

Engineering Geological Assessment of Selected Landslide Dams Formed from the 1929 Murchison and 1968 Inangahua Earthquakes

A thesis
submitted in partial fulfilment
of the requirements for the degree
of
Master of Science in Engineering Geology
at the
University of Canterbury
by
Timothy Richard Nash



UNIVERSITY OF CANTERBURY

2003

~~THESIS~~
QE
599
.N5
.N253
2003



L. Matiri

ABSTRACT

This study investigated the characteristics of 26 failed and non-failed landslide dams (Murchison dataset) formed in the northern part of the South Island, New Zealand, from the 1929 Murchison and 1968 Inangahua earthquakes. The dataset was compiled from a combination of engineering geological mapping, field investigations, aerial photography interpretation and a review of existing literature. Current analysis techniques have been applied to the investigated landslide dams to assess their ability to accurately predict the post-formation development (or 'evolution') of the dam over time. This has allowed the recognition of a number of additional landslide dam attributes that influence long-term stability, allowing modification of the stability analysis techniques in current use.

Dam, lake, catchment and landslide characteristics were collated and analysed for the Murchison dataset by distinguishing failed from non-failed landslide dams, and then assessing the parameters common to both. Parameters that influence the post-formation development of selected landslide dams in the dataset include the dam volume, catchment area above the point of blockage, average block size of material comprising the dam, slope angle of the downstream dam face, and rock mass and material characteristics in the source area of the dam-forming landslide. The stability of the dams in the Murchison dataset was not significantly affected by rock type, landslide movement, or the state, distribution and style of the dam-forming landslide.

Existing geomorphic indices were applied to selected dams in the dataset. The Impoundment, Blockage and Dimensionless Blockage Indices (Casagli and Ermini (1999); Ermini and Casagli (2003)) predicted the correct post-formation development for 58, 86, and 81% of the selected landslide dams in the Murchison dataset, respectively. Four landslide dams covering both failed and non-failed types were investigated in detail to assist with this analysis, two being stable dams impounding lakes, and two having failed 'catastrophically' post-formation. Detailed investigation was carried out on Lake Stanley landslide dam, which agrees with all three indices predicting post-formation development, and of Lake Matiri, Ram Creek and Rain Peak landslide dams for which the indices incorrectly predict their post-formation development.

This investigation has shown that the average block size (D_{50}) of the dam material strongly influences the post-formation development of the four dams studied in detail. Dams consisting of material with larger ($> 200\text{mm}$) average block sizes correspond to stable dams; while those with small ($< 100\text{mm}$) average block size correspond to failed dams. Rainfall duration/intensity and slope angle of the downstream dam face were also found to influence post-formation development of the dams. The recently formed and failed Poerua landslide dam on the West Coast of the South Island was included in the geomorphic index evaluation because of the excellent documentation available, together with the prediction of its long-term stability using the index approach.

The D_{50} of the material forming the landslide dam, and the landslide dam's basal (or footprint) length, were incorporated with the parameters used in the existing geomorphic indices to produce a new geomorphic index, the Modified Dimensionless Blockage Index (*MDBI*). This is defined as:

$$MDBI = \log \left(\left(\frac{A_c}{A_l} \right) \times \left(\frac{H_d}{L_f} \right) \times \left(\frac{V_d}{V_b} \right) \right)$$

where A_c is the catchment area (m^2), A_l is the lake area (m^2), H_d is the height of the dam (m), L_f is the length of the dam footprint (m), V_d is the volume of the dam (m^3), and V_b is the volume of the mean block size forming the dam (cube of the D_{50} expressed in m^3). Calculated *MDBI* values for the two stable landslide dams (Lake Stanley and Lake Matiri) are less than 10 (8.90 and 6.94 respectively), while those for three failed landslide dams (Rain Peak, Ram Creek and Poerua) are greater than 10 (10.75, 10.80 and 14.9, respectively).

This suggests that the *MDBI* can be tentatively used as a tool in forecasting the post-formation development of a landslide dam, with *MDBI* values > 10 corresponding to catastrophic dam failure, and an *MDBI* value < 10 corresponding to probable longer-term stability. However, it is recommended that a wider landslide dam dataset be applied to the *MDBI* to further test its accuracy, and to refine the parameters used both for short-term stability assessment following impoundment, and for longer-term prediction of post-formation dam (and lake) development. Rainfall duration and maximum block size of the dam material also require further evaluation, and a refinement incorporating grading parameters (such as D_{60}/D_{10}) may provide a better estimation of the post-formation landslide dam development. It is clear from this study that the block size and grading of the landslide dam material (in particular matrix or block support) exert significant influence on dam longevity and evolution, and this is reflected in the substantial weighting given to D_{50} in the *MDBI*.

Acknowledgments

I would like to thank many people for their contribution during this study. In particular:

David Bell for his help throughout this study especially near its completion where his red and green pen was strongly backed up by many in-depth discussions. His contributions greatly improved the content of this thesis.

Tim Davies who also contributed with advice and direction throughout the project

Simon Nathan for his interest in this project and his constant support

Pier Nicoletti, Grant Dellow, Nick Perrin and Stuart Read for their useful discussions and advice on landslide dams, particularly in the early stages of the study

Beatriz Estrada for being a great friend since we met in our fourth year

The Clockwork Muse for giving me the low-down on time management (pity it didn't work though!)

Mr. and Mrs. Inwood from Inangahua Junction for the great stories about the Ram Creek dam burst and the photos

My brother Daniel who accompanied me on several occasions in the field

Beatriz Estrada and Mandy Parker, who also braved the wasps and dodgy rivers in the Kahurangi

To my classmates Davi, Lieth, Richards, Antiskant, Gussage, Masti, Salty, Euwage, Barnyard, P.J., Verne, Dejoup, Bird, Blumenthal, Marshall, Penetrator, Muirson, , and of course Estrada

A big thanks to the geology admin girls Julie-Anne and Joan

Syd, Dick and Simon who flew me all over northwest Nelson and dropped me off at random locations in the Tasman Mountains

Kathy Walter (NIWA) and Debbie Fellows (NZAM) who put up with my consistent email enquiries

David Inch from Port Electrical of Nelson for supplying information regarding Lake Matiri

And finally to my family for supporting me throughout my time at university.

TABLE OF CONTENTS

TITLE PAGE.....	i
FRONTISPIECE.....	ii
ABSTRACT.....	iii
ACKNOWLEDGMENTS.....	v
TABLE OF CONTENTS.....	vi
LIST OF FIGURES.....	xi
LIST OF TABLES.....	xv

CHAPTER 1. INTRODUCTION

1.1	PROJECT BACKGROUND.....	1
1.2	SPECIFIC AIMS AND OBJECTIVES.....	2
1.3	SEISMOTECTONIC SETTING.....	3
1.4	NORTHWEST NELSON GEOLOGY AND GEOMORPHOLOGY.....	5
1.4.1	1929 MURCHISON EARTHQUAKE.....	7
1.4.2	1968 INANGAHUA EARTHQUAKE.....	7
1.5	THESIS METHODOLOGY.....	8
1.6	TERMINOLOGY.....	9
1.7	THESIS FORMAT.....	10

CHAPTER 2. REVIEW OF LANDSLIDE DAMS

2.1	BACKGROUND.....	11
2.2	FORMATION OF LANDSLIDE DAMS.....	12
2.2.1	SPATIAL AND TEMPORAL OCCURRENCE OF LANDSLIDE DAMS.....	12
2.2.2	TYPE OF DAM-FORMING LANDSLIDES.....	14
2.2.3	TRIGGERING MECHANISMS.....	17
2.2.4	LANDSLIDE VELOCITY.....	20
2.2.5	GEOMORPHIC CLASSIFICATION OF LANDSLIDE DAMS.....	20
2.2.6	EFFECT OF LANDSLIDE DAMMING.....	22
2.3	FAILURE OF LANDSLIDE DAMS.....	23
2.3.1	MODES OF DAM FAILURE.....	23

2.3.2	LONGEVITY OF LANDSLIDE DAMS.....	26
2.3.3	STABILITY OF LANDSLIDE DAMS.....	28
2.4	FLOODS ASSOCIATED WITH LANDSLIDE DAMS FAILURE.....	30
2.4.1	DAM FAILURE IMPACTS AND MITIGATION METHODS.....	31
2.4.2	DAM-BREAK STUDIES.....	32
2.4.3	CHANGES TO CHANNEL AND VALLEY MORPHOLOGY.....	34
2.5	LANDSLIDE DAMS IN NEW ZEALAND.....	35
2.5.1	NORTH ISLAND LANDSLIDE DAMS.....	35
2.5.2	SOUTH ISLAND LANDSLIDE DAMS.....	37
2.5.3	CHRONOLOGY OF LANDSLIDE DAMS RESEARCH IN NEW ZEALAND.....	37
2.6	CHAPTER 2 SYNTHESIS.....	38

CHAPTER 3. LANDSLIDE DAM DATABASE

3.1	INTRODUCTION.....	40
3.2	DATABASE CONSTRUCTION.....	41
3.2.1	DAM SELECTION.....	41
3.2.2	PARAMETER SELECTION.....	43
3.2.3	DAM-FORMING LANDSLIDES AND SOURCE AREA.....	44
3.2.4	DAM, LAKE AND CATCHMENT DATASHEET.....	46
3.2.5	ACQUISITION OF DATA.....	47
3.2.6	ERROR WITHIN THE DATASET.....	49
3.2.7	TERMINOLOGY.....	50
3.2.8	PRESENTATION OF DATA.....	51
3.3	LANDSLIDE DATASHEET ANALYSIS.....	51
3.3.1	SPATIAL DISTRIBUTION.....	51
3.3.2	SOURCE DIMENSIONS.....	52
3.3.3	SOURCE ROCK GEOLOGY.....	53
3.3.4	LANDSLIDE CLASSIFICATION.....	58
3.4	DAM, LAKE AND CATCHMENT ANALYSIS.....	62
3.4.1	ORIGINAL AND PRESENT DAM DIMENSIONS.....	63
3.4.2	DAM MATERIALS.....	68
3.4.3	BREACH CHARACTERISTICS.....	69
3.4.4	LAKE CHARACTERISTICS.....	71
3.4.5	CATCHMENT CHARACTERISTICS.....	73
3.4.6	DEATH AND DAMAGE.....	74

3.5	DAM DEVELOPMENT AND STABILITY ANALYSIS USING GEOMORPHIC INDICES.....	74
3.5.1	BACKGROUND.....	74
3.5.2	IMPOUNDMENT INDEX (<i>Ii</i>).....	76
3.5.3	BLOCKAGE INDEX (<i>BI</i>).....	78
3.5.4	DIMENSION BLOCKAGE INDEX (<i>DBI</i>).....	81
3.6	CHAPTER 3 SYNTHESIS.....	84

CHAPTER 4. LAKE STANLEY CASE STUDY

4.1	INTRODUCTION.....	86
4.2	LAKE STANLEY LOCATION AND GEOLOGICAL SETTING.....	87
4.2.1	GENERAL DETAILS.....	87
4.2.2	GEOLOGICAL SETTING.....	90
4.3	LANDSLIDE SOURCE AREA CHARACTERISTICS.....	91
4.3.1	ZONE I.....	91
4.3.2	ZONE II.....	92
4.4	TIMING OF LANDSLIDING.....	94
4.4.1	PRE-1929 LANDSLIDING.....	96
4.4.2	1929 LANDSLIDE.....	96
4.4.3	1929-1968 LANDSLIDE.....	97
4.4.4	1994 LANDSLIDE.....	97
4.5	LANDSLIDE DAM CHARACTERISTICS.....	97
4.5.1	GENERAL DESCRIPTION/DIMENSIONS.....	97
4.5.2	DAM MATERIAL.....	99
4.6	DRAINAGE OF LAKE STANLEY.....	101
4.6.1	SPILLWAY CHARACTERISTICS.....	101
4.7	LANDSLIDE DAM STABILITY ASSESSMENT.....	104
4.7.1	GENERAL STABILITY.....	104
4.7.2	GEOMORPHIC INDEX ANALYSIS.....	105
4.7.3	PARAMETERS INFLUENCING STABILITY.....	106
4.8	FUTURE DEVELOPMENT.....	107
4.8.1	LANDSLIDE ONTO THE DAM.....	107
4.8.2	LANDSLIDE INTO THE LAKE.....	109
4.9	FUTURE WORK.....	110
4.10	CHAPTER 4 SYNTHESIS.....	110

CHAPTER 5. LANDSLIDE DAM CASE STUDIES

5.1	INTRODUCTION.....	112
5.2	RAM CREEK LANDSLIDE DAM.....	113
5.2.1	INTRODUCTION.....	113
5.2.2	LANDSLIDE AND SOURCE AREA CHARACTERISTICS.....	115
5.2.3	LANDSLIDE DAM CHARACTERISTICS.....	116
5.2.4	FAILURE OF THE DAM.....	119
5.2.5	PARAMETERS AFFECTING DAM STABILITY.....	122
5.2.6	FUTURE DEVELOPMENT.....	124
5.2.7	RAM CREEK SYNTHESIS.....	124
5.3	RAIN PEAK LANDSLIDE DAM.....	125
5.3.1	INTRODUCTION.....	125
5.3.2	LANDSLIDE AND SOURCE AREA CHARACTERISTICS.....	127
5.3.3	LANDSLIDE DAM CHARACTERISTICS.....	128
5.3.4	FAILURE OF A DAM.....	131
5.3.5	PARAMETERS AFFECTING DAM STABILITY.....	134
5.3.6	FUTURE DEVELOPMENT.....	135
5.3.7	RAIN PEAK SYNTHESIS.....	136
5.4	LAKE MATIRI LANDSLIDE DAM.....	136
5.4.1	INTRODUCTION.....	136
5.4.2	HISTORICAL ACCOUNT OF DAMMING.....	139
5.4.3	LANDSLIDE SOURCE AND DEPOSIT CHARACTERISTICS.....	140
5.4.4	LANDSLIDE DAM CHARACTERISTICS.....	140
5.4.5	DAM MATERIAL.....	142
5.4.6	PARAMETERS AFFECTING DAM STABILITY.....	144
5.4.7	FUTURE DEVELOPMENT.....	145
5.4.8	LAKE MATIRI SYNTHESIS.....	146
5.5	CHAPTER 5 SYNTHESIS.....	147

CHAPTER 6. POST-FORMATION LANDSLIDE DAM DEVELOPMENT

6.1	INTRODUCTION.....	148
6.2	IMPOUNDMENT INDEX (I_i).....	149
6.3	BLOCKAGE INDEX (BI).....	152
6.4	DIMENSIONLESS BLOCKAGE INDEX (DBI).....	156
6.5	DEVELOPMENT OF A MODIFIED DBI ($MDBI$).....	159
6.5.1	BACKGROUND.....	159

6.5.2	<i>MDBI</i> DEVELOPMENT.....	160
6.5.3	<i>MDBI</i> APPLICATION TO SELECTED DAMS.....	162
6.5.4	ASPECTS OF THE <i>MDBI</i> CONTRIBUTING TO BETTER CORRELATION	165
6.6	CHAPTER 6 SYNTHESIS.....	167
 CHAPTER 7. SUMMARY & CONCLUSIONS		
7.1	INTRODUCTION.....	169
7.2	LANDSLIDE DAM DATASET.....	170
7.2.1	MURCHISON AND INANGAHUA EARTHQUAKES.....	170
7.2.2	DATABASE CONSTRUCTION.....	170
7.2.3	ANALYSIS OF THE MURCHISON DATASET.....	170
7.2.4	GEOMORPHIC INDICES.....	171
7.3	DETAILED INVESTIGATION.....	173
7.3.1	SELECTION CRITERIA.....	173
7.3.2	LAKE STANLEY LANDSLIDE DAM.....	173
7.3.3	RAM CREEK LANDSLIDE DAM.....	174
7.3.4	RAIN PEAK LANDSLIDE DAM.....	175
7.3.5	LAKE MATIRI LANDSLIDE DAM.....	175
7.3.6	GENERAL CONCLUSIONS.....	176
7.4	MODIFIED DIMENSIONLESS BLOCKAGE INDEX (<i>MDBI</i>).....	177
7.4.1	IMPORTANT ADDITIONAL PARAMETERS.....	177
7.4.2	FORMULATION OF THE <i>MDBI</i>	177
7.4.3	APPLICATION TO FIVE DAMS.....	178
 REFERENCES.....		 180
 APPENDICES		
Appendix A	Sample Landslide and Dam Datasheets.....	190
Appendix B	Murchison Datasheet (Raw Data on CD)	
Appendix C	Synthesised Murchison Data.....	197
Appendix D	Landslide Triggering Mechanisms.....	209
Appendix E	Predicting Flood Magnitude from Dam failure.....	213
Appendix F	Parameter Terminology.....	220
Appendix G	Rock Mass and Material Field Descriptions.....	228

LIST OF FIGURES

CHAPTER 1

Fig. 1.1	Tectonic setting of New Zealand.....	4
Fig. 1.2	DEM of the top north west of South Island, New Zealand showing lithological boundaries and major faults.....	5

CHAPTER 2

Fig. 2.1	Number of landslide dams relative to the type of landslide.....	16
Fig. 2.2	Examples of the main types of landslides that form dams.....	16
Fig. 2.3	Causes of dam-forming landslides.....	17
Fig. 2.4	Summary of forces acting on a slope produced during an earthquake.....	18
Fig. 2.5	One of the largest landslide dammed lakes in the world today (Lake Sarez)...	19
Fig. 2.6	Schematic diagrams showing classification of landslide dams.....	21
Fig. 2.7	Modes of failure of landslide dams.....	24
Fig. 2.8	Duration of landslide dams based on 187 failed landslide dams where the time to failure is known.....	27
Fig. 2.9	Types of landslides that have produced landslide dams.....	29
Fig. 2.10	Triggering mechanisms that produced dam-forming landslides.....	29
Fig. 2.11	Example of a typical hydrograph of discharge following the failure of landslide dams	33
Fig. 2.12	Location of landslide lakes in New Zealand showing approximate landslide volumes.....	36

CHAPTER 3

Fig. 3.1	Map showing locations of 26 landslide dams formed in part or whole by the 1929 Murchison and the 1968 Inangahua earthquakes.....	43
Fig. 3.2	Quantification of the rupture length (L_r), rupture width (W_r) and rupture depth (D_r) for initial dam-forming rotational landslides.....	53
Fig. 3.3	Rock material characteristics of initial dam-forming landslide source area from various dams, this thesis.....	56

Fig. 3.4	Distribution of the classification of the initial dam-forming landslides associated with dams from this dataset.....	61
Fig. 3.5	Schematic plan, section and 3-D illustrations of a typical landslide dam prior to failure and post failure.....	64
Fig. 3.6	(A) Landslide dam volume versus lake volume defining stable and unstable domains for 19 landslide dams formed in northwest Nelson. (B) Dam volume versus lake volume showing actual stage of landslide dams.....	77
Fig. 3.7	(A) Landslide dam volume versus drainage basin area for 23 dams located throughout northwest Nelson defining stable and unstable domains. (B) Comparison of actual stage of landslide dam to that forecast using the <i>BI</i>	80
Fig. 3.8	(A) Calculated dimensionless blockage index (DBI) for 22 landslide dams located throughout northwest Nelson indicating stable (<2.75) and unstable (>3.08) domains. (B) Comparison actual stage of landslide dam to that forecast using the <i>DBI</i>	83

CHAPTER 4

Fig. 4.1	Location map of Lake Stanley landslide dam.....	88
Fig. 4.2	View of Lake Stanley looking northeast with the landslide dam (ld) material in the background.....	89
Fig. 4.3	Aerial oblique photograph of Lake Stanley dam-forming landslide looking southwest.....	89
Fig. 4.4	Major joint sets dipping to the northwest at ~ 45-50° from the eastern lateral margin rock mass Zone I.....	93
Fig. 4.5	Closely jointed volcanoclastic sedimentary rock mass exposed in the upper western lateral margin of Zone I.....	93
Fig. 4.6	Planar joint surface at the base of zone II looking southwest at the head of the slide.....	95
Fig. 4.7	Typical planar joint surface in Zone III comprising the intrusive sill as in Zone II.....	95
Fig. 4.8	View of the dam material looking north illustrating zones within the vegetation that define landslide events.....	98
Fig. 4.9	View of the landslide complex from the dam material looking south east illustrating the damaged tree resulting from a landslide in 1994.....	98
Fig. 4.10	Illustration of the rock material exposed in the spillway walls.....	100
Fig. 4.11	View of the lake outlet looking northwest towards the Lake Stanley.....	102

Fig. 4.12	View of the spillway Section B looking downstream.....	103
Fig. 4.13	Stereographic projection for kinematic analysis of wedge and planar failure in Zone I rocks at Lake Stanley upper eastern lateral margin.....	108

CHAPTER 5

Fig. 5.1	Location of Ram Creek landslide dam and lake (pre failure).....	114
Fig. 5.2	Aerial oblique of Ram Creek landslide dam looking east.....	117
Fig. 5.3	Source rock mass characteristics.....	117
Fig. 5.4	Dam material comprising the landslide dam.....	118
Fig. 5.5	Flood debris 5.5 km downstream of dam.....	120
Fig. 5.6	Looking west illustrating the breached section of the landslide dam following failure.....	121
Fig. 5.7	1km downstream of the dam showing > 2m of aggradation from the breaching and failure of the Ram Creek landslide dam.....	121
Fig. 5.8	Location map of Lake Matiri (5) and Rain Peak (16) landslide dams.....	126
Fig. 5.9	Oblique aerial stereo pairs of Rain Peak landslide dam post failure looking north-northwest.....	129
Fig. 5.10	View looking southeast in the direction of flow at the breached section of the dam.....	129
Fig. 5.11	Stratified sediments 700m downstream of the Rain Peak lake overlying massive landslide deposits from movement in Zone II.....	130
Fig. 5.12	Finely laminated lake sediments overlying undifferentiated deposits inferred to be stream alluvium.....	130
Fig. 5.13	Panoramic view illustrating the present lake, breached section of the dam, landslide deposits and original lake level.....	133
Fig. 5.14	Photograph looking southwest at the Rain Peak dam and lake complex post failure illustrating the breach dam section, landslide, the present lake and lake sediments from the original lake prior to breaching.....	133
Fig. 5.15	Oblique aerial photograph of Lake Matiri landslide looking southeast.....	138
Fig. 5.16	Photo looking east at the steeply dipping (~ 60°) calcareous sandstone landslide source area.....	138
Fig. 5.17	Photo at the dam crest looking south at the main spillway.....	141
Fig. 5.18	View of the main spillway looking southwest at a position distal to the landslide source.....	141

Fig. 5.19	(A) Blocks lining the spillway on the downstream face of the dam. (B) view of the spillway on the downstream face of the dam looking southeast.....	143
-----------	---	-----

CHAPTER 6

Fig. 6.1	(A) Application of the <i>Ii</i> to 18 landslide dams (Casagli and Ermini, 1999) from the Northern Apennines, Italy. (B) Application of the <i>Ii</i> to 20 dams from the Murchison dataset.....	151
Fig. 6.2	(A) Application of the <i>BI</i> to c.60 landslide dams from the Northern Apennines, Italy (Casagli and Ermini, 1999). (B) Application of the <i>BI</i> to 23 dams from the Murchison dataset.....	154
Fig. 6.3	(A) Application of the <i>DBI</i> to 84 landslide dams worldwide (Ermini and Casagli, 2003). (B) Application of the <i>DBI</i> to 22 landslide dams from the Murchison dataset.....	157
Fig. 6.4	Graphical representation of <i>MBDI</i> values for five landslide dams.....	165

ATTACHED MAPS (in pocket)

Map 1	Engineering Geological Plan and Section of Lake Stanley Landslide Dam
Map 2	Engineering Geological Plan and Section of Ram Creek Landslide Dam
Map 3	Engineering Geological Plan and Section of Rain Peak Landslide Dam
Map 4	Engineering Geological Plan and Section of Lake Matiri Landslide Dam

LIST OF TABLES

CHAPTER 2

2.1	Classification of landslides based on the type of movement and material.....	14
2.2	Glossary of forming names of landslides.....	14
2.3	Relative abundance of earthquake induced landslides.....	20
2.4	Classification of landslide dams with known examples.....	21
2.5	Some effects of landslide damming on upstream and downstream environments.....	22
2.6	Summary table listing the advantages and disadvantages of available methods to predict the dam break flood characteristics and data required for the individual techniques.....	34

CHAPTER 3

3.1	List of the landslide dams used in the Murchison dataset.....	42
3.2	Mean and range source dimensions and volumes for all 26 dam-forming landslides in the dataset, this thesis.....	52
3.3	Summary of the original and present dam dimensions and composition from selected landslide dams from the Murchison dataset comparing failed dams to non-failed dams.....	65
3.4	Degree of modification (DOM) based on the volume of material eroded from the original dam volume.....	70
3.5	Summary of the present lake dimensions and catchment conditions from selected landslide dams, this study.....	71
3.6	Summary of effectiveness of the <i>Ii</i> , <i>BI</i> and <i>DBI</i> in forecasting the post-formation dam development.....	85

CHAPTER 4

4.1	Calculated index values for Lake Stanley (No. 1) landslide dam.....	106
-----	---	-----

CHAPTER 5

5.1	Calculated index values for Ram Creek (No. 25) landslide dam.....	122
5.2	Calculated index values for Rain Peak (No. 16) landslide dam.....	134
5.3	Calculated index values for Lake Matiri (No. 5) landslide dam.....	144

CHAPTER 6

6.1	Parameters used in the proposed <i>MDBI</i> summarising reasons for their inclusion and a brief description of each parameter.....	160
6.2	Data used to calculate the <i>MDBI</i> for four landslide dams from the Murchison dataset and the Poerua landslide dam.....	163
6.3	Summary of results from application of the I_i , BI , DBI and <i>MDBI</i> indices on four dams from the Murchison dataset and one recent landslide dam not included in the dataset (Poerua landslide dam).....	164
6.4	Summary of the individual <i>MDBI</i> index ratios used for the five applied dams demonstrating the variation and weighting of each ratio to the final <i>MDBI</i> value.....	166

Chapter 1

INTRODUCTION

1.1 PROJECT BACKGROUND

Hazards associated with natural damming of rivers, and catastrophic flooding from their failure, have long been recognised and documented in a plethora of historical accounts and case studies of landslide dams. Landslide dams form in all kinds of physiographic settings; however, they are commonly found in mountainous terrain typically associated with steep-walled narrow valleys with a high landslide frequency. The effects of landslide damming extend beyond the immediate on-site impacts on the fluvial system, such as full blockage or channel diversion, to off-site effects such as sediment transport changes both upstream and downstream of a landslide dam. Triggering mechanisms also vary, but most commonly involve earthquakes or rainfall and snowmelt.

Previous work on landslide dams has been largely descriptive in nature, as evident in the multitude of historical accounts and case studies that document the formation and failure of natural dams (Adams, 1981 a; Costa and Schuster, 1988; Costa and Schuster, 1991; Schuster, 1993; Schuster and Costa, 1986). Recent work has focussed on more quantitative methods in determining the post-formation development of a dam, in particular the controls on dam longevity (Casagli *et al.*, 2003; Ermini and Casagli, 2003; Manville, 2001; Schuster, 2000). However, there is still a general lack of understanding of the processes involved in landslide dam formation, and in particular, the short and long-term ability of a dam to impound water, partly due to the highly variable nature of landslide dams themselves.

It is therefore the purpose of this thesis to understand the dynamics of landslide dams and to provide a more accurate indicator of short-term stability for instantaneous hazard appraisals. In addition, this thesis attempts to better understand the spatial and temporal

influences on the ability of a natural dam to impound water. This is achieved by collating data for a group of landslide dams formed in the South Island of New Zealand through analysis of the individual parameters associated with the dam, lake and catchment. Current methods of predicting a dam's post-formation development and stability can then be applied tested and modified based on the database of landslide dams included in this study.

The thesis structure consists of 1) a literature review of landslide dams; 2) development of a methodology for the construction of a landslide dam dataset; 3) analysis of the landslide dam dataset; 4) discussions regarding the application of current methods to predict the post-formation development of landslide dams; and 5) development of a new method of predicting the post-formation development of landslide dams.

1.2 SPECIFIC AIMS AND OBJECTIVES

In order to understand the dynamics of landslide dams and to provide a more accurate indicator of short-term stability, the project was subdivided into four primary objectives:

- 1) To review available literature on landslide dam formation and failure;
- 2) To develop a database of large landslide dams in the northern part of the South Island;
- 3) To analyse results in terms of currently published geomorphic indices; and
- 4) To develop a revised geomorphic index that better predicts landslide dam development over time.

The primary objectives are further divided into subsidiary aims as follows:

- To understand important parameters influencing the ability of a landslide dam to resist erosion from overtopping of the dam crest and/or seepage through the dam;
- To critically analyse four selected dams from a dataset of landslide dams to highlight important parameters influencing their stability and longevity;
- To present and define terminology used to document the occurrence and characteristics of landslide dams;
- To assess the applicability of geomorphic indices that predict a dam's post-formation development by applying them to selected dams from the database collected as part of this study;

- To identify shortcomings in the ability of current indices to correctly predict post-formation development of a landslide dam;
- To refine the current methodology used to record the occurrence of landslide dams;

1.3 SEISMOTECTONIC SETTING

Earthquakes have long been recognised as a major cause of landslides, documentation of which dates back to around 370 B.C. (Keefer, 1984; Seed, 1968). Schuster (1993) analysed 394 historical cases of landslide dam formation and showed that earthquakes triggered almost 50% of the dam-forming landslides. The size and scale of earthquake-triggered landslides is highly variable, but is generally controlled by the geological and tectonic setting of a region; the current tectonic and geological setting of New Zealand creates an environment that is common to earthquake-triggered landsliding, as described below.

New Zealand is located at the boundary between the Australian and Pacific plates. The motion between these plates forms an opposite dipping and obliquely convergent subduction zone. The relative displacements along the plate margin range from 50 mm/yr in the north to 40 mm/yr in the centre, and 30 mm/yr in the south (Figure 1.1). Numerous active faults within New Zealand accommodate the plate motion. Two major fault zones, the Alpine Fault and Marlborough Fault Zone (MFZ) in the South Island, can be interpreted as a trench-trench transform fault zone, linking the subduction zones (Figure 1.1). A southeast dipping subduction zone at the southwest end of the country, the Puysegur trench, is linked to a major northwest-dipping subduction zone in the northeast, the Hikurangi subduction zone.

South Island tectonics are characterised by the east-dipping Alpine Fault, which displays oblique dextral shear and is the prominent component of the Alpine Fault system (Pettinga, 1997). The Alpine Fault system is comprised of a 200km wide band of deformation across the Southern Alps which transforms to the north onto the Marlborough Transfer Zone (MTZ) to accommodate the transition from continental collision to subduction, which promotes tectonic shortening, crustal thickening and uplift in the MTZ (Pettinga, 1997; Fig 1.1).

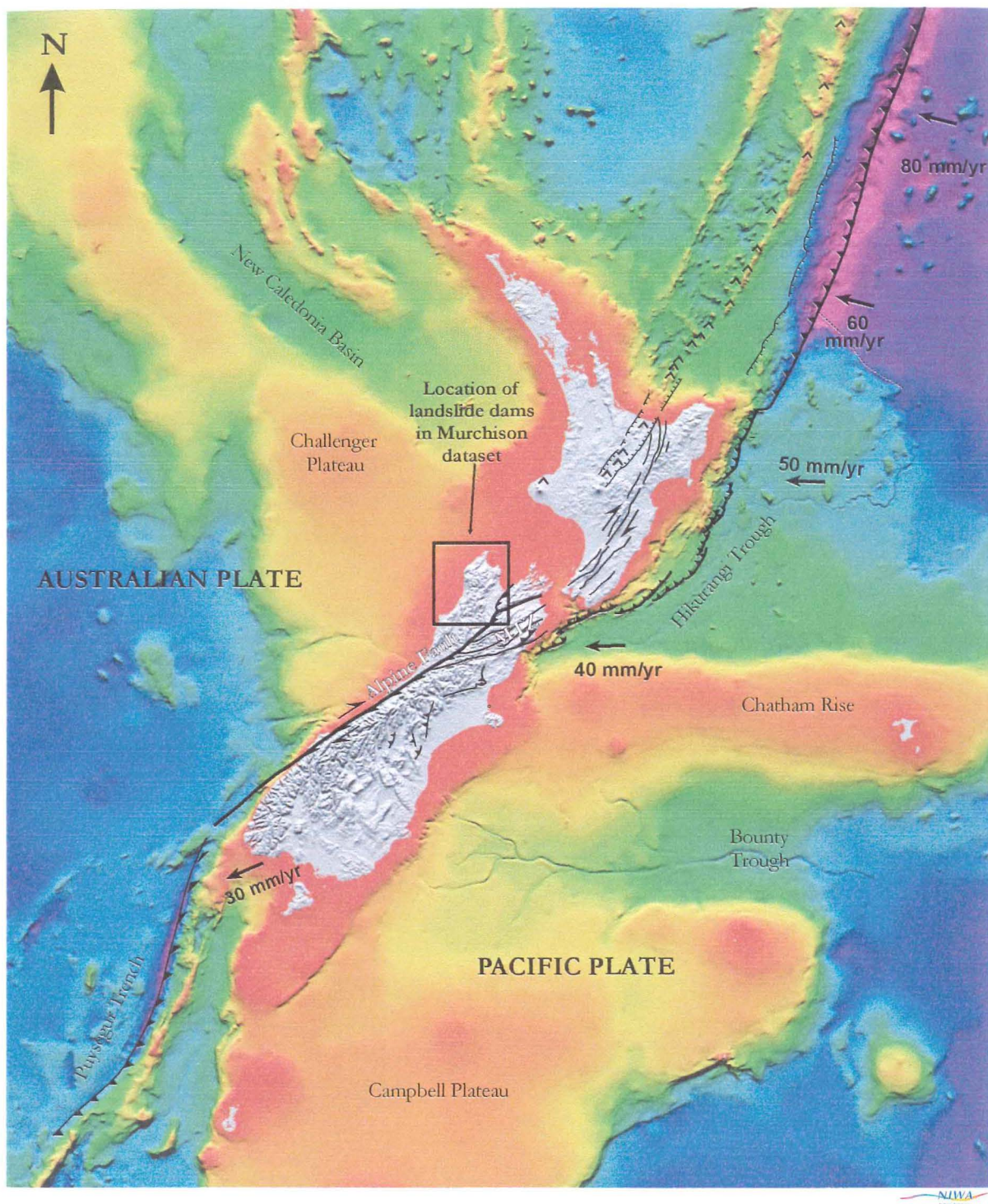


Fig 1.1. Setting of the New Zealand micro-continent straddling the obliquely convergent Australia-Pacific plate boundary zone. Numbered arrows show rates of relative convergence in mm/year.. Location of the study area is highlighted by the box and annotation at the top of the South Island (New Zealand Undersea image modified with permission from NIWA, 2003).

The subduction of the Pacific Plate beneath the Australian Plate generates seismicity which is concentrated in the Hikurangi Benioff zone, but it also extends onto the northern South Island terminating just south of Westport, making northwest Nelson one of the most seismically active parts of New Zealand (Anderson and Webb, 1994). To the south of this termination, the Alpine Fault shows a pre-history of surface rupture and associated large magnitude earthquakes (Benn, 1992). Evidence suggests the Alpine Fault has a recurrence interval of hundreds of years (Stirling *et al.*, 2002), with the most recent movement occurring ~ AD 1717 (Yetton, 2002). Therefore, the Alpine Fault system represents the principal seismic hazard to the central South Island and the likely source of future earthquake-triggered landslide (dams).

1.4 NORTHWEST NELSON GEOLOGY AND GEOMORPHOLOGY

Fig 1.2 shows the distribution of landslide dams used in this study, which covers an area of about 5,000 km² throughout northwest Nelson, South Island, New Zealand, and includes parts of the Tasman and Buller districts. The north-trending Buller and Takaka terranes are the oldest structural units in New Zealand, consisting of slightly metamorphosed quartz-rich turbidites and sedimentary/volcanic sequences of mid to late Palaeozoic age respectively which make up the bulk of basement rock in the study area (Rattenbury *et al.*, 1998). Granites from the Karamea Batholith are intruded into the Buller terrane rocks, and strike north south, covering the entire length of the field area. Likewise, but less extensively, the Takaka terrane is intruded by north-south trending granitic bodies of the Separation Point Suite (Rattenbury *et al.*, 1998). The remaining field area is comprised mainly of Tertiary marine sedimentary sequences, which are prominent in the middle and west of the field area and unconformably overlie the previously described basement rocks.

The main geomorphologic feature of northwest Nelson is the Tasman Mountains (Fig 1.2), which rise to a maximum elevation of 1,875 meters above mean sea level and have been extensively glaciated during the Pleistocene, with many of the younger valleys retaining the characteristic 'u' shape (Rattenbury *et al.*, 1998).

Average yearly rainfall is relatively consistent throughout the study area, receiving between 2.5 and 3.5m per annum (*pers comm.*, NIWA, 2003). Drainage throughout northwest Nelson is via several major east-west flowing rivers that dissect the north-south trending mountains such as the Buller, Mohikini and Karamea Rivers, as well as south-north flowing rivers such as the Takaka and Aorere Rivers (Fig 1.2).

The study area is dominated by mountainous terrain that is sparsely populated, with the larger urban centres located around the periphery of the field area, including Westport, Murchison, Karamea, and Inangahua (Fig 1.2). The major land uses are dairy, sheep and cattle farming, horticulture and exotic forestry (Rattenbury *et al.*, 1998). However, the majority of the field area (> 90%) is covered in uninhabited dense native bush.

Northwest Nelson is located in one of the most seismically active areas in New Zealand (Benn, 1992). Landslide dams investigated in this thesis formed from two major earthquakes generated in the area in the recent past, those being the Murchison 1929 and the Inangahua 1968 earthquakes.

1.4.1 1929 MURCHISON EARTHQUAKE

On the 17th of June 1929, the Murchison earthquake (M 7.8) was produced by oblique movement on the north south trending White Creek Fault about 12 km west of Murchison (Fig 1.2). An estimated 3.0 m of vertical movement occurred on the east side of the fault, with a maximum sinistral horizontal offset of 2.5 m (Berryman, 1980) and the 1929 rupture fault trace extended for ~ 8 km (Henderson, 1937). Prior to 1929, there was no evidence of displacement on the White Creek Fault for at least 18,000 years based on the age of fluvioglacial deposits inferred to be Last Glaciation (Berryman, 1980). The earthquake caused widespread landsliding over an area between approximately 6,000 km² throughout northwest Nelson, up to 100km north and 20km south of the epicentre at 41.7°S, 172.2°E (Hancox *et al.*, 2002). Many of these landslides dammed or partly dammed rivers, and in all 17 persons lost their lives, of which 14 were overwhelmed in slips (Henderson, 1937). Twenty-four of the larger landslide dams that formed in part or whole by landslides triggered during the 1929 Murchison earthquake are included in the dataset for this study.

1.4.2 1968 INANGAHUA EARTHQUAKE

On the 24th of May 1968, the Inangahua earthquake (M_w 7.2) occurred ~ 10 km north of Inangahua Junction (Fig 1.2) on the west coast of the South Island, New Zealand. The

earthquake was produced by the west-dipping, largely blind Rotokohu fault, with subsequent secondary surface rupture west side up on the Lyell and Inangahua faults which is in opposite sense to their long-term displacement (Yeats, 2000). Prior to 1968 on the Inangahua fault only 1.5m of vertical displacement had occurred since the last (Otira) glacial, 18, 000 years ago (Lensen and Suggate, 1968), however the number of movements associated with this displacement is unknown (Benn, 1992). In total, three people were killed as a result of the earthquake, with heavy damage to roading and other infrastructure occurring with many large bedrock and surficial landslides forming in the Buller area. One large landslide blocked the east-west draining Buller River, and another blocked a small tributary of the Buller River east of Inangahua junction. Both landslides formed dams, which are included in the dataset in this thesis.

1.5 THESIS METHODOLOGY

A preliminary desk study was conducted to select appropriate landslide dams for detailed analysis and inclusion in the landslide dam database (called ‘Murchison dataset’ in this thesis, even though 2 are Inangahua earthquake-related). Selection was based primarily on the landslide dam volume, with the largest dams (volume $> \sim 100,000 \text{ m}^3$) being chosen because they pose the greatest hazard to downstream settlements and infrastructure, and because their dam and lake attributes are better defined relative to small (volume $< \sim 100,000 \text{ m}^3$) landslide dams. Once selected, information relating to their formation and failure (if applicable) was collated and synthesised on spreadsheets (Appendix A and B), which detail the landslide source, dam, lake and catchment characteristics. Methods used to collate the information included existing published and unpublished reports, geologic and topographic maps, field investigations of dams that could be accessed on foot, and flights over the field area documenting the current state of each dam included in the Murchison dataset. A total of 40 days were spent in the field conducting reconnaissance and detailing landslide dam characteristics not able to be acquired through desk studies. These preliminary results were synthesised, analysed and applied to recent dam stability analysis techniques in current use, which raised further questions regarding the parameters that actually control the ability of a landslide dam to impound water. These so-called ‘geomorphic indices’ are further discussed in Chapter 2.

The next step focused on identifying the influence that specific dam, lake and catchment parameters had on dam longevity, through additional field reconnaissance and the production of detailed engineering geological maps for four of the identified dams (both failed and non-failed). The applicability of current stability indices was then determined for the selected dams to test the forecasted stability against their actual post-formation behaviour. The final research step was the application of additional parameters understood from this study to influence stability, and the development of a new index (Modified Dimensionless Index or *MDBI*), in an attempt to better forecast a landslide dam's post-formation development.

1.6 TERMINOLOGY

International terminology used to assess the state of a landslide dam is highly variable and often ambiguous, mainly because of the lack of parameter definition in the majority of landslide dam reports. One aim of this thesis is to clarify how the landslide dam parameters are quantified in order to permit the comparison of dams forming in geographically different regions. Appendix D lists definitions for all parameters used in the dataset generated for this thesis (termed the 'Murchison dataset').

The term 'evolution' of a dam is commonly used in the literature to describe the development of a dam after its formation. The term 'evolution' has been substituted in this thesis by 'post-formation development'. In their most recent paper Ermini and Casagli (2003) define a landslide dam as either being 'stable' or 'unstable'. 'Stable' refers to a landslide dam that has remained stable since its formation and has not encountered a breach, thus still impounding an existent or relict lake. 'Unstable' refers to a landslide dam that has undergone erosion or collapse leading to a catastrophic breach, with the subsequent release of the impounded lake waters. These two terms have been further divided as part of the Murchison study into highly stable (HS), stable (S), moderately stable (MS), largely failed (LF) and completely failed (CF), based on the amount of dam material eroded from the original dam volume (see section 3.2.5 for discussion).

When referring to a dam in the Murchison dataset, the name of the dam is followed by the database reference number (e.g. Matakkitaki No. 2), which links the landslide dam to its appropriate datasheet in Appendix B.

1.7 THESIS FORMAT

Chapter 2 focuses on the formation and failure of landslide dams, both globally and within the New Zealand context. In particular, the chapter focuses on the environmental controls needed for dam formation, and the short and long-term effects that dam formation has on other natural processes such as river flow and sediment transport. Dam failure is generally concerned with describing downstream hazards associated with catastrophic dam failure or lowering, and techniques used to estimate flood flows quantitatively. The final section briefly describes the current status of research on landslide dams in New Zealand.

Chapter 3 details the methodology used to build the landslide dam database, which is followed by analysis and discussion of each parameter to highlight those relating to dam failure. The last section details the use of geomorphic indices to predict the evolution (termed ‘post-formation development’ this study) of selected landslide dams from the Murchison dataset, and highlights their applicability.

Chapters 4 and 5 investigate four landslide dams in detail whose actual post-formation development either agrees or disagrees with that predicted using geomorphic indices. The intention is to demonstrate the key parameters influencing their development, and to use these to better formulate a revised geomorphic index.

Chapter 6 critically reviews the current geomorphic indices available in the literature to predict a landslide dam’s post-formation development. A modification of the latest index is proposed to better predict the development of landslide dams following their formation. Application of the modified index to five landslide dams is discussed, followed by suggestions to improve the modified index.

Chapter 2

REVIEW OF LANDSLIDE DAMS

2.1 BACKGROUND

The term “landslide dam” identifies the natural blockage of river channels caused by slope movements (Casagli and Ermini, 1999). The river blockage may be complete or partial; in both instances, an impoundment may be formed upstream. Costa and Schuster (1988) list the wide range of dams that form in nature. These include landslide dams, glacier-ice dams, moraine dams, volcanic dams, fluvial dams, aeolian dams, coastal dams, and organic dams; three of these pose a widespread threat to people and property, namely landslide dams, glacier-ice dams, and late-neoglacial-age moraine dams.

Hazards from landslide dams derive from their relatively short-lived nature. According to Costa and Schuster (1988), who sampled 73 landslide dams with known time to failure, 85% of landslide dams failed within 1 year of formation. In contrast, blockages can also impound water for millennia due to their natural stability and resistance to erosion (Adams, 1981 a; Nicoletti and Terranova, 1998; Riley and Read, 1991). In general, however, landslide dams have a low resistance to both internal erosion and especially when overtopped by the impounded water. In many cases failure may be catastrophic, causing major downstream flooding, or in others it may be slow resulting in minimal downstream damage (Schuster, 2000). Additional hazards, such as backwater flooding, occur upstream of a landslide dam as the impoundment fills; the rate of filling is generally a slow process depending on the size of the catchment above the point of blockage however, it can potentially inundate communities and valuable agricultural land (Schuster and Costa, 1986).

The impacts of landslide dams can be subdivided into short and long-term impacts. Short-term impacts involve upstream and downstream flooding; downstream flooding is the most

hazardous to populated areas and infrastructure in the potential flood path and therefore receives significant attention. Initial assessment of a landslide dam to identify the probability of catastrophic failure associated with impounded water is essential for emergency management. Current research is therefore focussed on predicting a dam's post-formation development for early identification of its potential for catastrophic dam failure through empirically derived geomorphic indices, and is the basis of the research in this study. Long-term impacts receive less attention because they concern the effects the landslide dam has on sediment transport and overall hydrological impacts, which does not pose an immediate threat to populated areas downstream of a landslide dam.

This chapter documents and illustrates the multiple boundary conditions required for the formation and failure of a landslide dam, the long and short-term hazards associated with their formation and failure, and landslide damming within the New Zealand.

2.2 FORMATION OF LANDSLIDE DAMS

This section presents the formation of a landslide dam with particular reference to the typical geomorphic settings, type and characteristics of dam-forming landslides, and the effects of landslide dam formation. The formation of a landslide dam is dependent on many factors such as the type of landslide, the velocity of the landslide, landslide material, valley morphology, and the distribution of landslide debris within the valley floor. Once formed, a landslide dam may last several minutes or for several thousand years (Schuster, 1993; Schuster and Costa, 1986)

2.2.1 SPATIAL AND TEMPORAL OCCURRENCE OF LANDSLIDE DAMS

The term 'landslide' comprises almost all varieties of lateral and down slope mass movements including rock-falls, topples, and debris flows that involve minimal or no true sliding; various interactions and conditions affect slope stability such as lithology, geological structure, geomorphology, hydrological conditions (climate), and vegetation (Cruden and Varnes, 1996; Varnes, 1984).

Landslide dams form in various kinds of geomorphic settings. They generally form in steep-walled narrow valleys bordered by high rugged mountains, a setting commonly found in geologically active regions where uplift or mountain building, associated with

active tectonics, is the dominant process (Costa and Schuster, 1988; Schuster and Costa, 1986). This type of setting augments the chances of a landslide dam forming because 1) steep-walled valleys are particularly prone to slope failures; and 2) their narrow cross sections require relatively small amounts of debris to block the flow of water (Schuster, 1993). However, the occurrence of landslide dams is not restricted to this particular setting; landslide dams, albeit uncommon, also form in broad flat river valleys (Hancox *et al.*, 2002).

Schuster *et al.* (1989) listed four groups of factors that governed the spatial distribution of landslide dams formed from the 1989 Californian Loma Prieta earthquake including 1) seismic intensity (both the peak acceleration and duration of shaking, defined by the Arias intensity I_a); 2) topography and high slope gradient; 3) lithologic and weathering properties of the rock material; and 4) soil moisture and groundwater considerations. This list is specific to the Loma Prieta earthquake; however, in general, it is representative of some of the more common conditions influencing the spatial and temporal occurrence of landslide dams. In addition, Schuster *et al.* (1989) state the influence of climate and hydrogeology of a region as being an important factor in the distribution of landslide dams. For example, in the seismically active region of Southern California, few landslide dams have occurred because seasonal rainfall, hillside ground water levels, and stream flow is generally lower than in central and northern California, which is commonly affected by these phenomena.

The temporal occurrence of landslide dams can be a function of climatic and/or seasonal rainfall patterns (Van Asch *et al.*, 1999). Essentially, however, the temporal occurrence of a landslide dam is a function of the frequency of triggering mechanism, whether it is earthquake, volcanic or excessive rainfall (section 2.2.4). Attempts have been successful in correlating the formation of landslide dams with 1) paleosiesmicity of a region (Eden and Page, 1998; Hancox *et al.*, 2002; Reneau and Dethier, 1996; Wayne, 1999); 2) paleoclimatic conditions (Dethier and Reneau, 1996; Eden and Page, 1998; Trauth *et al.*, 2000; Trauth and Strecker, 1999); and 3) other triggering mechanisms of dam-forming landslides such as anthropogenic causes (Reneau and Dethier, 1996; Trauth *et al.*, 2000). For instance, Nicoletti and Scalzo (1998) were able to correlate the temporal occurrence of a 1693 earthquake with the formation of a landslide dam and the resulting recrudescence of malaria due to the formation of a lake.

2.2.2 TYPE OF DAM-FORMING LANDSLIDES

The following landslide terminology is largely based on Varnes (1978) and Cruden and Varnes (1996) in their classification of landslides, with emphasis on the type of movement and material involved (Table 2.1 and 2.2). Ultimately, however, the kinematics of a landslide i.e. how the movement is distributed through the displaced mass, is a principal criteria for classifying landslides (Cruden and Varnes, 1996). Using the method of Cruden and Varnes (1996) to classify landslides is limited, especially when faced with a slide that may initiate as a coherent mass that has failed on a distinct shear surface, yet has achieved most of its translational movement by flowage (as with a lot of dam-forming landslides). Thus the classification must relate to the process being studied, i.e. analysis of the conditions causing failure or the result of movement (Crozier, 1986).

Table 2.1. Classification of landslides based on the type of movement and material. When naming the slides, the first noun should describe the material involved; the second describes the type of movement (Varnes, 1978; Cruden and Varnes, 1996) Source: Cruden and Varnes (1996).

Type of Movement	Type of Material		
	Bedrock	Engineering Soils	
		Predominantly Coarse	Predominantly Fine
Fall	Rock Fall	Debris Fall	Earth Fall
Topple	Rock Topple	Debris Topple	Earth Topple
Slide	Rock Slide	Debris Slide	Earth Slide
Spread	Rock Spread	Debris Spread	Earth Spread
Flow	Rock Flow	Debris Flow	Earth Flow

Table 2.2. Glossary for forming names of landslides. The suggested sequence in naming a slide is the activity and movement. For example: state, distribution, style, rate, water content, material and type of material. Source: Turner and Schuster (1996).

Activity			Description of first movement			
State	Distribution	Style	Rate	Water content	Material	Type
Active	Advancing	Complex	Extremely rapid	Dry	Rock	Fall
Reactivated	Retrogressive	Composite	Very Rapid	Moist	Soil	Topple
Suspended	Widening	Multiple	Rapid	Wet	~ Earth	Slide
Inactive	Enlarging	Successive	Moderate	Very Wet	~ Debris	Spread
Dormant	Confined	Single	Slow			Flow
Abandoned	Diminishing		Very Slow			
Stabilized	Moving		Extremely Slow			
Relict						

Natural dams form from a variety of mass movements, as shown by Schuster (1993) in a study of 477 landslide dams of which the type of landslide based on Cruden and Varnes (1996) was determined in 390 cases (Fig 2.1). This study indicates that earth slumps and slides (c.50%) are the most common mass movements damming rivers, followed by debris, mud and earth flows (c.25%), rock and debris avalanche (c.19%), with sensitive clay failures and rock and earth falls (c.6% combined) being the least likely types to form landslide dams (Schuster 1993).

Earth slumps and slides show down slope movement dominated by sliding on relatively thin zones of intense shear strain or on surfaces of rupture (Turner and Schuster, 1996). Slides can be subdivided further based on the internal characteristics of the slide mass, and the failure surface into either a rotational or translational style (Varnes, 1978). Rotational slides tend to have well defined curved or concave upward failure surfaces, and move down slope as a relatively coherent mass along zones of high shear strain. Translational slides show generally planar or gently undulating failure surfaces and tend not to rotate or 'slump' about an axis, preferring instead to slide out over the original ground surface (Turner and Schuster, 1996).

Debris, mud and earth flows (Fig 2.2) are characterised by their spatially continuous movement in which surfaces of shear rapidly change throughout the movement and are closely spaced (Turner and Schuster, 1996). Flows can generally be described as highly viscous liquids given the variation in internal velocities; earth flows are particularly prone to formation during intense rainfalls when water infiltration is higher than normal, saturating the ground.

Rock and debris avalanches (Fig 2.2), belong to the flow group of landslides. They are however generally larger and show higher velocities than the aforementioned flows. In addition, there is often a continuum between a rock or earth slide and a rock and debris avalanche, with the former disintegrating into the later upon down slope movement.

Sensitive clay failures tend not to form dams due to their relative slow emplacement, and because they are not normally found in mountainous settings favourable for dam formation. In addition, rock falls are not known to form dams because these types of failures are usually small in volume (Schuster, 1993).

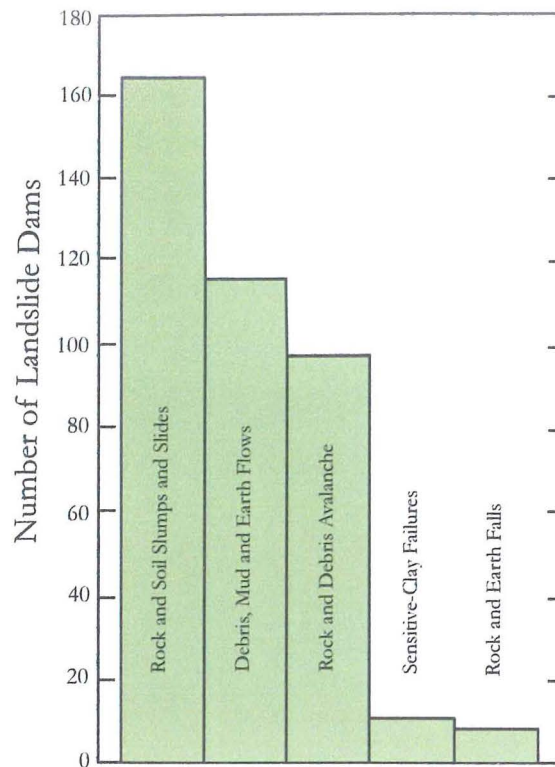


Fig 2.1. Number of landslide dams relative to the type of landslide. Graph based on 390 damming cases from Costa and Schuster (1991) and Schuster (1993). Landslide classification based on Varnes (1978). (Redrawn from Schuster (1993)).

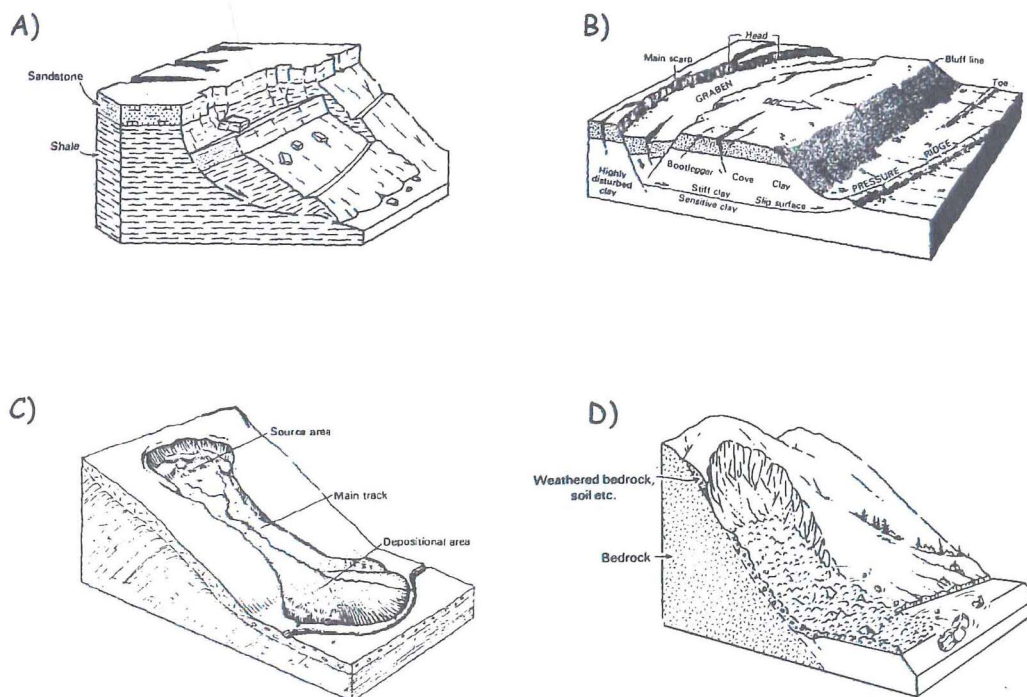


Fig 2.2. Examples of the main types of landslides that form dams: A) rotational rockslide in shale showing a concave failure plane, B) translational earth block slide illustrating the planar nature, C) debris, mud or earth flow and D) rock or debris avalanche. From Turner and Schuster (1996); Varnes (1978).

2.2.3 TRIGGERING MECHANISMS

Dam-forming landslides are generally initiated by natural mechanisms that act to reduce the internal strength of the rock mass or material. Analysis of 394 historical cases of landslide dam formation with known triggering mechanism by Schuster (1993) suggests that the most important natural processes influencing the initiation of dam-forming landslides are excessive rainfall, snowmelt and earthquakes which, when combined represent 90% of the landslide dams investigated (Fig 2.3). Volcanic eruptions and other mechanisms such as anthropogenic activity and removal of toe support represent the remaining percentage of triggering mechanisms. Earthquake triggering of landslides is described below in detail because the dataset collected as part of this thesis is based on landslide dams triggered by two large earthquakes. Detailed information relating to the additional triggering mechanisms is presented in Appendix D.

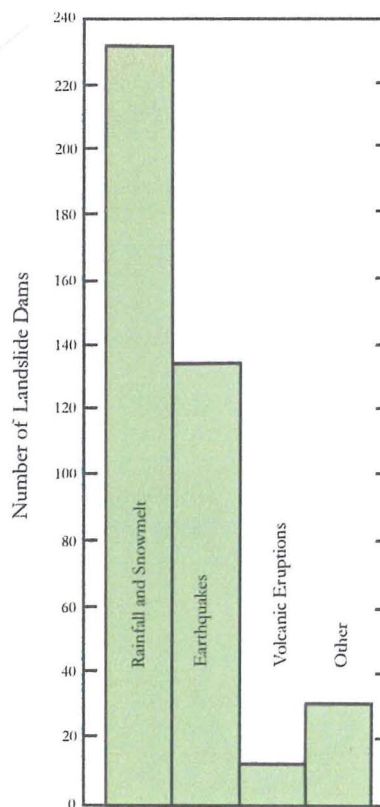


Fig 2.3. Causes of dam – forming landslides. Graph redrawn from Schuster (1993) based on 394 historical landslide dam occurrences from Costa and Schuster (1991).

Earthquakes have long been recognised as a major cause of landslides, documentation of which dates back to around 370 B.C. (Keefer, 1984; Seed, 1968). Earthquake motions can induce significant horizontal and vertical dynamic stresses in slopes of any rock type (Fig 1) (Kramer, 1996). These stresses act to produce dynamic normal and shear stresses along potential failure surfaces, previously in a state of static equilibrium, which may or may not exceed the available shear strength within the rock or soil mass. Peak ground acceleration and duration of strong shaking are also important factors leading to the failure of natural slopes (Schuster and Wieczorek 1989).

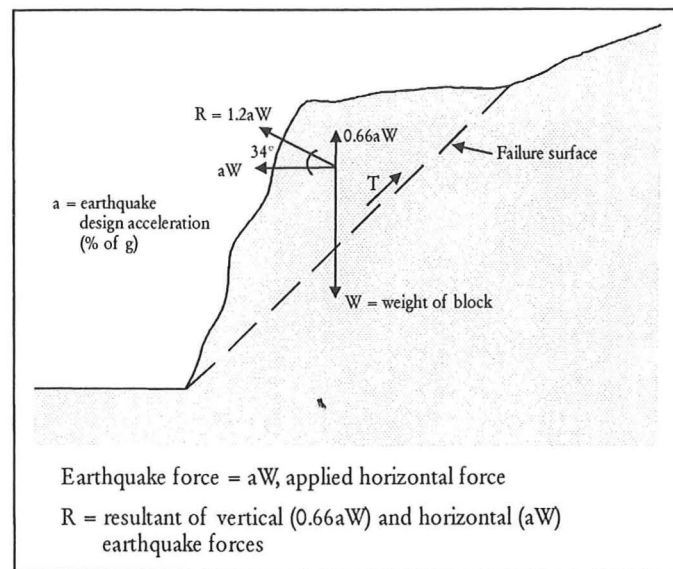


Fig 2.4. Summary of forces acting on a slope produced during an earthquake.

The size and scale of earthquake-triggered landslides varies and is generally controlled by the geological setting of a region. For example, in the Pamir Mountains, Tajikistan, the Murgab River was dammed when a 'strong earthquake' (of unknown magnitude) triggered rock slide, with a volume of $8 \times 10^9 \text{ m}^3$, fell into the valley forming Lake Sarez presently, $4 \times 10^{12} \text{ m}^3$ in volume (Fig 2.5) (ISDR, 2000). In June 1929 an M_s 7.8 earthquake in northwest Nelson, South Island, New Zealand, caused landsliding over an area of $\sim 7000 \text{ km}^2$ and formed a minimum of 39 landslide dams over $500\,000 \text{ m}^3$ in volume (Hancox *et al.*, 2002).

40 historical earthquakes from around the world documented by Keefer (1984), illustrate the most common landslides produced from earthquakes. The type of landslide and area

affected by landsliding does vary remarkably; however, it is generally a function of the magnitude of the earthquake, its focal depth, the topography, geology, antecedent ground moisture conditions, and the amplitude, frequency composition, and duration of ground shaking.

Keefer (1984) identified and characterised fourteen types of landslides based on material type (rock or soil), nature of movement, velocity, depth to failure surface, and water content. The most common of which were rock falls, disrupted soil slides, and rock slides. In addition, Keefer (1986) lists rock falls, rockslides, soil falls, and disrupted soil slides as being initiated by the weakest shaking; larger deep-seated landslides are generally initiated by stronger and higher duration shaking generally situated proximal to the seismic source.

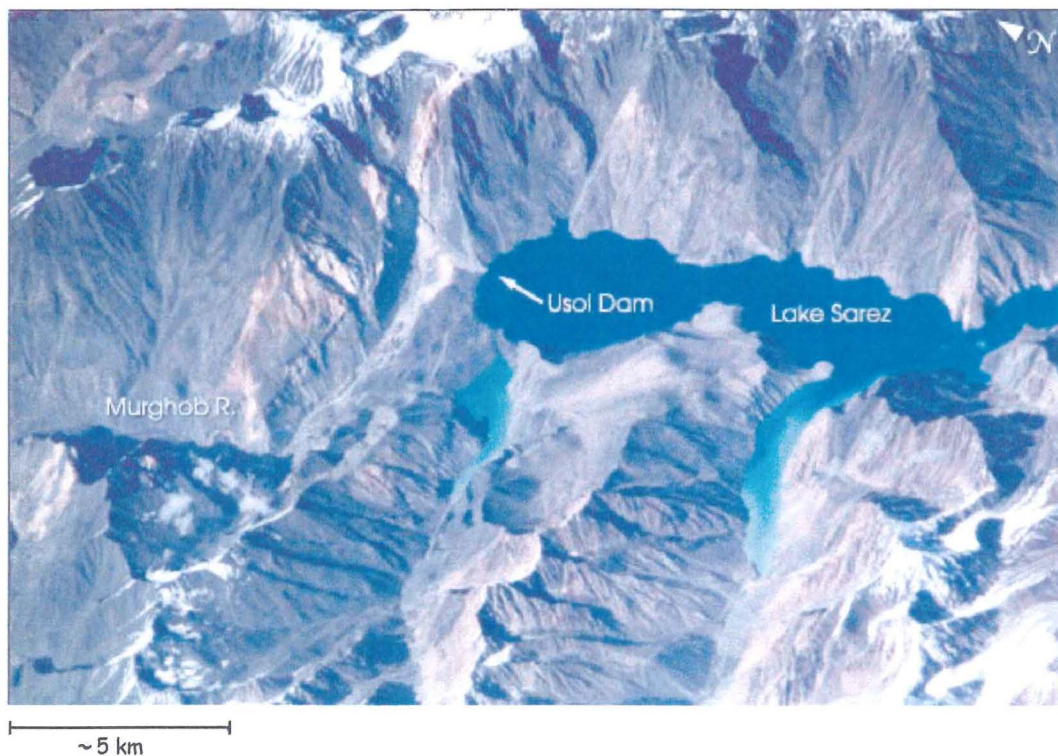


Fig 2.5. One of the largest landslide dammed lakes in the world today. Lake Sarez is 17 km^3 and is impounded by a 2 km^3 rock slide in the Murghob River, Tajikistan. (Photo source: <http://earthobservatory.nasa.gov/>)

Table 2.3. Relative abundance of earthquake-induced landslides from a study of 40 historical earthquakes ranging from $M_s = 5.2$ to $M_w = 9.5$ (Source: (Keefer, 1984; Kramer, 1996))

Abundance	Description
Very abundant ($>100,000$ in the 40 earthquakes)	Rock falls, disrupted soil slides, rock slides
Abundant ($10,000$ to $100,000$ in the 40 earthquakes)	Soil lateral spreads, soil slumps, soil block slides, soil avalanches
Moderately common (1000 to $10,000$ in the 40 earthquakes)	Soil falls, rapid soil flows, rock slumps
Uncommon	Subaqueous landslides, slow earth flows, rock block slides, rock avalanches

2.2.4 LANDSLIDE VELOCITY

The rate of movement, like landslide type, is an important parameter influencing the probability of channel blockage (Casagli and Ermini, 1999). Typically slower moving mass movements (less than c. 1.5m/yr) tend not to cause any type of damming; landslides with higher velocities (c. 1.8m/hr to c. 5m/s) generally facilitate some form of damming (Casagli and Ermini, 1999; Swanson *et al.*, 1986). The velocity of a landslide is closely linked to the amount of debris deposited within the channel and the time available for natural or anthropogenic processes to erode or control the landslide debris. This allows the safe passage of water around or through the dam material respectively (see Appendix E for landslide velocity definitions).

2.2.5 GEOMORPHIC CLASSIFICATION OF LANDSLIDE DAMS

The distribution of debris in a valley floor following a landslide is a function of the width of the channel and the velocity, type and volume of the landslide (Swanson *et al.*, 1986). These interactions are some of the most important factors in determining whether a landslide will totally, partially or not block a drainage system. The occupation of debris throughout a length of channel has the potential not only to block the main channel but its tributaries, which may form multiple lakes (Swanson *et al.*, 1986). Swanson *et al.* (1988) proposed a geomorphologic classification scheme for landslide dams based on the relationships with the valley floor. This geomorphologic classification was modified by Costa and Schuster (1988) who were able to identify six groups of landslide dams (Fig

2.6). Table 2.4 gives a description of the classification scheme and an example for each class.

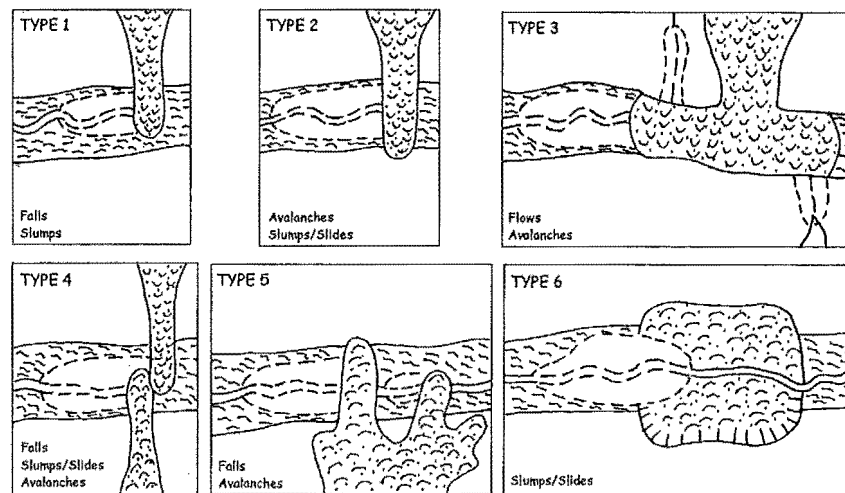


Fig 2.6. Schematic diagrams showing classification of landslide dams (from Costa and Schuster, 1988). The lower left corner of each diagram lists the likely slope movements associated with the particular landslide dam. The main valley flow is from left to right.

Table 2.4. Classification of landslide dams with known examples (Descriptions following Costa and Schuster 1988; Swanson et al. 1986).

Type	Description	Example
1	Volume of landslide debris reaching the channel is small with respect to valley width; debris does not reach the opposite side of the valley.	Maruia Falls landslide Hancox <i>et al.</i> (2002)
2	Debris spans the entire width of the valley occasionally extending up the opposite side; characterised by a long narrow shape.	Mt Adams rock avalanche Hancox <i>et al.</i> (1999)
3	Greater volume of debris filling valley from side to side; distribution of debris upstream and/or downstream from point of entry.	Mt St Helens eruption Meyer <i>et al.</i> (1986)
4	Contemporaneous movement of two landslides from opposite sides of the valley; mirrored failures within a valley or slides from opposite sides that are juxtaposed, can result in dam formation.	Yinping rock avalanche Li <i>et al.</i> (1996)
5	Different lobes of the same landslide cause multiple dams to form within the same reach of river.	Slide Lake rockfall avalanche Butler <i>et al.</i> (1986)
6	Landslide failure surface extends beneath the channel to emerge on the opposite side of the valley from the landslide source; bed uplift generally dams the river.	Kamenose landslide (Yamato River) Swanson <i>et al.</i> (1986)

2.2.6 EFFECTS OF LANDSLIDE DAMMING

The formation of a landslide dam affects the fluvial, sedimentological and anthropogenic regimes of the surrounding area. Table 2-5 outlines some of the effects of landslide dam formation with examples. By far the most important factor in landslide dam formation is the potential for a catastrophic release of reservoir water creating greater than normal flows downstream. Upstream flooding (also referred to as backwater flooding), is the immediate effect of damming, however sufficient time is normally allowed for the safe evacuation of people from potential flood areas. These two factors, along with the deterioration of aquatic habitats and water quality, can be described as the short-term effects of damming; long-term effects relate to the sediment and fluvial regime changes post dam formation.

Table 2.5. Some effects of landslide damming on upstream and downstream environments

Effect	Description	Example	References
Downstream Flooding	The release of water impounded upstream of a landslide dam normally catastrophically. This releases high volumes of water into the system increasing the flow of water to higher than normal levels	The 1985 Bairaman landslide dam in Papua New Guinea failed releasing $50 \times 10^6 \text{ m}^3$ of water wiping out a village 39km downstream with a flood wave 8m high	King <i>et al.</i> (1989)
Upstream Flooding	The progressive infilling of a reservoir upstream of a landslide dam leads to inundation of land and settlements. The reservoir or lake area is a function of the dam size and hydrological input.	Thistle, Utah landslide 1983 dammed the Spanish Fork River, which submerged the town of Thistle and destroyed houses, businesses and infrastructure.	Kaiser and Fleming -1986
Deterioration of Water Quality	Sediment deposited in the river or stream can be transported downstream progressively or spontaneously upon dam failure thus reducing the water quality some distance from the source.	The Loma Prieta earthquake of 1989 formed 5 landslide dams. upon failing they carried fine sediment from aggradation behind the dam and dam material some distance downstream reducing water quality	Schuster <i>et al.</i> (1989)
Deterioration of Fish Habitats	Sediment input into the streams and rivers deteriorates the aquatic habitat. Dams also impose a physical barrier on the upstream migration of spawning fish.	Sedimentation immediately downstream of the dams after failure affects the spawning of Steelhead Trout which require stable gravelly stream bottoms as spawning beds	Schuster <i>et al.</i> (1989)
Upstream/Downstream Aggradation	Deposition of lacustrine sediments in the reservoir; deposition of sediment from the dam material and/or lacustrine sediments immediately downstream or at a distance from the dam depending on the scale.	50m of sediment was deposited behind the 1941 Ling landslide dam, Taiwan; the failure of a Peruvian landslide dam deposited huge amounts of material immediately downstream of the dam altering the fluvial regime of the river	Chang (1984) Kojan and Hutchinson (1978)

2.3 FAILURE OF LANDSLIDE DAMS

The term 'failure' refers to the reduction in volume of reservoir water and the subsequent removal of dam debris. This failure process is highly varied and is generally a function of the type of breach and the materials forming the dam. Types of breaching include 1) overtopping of the dam by the rising water; 2) piping through the dam causing internal erosion; 3) heave, which is normally followed by slope failure of a portion of the dam; and 4) engineered structures such as tunnels or spillways, which act to safely reduce the risk for the above to occur. If the process of failure is slow, resulting downstream damage will be minimal. However if the process is rapid or catastrophic releasing large amounts of water bulked with debris from the dam and stream channel, the effects downstream can be severe (Table 2.5) (Schuster, 1993).

2.3.1 MODES OF DAM FAILURE

2.3.1.1 Overtopping

The leading cause of dam failure is generally thought to be overtopping. Overtopping failure is caused by water spilling over the dam crest subsequently eroding a channel along the downstream face of the dam (Manville, 2001). Growth of the breach generally involves erosion of the channel base via entrainment of sediment along with mass failure of the channel sidewalls and downstream dam face. Costa and Schuster (1998) in a study of 73 landslide dams from around the world, found 70% failed due to overtopping (Fig 2.7). In a later study of 202 landslide dams by Schuster (1993), 97% failed by overtopping.

Overtopping failure of a landslide dam is highly dependent on the ability of the dam material to resist erosion from the impounded water spilling over the dam crest. The ability of the impounded water to overtop the blockage is dependent on the rate of water flowing into the reservoir area (which is a function of catchment size above the point of blockage) and the dam volume, which controls the amount of water that can be stored. However, if the amount of water entering the impoundment is less or equal to the amount of water exiting the impoundment via evaporation, or seepage through the dam material, the lake level can stabilise below the minimum crest level without overtopping. additional mechanisms for stabilising the lake level below the crest of a dam include the withdrawal of water for irrigation and tunnelling through the abutment rock forming a conduit for drainage (Hansen and Morgan, 1986; Sager and Chambers, 1986).

Nevertheless, not all landslide dams fail once overtopped. Depending on the properties of the dam material, water can flow over the dam crest and down the face without eroding it (Riley and Read, 1991). The dam composition is therefore important in determining whether it will resist erosion due to overtopping (e.g. Yinping landslide dam (Li *et al.*, 1986)). However, the erosive power of water is generally related to the type of flow and its velocity. A naturally formed spillway may resist erosion during normal overflow conditions; higher discharges during periods of intense rainfall, may overcome the channel materials frictional resistance initiating the erosion process leading to failure (Hancox *et al.*, 1999), Poerua River dam failure).

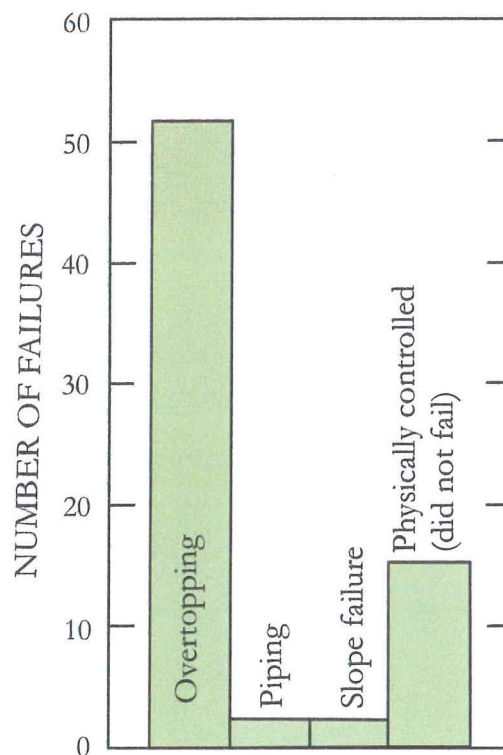


Fig 2.7. Modes of failure of landslide dams, based on 103 failures (Schuster and Costa, 1986)

2.3.1.2 Piping

Piping is described as the removal of soil along discontinuities in an earth structure or its foundation; removal of particles begins at the downstream surface, enlarging and working its way backwards to form irregular channels or pipes (Meyer *et al.*, 1994). In the case of landslide dams, the downstream surface is located at one or more points on the dam face predominantly characterised by the presence of springs. Support for the dam crest is removed as the pipes grow head ward and enlarge, resulting in the collapse and development of an open breach (Manville, 2001).

Piping failure occurs when water percolates through the dam causing internal erosion and subsequently producing pipes within the dam (Manville, 2001). Landslide dams are particularly susceptible to piping due to their heterogeneous nature unlike man made structures, such as embankment dams, which have undergone systematic compaction to reduce the permeability which minimises the potential for piping (Meyer *et al.*, 1994).

The ability to produce piping via internal erosion in landslide dams is a function of the material comprising the dam. Because the majority of dams are caused by avalanches, slides and flows and not by slope failures in sensitive clays, landslide dams are not typically subjected to failure by internal piping erosion (Costa and Schuster, 1988; Ermini and Casagli, 2003). In a study of 73 landslide dams by Costa and Schuster (1988) only 2 failed by piping (Fig 2.7).

Landslide dams can be assessed for their susceptibility to piping failure following Bell (1983) showing the critical hydraulic gradient of the dam material as:

$$i_c = \frac{G_s - 1}{1 + e}$$

where G_s is the specific gravity of the solid particles, and e is the void ratio.

2.3.1.3 Slope failure/Heave

Slope failure is commonly associated with both piping and overtopping when vertical erosion oversteepens the breach sidewalls leading to gravitational collapse (Manville, 2001). Slope failure within slices of the dam material is less common; however, given that very few landslide dam breaches have been witnessed this mode of failure should not be overlooked. This phenomenon occurs when the hydraulic pressure exerted by the impounded water overcomes the dam materials' frictional and cohesion resistance to shear, leading to dam collapse. This process is synonymous with heave which is the upward movement of a mass of rock or debris when subjected to a high seepage gradient in the exit flow region (Meyer *et al.*, 1994).

The stability of a dam against gravitational failure is assessed using the infinite slope analysis where the factor of safety (FOS) is defined as:

$$F = \frac{c' + (\sigma - u) \tan \phi'}{\tau}$$

where c' is the effective cohesion of the material, σ is the total normal stress, u is the pore water pressure, ϕ' is the effective friction angle, and τ is the shear stress. Additional forces such as surcharges from the lake volume on the upstream portion of the dam can decrease the FOS .

2.3.1.4 Controlled failure

When a landslide dam blocks a major tributary, leading to the formation of a large lake upstream of populated areas or major infrastructure, there may be a need to minimise the impact of an inevitable outburst flood. The most effective way to achieve this is to reduce the capacity of a dam to store water by lowering the dam crest through construction of a spillway over the dam (e.g. Evans, 1986; Casagli and Ermini, 2000). Other methods include blasting of the dam using explosives; however, this technique is not as controlled as spillway construction. Perhaps the most effective way to reduce the probability of catastrophic dam failure is to stop the impoundment from overtopping the dam. This is best achieved through tunnelling into abutment rocks below the minimum crest height allowing drainage of lake water stabilising the impoundment below the dam crest (e.g. Hansen and Morgan, 1986). The high cost associated with tunnelling restricts the use of this approach.

2.3.2 LONGEVITY OF LANDSLIDE DAMS

The longevity of landslide dams ranges from several minutes to several thousand years (Costa and Schuster, 1988; Schuster, 1993; Schuster and Costa, 1986; Swanson *et al.*, 1986). This depends on factors such as 1) the rate of sediment and water flow into the upstream reservoir area; 2) physical characteristics of the dam such as shape, size, and the geotechnical properties; and 3) the amount of water loss via seepage through the dam, evaporation and groundwater recharge into abutment rocks (Ermini and Casagli, 2003). Schuster (1993) argued that 35% of 187 investigated landslide dams failed within one day of formation and 89% failed within one year (Fig 2.8). Ermini and Casagli (2003) found similar results upon investigating 205 failed landslide dams indicating c.20% failed within a day with c.80% failing within one year after formation.

Essentially a dam's survival rate is dependent on its resistance to all fluvial erosion, including overtopping, internal erosion from piping, and slope failure or heave. This is highly dependent on the geotechnical properties of the rock or soil material and mass characteristics such as weathering, strength, average unit block size, and grading of the rock material comprising the dam. Dams comprising highly erodible rocks such as poorly indurated mudstones and sandstones have a higher probability of failure especially upon overtopping of the impoundment. A natural spillway may develop but generally holds little resistance to the turbulent flowing water and soon erodes the dam material either catastrophically or gradually. Contrastingly, a dam comprised of strong, unweathered rock with a large unit block size may resist erosion from overtopping and seepage (Schuster, 1993). The USOI dam in Tajikistan is an excellent example of a dam comprised of quartzite and schist, a relatively strong material when not weathered. Seepage through the dam ranging from 28 and 84 m³/s has stabilised the lake level to about 70m below the dam crest demonstrating the ability for certain material to pass water without internal erosion (ISDR, 2000). Lake Matiri landslide dam (No. 5, this thesis) is an example of a dam comprised of large boulders that resist erosion from overtopping.

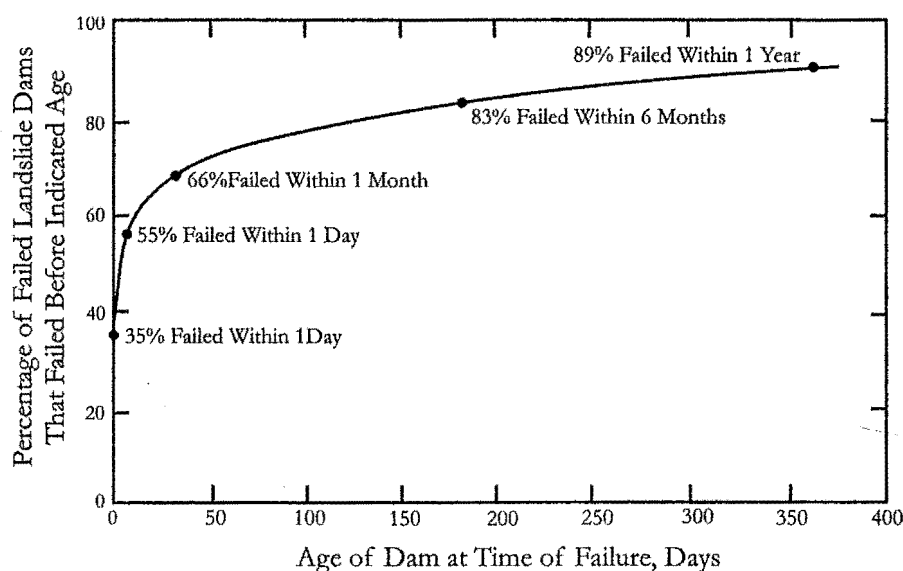


Fig 2.8. Duration of landslide dams based on 187 failed landslide dams where the time to failure is known. The percentages pertain only to 187 of 477 total landslide dams; the remaining 290 are either stable or the time to failure is not known (Costa and Schuster, 1991; Schuster, 1993; Schuster and Costa, 1986).

2.3.3 STABILITY OF LANDSLIDE DAMS

The stability of a landslide dam is not generally controlled by a single parameter such as a landslide dam's volume or catchment area above the point of blockage, but a combination of multiple parameters that control a landslide dam's resistance to erosion (Swanson *et al.*, 1986; Schuster, 1993). Characteristics of the dam material, such as grain size distribution, strength and texture, are important factors in determining a dam's resistance to erosion either from seepage through the dam or overtopping of the reservoir water and ultimately reflect the dam stability. The grain size distribution has a direct influence on the hydrogeological behaviour of the dam material. For example, the erodibility of the grains by flowing water when overtopped, the stability of the dam slopes as a function of the shear strength, and the resistance to internal seepage and piping as a function of the permeability of the material (Casagli and Ermini, 1999). In addition, landslide dams consisting of coarse grain sizes and high strength are more stable than dams composed of soft, fine grain sizes because the latter are more susceptible to erosion (Schuster, 1993). 67 case histories of landslide dam formation in Italy documented by Casagli and Ermini, (1999) were analysed indicating that matrix supported landslide dams tend to either not completely form or show high instability, whereas grain supported landslide dams tend to produce stable blockages.

The type of dam-forming landslide is shown not to significantly influence a dam's stability (Fig 2.9) (Ermini and Casagli, 2003). Contrastingly, landslide dams formed because of earthquakes and snowmelt are normally more stable than dams generated by intense rainfall events (Fig 2.10). The increased stability of earthquake triggered landslide dams is thought to be a function of the increased volume of debris reaching the valley floor as opposed to rainfall triggered landslide dams. Ermini and Casagli (2003), argue that c. 57% of the total volume of an earthquake-triggered landslide reaches the valley bottom as opposed to c. 40% of the total landslide volume in rainfall-triggered landslides.

In addition to the geotechnical properties of dam material, there are also certain geomorphic parameters that can influence the stability of a dam such as 1) the dam volume and catchment area above the point of blockage; and 2) the dam height and lake volume, which are considered to be the most important geomorphic parameters in assessing the stability of a landslide dam (Casagli and Ermini, 1999; Ermini and Casagli, 2003; Swanson *et al.*, 1986)

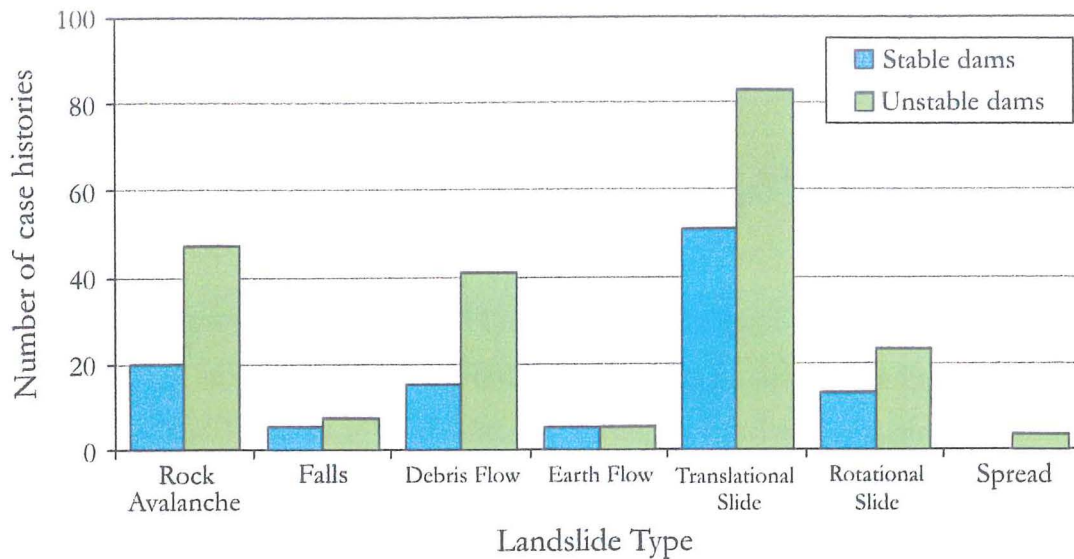


Fig 2.9. Types of landslides that have produced landslide dams, based on 353 case histories (reproduced from Ermini and Casagli, 2003).

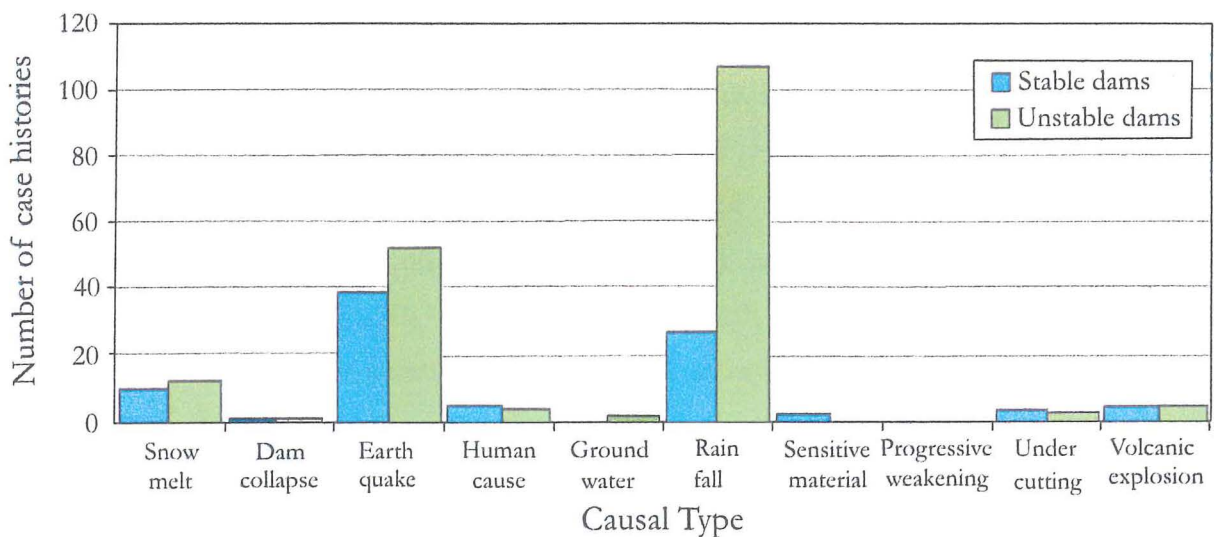


Fig 2.10. Subdivision of the types of triggering mechanisms that produced dam-forming landslides for 353 case histories collated by Ermini and Casagli, 2003.

Various combinations of these parameters thought to control the ability of a landslide dams to resist erosion and catastrophic failure are used to predict the post-formation development of a landslide dam (termed ‘evolution’ by Casagli and Ermini, 1999 and Ermini and Casagli, 2003) using three empirically derived geomorphic indices namely 1) Impoundment Index (I_i , developed in 1999); 2) Blockage Index (BI , developed in 1999); and 3) Dimensionless Blockage Index (DBI , developed in 2003). Discussions regarding the

applicability and accuracy of these indices to predict the post-formation development of a landslide dam are discussed in detail in Chapters Three to Six.

2.4 FLOODS ASSOCIATED WITH LANDSLIDE DAM FAILURE

The potential for downstream flooding following the breaching of landslide dams has long been recognised. The earliest known records of dam failure causing flooding date back to A.D. 563 when a landslide dam in St Barthelemy Basin, Switzerland, breached killing many people (Eisbacher and Clague, 1984). Floods from landslide dam failures have produced some of the largest floods in human history. For example, the Tanggudong landslide, China occurred in June of 1967 damming a major tributary of the Yangtze River. The slide volume was $68 \times 10^6 \text{ m}^3$ and dammed the river to a height of 175 m above the original valley floor. The resulting lake attained a maximum length of 53 km and a maximum volume of $680 \times 10^6 \text{ m}^3$.

Nine days later the lake overtopped the landslide dam breaching to a depth of 88m over a 1-hour period. The resulting flood travelled 1,000 km downstream with the frontal flood wave recorded as being c.50m 6km downstream of the dam and c.17m 551km downstream. The maximum discharge was recorded as being 53,000 m^3/sec 6km downstream of the blockage. No lives were lost as a result of evacuation of people in the path of the flood, however substantial housing and infrastructure was destroyed by the flood (Li *et al.*, 1986).

Perhaps the worst case of lives lost as a result of a landslide dam breach was again in China when in 1786 an earthquake triggered landslide blocked the Dadu river for 10 days after which overtopping released a flood wave that killed 100,000 people and travelled 1,400 km downstream (Li, 1989).

The failure process varies within each dam, in some the failure will be slow, in others the failure will be quite rapid leading to minimal or catastrophic downstream flooding respectively. Schuster (2000) indicates the variability in the severity of downstream flooding depends on 1) volume and rate of outburst flows; 2) type of material comprising the dam; 3) amount and availability of lacustrine sediment; and 4) amount of loose, easily erodible material lining the downstream channel available for the bulking process (i.e. entrainment of loose materials). It is important to note, however that floods downstream of

landslide dams not only result in the failure of a blockage by overtopping, piping or heave, but also can arise from additional landslides into the impounded lake displacing large quantities of water over the dam. In the case of the Usoi landslide dam, Tajikistan, a major landslide on the right bank of the lake is considered unstable and has the potential to displace a large volume of water over the dam causing downstream flooding and threatening the credibility of the dam (ISDR, 2000).

2.4.1 DAM FAILURE IMPACTS AND MITIGATION METHODS

The impact of a dam failure can be characterised into long and short term. The long-term impacts are generally concerned with geomorphic impacts on natural processes such as sediment fluxes in the channel and fluvial systems, whereas short term affects generally concern the flood wave of water and entrained sediment associated with dam failure. Because of the impacts dam failure floods have on the downstream environment, it is not surprising that research has focussed on trying to understand the mechanisms and type of floods produced from natural (and man made) dam failure while little attention has been given to the long term impacts of natural dam failures. There is however, a plethora of information regarding the formation and failure of landslide dams detailing the complex geomorphological, geofluvial and poleoseismic relationships that set precedent for landslide dam investigations (Casagli and Ermini, 1999; Dethier and Reneau, 1996; Nicoletti and Scalzo, 1998; Nicoletti *et al.*, 1998; Nicoletti and Terranova, 1998; Philip and Ritz, 1999; Wayne, 1999). However, the lack of preservation potential of dam material, outwash deposits from a dam failure and lacustrine deposits from sedimentation upstream of a dam can conceal dam-forming locations and hence the frequency of landslide dam formation (Hewitt, 1998).

Minimising the impacts of a flood from dam failure particularly minimising the number of deaths, can be achieved via an early warning systems downstream of the dam or within the lake to detect sudden changes in water level. Such a method is to be applied to the USOI landslide dam, Tajikistan, in the unlikely event of dam failure or an overtopping wave (ISDR, 2000). The best method to minimising the severity of downstream flooding following dam failure is to reduce the potential for flooding by artificially lowering the dam crest therefore reducing the capacity and potential energy of the impounded water. This is possibly the most cost-effective and quickest method of mitigating a flood hazard from a newly formed dam. This method does not stop the dam failure but minimises the

severity of the resulting flood. A commonly used method is to construct protected spillways either across adjacent bedrock abutments or over the dam material (Schuster, 1993) to allow safe overtopping of water from the impoundment once the crest is reached. In certain instances however, there may be more time available to implement other methods that stabilise the impoundment at a safe level well below the minimum crest level. Such methods include the use of siphon pipes, pumping systems and tunnel outlets and diversions (Hansen and Morgan, 1986; Sager and Chambers, 1986; Schuster, 1993)

Mitigation of an outburst debris flow after it forms embodies traditional methods used to reduce the downstream effects of debris flows including 1) debris retention structures, most commonly concrete or rock fill check dams; and 2) debris basins, diversion structures, commonly walls or channels that attempt to deflect the flow away from infrastructure (Schuster, 2000).

2.4.2 DAM-BREAK STUDIES

Rapid analysis of the potential magnitude of a dam-break flood is essential in mitigating loss of human life and infrastructure due to the rapid failure of many natural dams (Manville, 2001). Dam break studies have focussed on trying to predict the magnitude of dam break floods and the breach development time from initial overtopping to full breaching to reach its maximum discharge (i.e. outflow hydrographs illustrated in Fig 2.11). Methods in determining the aforementioned predictions vary from simple estimations based on empirical data from historical dam failures (Costa, 1988), to complex numerical and physically based mathematical techniques incorporating many variables (Fread, 1988; Manville, 2001). Four important factors determine the magnitude of the dam-break flood and its outflow hydrograph 1) volume and height of the lake; 2) depth of the lake at the upstream dam face; 3) average width of the breach; and 4) the breach development time (Manville, 2001).

The simplest approach in estimating the peak discharge from dam-breaks is to use empirically derived correlations relating observed values of peak discharge to some measure of the impoundment or dam such as lake volume, depth of the lake and/or the total drop in lake level during a flood (e.g. Costa, 1988; Costa and Schuster, 1988; Evans, 1986; Manville, 2001; Walder and O'Connor, 1997).

Many of these empirically derived regression relationships have been produced to predict dam-break flooding for both constructed and natural earthen dams, many of which show the following form:

$$Q_{max} = a X^b$$

Where X is the impoundment or dam characteristic such as lake depth (d) or lake volume (v), and a and b are empirically derived coefficients (Manville, 2001). Inaccuracies when using regressions relationships in the form given above lead to the underestimation of the peak discharge immediately downstream of a failed dam. However, regression relations remain a useful tool for rapid assessment of the flood potential following a breach. (Walder and O'Connor, 1997).

A large number of complex mathematically based dam breach models have been developed to predict dam breach characteristics (i.e. size and time of formation) and the discharge hydrograph (a plot of discharge vs. time) deriving from the breaching of both natural and man made earth dams summarised in Table 2.6 (Fread, 1988). Mathematical techniques are more precise at predicting the flooding potential following dam failure; however are more labour intensive and sensitive to a number of input parameters. Appendix E discusses in more detail available techniques to predict the flood magnitude from dam failures; Table 2.6 gives a summary of the available techniques.

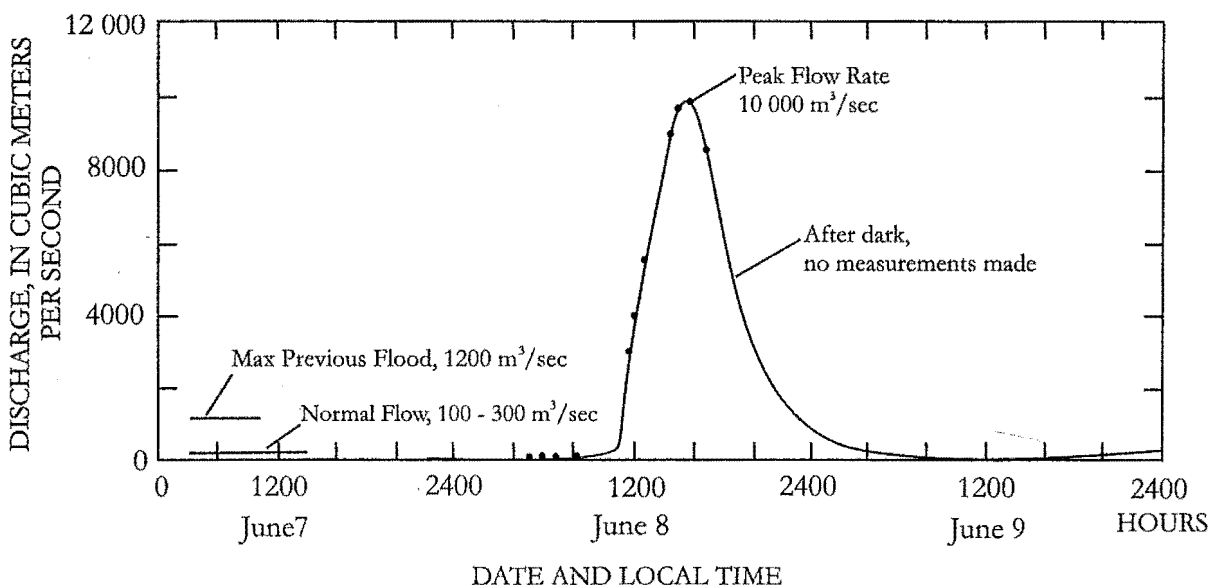


Fig 2.11. Example of a typical hydrograph of discharge following the failure of landslide dams. This particular hydrograph is from the failure in 1974 of the Mayunmarca landslide dam, Peru (Source: Costa, 1988).

Table 2.6. Summary table listing the advantages, disadvantages of available methods to predict the dam break flood characteristics and data required for the individual techniques (reproduced from Manville, 2001)

Method	Advantages	Disadvantages	Data required
1 Empirical regression equations(lake and dam characteristics)	Very rapid and simple	Questionable accuracy Large coice of regression relationships	Lake volume, dam height
2 Empirical breach characteristics	Very rapid and simple Can supply first - order input parameters for more sophistocatedmodels	Uncertain accuracy Based on empirical data	Lake volume, depth and surface area
3 Parametric	Rapid (if model is available)	Several choices of weir - flow equation DAMBRk requires some familiarity to operate	Breach dimintions, geometry and development time. Lake volume and geometry
4 Dimensionless	Rapid	Sensitive to lake depth Sensitive to breach width depth ratio. Little - tested in New Zealand. Requires use of graphs and calculations	Breach development time Lake volume and geometry
5 Physically based	Potentially the most accurate	Requires experience to operate, can be temperamental. Data input slower than other methods. Little-tested in New Zealand	Dam geometry and dimensions. Geotechnical properties of dam material. Lake volume and geometry

2.4.3 CHANGES TO CHANNEL AND VALLEY MORPHOLOGY

A channel or valley's reaction to the failure of a landslide dam will vary relative to the amount of sediment transported, velocity of floodwaters, duration of flooding and the slope of the channel immediately downstream of the dam (Costa, 1988; Korup, 2002; Schuster, 2000). Rapid drawdown of a reservoir can lead to the collapse of slopes along the shore by removal of the water's lateral support immediately following dam failure and lake drainage (e.g. Hancox et al., 1999). This also increases the amount of sediment potentially available for transport during reservoir release or normal/above normal flows. Downstream of the dam the degradation of the channel caused by higher than normal flows during breaching, may remove the support at the toe of a slope leading to collapse of the valley slide.

When a landslide dam fails, large amounts of sediment from the dam mass and any backwater or lacustrine sediment, are available for sediment transport resulting in possible widespread aggradation downstream of the dam. In additional loose sediment lining the

channel immediately downstream of the dam may also be incorporated into the flood waters and deposited further down valley. The increase in sedimentation may cause channel avulsion by reducing the stream gradient (Schuster, 1993). Bathurst and Ashiq (1998) showed that the localised bed aggradation due to excessive increases in sediment yield has been observed to seriously affect the medium and long term channel morphology and stability.

2.5 LANDSLIDE DAMS IN NEW ZEALAND

New Zealand occupies a complex geological setting caused by the convergence of the Pacific and Australian plates allowing the growth of mountains through rapid uplift. As a result, a high percentage of New Zealand is represented by high mountainous terrain and is subject to high seismicity. In addition, a relatively high precipitation throughout the country, owing to a mainly oceanic climate, augments the formation of stream blockages by landslides.

Landslide dams are located mainly in areas with geology and topography favourable to landslide formation and stream blockage such as eastern central North Island, Northwest Nelson, North Westland, western Canterbury and Fiordland in the South Island (Fig 2.12) (Perrin and Hancox, 1992).

2.5.1 NORTH ISLAND LANDSLIDE DAMS

The formation of landslide dams in the North Island of New Zealand, tend to occur in softer marine sedimentary rocks typically found in central eastern areas (Perrin and Hancox, 1992). Lake Waikaremoana, located on the east coast of the North Island, formed 2,200 years ago and is considered the largest existing landslide dammed lake in New Zealand with a dam volume of $5.2 \times 10^9 \text{ m}^3$ (Fig. 2.12) (Read *et al.*, 1992). Lake Waikaremoana is 582m above mean sea level creating a storage and head for three consecutive hydroelectric power stations with a total output of 124MW. This along with the 5,000 people occupying a settlement 40km downstream, required an assessment of the landslide dam's stability which has been completed in a comprehensive study by Riley and Read (1992). They concluded that the combination of 1) seepage through the dam; 2) a high dam thickness; 3) the presence of a large ($> 8 \text{ km}^3$) intact rock block; and 4) the prevention of downstream movement of the intact block due to the pre-landslide valley shape, indicates the relative stability of the dam.

Although central North Island is seismically active, triggering of dam forming landslides by intense rainfall events is more common. For instance, Cyclone Bola in 1988 resulted in the formation of several small transient landslide dams in the Gisbourne area (Hancox and Perrin, 1992).

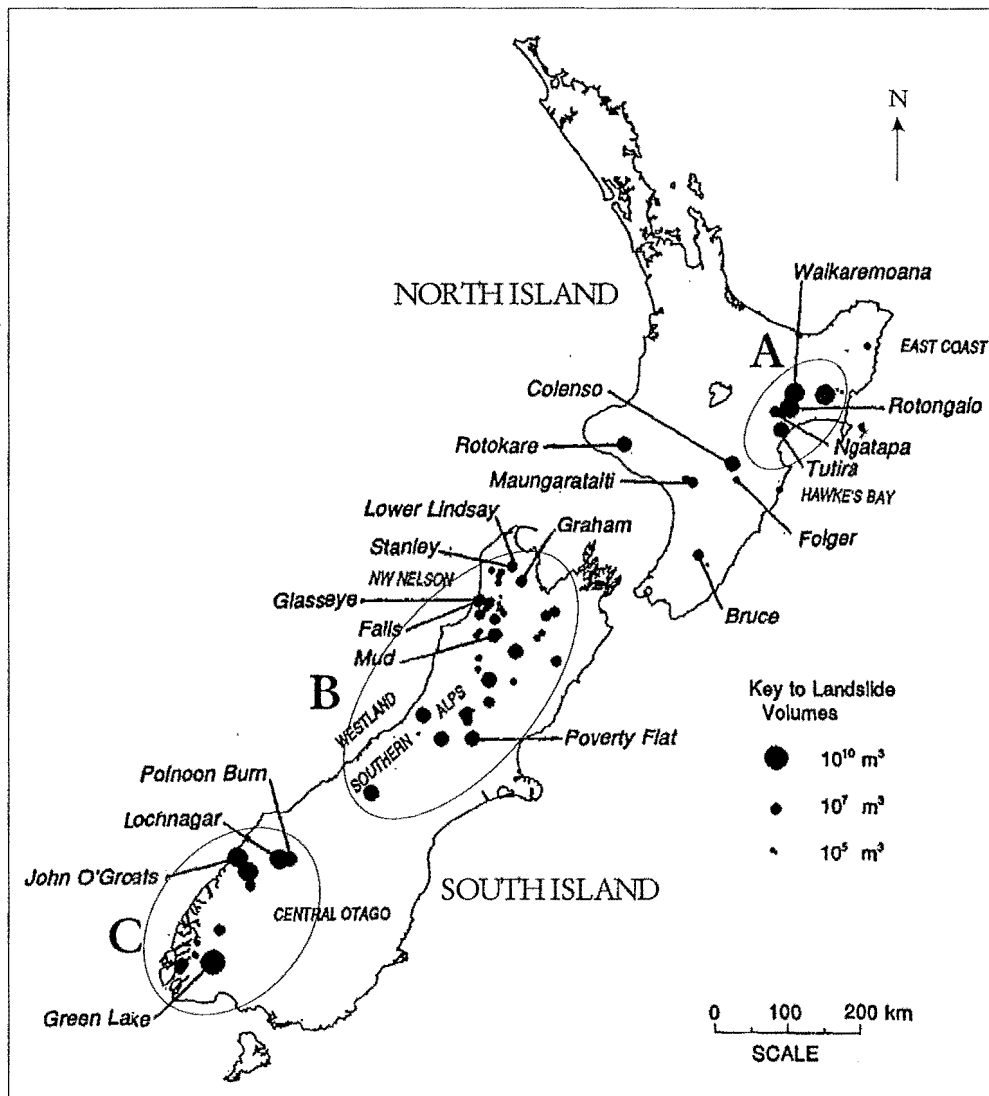


Fig 2.12. Location of landslide-dammed lakes in New Zealand showing approximate landslide volumes. The areas circled illustrate regions in which most of the landslide dams in New Zealand form given by A. central East Coast of the North Island; B. northwest Nelson and Westland; and C. Fiordland. (Modified from Perrin and Hancox, 1992)

2.5.2 SOUTH ISLAND LANDSLIDE DAMS

Most of New Zealand's landslide dammed lakes are in the more mountainous and glaciated regions of the South Island (Perrin and Hancox, 1992) (Fig 2.12). Landslide dams tend to cluster in two distinct regions of the South Island namely Fiordland and Northwest Nelson.

Geologically, Fiordland does not generally permit the formation of a landslide dam due to the slow moving nature of landslides in the schist terrane. However, some very large landslide dams such as Green Lake and Lochnagar (Fig 2.12) have formed as a result of massive failure (e.g. Perrin and Hancox, 1992; Hancox and Perrin, 1994). Green lake is located in the glaciated Hunter Mountains in Fiordland, and is considered the largest ancient landslide dam in New Zealand with an estimated volume of about 27 km^3 forming a dam c.800m high (Hancox and Perrin, 1994).

Northwest Nelson and the northern Westland (Fig. 2.12) show the highest concentration of landslide dams in the South Island which is attributed to the frequency of large earthquakes of $M_s \geq 7$ during the last 150 years (e.g. 1929 Murchison $M7.8$ earthquake and the 1968 Inangahua $M_s 7.2$ earthquake) (Perrin and Hancox, 1992). The highly mountainous terrane and geological composition of the area also favour the formation of landslide dams, with a number of active faults dissecting the region, which triggers large landslides in coherent bedrock allowing landslide dams to form.

2.5.3 CHRONOLOGY OF LANDSLIDE DAM RESEARCH IN NEW ZEALAND

Ongley (1932) and Henderson (1937) were among the first to recognise and described landslide dams within the New Zealand environment. Henderson (1937) reported on the formation and failure of many landslide dams formed from the 1929 Murchison earthquake, Northwest Nelson, while Ongley was first to recognise the origin of Lake Waikaremoana as being landslide dammed.

Individual landslide dam studies have occurred throughout the later half of the 20th century (e.g. Johnston, 1974; Speight, 1933), however it was not until 1981 when Adams (1981a) documented the occurrence of 38 temporary and permanent landslide dams throughout New Zealand, inferred to have formed from historical and prehistorical earthquakes. Adams (1981a), illustrated the longitudinal profiles of several landslide dams as well as

highlighting the potential for using groups of landslide-dammed lakes of a single age, to identify the palaeoseismic earthquake magnitude.

Following Adams (1981a), Perrin and Hancox (1992), used topographic and aerial methods to identify existing and former landslide dammed lakes in New Zealand leading to the recognition of 53 existing lakes formed where landslides have blocked rivers or streams. A further 24 former landslide dammed lakes were also identified, 22 of which have breached, and 2 that have infilled leaving the landslide dam intact.

Further investigations by Hancox et al. (1997), lead to the identification and documentation of landslides caused by 22 historical earthquakes. Information ascertaining to the landslide dam and earthquake were plotted on maps and entered into what now forms a national database of historical earthquake induced landslides in New Zealand (*pers comm.*, G. Dellow, 2002). The formation of the national database from the amalgamation of the above sources, identifies c. 130 landslide locations (Korup, 2002), and locates many landslide dams throughout the country.

2.6 CHAPTER 2 SYNTHESIS

- The term “landslide dam” identifies the natural blockages of river channels caused by slope movements (Casagli and Ermini, 1999). The formation of a landslide dam is dependent on many factors such as the type of landslide, the velocity, landslide material, valley morphology, and the distribution of landslide material; they commonly form in steep-walled narrow valleys bordered by high rugged mountains, a setting commonly found in geologically active regions. Once created, a landslide dam may last several minutes or for several thousand years (Schuster, 1993; Schuster and Costa, 1986)
- The spatial distribution of landslide dams depends on the seismic intensity, topography, slope gradient, rock material characteristics of the rock material, and soil moisture and groundwater content in the region.
- Earth slumps and slides are the most common mass movements causing landslide dams followed by debris, mud and earth flows, rock and debris avalanche, with sensitive clay failures and rock and earth falls being the least likely types to form landslide dam (Schuster, 1993).

- Triggering mechanisms for dam forming landslides include excessive rainfall, snowmelt and earthquakes, volcanic eruptions anthropogenic activity, and removal of toe support.
- Hazards following the formation of a landslide dam include downstream flooding resulting from the subsequent release of the impounded water after a dam breach and upstream or backwater flooding the immediate hazard associated with damming of a river or stream.
- Breaching of a dam can result from overtopping of reservoir water, piping through the dam, heave (normally followed by slope failure of a portion of the dam) and engineered structures such as tunnels or spillways providing protected conduits for the safe passage of water from behind the dam.
- The longevity of a landslide dam depends on factors such as the rate of sediment and water flow into the upstream reservoir area, the physical characteristics of the dam such as shape, size, and the geotechnical properties, and the amount of water loss via seepage through the dam, evaporation and groundwater recharge into reservoir slopes (Ermini and Casagli, 2003).
- Four important factors determine the magnitude of the dam-break flood and its outflow hydrograph: 1) volume and height of the lake; 2) depth of the lake at the upstream dam face; 3) average width of the breach; and 4) breach development time (Manville, 2001).
- Most of New Zealand's landslide dammed lakes are in the more mountainous and glaciated regions of the South Island (Perrin and Hancox, 1992), however regions such as the eastern central North Island, and Northwest Nelson, North Westland, western Canterbury and Fiordland in the south, also show high landslide dam frequency.

Investigating reasons why some landslide dams fail while others survive is the overall aim of this study. This is achieved through the production of a detailed database of landslide dams in the northwest Nelson region. Chapter Three presents the methodology used to build this dataset and discusses characteristics of failed dams as opposed to surviving dams to understand what parameters influence stability.

Chapter 3

LANDSLIDE DAM DATABASE

3.1 INTRODUCTION

Globally, documentation of landslide dam occurrence has so far barely gone past the descriptive stage, with many authors citing incompleteness and deficiencies in the data-gathering process (Korup, 2002). This potentially limits the degree of accuracy, as well as the type of analytical applications, in landslide dam data analysis. Casagli and Ermini (1999), in their inventory of c.65 landslide dams in Italy, outline some important parameters required when detailing landslide dams. They identify the importance of recognising and determining the characteristics of both the landslide and the dam, which can help in assessing their past and present condition. The landslide and dam attributes can also lead to the prediction of a dam's post-formation development by assessing key relationships such as dam volume versus lake volume for example.

So far, in the New Zealand context, the recognition of landslide dams has been via a number of studies (e.g. Henderson, 1937; Adams, 1981a and b; Perrin and Hancox, 1992, Hancox *et al.*, 1997 Hancox *et al.*, 2002). Detail relating to the landslide and dam characteristics from the above studies is limited to both general quantitative and qualitative information. There has however, been no systematic or standardised detail given for any of the studied dams. This reinforces the need for detailed investigation of groups of landslide dams within New Zealand, and is the basis for producing the present database.

The aims of this chapter are to:

- A. Document the principles and methodology used during this study in the construction of a database for selected landslide dams within a particular region of New Zealand. This includes how the dams were selected, what parameter values

were obtained, terminology used, how the data was acquired and finally presentation of the data.

- B. Summarise and discuss the data to aid interpretation in chapters; and
- C. The application of empirically derived geomorphic stability indices, which incorporate four main geomorphic parameters that are understood to control the stability of the dam against failure.

It is my intention to draw conclusions from this chapter in order to highlight any deficiencies found in current international techniques for assessing dam stability, and from the construction of this dataset. Detailed analysis in Chapters Four and Five will attempt to highlight ambiguities from the analysis of the database.

The main aims in building a database of the occurrence of landslide dams in a particular region of New Zealand is 1) to try and understand the key parameters controlling the longevity and stability of landslide dams; 2) to test the application of internationally accepted empirical stability indices such as the Impoundment Index (I_i), Blockage Index (BI), and Dimensionless Blockage Index (DBI); 3) to understand what threshold(s) are involved in controlling a dam's stability in a particular topographically similar region of New Zealand; and 4) to attempt to standardise the terminology used in the assessment of landslide dams.

3.2 DATABASE CONSTRUCTION

3.2.1 DAM SELECTION

The M_s 7.8 Murchison earthquake of June 1929 and the May 1968 Inangahua earthquakes that occurred in the mountainous region of north-west Nelson, South Island, New Zealand, triggered many landslides throughout the northwest of the South Island, some of which dammed or partly dammed rivers and streams, creating temporary and permanent lakes. Henderson (1937) documented the occurrence and, in some cases, the characteristics of many of the larger dams in a detailed report of the 1929 Murchison earthquake. His report was the basis of later investigations regarding the occurrence of landslide dams throughout the NW Nelson and Buller districts by Adams (1981a and b), Perrin and Hancox (1992), Hancox *et al.*, (1997), and Hancox *et al.*, (2002). Of these studies, Hancox *et al.*, (2002) documented the occurrence of 66 landslides with volumes greater than about 100,000 m³,

and identified 40 failed or existing landslide dams caused by the 1929 Murchison earthquake. However, it was found during this study that some of the dams documented as being formed from this earthquake, have formed pre-1929, for example Lake Matiri (No. 5) and Lake Stanley (No. 1).

Hancox *et al.*, (2002) detail the characteristics of landslides from the 1929 Murchison earthquake such as the distance from epicentre and landslide dimensions. Their study constitutes the primary source of data used in creating the database developed here. Of the 40 landslide dams identified by Hancox *et al.*, (2002), 24 that formed in part, or wholly from the 1929 Murchison earthquake, were included in the database. In addition, two landslide dams resulting from the 1968 Inangahua earthquake were included in the database from different including Johnston, 1974; Perrin and Hancox; 1992; and *pers comm.*, S. Nathan, 2003). Consequently, 26 landslide dams are included in the dataset in this thesis herein called ‘Murchison dataset’ (Table 3.1 and Fig 3.1).

Table 3.1. List of the landslide dams used in the Murchison dataset. The location of the dams is illustrated in Fig 3.1 and the numbers relate to the datasheets in Appendix B.

1 Lake Stanley	10 Matiri (right branch)	19 Lower Lindsay
2 Matakitaiki (Mud)	11 Maruia Falls	20 Mercury
3 Falls	12 Lower Stanley	21 Ferris
4 Glasseye	13 Allen	22 Garabaldi
5 Lake Matiri	14 Beautiful	23 Lake Moonstone
6 Lake Marina	15 Lake Elmer	24 Lake Barfoot
7 Dora	16 Tangent	25 Ram Creek
8 Kakapo/Haystack	17 Rain Peak	26 Buller
9 Lake Perrine	18 Upper Matiri	

3.2.2 PARAMETER SELECTION

Parameters required in the inventory of the 26 landslide dams were based on the parameters outlined by Casagli and Ermini (1999) in their study of landslide dams in Italy. They recognise the importance in determining the characteristics of the dam-forming landslide, dam, lake and catchment, which were recorded on two forms. One details the dam-forming landslide and source rock characteristics, while the other records the dam, lake and catchment characteristics (Appendix A).

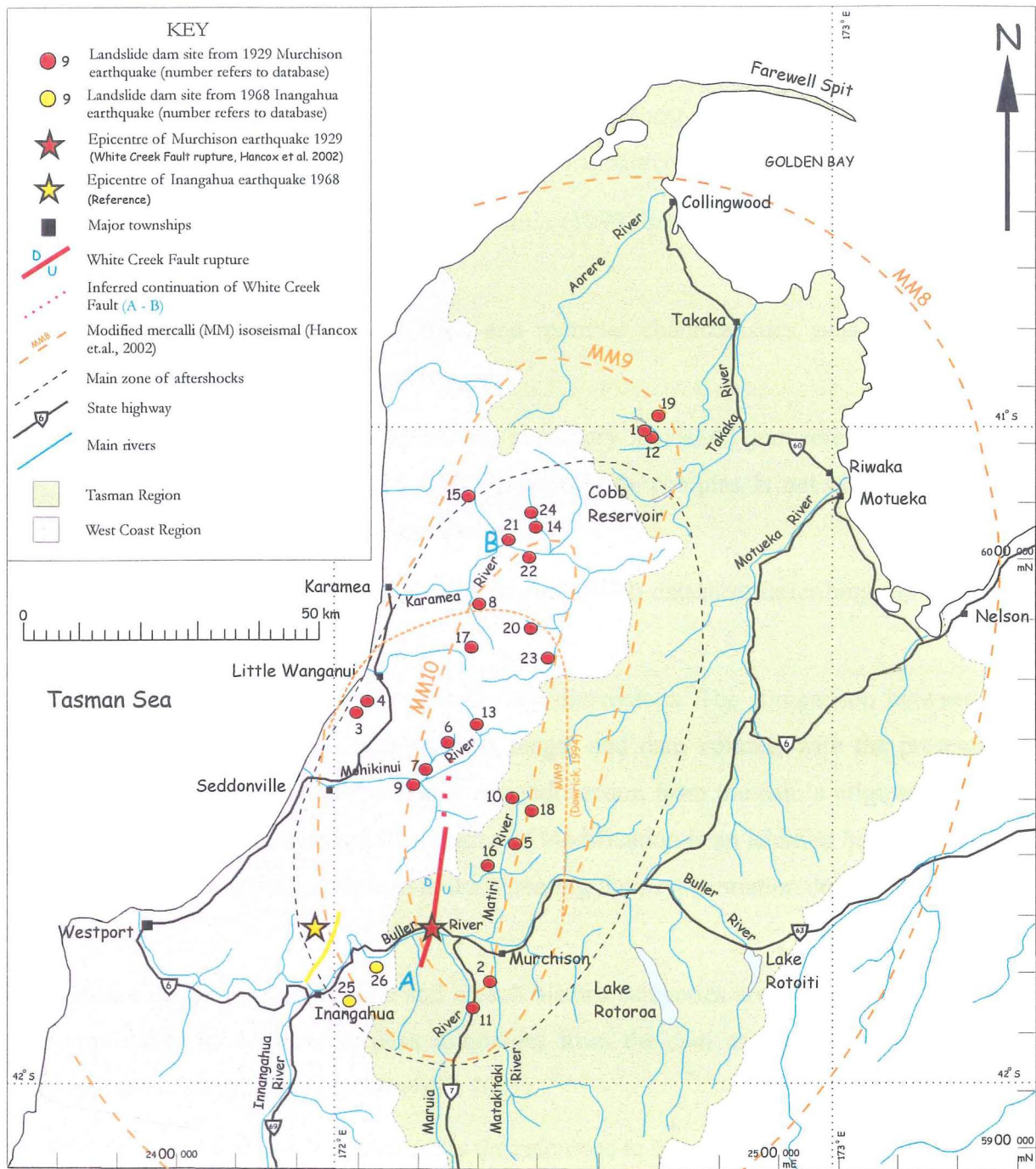


Fig 3.1. Map showing locations of 26 landslide dams formed in part or whole by the 1929 Murchison and the 1968 Inangahua earthquakes. Numbers associated with dam location (red and orange dots) refer to the database number this study. Modified mercalli isoseismal information and approximate epicentre location (orange line and star) are for the 1929 Murchison earthquake (modified from Hancox et al., 2002).

Parameters used by Casagli and Ermini (1999) have been supplemented with important geotechnical parameters such as rock mass and material characteristics of the dam material, which are considered to be significant factors in controlling a dam's stability (Casagli *et al.*, 2003). Some parameters in the original datasheet were considered irrelevant and were not included in the datasheets developed in the Murchison study.

The main modifications from Casagli and Ermini's (1999) datasheet that details the dam-forming landslide are:

- 1) Inclusion of the source rock mass and material characteristics such as defect spacing and weathering respectively; and
- 2) Exclusion of detailed description of secondary landslide movements because additional landslide movement within the landslide complex is not considered as important as initial dam-forming movement.

The main modification from the Casagli and Ermini (1999) datasheet describing the dam, lake and catchment characteristics are:

- 1) The inclusion of original and present dam dimensions. The comparison between original dam dimensions such as crest length and dam volume, with the present dam dimensions indicate the degree of modification from the dam's original state (expressed as a percentage). The degree of modification is an addition because it is considered an important feature in documenting the post-formation development of a dam;
- 2) Breach height, breach volume and breach history categories are added due to their importance in determining peak discharges from the dam using physically based mathematical models (e.g. Manville, 2001).

One of the main additions to the datasheet is the reference to the way the attributes, such as dam volume, dam height and dam crest length, were quantified (Appendix F), which is lacking in the datasheets presented by Casagli and Ermini (1999).

3.2.3 DAM-FORMING LANDSLIDE AND SOURCE AREA

The Murchison landslide datasheet (Appendix A) is further subdivided into 1) general information; 2) source dimensions; 3) geology; 4) landslide classification; and 5) causes of failure.

1. General information

The general information includes NZMG coordinates locating the dam site, reference name and number linking the dam to the dataset of 26 dams, the date of initial dam-forming landslide, and subsequent landsliding within the initial slide boundaries. Additional general information is included such as the appropriate topographic map edition and scale for the dam, approximate elevation of the landslide centre and the geographical district in which the dam formed.

2. Source Dimensions

This section is concerned with the initial dam-forming landslide extent, which is important in determining the percentage of landslide material contributing to the landslide dam. The main dimensions acquired are the rupture length, width and depth, which are needed when calculating an approximate landslide volume. The final slide volume is estimated using a dilation coefficient of 33% (Nicoletti and Sorriso-Valvo, 1991), a better estimate of the actual volume of landslide material upon deposition. Information concerning the landslide head and toe elevation, slope, and facing direction is also included in this section (based on Cruden and Varnes, 1996).

3. Geology

This section details the geological composition of the dam-forming landslide source rock, which is directly related to the material comprising the dam, which is achieved through a detailed geological description of the source rock mass and material characteristics. Source rock descriptions include age, history and current tectonic influences. Rock material descriptions of the source rock, following Bell and Pettinga (1983), list weathering, strength and fabric details. Rock mass descriptions detail the defects within the source rock through defect spacing, persistence and unit block sizes and joint orientation.

4. Landslide Classification

The classification of the landslide is concerned with describing the initial landslide based on its movement (following Cruden and Varnes, 1996). This section is further subdivided into 2 categories: 1) a description of the initial failure type; and 2) the landslide activity.

- 1) The description of the initial failure is concerned with landslide movement (kinematics of a landslide – how movement is distributed through the displaced mass) and the velocity at which the slide has moved. Categories for the movement

of a slide include fall, rock avalanche, translational slide, rotational slide, spread, and flow. The velocity of the initial dam forming landslide is also recorded.

- 2) The landslide activity describes the internal slide dynamics and timing under three main categories. a. The state of activity describes what is known about the timing of movements; b. landslide movement defines broadly where the landslide is moving; and c. style of activity, which indicates the manner in which different movements contribute to the landslide. A landslide's activity can indicate trends that might suggest further landsliding, and is therefore important when assessing further hazards.

5. Causes of landsliding

The final category describes the cause(s) of landsliding through descriptions of 1) pre-existing geological controls such as major jointing; 2) triggering mechanisms such as rainfall or earthquakes; and 3) description of subsequent failure within the initial landslide boundaries.

3.2.4 DAM, LAKE AND CATCHMENT DATASHEET

The dam, lake and catchment datasheet (Appendix A) is subdivided into 1) general information; 2) original/present dam dimensions; 3) dam materials; 4) breach characteristics; 5) lake and catchment characteristics; and 6) damage.

1. General information

This section lists information regarding dam name and database reference number, dates of dam formation and dam failure (where applicable), geomorphic classification of the landslide dam and its location with reference to the NZMG.

2. Original/Present dam dimensions

Parameters recorded in this section include crest length, crest width, crest height, area of landslide dam, volume of landslide dam, average baseline length, slope of the downstream dam face, and the slope of the upstream dam face.

3. Dam materials

This section describes the rock material comprising the dam relating to the size and interaction of the clasts, which influences the ability of the dam to resist internal and

external fluvial erosion. Details such as grain - matrix ratios, clast angularity, grading, and the range of material clast sizes are included in this section.

4. Breach characteristics

Important breach parameters include average breach depth, width and shape, which are used to calculate breach volume. The degree of modification is a new term developed from the Murchison study that calculates the volume of dam material eroded following a breach expressed as a percentage of the original dam volume.

E. Lake and catchment characteristics

The characteristics of the lake are important because: 1) the condition of an impounded lake post-formation can indicate the current state of a dam and its ability to impound water; 2) lake dimensions can indicate the potential hazard associated with the impoundment; and 3) lake volume is one parameter used for the stability analysis of a landslide dam.

In particular, information relating to the lakes original and present volume, lake surface elevation, lake length, width and maximum depth are incorporated in this section. The duration of the lake if known, is normally indicative of the dam longevity and is therefore an important attribute. Finally, the present lake condition gives a general indication of the post-formation dam development.

The size of the catchment above the point of blockage determines the rate of inflow into the impoundment and indirectly the valley morphology at the point of blockage. These are important parameters that influence the flow and hence erosivity of the river or stream.

F. Damage

The final section details damage to infrastructure and deaths resulting from the formation or failure of landslide dams in the Murchison dataset.

3.2.5 ACQUISITION OF DATA

The selection of 26 landslide dams was based on the availability of quality information detailing the dam characteristics via aerial photographs, historical evidence, published and unpublished reports, geological maps and reports, and accessibility to the dam site. Landslide dams lacking well-defined boundaries, such as upstream and downstream damming extent and crest height, typically not well defined for dams $< 100,000 \text{ m}^3$ in volume, were omitted from the dataset. The scale of damming also influenced the

selection. Hancox *et al.*, (2002), identified landslide dams large enough to be recognised using stereo aerial photography, all of which showed volumes ranging from about 100,000 m³ to 18 x 10⁶ m³. Landslide dams smaller than 100,000 m³ could not be easily identified and therefore were not included in either their dataset or the Murchison dataset. Dams with volumes greater than 100,000 m³ identified by Hancox *et al.* (2002) were the main dams used in this study because of their higher degree of dam material preservation after dam failure, and because the dam parameters are easily recognised and quantified compared with smaller landslide dams.

Data relating to the 26 selected landslide dams (Table 3.1) were obtained from various sources being:

1. **Literature review:** A detailed account by Henderson (1937) of several landslide dams formed by the earthquake of 1929 was used. This report included important information regarding the timing of failure of the larger landslide dams such as Lake Perrine (No. 9 this database). Another particularly useful source of historical data was from personal communication with local residents who, in some cases, witnessed the formation and failure of landslide dams in their region (e.g. Matakita, No.2).

Local museums, such as those in Nelson, Westport and Murchison, provided accurate historical information relating to the landslide dams forming, in particular from the 1929 Murchison earthquake. A number of historical accounts have also been published detailing the sequence of events relating to landslide dams from the 1929 earthquake (Brown, 1976; Grigg, 1947). Hancox *et al.*, (2002) was the main reference used to locate suitable dams to include in the dataset.

Johnston (1974) gave a good account of the geology, dimensions and duration of the landslide and associated dam that temporarily blocked the Buller River resulting from the Inangahua earthquake of 1968. Personal communication with S. Nathan (2003) provided information relating to the formation and failure of the 1968 Inangahua earthquake-triggered Ram Creek landslide dam. Published 1:50,000, 1:63,360 and 1:250,000 geological maps varying in age from 1961 to 1998, published and unpublished reports and university theses were among other references used to obtain data.

2. **Field Reconnaissance:** 15 of the 26 landslide dams investigated were field checked to obtain information related to important parameters not acquired from other sources

(such as aerial photography). These parameters include the rock mass and material properties of the landslide source (where possible), dam material properties, and the current lake condition, which may have changed since the aerial photography reconnaissance flights. The isolation of the unchecked dams made it difficult to obtain ground-truthed data. Many of the accessed dams required up to two days tramping to get to the site, such as Lake Moonstone (No. 23) which is located on the Karamea/Leslie track in the Kahurangi National Park. Aerial reconnaissance of the dams was carried out between December 2002 and February 2003 in order to obtain oblique aerial photographs of each dam in the database (Appendix B) to document the current state of the dam, lake and landslide.

3. **Cartography:** Schematic maps for each landslide dam illustrating the important geometric relations and relative proportions of features, such as dam vs. lake area, were produced using 1) 1:50,000 topographic maps; and 2) 1:50,000, 1:63,000 and 1:250,000 Geological Maps of New Zealand.

3.2.6 ERROR WITHIN THE DATASET

The estimation of some landslide attributes considered in the dataset involve errors due to the scale and level of investigation. Base maps and cross section were drawn for all landslide dams studied from the Land Information New Zealand 20m contour dataset, which is probably only accurate to $\pm 10\text{m}$ (Appendix B). The scale used to determine the dam, landslide and lake dimensions for 22 of the 26 landslide dam cases, varied depending on the size of the dam and landslide however, the scale generally ranged from 1:30,000 to 1:50,000, introducing an error of $\pm 5\%$.

Some of the dam sites showed significant vegetation regrowth since their formation making the identification of dam and landslide attributes more difficult. Complications arise also when there is further landsliding within the original slide that formed a dam, or on valley sides opposite to the original landslide. This makes it harder to difficult to estimate the longevity and characteristics of the original dam and lake.

Rock mass and material information relating to the source area and dam material are limited. This is attributed to the isolation of many of the dams, 12 of which were so isolated that a helicopter would have been required for field investigations, which is outside the scope of this project. Accessing the remaining 14 sites required walking or

tramping, with travel times ranging from 3 minutes to 3 days to acquire source rock and landslide (dam) characteristics such as strength, block size and dam status.

3.2.7 TERMINOLOGY

A description of several terms currently in use throughout the literature, and descriptions of terminology used in the analysis of the Murchison dataset are given below. Appendix F details the specific parameter terminology used in the Murchison study.

Casagli and Ermini (1999):

1) Dams not formed: partial blockage, channel deviation, erosion of the landslide toe, in which the formation of a complete dam is prevented; 2) Collapsed dam: all cases of catastrophic failure; 3) Artificially controlled: remedial works changes the natural evolution of the phenomenon; 4) Slow erosion: lake extinguishes because of slow progressive erosion of the dam without catastrophic events; 5) Filling: lakes that extinguish due to infilling of the impoundment; and 6) Existing: lakes existing at present.

Ermini and Casagli (2003):

1) Stable dam: landslide dam that has remained stable and has not encountered a breach thus still impounding an existent or relict lake; 2) Unstable dam: landslide dam that has undergone erosion or collapse leading to a catastrophic breach, with the subsequent release of the impoundment lake waters.

Murchison Study (2003):

A. Dam Status

1) Highly stable (HS): landslide dam displaying less than 10% erosion of the original dam volume (degree of modification < 10%) and currently impounds a lake; 2) Stable (S): landslide dam that has gradually eroded between 10 and 35% of the original landslide dam volume without catastrophic dam failure and currently retains a lake; 3) Marginally stable (MS): landslide dam displaying between 35 and 65% erosion of the original dam volume through gradual erosion or episodic catastrophic erosion of dam material. retains a relict lake behind remaining dam material; 3) Largely failed (LF): landslide dam that has eroded between 65 and 90% of the original dam volume via one or more catastrophic failure events. Drainage of all or part of the original lake volume; 5) Completely failed: greater than 90% of the dam material eroded in one or more catastrophic failure events. No remnants of original lake remain upstream of the point of blockage.

B. Failed Dam: landslide dams with a dam status of completely failed (CF), largely failed (LF) or marginally stable (MS).

C. Stable Dam: landslide dam with a dam status of Stable (S) or Highly stable (HS).

3.2.8 PRESENTATION OF DATA

Raw data from the 26 landslide dams included in the dataset are presented on two Excel datasheets detailing the landslide and dam attributes as previously discussed. A plan and section map for each dam is included with the spreadsheets (Appendix B).

Due to the large amount of data in Appendix B, it has been condensed into two spreadsheets, one detailing the dam-forming landslide attributes, the other describing the dam, lake and catchment attributes (Appendix C). Qualitative information such as breach shape and rock material terminology are linked to a reference number, which describes the attribute and accompanies the synthesised data in Appendix C.

3.3 LANDSLIDE DATASHEET ANALYSIS

This section analyses data from the 26 dam-forming landslides included in the Murchison dataset relating to the landslide datasheet (Appendix A). Presentation of the parameters will match the format of the spreadsheet, which is divided into four groups detailing; 1) landslide spatial distribution; 2) initial landslide source dimensions; 3) geological composition of slide source rock; and 4) initial landslide classification. Discussion of the parameters with respect to the current dam status will follow each section.

3.3.1 SPATIAL DISTRIBUTION

The 1929 Murchison earthquake produced several thousand landslides ranging from shallow regolith slides with volumes between 1 and $20 \times 10^3 \text{ m}^3$, to large bedrock failures up to $210 \times 10^6 \text{ m}^3$ in volume affecting a total area of $\sim 7000 \text{ km}^2$ (Hancox *et al.*, 2002). Hancox *et al.*, (2002) used the distribution of 66 Murchison earthquake-induced landslides with volumes over about $100,000 \text{ m}^3$, and several hundred other known significant slides less than $100,000 \text{ m}^3$ in volume, to define MM intensity, which differs from Dowrick (1994) who defined MM9 intensity based on building damage (Fig 3.1).

From the Murchison earthquake-induced landslides, 24 of the larger dam-forming slides were included in this thesis, along with 2 additional Inangahua earthquake-induced

landslides, which are identified in Fig 3.1. All of the 24 landslides from the Murchison earthquake included in this study, lie within the MM9 isoseismal (up to 90 km north and 20km south of the epicentre) defined by Hancox *et.al.*, (2002) with 62% lying within the stronger shaken MM10 intensity zone (within 40-50 km north of the epicentre) as defined by Hancox *et.al.*, (2002). None of the 24 Murchison-related landslides included in this study were located outside of the MM9 intensity zone (Fig 3.1).

3.3.2 SOURCE DIMENSIONS

The source dimensions relate to the initial dam-forming landslide (herein called landslide) dimensions. Their products lead to estimates of the in-situ and final bulked volume of the landslide, important in determining the amount of material available for damming. Fig 3.2 illustrates how the rupture length (L_r), rupture width (W_r) and rupture depth (D_r) of the landslides were quantified as part of the Murchison study. These dimensions are used with an assumption about the shape of the landslide to approximate the in-situ volume using

$$V_{ls} = \frac{1}{6} \pi D_r W_r L_r \text{ for rotational failures, whereas the volume of a planar failure is simply}$$

the product of the L_r , W_r , and D_r . The final bulked volume of the slide material after dilation for all failure types is estimated by applying a swell factor of 33% (Nicoletti and Sorriso-Valvo, 1991). The head and toe elevation of the landslide is taken as their height (m) above mean sea level (Fig 3.2). The travel angle and azimuth are taken as the angle ($^\circ$) between the failure surface and the horizontal and the initial landslide failure propagation angle ($^\circ$) relative to north. The average and range of source dimensions for all 26 landslides are given in Table 3.2.

Table 3.2. Mean and range source dimensions and volumes for all 26 dam-forming landslides in the dataset this thesis. Dimensions in the table relate to failed dams (f) and non-failed dams as defined by the dam status.

LANDSLIDE DIMENSIONS	Max	Min	Average	Max (F)	Min (F)	Average (F)
Rupture length (m)	1170	320	685	970	400	574
Rupture width (m)	1270	170	487	510	330	426
Rupture depth (m)	83	10	30	50	15	28
Ladslide area ($\times 10^3 \text{ m}^2$)	700	0.82	273	320	58	209
In - situ volume ($\times 10^6 \text{ m}^3$)	22	1.1	6.8	4.4	1.6	3.4
Final bulked volume ($\times 10^6 \text{ m}^3$)	25	1.5	8.2	5.8	2.1	4.5
Head elevation (m.a.s.l.)	1595	280	997	1500	295	750
Toe elevation (m.a.s.l.)	940	60	496	680	135	274
Slope angle ($^\circ$)	48	8	32	50	17	27

3.3.3 SOURCE ROCK GEOLOGY

The geological composition of the source area in which the initial landslide developed can influence and/or control the dynamics of the landslide from triggering mechanisms. For example, close proximity to an active fault, or deep weathering profiles, which influence the stability of a slope. Information relating to the rock mass and material properties of a particular geological unit in the landslide's source area can indicate source rock characteristics that may influence the landslide development. These parameters have been recorded for the selected dams in this thesis (Fig 3.3) following rock mass and material terminology by Bell and Pettinga (1983) (Appendix F).

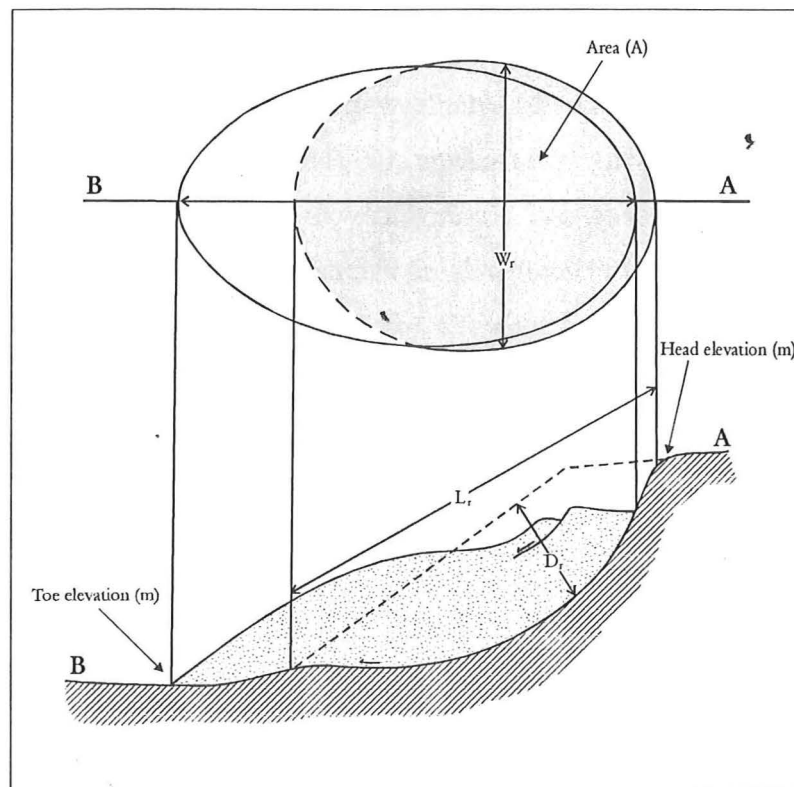


Fig 3.2. Quantification of the rupture length (L_r), rupture width (W_r) and rupture depth (D_r) for initial dam-forming rotational landslides, their product leads to the approximation of landslide in-situ volume. Planar failure volume quantification adopts the terminology used as for rotational slides, and is simply the product of L_r , W_r , and D_r . (modified from Cruden and Varnes, 1996).

3.3.3.1 Rock material

The rock material parameters recorded from landslide dams in the Murchison dataset describe the material shed from the initial dam-forming landslide source area (herein called source rock), in particular the weathering, strength, fabric and rock type as summarised in

Figure 3.3 a. Not all dams could be included in the rock material analysis because of their isolation, therefore, only dams that were visited are included in the description. The number of dams used for each parameter is shown as an 'n' value in Figure 3.3 a.

Rock material characteristics associated with failed dams are indicated by shading in Fig 3.3a; the following section discusses the rock material properties of the landslide source rock (Fig 3.3a).

The extent of weathering is dominantly moderately weathered at 75% (penetrative discolouration and alteration of rock material, with some loss of strength). The remaining 25% of source rock material is either highly weathered (material pervasively altered with discolouration and loss of strength; fabric preserved; lithorelicts) or slightly weathered (slight discolouration of rock fabric; no loss of material strength). No landslide source material is characterised as residual soil (discolouration and complete transformation to soil, original fabric destroyed), completely weathered (discolouration and transformation to soil, original fabric largely preserved), or unweathered (no discolouration or loss of strength, or any other effects due to weathering). The absence of residual soils and completely weathered material demonstrates the dynamics of the general area as relatively fresh rock is continually being exposed not allowing time for material to completely weather. The time since this material was emplaced is ~ 70 and 30yrs, therefore rock material properties described presently may not reflect the nature of the material at the time of landsliding.

Of the 17% of landslides that are highly weathered, 100% failed. Of the 75% of landslides that are moderately weathered, 33% failed. The remaining 8% of slides that are slightly weathered none failed.

The distribution of strength properties of the rock material shows a similar distribution to weathering, as strength is largely a function of the degree of weathering, among other things. Strength characteristics are described qualitatively, like weathering, based on the descriptive terms given by Bell and Pettinga (1983) (Appendix G). Moderately strong and strong material (breaks readily with one hammer blow and few firm blows of hammer required to break specimen respectively) dominate the source rock material representing 90% of the landslide source rock where the strength characteristics are known. The remaining 10% are represented by moderately weak material (broken by hand only with difficulty; small thin pieces broken by finger pressure) (Fig 3.3a).

Extremely strong and very strong (can only be chipped with geological hammer and several hard blows required to break hand specimen respectively) and very weak and weak (crushed or remoulded by hand and broken by hand, pieces 25mm or more broken by finger pressure) dam-forming landslide source rock strength characteristics are not represented in any case.

Of the 17% of landslides that are moderately weak, 100% failed. Of the 50% of landslides that were moderately strong, 67% failed. The remaining 33% of slides material that was strong none failed (Fig 3.3a). This is attributed to the material being strong enough (assuming this material comprised the bulk of the dam material) to resist erosion from overtopping and internal piping.

The fabric of a rock material reflects the arrangement of crystals or grains with respect to one another at the scale of hand specimen (Bell and Pettinga, 1983). The fabric of rock material for the dams in this database is qualified from field reconnaissance and geological reports/maps based on the terminology used by Bell and Pettinga, (1983). All three fabric categories are represented in by the landslide source rock material (massive, coarsely layered and finely layered) however, massive (hand specimen displays no layering either sedimentary or flow banding etc) dominated at 59%, with 35% coarsely layered (layering present in hand specimen <100mm spacing) and only 6% finely layered (fine laminations present in hand specimen). The reason for the high percentages of massive source rock could be due to the high number of landslides in granite, which is generally massive in nature.

Of the 59% of landslides that are massive, 30% of the associated dams failed and of the 35% of landslides that are coarsely layered, 50% failed. No dams failed that are associated with the remaining 6% of slides material classified as finely layered (Fig 3.3a).

Landslide source rock type in this case, is largely controlled by the proximity to triggering mechanism and present lithological composition of the region. For example, the Karamea granite is represented throughout the length of the study area (Figure 1.2). Because of the widespread nature of this granite and its close proximity to active faults, such as the White Creek Fault, it is particularly prone to landsliding hence its domination in dam-forming landslides from this dataset. The source rock material represents 6 broadly classified lithologies namely (in order of abundance): granite, sandy/muddy limestone, sandstone, alternating sandstone/mudstone, conglomerate and limestone (Fig 3.3a).

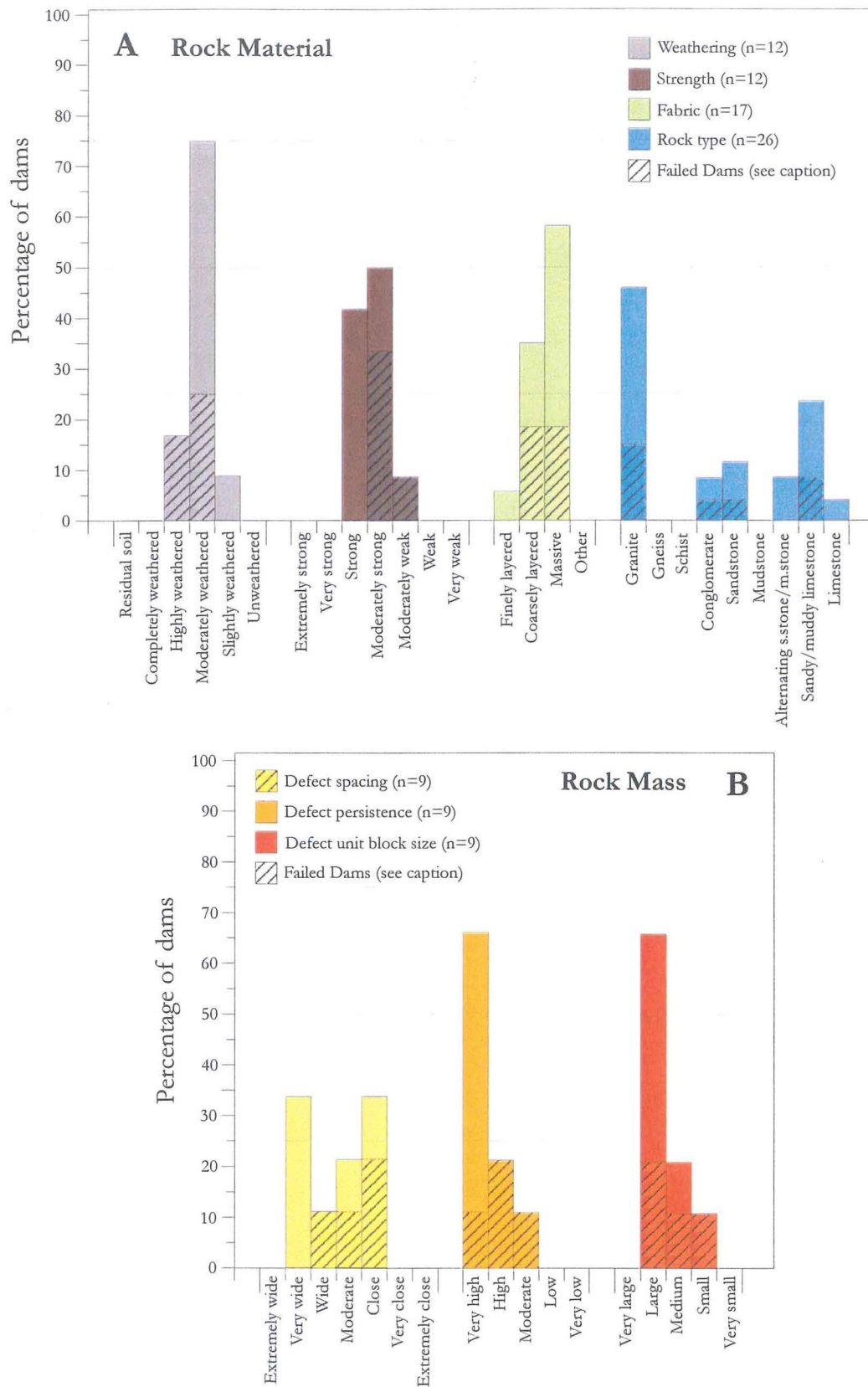


Fig 3.3. Rock material characteristics of initial dam-forming landslide source area from various dams this thesis. Key in top right corner of histogram also indicates the number of dams used in the analysis of the associated parameter. Terminology based on Bell and Pettinga (1983) (see text for discussions relating relevance of these landslide parameters to damming).

Mudstone, gneiss and schist are not represented in any cases. Gneiss and schist are largely absent from the region, which explains why they are not represented; mudstone is present however has not produced any significantly large dam-forming landslides.

Failed dams are represented in four of the six lithologies that comprise all 26 landslide dams in the dataset, with no failure in dams comprising alternating sandstone/mudstone or limestone (Fig 3.3a). The lithology of the source rock material does not significantly influence the stability of dams in this dataset.

3.3.3.2 Rock mass

The rock mass of the initial dam-forming landslide source rock describes the defects that are present within the mass, and can dictate the formation and dimensions of material shed from it, for example, during a landslide (terminology following Bell and Pettinga, 1983; Appendix G). As with the rock material, analysis of the source rock mass is achieved through qualitative field measurements of defect characteristics, and has been achieved during this study for a number of dam-forming landslide sites. The number of landslides analysed for rock mass characteristics is restricted to nine for all three rock mass parameters because of the aforementioned hazards and difficulties associated with access (Fig 3.3 b).

One rock mass parameter is defect spacing (the distance between defects or fractures in the rock mass). The analysis of nine dams shows the general even distribution of defect spacing represented in the source rock namely: close (25-100mm), moderate (100-200mm), wide (200-500), and very wide (500-2000mm). No source rock mass is represented by extremely wide (> 2,000mm), very close (5-25mm) or extremely close (< 5mm) defect spacing (Fig 3.3b). The high range of spacing may reflect the high lithological variation in the region.

Of the nine landslides assessed for defect spacing, four associated dams have failed and are represented by close, moderate and wide defect spacing. No dams with a very wide source rock mass have failed. A very general trend shown is the smaller the defect spacing the more susceptible the dam is to failure (Fig 3.3b).

The defect persistence of a rock mass quantifies the distance over which an individual defect can be traced (Bell and Pettinga, 1983). As for defect spacing, nine sites were used for the analysis of defect persistence, of which nearly 70% were shown to be very high (> 10m), the remaining 30% have either high or moderate defect persistence (5-10m, 2-5m

respectively) (Fig 3.3b). Low (0.5-2m) and very low (< 0.5) defect persistence is not represented.

Of the nine landslides assessed for defect persistence, four associated dams have failed and are represented in source rock at the higher end of the defect persistence spectrum (Fig 3.3b). Of the 70% of landslides displaying very high defect persistence, only 17% failed, whereas all of the dams displaying high and moderate defect persistence failed (Fig 3.3b). This suggests dams with source rock mass characteristics displaying a low defect persistence tend to fail more than dams with a higher source rock defect persistence. This could be related to the degree of fragmentation associated with rock displaying a low defect persistence creating a smaller average block size, which increases the erosivity of the dam material.

The final rock mass parameter analysed is the defect unit block size. This describes the effect of intersecting defect sets on rock mass geometry (Bell and Pettinga, 1983). The dominant source rock defect unit block size is large (500-1,000mm equivalent cube side) at 67%, while medium (100-500mm equivalent cube side), and small (10-100mm equivalent cube side) comprise the remaining 37% of dam source rock. Very large and very small ($> 1,000\text{mm}$ and $< 10\text{mm}$ respectively) were not represented by any of the nine dams analysed for defect unit block size (Fig 3.3b).

Of the nine landslides assessed for defect unit block size, four associated dams have failed and are represented in all three block sizes (Fig 3.3b). However, only 33% of landslide source rock displaying large defect block size failed, while two thirds of dams displaying medium and small defect unit block sizes failed. The general trend indicates the source rock with a smaller defect unit block size is more likely to fail over source rock comprised of a large unit block size. The reason for this may be that source rock mass characteristics control the resulting rock material characteristics, which in turn, influence and control a dam's ability to resist erosion from overtopping or internal piping.

3.3.4 LANDSLIDE CLASSIFICATION

The term landslide denotes the movement of a mass of rock, debris or earth down a slope (Cruden, 1991). The classification of landsliding is based on Cruden and Varnes (1996) who use the type of movement to establish principal groups of landslides. The classification of the landslides in this thesis is concerned with the initial dam-forming landslide (herein called landslide), which in 24 cases, occurred in 1929 with two occurring

in 1968. The classification of these relatively old landslides is therefore inferred and is largely based on field reconnaissance, published/unpublished reports and aerial photographic evidence. Vegetation regrowth throughout some of the landslide source area is relatively high, making it difficult to establish landslide characteristics.

The following section presents and discusses the landslide characteristics with respect to failed and existing dams (terminology as defined in section 3.2.5)

3.3.4.1 Description of initial failure

The kinematics of a landslide – how movement is distributed through the displaced mass – is one of the principal criteria for classifying landslides. Five distinct kinematically types of landslide movement are used to classify the landslides in this dataset. The classification of the landslides in this thesis is considered important when determining what type of landslides dam rivers, and to assess the influence of landslide type on the stability of a dam. The following terminology is taken from Cruden and Varnes (1996), unless otherwise stated:

The majority of the landslide movement was classified as rock avalanches (54%) (very rapid downslope flowage of rock fragments (Bishop, 2002)) closely followed by translation slides (31%) (the mass displaces along a planar or undulating surface of rupture, sliding out over the original ground surface). The remaining 15% of slide movement was classified as rock fall and rotational slide (the detachment of rock from a steep slope along a surface on which little or no shear displacement takes place; and moves along a surface of rupture that is curved or concave) (Fig 3.4). The domination of rock avalanches is likely to be a function of the triggering event and the geological composition of the region (e.g. the Karamea granite), which tends to favour their formation. No dams have formed from landslides classified as spread or flow (lateral movement in a soil or fractured rock mass resulting from liquefaction or plastic flow of underlying materials; and spatially continuous movement in which surfaces of shear are short-lived, closely spaced, and usually not preserved) (Fig 3.4). This may be due to the lack of this type of landsliding from the two earthquake events considered in this thesis.

Of the 12% of landslides described as rock fall, two thirds of the dams failed; of the 85% of landslides described as a rock avalanche or translational slide, only 23% of the associated dams failed. The one dam that formed because of rotational failure did not fail

(Fig 3.4). Therefore, there seems to be no strong correlation between landslide type and stability of a dam from this dataset.

The inferred velocity of the landslides is dominated by extremely rapid and very rapid (> 5 m/s and 3 m/min - 5 m/s). Very slow (1.6 m/yr), slow (1.6 m/yr - 13 m/month), moderate (13 m/month - 1.8 m/hr) and rapid (1.8 m/hr - 3 m/min) are not represented in the dataset mainly due to the triggering mechanism, which caused the sudden collapse of rock masses under high ground accelerations during earthquakes (Fig 3.4).

3.3.4.2 Landslide activity

The activity of a landslide defines the timing of movements, where the landslide is moving and the manner in which different movements contribute to the landslide as defined by: 1) state; 2) distribution; and 3) style of activity. As for the type of landslide, terminology regarding slide activity is taken from Cruden and Varnes (1996) and applied to the initial dam-forming landslides in this dataset (landslides). The aim is to assess the influence that landslide activity has on the stability of a dam.

The state of activity of the landslide describes what is known about the timing of movements. Fig 3.4 illustrates the distribution of state of activity for 26 landslides in the Murchison dataset. The landslides are dominantly described as having a dormant state of activity (inactive landslide where the causes of movement remain apparent) (65%; Fig 3.4). The remaining 35% of landslides are described as active (landslides that are currently moving), reactivations (a landslide that is currently active after being inactive), and stabilised (the toe of the slope has been protected against erosion effectively stopping movement). Suspended (movement within the last annual cycle of seasons but that are not moving at present) and abandoned (river eroding toe of the moving slope changes course) landslides are not represented in the dataset of 26 landslides.

Of the landslides described as active or stabilised, all of the associated dams failed, 12% of the dams associated with dormant landslides failed, and no dams associated with a reactivated landslide failed (Fig 3.4).

The distribution of activity, as the name suggests, describes the activity distribution within a landslide complex defined by: 1) advancing; 2) retrogressive; 3) widening; 4) enlarging; 5) diminishing; and 6) confined.

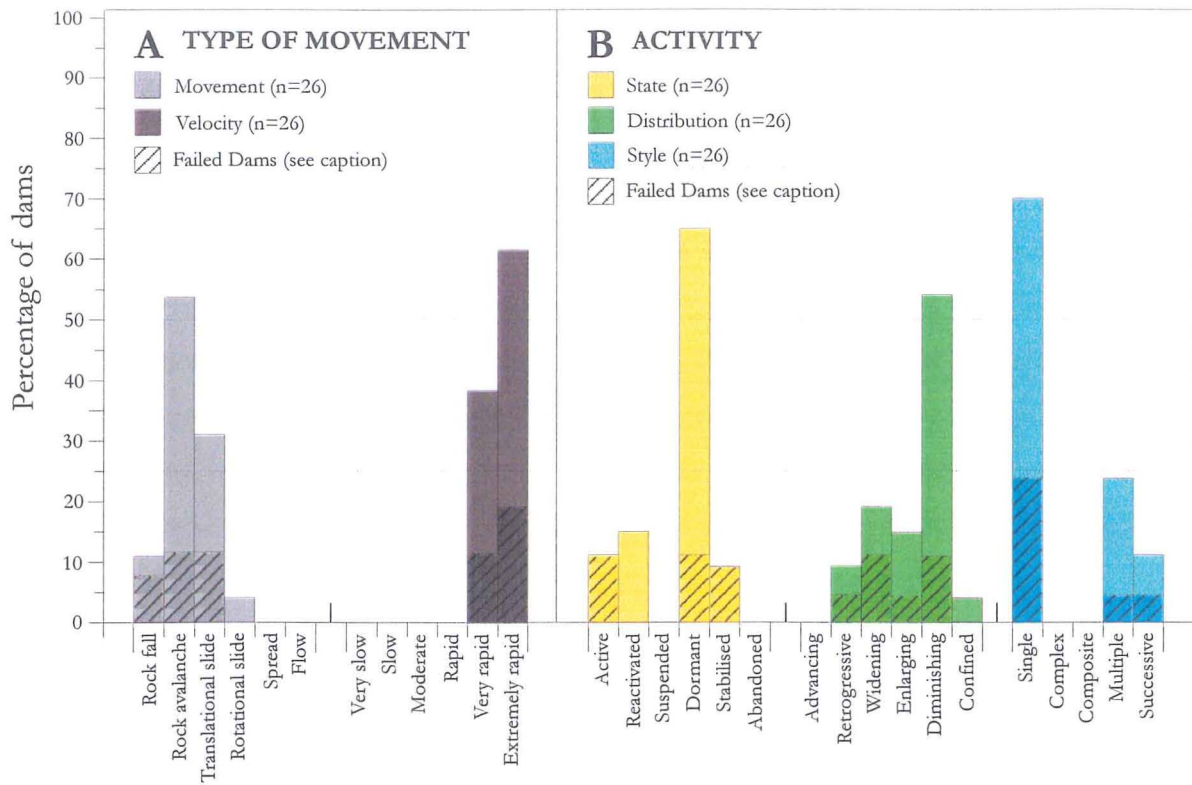


Fig 3.4. Distribution of the classification of the initial dam-forming landslides associated with dams from this dataset. Failed dams refer to a dam status of MF, LF or CF (shaded areas). Non-failed dams represent a dam status of HS and S.

Approximately 50% of the landslides are evenly distributed between retrogressive (surface of rupture extending in the direction opposite the movement), widening (surface of rupture extending at one or both lateral margins), enlarging (movement limited to displacing material), and confined (have a scarp but no visible surface of rupture) (Fig 3.4). The remaining 50% of landslides are described as diminishing (the volume of material being displaced grows less with time), which is likely to be a function of the age of the slides since initial movement (i.e. 1929 and 1968). Advancing landslides (surface of rupture extending in the direction of movement) is not represented by any of the slides in the dataset.

There seems to be a low correlation with landslide distribution between failed and non-failed dams shown by the even distribution throughout four of the five represented categories.

Finally, the style of activity describes the way in which different movements contribute to the landslide defined by: 1) single; 2) complex; 3) composite; 4) multiple; and 5) successive.

70% of the 26 landslides in the dataset are classified as single (single movement of displaced material often as an unbroken block) (Fig 3.4). The 'single' definition is not strictly applicable to many of the landslides in this dataset mainly because the displaced material (which may have originated as a single block) has disintegrated once mobilised, augmented by the relatively high average vertical fall distance of about 500m between the head and toe of the landslides. Multiple (repeated movements of the same type, often followed by enlargement of the surface of rupture) and successive (identical in type to an earlier movement but does not share the displaced material or surface of rupture) define the remaining 30% of landslides in the dataset. Complex (landslides displaying at least two types of movement) and composite (different types of movement occur in different areas of the displaced mass) are not represented in the landslides in this dataset (Fig 3.4).

This highlights the difficulties when applying this classification scheme to old landslides when evidence for the style of initial landsliding cannot be directly observed because further slope movements and vegetation regrowth within the slide mask the initial slide characteristics.

The association of the style of landsliding with dam failure is dominated by slides defined as single (33%) with 22% of multiple and successive dams failing. This shows a relatively poor correlation between landslide style and dam failure (Fig 3.4).

Finally, the material comprising the 26 landslides in this thesis is dominated by rock (firm intact bedrock failures at 90%) with the remaining 10% being debris (loose unconsolidated or poorly cemented aggregate of particles). Landslides comprising earth (superficial slide debris involving the top 2–3 m of colluvium/organic matter) are not represented in the dataset. The dominance of firm intact bedrock landslides associated with damming could be because the earthquake triggering mechanism is sufficient to mobilise rock. It may also indicate the inability of landslides comprising debris and earth to form landslide dams.

3.4 DAM, LAKE AND CATCHMENT ANALYSIS

The following section analyses data relating to the 26 landslide dams included in the dataset, this thesis, following the format of the dam, lake and catchment datasheet illustrated in Appendix A. Presentation of the parameters will match the format of this spreadsheet, which is divided into four groups, detailing; 1) general stability; 2) original/present dam dimensions; 3) breach characteristics; and 4) lake and catchment

characteristics. This section focuses on comparing and contrasting failed vs. non-failed landslide dam characteristics. Parameters not considered significant are mentioned but not discussed in detail.

3.4.1 ORIGINAL AND PRESENT DAM DIMENSIONS

The following section presents and discusses original landslide dam dimensions following formation, and the present dam dimensions for the selected dams in the Murchison dataset. Table 3.3 summarises this data and indicates the number of dams analysed for each parameter. The number of dams analysed does vary because of the difficulties involved in studying dams that are up to and greater than 70 years old. Therefore, dams whose features are difficult to quantify, due to isolation or high vegetation regrowth for example, are omitted from analysis of some parameters. Table 3.3 differentiates between failed (f) and non-failed dams to assess the parameter influence on dam stability. Failed dam dimensions are taken as their dimensions prior to failure. Figure 3.5 illustrates how the original and present dam dimensions have been quantified, something which is lacking in the current literature and yet is considered in this study as an important feature necessary when comparing different landslide dam datasets.

3.4.1.1 Crest length, width and height

The crest length (horizontal distance between original valley walls perpendicular to valley axis at the maximum lake level, Fig. 3.5) show an average reduction in original length relative to their present length from 360m to 261m. However, the original crest length is only calculated for 14 dams due to insufficient data, while the present crest length is calculated for 17. Reducing the crest length is normally achieved by a lowering of the crest height (height in meters from the original valley floor to the maximum lake level, Fig. 3.5), which is the case for the dams in the dataset, with the average crest height reducing from an original height of 42m to the present calculated height of 35m (Table 3.3).

Comparison between non-failed and failed original dam crest length shows a slight reduction in the average crest length from 360 to 305 m respectively, which is not considered significant.

Again, the sample size used to calculate the average failed dam crest length is six compared to 14 for the non-failed dams.

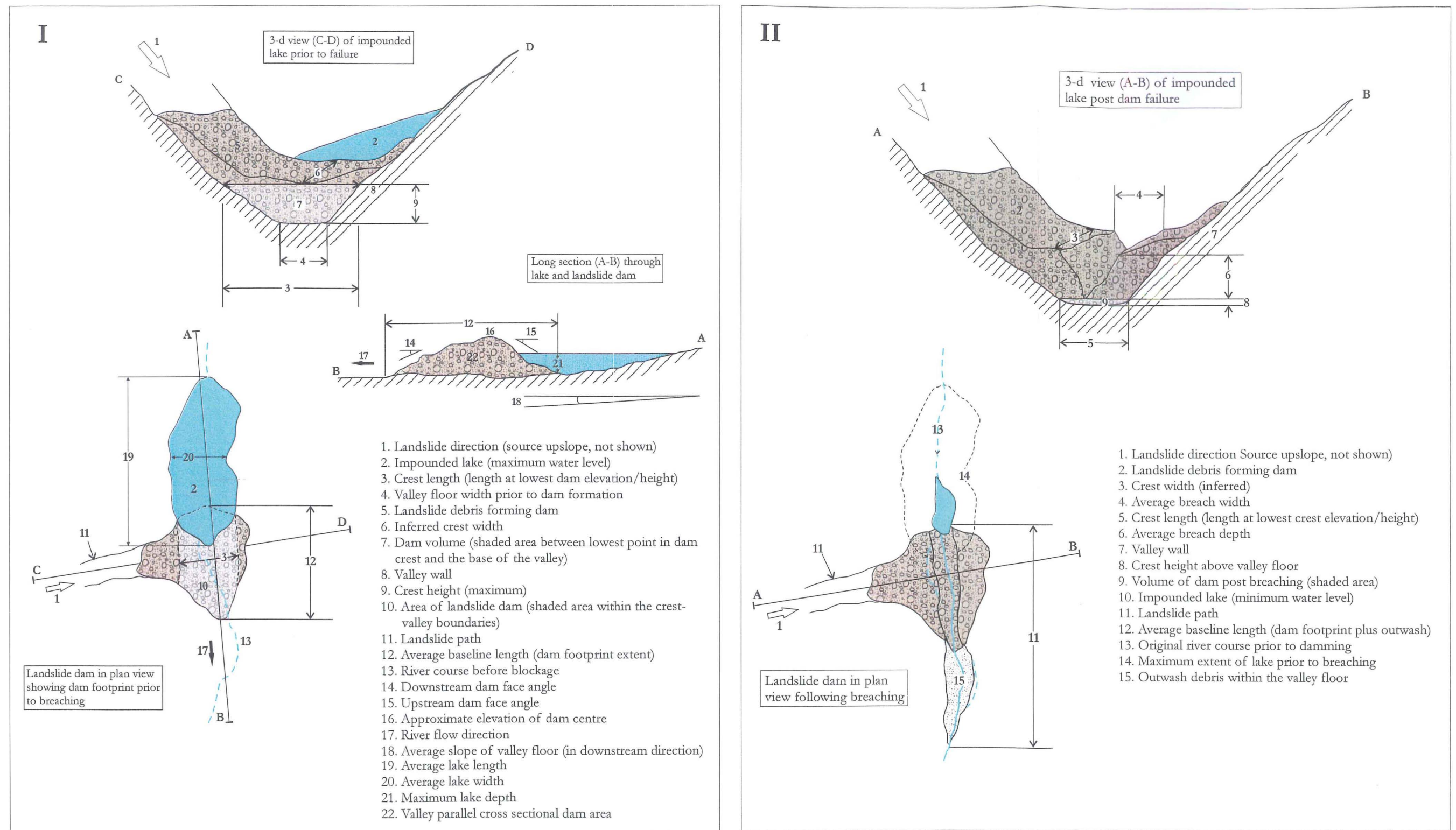


Fig 3.5. Schematic plan, section and 3-D illustrations of a typical landslide dam prior to failure (I) and post failure (II) documenting how the dam parameters from dams in the dataset this thesis have been quantified. Note these illustrations are idealised and do not represent every dam investigated in the dataset. Slight modifications to the above methods may be required given different circumstances. For terminology definitions see text.

There is however, a large contrast between the maximum crest lengths in the non-failed dams (1,200m) relative to the failed dam maximum crest length of 560m. The 1,200m maximum crest length belongs to the Matakiki (No.2) landslide dam, which survived up to 10 years but was subsequently gradually removed artificially using explosives. If this crest length is excluded, there is no significant difference between the failed and non-failed maximum crest length. Table 3.3 shows a 50% reduction in the original average crest height for the failed dams relative to the non-failed dams, inferring this parameter may be important in determining the stability of a dam. All but one of the failed dams shows a total reduction in present dam crest height (Table 3.3).

The crest width (horizontal valley parallel length of the dam crest, Fig. 3.5) shows a drop from the original to present width of 120m. It is important to note the difficulties in defining the crest width of a landslide dam because, unlike man-made dams, natural dams do not show a definite flat valley-parallel crest because of the rapid emplacement and hummocky nature of a landslide dam. The determination of the crest width of the dams in this dataset was not well defined from the outset of the project; the results are therefore not considered significant, and are not discussed further.

Table 3.3. Summary of the original and present dam dimensions and composition from selected landslide dams from the dataset this study comparing failed dams (f) to non-failed dams. The number of dams analysed for each parameter (No.) is also given.

ORIGINAL DAM DIMENSIONS	Max	Min	Average	No.	Max (f)	Min (f)	Average (f)	No. (f)
Crest length (m)	1200	90	360	14	560	205	305	6
Crest width (m)	1350	30	518	13	550	130	332	6
Crest height (m)	100	20	42	14	40	10	24	6
Dam area ($\times 10^3 \text{ m}^2$)	350	25	140	12	121	23	82	6
Dam volume ($\times 10^3 \text{ m}^3$)	24000	200	4577	13	2800	400	1470	7
Dam baseline length (m)	1350	400	761	11	830	320	546	7
Dam slope (downstream) ($^\circ$)	10	6	8	3	13	12	12.5	2
Dam slope (upstream) ($^\circ$)	13	3	8	2	13	9	10.5	2
PRESENT DAM DIMENSIONS	Max	Min	Average	No.	Max (f)	Min (f)	Average (f)	No. (f)
Crest length (m)	500	90	261	17	200	200	200	1
Crest width (m)	875	30	389	16	500	500	500	1
Crest height (m)	85	10	35	17	15	15	15	1
Dam area ($\times 10^3 \text{ m}^2$)	410	20	141	13	nd	nd	nd	0
Dam volume ($\times 10^3 \text{ m}^3$)	12500	200	2625	15	2500	500	1500	1
Dam baseline length (m)	1250	300	724	14	650	385	553	3
Dam slope (downstream) ($^\circ$)	18	6	10	5	nd	nd	nd	0
Dam slope (upstream) ($^\circ$)	3	13	8	4	nd	nd	nd	0
DAM COMPOSITION	Max	Min	Average	No.	Max (f)	Min (f)	Average (f)	No. (f)
Grain size (mm)	20 000	2	500	6	4000	1	300	5

3.4.1.2 Dam area

The dam area is defined as the area inside the dam material extent (the dam footprint) (Fig 3.5). Results from analysis of the original and present dam area using 12 and 13 dams respectively, do not show any significant change with the average area for both being about 140,000 m². A comparison of the original dam area between non-failed and failed dams (12 and 6 dams' analyses respectively) shows nearly a 50% reduction in the average dam area from 140,000 to 80,000m². The reason for this is not clear, however this parameter is thought to indicate dam volume and hence the amount of material that needs to be eroded to achieve failure; the greater the area the more material available to resist erosion therefore increasing dam stability. The maximum dam area also decreases significantly within the failed dams, while the minimum dam are remains very similar (Table 3.3).

3.4.1.3 Dam volume

Dam volume indicates the amount of landslide material available to block a stream or river and is typically significantly less than the total landslide volume. Dam volume is defined as the volume of material below the lowest crest level in a line perpendicular to the valley axis extending to the original valley walls, to the base of the original valley floor and to the upstream and downstream limits of the dam material (dam footprint) (Fig 3.5). Following the above discussion on dam area, the dam volume should show similar trends between the original (pre-failure) failed and non-failed dam dimensions. The analysis of seven failed and 13 non-failed dams shows the average dam volume for the failed dams is less than 50% of the dam volume for the non-failed dams (Table 3.3). These observations indicate that dam volume is an influential parameter in determining weather the landslide dams in this dataset will fail or not.

Another important observation is the 50% reduction in average dam volume for non-failed dams between their original and present state (Table 3.3.) indicating significant (non-catastrophic) gradual erosion of the dam material since emplacement (note 15 dams were analysed for their present dam volume as opposed to 13 for original dam volume). This reduction from original to present volume is supported by the reduction in other dam dimensions such as crest length and height.

3.4.1.4 Dam baseline length

Dam baseline length defines the valley parallel extent (in meters) of the dam footprint (Fig 3.5). 11 and seven original landslide dam dimensions were analysed for non-failed and failed dams respectively. Observations show that non-failed dams have an average baseline length of 750m, whereas failed dams have an average baseline length of 550m, 25% less than the non-failed dams. Based on dam area and volume observations, you would expect the failed dams to show a lower baseline length however, a 25% reduction observed in the failed dam baseline length is not as pronounced as the dam and area reductions of $\sim 50\%$. As with the crest width, baseline length highlights the difficulties in defining this parameter in the field and may explain the low correlation observed. The reduction from original dam baseline length to the present dam baseline length is very low, which also supports the disuse of the term.

3.4.1.5 Upstream and downstream slope of dam face

The final dam parameters discussed in the dam dimensions section are the upstream and downstream dam face, defined as the angle between the horizontal and the average slope of the dam material upstream and downstream of the crest (Fig 3.5). The original dam slopes are particularly difficult parameters to acquire mainly on old dams such as those included in this dataset because of the lack of evidence preserved, especially in the failed dams. As a result, the downstream face slope could be calculated for three non-failed and two failed dams, and the upstream face slope could be calculated for two non-failed and two failed dams. (The two failed dams are studied in detail; see Chapter 5) allowing sections to be drawn at a scale that permits the calculation of the dam face slope). The observations show that the average slope is higher in the failed dams (prior to failure) relative to the average slope in the non-failed dams (original dimensions) (Table 3.3). Similar results are achieved when comparing the present non-failed dam upstream and downstream slopes with the original failed dam slopes.

However, quantification of the dam slope angle based on valley parallel sections may not represent the actual angle of a naturally formed spillway as demonstrated by detailed investigations of Lake Stanley (No. 1), a non-failed dam (Chapter 4). This dam has developed a natural spillway with a slope angle of $\sim 5^\circ$ that is eroded into the dam material. This differs from the valley parallel sectional dam slope of 18° , the value attributed as its downstream dam slope in the dataset. Considering the slope angle of the

spillway is a better representation of the reservoirs potential energy available to erode the dam material for dams with a natural spillway, this angle should be calculated and added to future landslide dam databases.

3.4.2 DAM MATERIALS

The following dam material section is concerned with the interaction and characteristics of the rock material comprising the landslide dams in the dataset, this thesis, which is closely related to the rock material characteristics from the landslide source area.

Table 3.3 summarises the grain size distribution for six non-failed and five failed dams in the dataset based mainly on estimates from field observations and published reports (e.g. Henderson, 1937). The isolation of the remaining 15 dams in the dataset meant estimates of the grain size could not be acquired. Observations from six non-failed dams suggest an average grain size of 0.5m in diameter, and a maximum of 20m as opposed to the average, and maximum for five failed dams of 0.3 and 4m respectively. This 40% reduction in average grain size for a similar number of failed dams is a significant value and may control or influence the ability of the dam material to resist erosion. The two smallest average grain sizes obtained from landslide dams in the dataset were Ram Creek (No. 25) and Rain Peak (No. 16), with 70 and 60mm respectively. Other dams such as Lake Matiri (No. 5) and Lake Stanley (No. 1), two non-failed dams, display relatively high average grain sizes of 2m and 250mm respectively. This shows that grain size may be an important factor controlling or influencing the overall dam stability.

The interaction of the material comprising the dam is divided in three groups: 1) grain supported (coarser particles forming the dam are in contact with each other and the fine matrix is present at an interstitial level (Blikra and Nemec, 1998); 2) matrix supported (coarser particles forming the dam are scattered inside a prevailing fine matrix, as they are not in contact with each other (Blikra and Nemec, 1998); and 3) intermediate supported (intermediate between grain and matrix supported). As with most of the dam material analysis of dams in this dataset, the analysis of the dam material support is dependent on accessibility and requires the sampling of the dam material internally (normally achieved through the spillway walls where erosion is occurring exposing the dams internal structure).

Due to the difficulties described above, the support could only be acquired for six non-failed dams and four failed dams. Observations show five of the six non-failed dams are

grain supported and one was intermediate. None of the non-failed dams are matrix supported. For the four failed dams, two are grain supported, one was intermediate and one was matrix supported. These very general observations shown that non-failed dams tend to have a higher grain-to-matrix ratio than failed dams for the selected dams in the dataset. This higher ratio is thought to increase the strength and permeability of the dam material, allowing it to resist overtopping and internal erosion.

The grading of the dam material describes the relative proportion of particle sizes present, which is characterised into three classes: 1) poorly graded (consisting of predominantly one size class); 2) well graded (equal amounts of particles ranging from large to small); and 3) moderately graded (intermediate between poorly and well graded). As for grain support, the grading of the dam material is based on visual estimates during field reconnaissance and is reliant on a sample of dam material that best represents the overall grading (normally found in the spillway walls). Observations from the six non-failed dams indicate that four are moderately graded and two are well graded. Observations from the four failed dams indicate that three are well graded and one was moderately graded (Appendix C). In both cases, poorly graded material was not encountered, mainly because all of the dam-forming landslides are bedrock failures, which produces a relatively large variation in clast size. The general well-graded nature of the failed dams represents the presence of both large and small (matrix) particles evident in the previous support section; this may have some control on dam stability.

3.4.3 BREACH CHARACTERISTICS

Breach characteristics refer to the dimensions and shape of a void in the dam material following complete (catastrophic) removal of the dam material or partial removal from gradual erosion of a naturally formed spillway. Breach characteristics are particularly important when estimating peak flows immediately downstream of the dam following a complete dam failure. In addition, information regarding the breached section of a landslide dam can also provide insight as to the amount of erosion since formation, particularly useful for dams that have retained an impoundment but show signs of crest lowering over time. The volume of material eroded from the original dam volume (expressed as a percentage of initial dam volume) is termed degree of modification (DOM), which is an indicator of the dam's stability, as defined in Table 3.4. The DOM

when used with the current dam and lake condition allows the classification of the dam status as shown in Table 3.4.

Breach characteristics of landslide dams are estimated from sections drawn perpendicular to the valley axis using 20m contour data (Fig 3.5) and field observations, which are the best indication of breach dimensions.

Table 3.4. The degree of modification (DOM) based on the volume of material eroded from the original dam volume, which is linked to a modification index. The associated dam and lake conditions for the particular index are listed; question mark indicates some dam material or lake may remain. The dam status defines the current state of the dam where HS = highly stable, S = stable, MS = marginally stable, LF = largely failed and CF = completely failed based on the DOM and dam/lake conditions.

DOM (%)	Modification index (MI)	Dam present (✓ = yes ✗ = no)	Lake present (✓ = yes ✗ = no)	Dam status
< 10	1	✓	✓	HS
10-35	2	✓	✓	S
35-65	3	✓	✓	MS
65-90	4	✓?	?	LF
> 90	5	?	✗	CF

None of the dams studied in this thesis showed a 100% reduction in dam volume, even the dams known to have failed catastrophically, drain the entire lake but fail to remove all of the dam material (based on Figure 3.5). 25 of the 27 dams indicate gradual or catastrophic erosion of the original dam volume via overtopping of the reservoir water (inferred failure mechanism for catastrophic breaching). Matiri Right Branch (No. 10) dam was the only example where there is no evidence indicating overtopping. Field reconnaissance suggests there has never been water impounded behind the blockage; presumably because of the very small catchment size and high permeability of the dam material. In addition, there were no cases of piping failure or mass sliding of dam material creating catastrophic failure or gradual erosion of the landslide dams in the dataset. The Matakkitaki (No. 2) landslide dam was the only known case where engineering works were used to exacerbate the natural erosion of the dam material due to overtopping.

Comparison of breach dimensions for non-failed and failed dams shows a higher maximum and average breach volume for non-failed dams (Table 3.5). This is not considered significant unless it can be related to the original dam volume. The average breach depth of the failed dams is significantly higher in the failed dams, which is expected with dams displaying a high DOM.

Table 3.5. Summary of the present lake dimensions and catchment conditions from selected landslide dams, this study (see appendix one and three for terminology and source respectively)

BREACH DIMENSIONS	Max	Min	Average	No.	Max (f)	Min (f)	Average (f)	No. (f)
Breach depth (m)	45	5	14	11	40	5	18	4
Breach width (m)	100	20	58	11	330	40	142	5
Breach volume ($\times 10^3 \text{ m}^3$)	2500	200	880	10	1000	200	570	5
LAKE DIMENSIONS	Max	Min	Average	No.	Max (f)	Min (f)	Average (f)	No. (f)
Volume (original) ($\times 10^3 \text{ m}^3$)	3500	0	1800	5	15000	150	3950	5
Volume (present) ($\times 10^3 \text{ m}^3$)	6500	0	1900	12	2000	0	286	2
Surface elevation (m.a.s.l.)	930	30	470	13	450	100	248	6
Length (m)	2190	130	1040	13	6000	230	3297	6
Width (m)	420	60	200	13	450	100	221	6
Depth (m)	50	5	25	13	30	12	20	6
Area ($\times 10^3 \text{ m}^2$)	730	6	175	13	2000	15	597	5
CATCHMENT CONDITIONS	Max	Min	Average	No.	Max (f)	Min (f)	Average (f)	No. (f)
Drainage Basin Area (km^2)	875	2	79	18	4400	4	861	8
Yearly precipitation (mm)	3694	1255	2378	18	3694	1931	2505	8
Monthly precipitation (mm)	307	104	198	18	307	160	208	8
Maximum monthly precipitation (mm)	856	360	591	18	1029	182	663	8
Mean monthly discharge (m^3)	55	11	33	2	470	58	184	4
Maximum monthly discharge (m^3)	170	38	104	2	1616	125	612	4
Valley width (m)	1500	50	259	18	650	50	265	8
Valley elevation (m)	870	15	464	17	600	95	271	8
Valley gradient downstream of dam ($^\circ$)	13	0.5	3.0	18	8.0	0.5	3.0	8
Valley gradient upstream of dam ($^\circ$)	9	0.5	2.5	17	9.5	0.5	3.0	8

3.4.4 LAKE CHARACTERISTICS

The lake characteristics are concerned with the dimensions of an impounded body of water (herein called lake) behind a landslide dam. With particular reference to the dams in this dataset, the lake dimensions are taken from the present lake for dams that still impound water. For the dams that do not retain a lake, such as the eight dams in the previous section with Modification Index (MI) of 3, 4 or 5, the dimensions of the lake prior to failure are recorded. These lake dimensions prior to failure can be used to assess the stability of the dam using empirically derived indices (see section 3.5) and to estimate the peak flows that occurred immediately downstream of the dam following failure. For the non-failed dams that currently retain a lake, the dimensions are important in estimating the flood hazard from a possible future dam failure.

The present lake volume is estimated based on the current depth, length and width of the lake (Fig 3.5) and the valley floor gradient taken from 20m contour topographic maps and schematic cross sections. The original lake volume estimations are based on documented

reports, which usually give lake area and depth information (e.g. Henderson, 1937). Field reconnaissance can also indicate original lake dimensions (Section 5.4 on Rain Peak landslide dam, No. 16) (Table 3.5).

The original lake volume could only be estimated for 5 of the 18 non-failed dams because of a lack of sufficient evidence. Thus the maximum original volumes for non-failed dams is 50% less than the present volume, which could be estimated for 12 of the 18 non-failed dams, and is therefore not considered relevant.

The original lake volume could be estimated for five of the eight failed dams in the dataset, which show an average volume almost 50% larger than the five non-failed dams (Table 3.5). In addition, the maximum lake volume (prior to failure) was $15 \times 10^6 \text{ m}^3$ as opposed to the maximum non-failed dam volume (in both the present and original) of $6.5 \times 10^6 \text{ m}^3$. Together, the average and maximum lake volumes suggest an important relationship between lake volume and dam failure, suggesting the dams associated with large impoundments tend to fail as opposed to dams associated with smaller impoundments. This fact is supported by the smaller lake lengths in the non-failed dams as opposed to failed dams (Table 3.5). A similar pattern to lake volume is seen in the lake area estimated from 20m topographical maps, with the failed dams having on average a 70% larger lake area, which should correspond to a larger lake length and volume (which is what we see in Table 3.5). This suggests that dams associated with lakes with a large surface area tend to fail as opposed to dams with smaller lake areas. Note the average lake surface area for failed dams is estimated for five dams as opposed to 13 for the non-failed dams.

Lake surface elevation is the height (in meters) of the lake surface above mean sea level, which is estimated from topographic maps and sections through the landslide dam perpendicular to the valley axis. This could be estimated for 13 of the 18 non-failed landslide dams using the original lake elevation, which if not known, its present elevation is used, likewise for six of the eight failed dams. The results indicate that the average surface elevation of the failed dams is almost 50% lower than the average surface elevation for the non-failed dams (248 and 470 m.a.s.l. respectively, Table 3.5). This suggests that the lower the lake elevation the lower the stream order (i.e. larger catchment), which decreases the dams ability to resist erosion.

3.4.5 CATCHMENT CHARACTERISTICS

The catchment characteristics (also known as watershed) are important in determining the amount of water available to remove the dam material that is blocking the flow in a river. In particular, the size of the catchment at the point of blockage and the amount of rainfall within the catchment will largely control the amount of water passing the point of blockage. These two attributes have been recorded for the landslide dams in the dataset, and are summarised in Table 3.5. The catchment area is defined as the total area from which a single river collects surface runoff (drainage basin area) and is measured in this dataset in km^2 . When comparing the average catchment area for all 18 non-failed dams with the eight failed dams in the dataset (Table 3.5), the catchment area of failed dams is over 90% larger than that from the non-failed landslide dams. The average area for failed dams is particularly high due to the Buller (No. 26) landslide dam, which has an area of 4400 km^2 . However, the average area for the remaining seven failed dams is still 78% larger than the average area for the 18 non-failed dams, suggesting that the larger the catchment area above the point of blockage, the less likely the dam will survive. It is important to note that two dams (Rain Peak and Ram Creek, No. 16 and 25) which have relatively small catchments, have failed suggesting that the catchment area is not the sole control on dam stability. These two dams are analysed in detail in Chapter 5.

3.4.5.1 Hydrology

The precipitation throughout the dam's catchment area is relatively uniform averaging $\sim 2.5\text{m}$ per annum for both failed and non-failed dams (values are based on the closest rain gage to the dam site (*pers comm.*, K. Walter, NIWA, 2003)).

The discharge of the river past the point of blockage could only be quantified for two of the 18 non-failed dams and four of the eight failed dams. Results show that the failed dams have a higher average discharge than the non-failed dams. This could be related to the higher average catchment area associated with the failed dams (Table 3.5).

3.4.5.2 Valley morphology

Valley width measures the horizontal distance on the valley floor from one valley side to the other at the point of blockage (Fig 3.5). Table 3.5 lists the resulting valley widths, which show little variation in the average width between failed and non-failed dams. Valley elevation is defined as the height of the valley floor in meters above mean sea level

at the point of blockage prior to dam formation. The resulting heights are summarised in Table 3.4, which show similar results to the lake surface elevation trends with the non-failed dams tending to form in valleys with an elevation $\sim 50\%$ higher than in failed dams. This suggests that dams that form at a higher elevation may have a lower stream order (have a smaller catchment area) with less stream power to erode the dam material.

The valley gradient defines the average slope of the valley floor prior to dam formation, and is recorded upstream and downstream of the point of blockage. The resulting gradients for the dams in the dataset are summarised in Table 3.5, which show little variation in average gradient between failed and non-failed dams both upstream and downstream of the dam. This suggests that the valley gradient does not directly affect the stability of a dam however; it is likely to influence other parameters such as lake dimensions etc.

3.4.6 DEATHS AND DAMAGE

Fortunately, there has been no loss of life from the failure of any landslide dams in the Murchison dataset. However, there has been significant damage to infrastructure caused by the failure of three landslide dams in the dataset namely Garibaldi (No. 22), Lake Perrine (No. 9) and Ram Creek (No. 25). Garibaldi and Lake Perrine landslide dams formed in 1929 from the Murchison earthquake and failed six months and two weeks later, respectively. Lake Perrine failure caused a flood that covered the Seddonville flat about 10 km west of the dam and shifted houses from their foundations. The failure of Garibaldi caused extensive flooding in Karamea, 25 km to the southwest of the dam.

Ram Creek landslide dam formed from the 1968 Inangahua earthquake. Its catastrophic failure in 1981 destroyed a bridge 5km downstream and nearly swept two occupants of a car on the bridge away. The flood also deposited up to 10 m of sediment over about 120,000 m² of farmland.

3.5 DAM DEVELOPMENT AND STABILITY ANALYSIS USING GEOMORPHIC INDICES

3.5.1 BACKGROUND

Swanson (1986), Canuti *et al.* (1998) and Casagli and Ermini (1999) demonstrated how a number of geomorphic parameters such as dam height, dam and lake volume, and

catchment area control the post-formation development of a dam (i.e. catastrophic failure, gradual erosion or no erosion of the dam material post-formation). They all consider dam volume to be an important factor in influencing post-formation development of a dam since it controls the dam self-weight; the catchment area at the point of blockage is also considered another main destabilising factor since it controls the channel discharge and stream power and, indirectly, the dam shape.

Canuti *et al.* (1998) and Casagli and Ermini (1999) used a dataset of about 60 landslide dams formed in the Northern Apennines, Italy, to produce an impoundment index (I_i) defined as the volume of the impounded water (lake) to the volume of the dam, to assess the stability of an already formed dam.

$$I_i = \log\left(\frac{V_d}{V_l}\right) \quad \text{Equation 3.1}$$

where V_d is the dam volume (m^3) and V_l the impoundment volume (m^3).

Canuti *et al.* (1998) and Casagli and Ermini (1999) used the same dataset to define a blockage index (BI) as a preliminary forecast of the dam development according to the expression:

$$BI = \log\left(\frac{V_d}{A_b}\right) \quad \text{Equation 3.2}$$

where V_d is the dam volume (m^3) and A_b the catchment area (km^2). In an attempt to improve this model, Ermini and Casagli (2002), used a larger dataset of 84 landslide dams occurring throughout the world to test a new dimensionless blockage index (DBI) according to:

$$DBI = \log\left(\frac{A_b \times H_d}{V_d}\right) \quad \text{Equation 3.3}$$

where H_d represents height of the dam (m), A_b the catchment area (m^2), and V_d the dam volume (m^3). They identify dam height as being an important parameter in assessing the stability of a landslide dam against both overtopping and piping failure mechanisms (Section 2.3.3). The dam height influences the steepness, among other things, of the dam slope downstream and hence the velocity and erosivity of the water when the dam crest is overtopped; while in piping failure it controls the position of the water table through the dams and, in particular, the hydraulic gradient (Ermini and Casagli (2002)).

The aforementioned geomorphic indices are applied to the landslide dams in this study to assess their applicability and accuracy in determining the dam development, and to establish if dam development can be accurately assessed using only the parameters applied in the indices. Terminology is adopted from Ermini and Casagli (2002) which characterises the landslide dams into two broad classes, based on their observed/inferred evolution. This terminology is tested in the selected dams in the Murchison dataset, using re-defined terminology (see section 3.2.5 for definitions).

Dam volume and height of the dam crest above the original valley floor data used to test the indices are based on the original dam dimensions, where known, allowing contrasts between the predicted dam development to the actual dam development, or state, of the dams. If the original dam dimensions are not known the present dimensions are used to predict the I_i , BI and DBI based on the assumption that there has been little change from the original dimensions. The I_i is thought to be useful in predicting the stability of an already existing landslide dam that impounds water, however where known, the original dam and lake volumes are used to compare what was predicted by the index with the current state of the dams. The following section documents and discusses the accuracy of the I_i , BI and DBI when applied to the landslide dams in the dataset, this thesis.

3.5.2 IMPOUNDMENT INDEX (I_i)

The I_i is defined as the logarithm of the ratio between dam volume and lake volume Equation 3.1 (Casagli and Ermini, 1999), and is thought to be useful for assessing the stability of an already formed dam. Casagli and Ermini (1999) used approximately 25 landslide dam cases from the Northern Apennines, Italy, where the dam and lake volume could be accurately quantified to plot a bi-logarithmic graph of dam volume against lake volume. They found that 100% of the stable dams had I_i values > 0 , and 80 % of the dams that failed had I_i values < 0 (i.e. if $V_d > V_l$, its log of this ratio is positive; if $V_d < V_l$, the log of this ratio is negative). This formed two distinct zones separated by the $I_i = 0$ fixed value line, which is inferred to separate stable from unstable dams based on Ermini and Casagli (2003) stability definitions. As for the previous sections, this index has been applied to the dams in this study to test the applicability and accuracy of the forecasted evolution.

In 20 of the 26 dams in this study, the lake volume could be estimated, and the I_i value calculated and plotted against the dam volume (Fig 3.6 a).

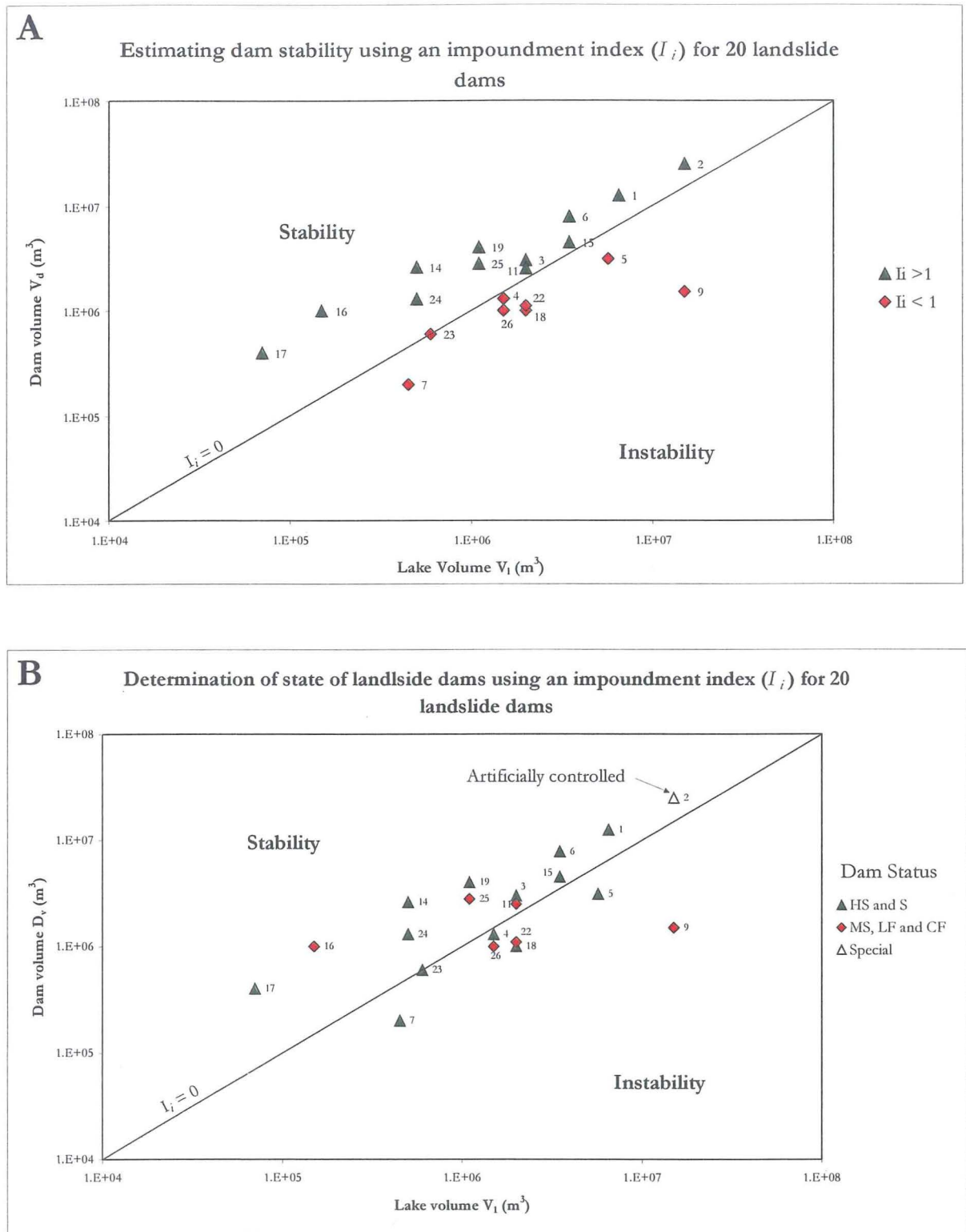


Fig. 3.6. A. Landslide dam volume versus lake volume defining stable and unstable domains for 19 landslide dams formed in northwest Nelson. Numbers adjacent to points refer to database reference number. **B.** Dam volume versus lake volume showing actual state of landslide dams from Fig. 24. Terminology is based on Casagli and Ermini (1999) in their description of stability and instability related to the state of a landslide dam (see text for terminology definition). Annotations relate to the dams labeled special.

12 of the 20 dams plot in the stability domain ($I_i > 0$), while the remaining eight plot in the instability domain ($I_i < 0$) (Fig 3.6 a). This is the predicted post-formation development of the 20 dams based on their dam and lake volumes following their formation.

To test the applicability of the I_i , the 20 dams were characterised, based on their dam status, as being either highly stable (HS), stable (S), marginally stable (MS), largely failed (LF), and completely failed (CF) (Table 3.4). Using the same index, the dams could then be colour coded to match their current state of stability to compare the forecasted with their actual post-formation development (Fig 3.6 b).

The results are as follows:

- Eight of 13 dams characterised as HS or S (excluding Matakkitaki No. 2) plot correctly in the stability domain on the log-log graph ($I_i > 0$), the remaining five plot incorrectly in the instability domain ($I_i < 0$) (Fig 3.6 b)
- Three of six dams characterised as MS, LF or CF plot correctly in the instability domain, the remaining three dams plot incorrectly in the stability domain.
- One dam (Matakkitaki No. 2) was artificially lowered, however plots in the stability zone and has not been considered when assessing the applicability of the index.

Clearly, the I_i is a relatively simple index that only considers two parameters in the prediction of a dam's post-formation development. As a result, the prediction of the dams' correct post-formation development was only achieved for 11 of the 19 assessed dams in the dataset, this thesis. Lake Matiri (No. 2, Fig 3.6 b) for example, is a highly stable dam, which has survived for ~ 300 yrs yet has an I_i value < 0 that corresponds to the unstable domain (this dam is discussed in detail in Chapter 5). This suggests that other parameters other than dam and lake volume influence dam stability. The dam status of Ram Creek (No.25), Rain Peak (No. 16) and Lake Perrine (No. 11) landslide dams is characterised as CF (completely failed) (Fig 3.6 b), yet their I_i values are > 0 suggesting the dams should be stable, based on the stability definition by Ermini and Casagli (2003).

3.5.3 BLOCKAGE INDEX (BI)

The BI is defined as the logarithm of the ratio between dam volume and catchment size at the point of blockage (Equation 1 after Casagli and Ermini, 1999). Results obtained from c. 65 landslide dams formed in the Northern Apennines allowed Canuti et al., (1998) and Casagli and Ermini (1999) to propose upper and lower bounds to predict the post-

formation development of a dam (described as ‘blockage evolution’ by Casagli and Ermini (1999)). Fixed values of the index (i.e. $V_d = 1$ and $A_b = 1$) plot as a straight line on bi-logarithmic graph paper, suggesting that an upper boundary for failed dams is given by $BI = 5$, and the lower boundary for stable dams is given approximately by $BI = 4$, while a lower boundary for cases of complete dam formation is given by $BI = 3$ (Terminology based on Casagli and Ermini (1999) and Ermini and Casagli, 2003, section 3.2.5). These boundary conditions allowed the division of the c.65 Italian case examples into four domains based on their observed post-formation development as either:

1. Dams not formed ($BI < 3$)
2. Unstable dams (BI between 3-4)
3. Uncertain evolution (BI between 4-5)
4. Stable dams ($BI > 5$)

Casagli and Ermini (1999) suggested that the BI could be employed to forecast the ‘evolution’ of future landslide-damming events (in the Northern Apennines). The terminology used to define the domains is taken from Casagli and Ermini (1999) but these authors do not reference to their exact meaning but it is interpreted here as the post-formation development of a dam.

Dam volume could only be estimated for 23 of the 26 landslide dams when assessing the applicability of the BI in forecasting the post-formation development of dams in the dataset, this thesis; BI values for the 23 landslide dams are plotted on a bi-logarithmic graph (Fig 3.7 a), and should predict the post-formation development of the individual dams. The dam volumes for the remaining three (Lake Dora, No. 7; Lower Stanley, No. 12; Ferris, No.21) could not be accurately calculated and were therefore omitted from the index calculations.

Fig 3.7 a shows that the dams are represented in all four possible domains. 11 of the 23 dams have a BI value > 5 which plot in the stability domain; six plot in the uncertain domain (BI between 4-5); five dams plots in the unstable domain (BI between 3-4) with the remaining one dam plotting in the dams not formed domain ($BI < 3$) (terminology follows Casagli and Ermini, 1999).

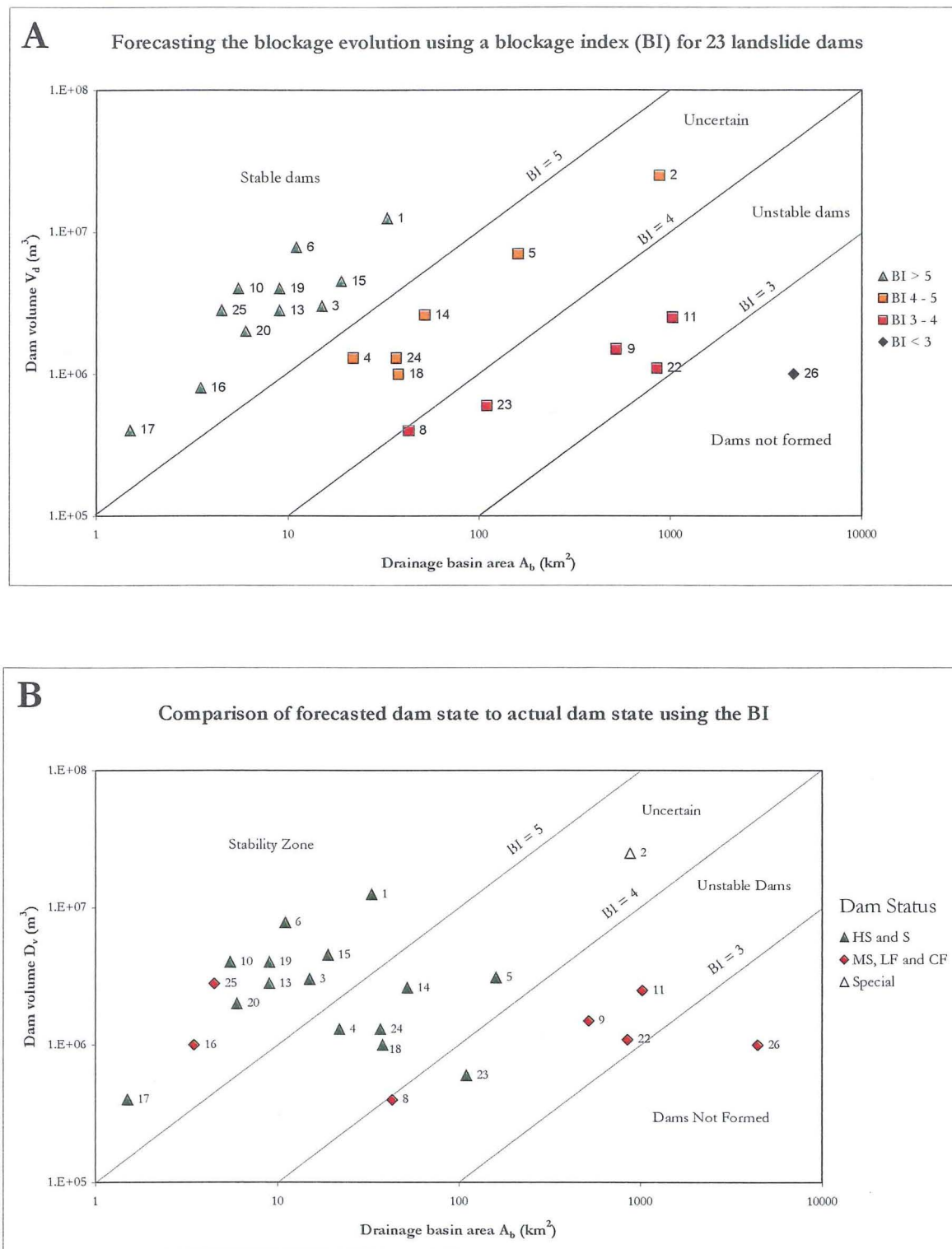


Fig. 3.7. A. Landslide dam volume versus drainage basin area for 23 landslide dams located throughout northwest Nelson defining stable and unstable domains. Numbers adjacent to points refer to database reference number. **B.** Comparison of actual state of landslide dam to that forecast using the BI. The terms stable and unstable are defined by Casagli and Ermini (1999); they have been used to describe the state of landslide dams in northwest Nelson (see text for definitions). Dams not formed and special cases are highlighted where appropriate.

To test the applicability of this index in 23 landslide dams in this dataset, each dam was characterised based on its dam status as being either highly stable (HS), S (stable), marginally stable (MS), largely failed (LF), and completely failed (CF) (Table 3.4). Using the same index, the dams could then be colour coded to match their current state of stability to compare the forecasted with their actual post-formation development (Fig 3.10).

The results (Fig 3.10) show that:

- 14 of the 15 dams characterised as HS or S plot above the lower boundary for stable dams (i.e. $BI > 4$) with one plotting in the unstable domain, suggesting this dam should have failed yet it has not.
- Five of the seven dams characterised as MS, LF or CF plot below the upper boundary for unstable or failed dams ($BI < 5$); the remaining two plot within the stability domain indicating they should not have failed but have done so some time after dam formation.
- One dam (Matakitaki, No. 2) has been classed as special because it was artificially controlled by blasting of the dam material; however, it does plot in the uncertain domain but it is not considered in this analysis when assessing the applicability of the BI .

Overall, the BI seems to have predicted the correct post-formation development for 19 of the 22 dams analysed (excluding Matakitaki, No. 2). However two of the three dams that are predicted to be stable (Ram Creek, No. 25 and Rain Peak, No. 16), failed catastrophically some time after formation. The Ram Creek landslide dam completely failed almost 13 years after its formation, while Rain Peak landslide dam failed completely during a series of catastrophic breaching events over a 50-year period. This suggests that parameters other than those used by the BI have controlled the post-formation development of these two dams. However, the BI did predict their short-term (< 10 year) post-formation development correctly.

3.5.4 DIMENSIONLESS BLOCKAGE INDEX (DBI)

The DBI is defined as the logarithm of the ratio between the product of the catchment area multiplied by the height of the dam and the dam volume (Equation 2 from Ermini and Casagli, 2002), which incorporates similar parameters to the BI , the difference being the

inclusion of the dam height, making the index dimensionless. Ermini and Casagli (2002) applied the index to 84 landslide dam cases inventoried worldwide (Chapter 2), to defined three main domains as follows:

- $DBI < 2.75$ Stability Domain
- $2.75 - 3.08$ Uncertain Domain
- $DBI > 3.08$ Instability Domain

Where ‘stability’ is defined as a landslide dam that has remained stable and has not encountered a breach thus still impounding an existing or relict lake; and unstable defined as landslide dam that has undergone erosion or collapse leading to the catastrophic breach, with subsequent release of impounded lake waters (Ermini and Casagli, 2003).

Ermini and Casagli (2003) cite five exceptions within the 84 cases (6%) that display *DBI* values that do not correspond to the actual state of the dam, and do not consider the age of the landslide dams. In three of the five cases, the *DBI* predicted the dams should be stable but have failed, and the causes of failure were attributed to high rainfall and overtopping waves produced in the impoundment. Two of the five dams plotted in the instability domain yet are currently stable after an unknown period since their formation; this has been attributed to high rates of seepage through the dam and dam material comprising heterogeneous mass of large ($> 5\text{m}$) blocks of rock. The remaining 79 dams (94%) behave as the model predicts. This is a good correlation coefficient and is therefore the basis for the domain selection.

DBI values are calculated for 22 of the 26 landslide dams in this study, four not being considered because accurate estimations of dam height were not available. These are then graphed on a bi-logarithmic plot to illustrate the predicted post-formation development of the dams using their *DBI* value (Fig. 3.8 a).

DBI calculations show 12 of the 22 Murchison and Inangahua dams plot in the stability domain ($DBI < 2.75$), five dams plot in the uncertain domain ($DBI 2.75 - 3.08$) and the remaining five dams plotting in the instability domain ($DBI > 3.08$).

As for the *BI*, the applicability of the *DBI* can be tested for the 22 landslide dams by characterising them into groups based on their dam status (e.g. HS, S, MS, LF, and CF; Table 3.4). The individual dams can then be re-plotted on the bi-logarithmic graph and colour-coded to show their current state to compare with the predicted state of stability (Fig 3.8 b)

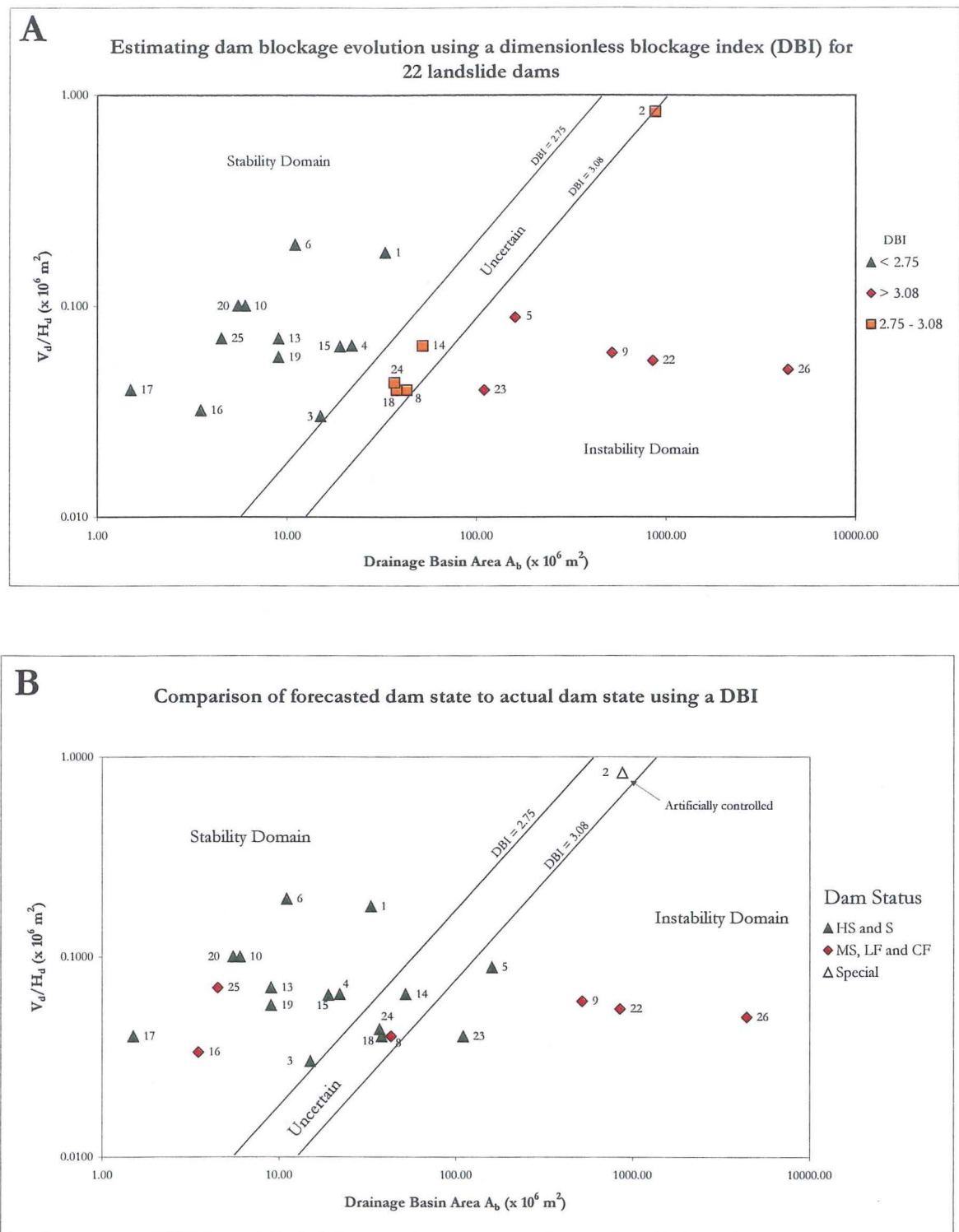


Fig 3.8. A. Calculated dimensionless blockage index (DBI) for 22 landslide dams located throughout northwest Nelson indicating stable (<2.75) and unstable (>3.08) domains. Numbers adjacent to points refer to database reference number. **B.** Comparison of actual state of landslide dam to that forecast using the DBI. The terms stable and unstable are defined by Casagli and Ermini (1999); they have been used to describe the state of landslide dams in northwest Nelson (see text for definitions).

The results show that:

- 10 of the 15 dams characterised as HS or S plot correctly within the stable domain ($DBI < 2.75$), three dams plot in the uncertain domain ($DBI 2.75-3.08$) with two dams plotting in the instability domain ($DBI > 3.08$) suggesting these dams should have failed yet have not.
- Three of the six dams characterised as MS, LF or CF plot correctly within the instability domain, one dam plots in the uncertain domain and two plot incorrectly in the stability domain indicating they should not have failed yet they have failed some time after dam formation.
- The Matakita, No. 2 landslide dam, as with the BI and I_i , is not considered in this assessment of DBI as it has been artificially controlled.

Assuming the post-formation evolution of the dams that plot in the uncertain domain are correctly predicted, the DBI predicted the post-formation development correctly for 17 of the 21 dams (81%), and incorrectly for four (19%).

As with the BI and I_i , the DBI incorrectly predicts Ram Creek (No. 25) and Rain Peak (No. 16) landslide dams to be stable, yet they have a current dam status of CF (completely failed). Likewise, with Lake Matiri (No. 5) and Lake Moonstone (No. 23), however in this case the DBI incorrectly predicts the dams to be unstable yet the dam status of both dams is HS. Thus the accuracy of the DBI in predicting the post-formation development of 17 dams in the Murchison dataset is lower than the accuracy obtained from the c. 85 landslide dams used in Ermini and Casagli's (2003) study. (i.e. 81% accuracy, Murchison study, as opposed to 94% from Ermini and Casagli (2003)).

3.6 CHAPTER 3 SYNTHESIS

The M 7.8 Murchison earthquake of 1929 and the M_s 7.2 Inangahua earthquake of 1968 produced innumerable landslides and formed hundreds of landslide dams, of which 26 of the largest ($> 100,000 \text{ m}^3$) were used to form a dataset of landslide dams in northwest Nelson.

Dam-forming source landslide, dam, lake and catchment characteristics are all parameters considered important in characterising a landslide dam, and are included in the Murchison dataset.

Dam, lake, catchment and landslide characteristics from the 26 failed and non-failed landslide dams in the Murchison dataset were collated and analysed by distinguishing failed from non-failed dams, and then assessing the parameters common to both. Parameters relating to the dam-forming landslides that were assessed included the source rock mass and material characteristics, and the type and dimensions of landsliding. Parameters relating to the dam, lake and catchment included dam material characteristics, dam dimensions, lake dimensions and the catchment area.

Parameters that influence the post-formation development of selected landslide dams in the dataset include the dam volume, catchment area above the point of blockage, average block size of material comprising the dam, slope angle of the downstream dam face, and rock mass and material characteristics in the source area of the dam-forming landslide. The stability of the dams in the Murchison dataset was not significantly affected by rock type, landslide movement, and the state, distribution and style of dam-forming landslide activity.

Geomorphic indices use a combination of dam volume, dam height, lake volume and catchment area above the point of blockage to predict the post-formation development of a landslide dam. The geomorphic indices analysed here include the Impoundment Index (I_i), Blockage Index (BI), and a Dimensionless Blockage Index (DBI) as developed by Casagli and Ermini (1999) and Ermini and Casagli (2003).

Application of geomorphic indices to selected dams in the dataset gave generally good results (Table 3.6). The Impoundment Index (I_i) predicted the correct post-formation development for 58% of the dams used for its analysis; Blockage Index (BI) correctly predicted the post-formation development for 86% of the dams; and the Dimensionless Blockage Index (DBI) correctly predicted the post-formation development for 81% of the applied dams.

Table 3.6. Summary of the effectiveness of the I_i , BI and DBI in forecasting the post-formation dam development. The number of dams used for the DBI does not include the 4 dams that plotted in the uncertain domain.

Index	Number of dams used for index	Total No. of dams correctly predicted	Percentage of dams correctly predicted
I_i	19	11	58
BI	22	19	86
DBI	21	17	81

Chapter 4

LAKE STANLEY CASE STUDY

4.1 INTRODUCTION

Following the discussion at the end of Chapter Three, it is clear that the geomorphic indices used to forecast the post-formation development of a landslide dam give ambiguous results. Therefore, in order to assess additional parameters that may influence or control the post-formation development of a dam, a detailed analysis of one landslide dam, Lake Stanley (No. 1), that agrees with the predicted post-formation development according to geomorphic indices is analysed in Chapter 5. Three additional dams, Lake Matiri (No. 5), Rain Peak (No. 16), and Ram Creek (No.25) whose post-formation differs from that predicted by the indices, are analysed in Chapter 5.

Chapter 4 is concerned with the Lake Stanley landslide dam, which is the largest in the database with a volume of at $12.5 \times 10^6 \text{ m}^3$. The I_i , BI and DBI all predict the dam should remain stable; it is the aim of this chapter to assess the overall stability of the landslide dam as compared to the predicted index, based on the historical and observed evolution.

The aims of this chapter are to:

- Provide a detailed account of Lake Stanley landslide dam formation and evaluate current hazards associated with Lake Stanley landslide dam;
- Evaluate future performance of Lake Stanley landslide dam;
- Evaluate the application of the Impoundment Index (I_i), Blockage Index (BI) and the Dimensionless Blockage Index (DBI) proposed by Casagli and Ermini (1999) and Ermini and Casagli (2003); and
- Discuss the primary influences on Lake Stanley landslide dam stability.

4.2 LAKE STANLEY LOCATION AND GEOLOGICAL SETTING

4.2.1 GENERAL DETAILS

Lake Stanley is located in northwest Nelson, South Island, New Zealand, within the Kahurangi National Park (Fig 4.1). The Stanley River drains southeast into the Waingaro River, which flows north to its confluence with the Takaka River, 2 km south of Takaka Township, Golden Bay. The lake was formed from a succession of landslides from the southern valley wall spanning several hundred years, which blocked the Stanley River forming Lake Stanley. The lake has a surface elevation of 770 m above sea level (m.a.s.l.), is currently 2,200m long, approximately 300 to 400m wide and has a current depth of 20m (Muller, 1997). The lake has a present estimated volume of approximately $6.5 \times 10^6 \text{ m}^3$ and a surface area of $0.75 \times 10^3 \text{ m}^2$ (Map1)

Drainage of the lake is via overtopping at the minimum crest height (770 m.a.s.l.) through a natural spillway consisting of large angular volcanogenic sedimentary and igneous rocks at the base of the southern valley wall. The total volume from all landsliding from the southern valley wall source is approximately $18 \times 10^6 \text{ m}^3$, and their movement is known to have occurred from multiple events separated by several centuries. This debris has contributed to the total landslide dam volume of $12.5 \times 10^6 \text{ m}^3$ (based on the definitions in chapter 3), with redistribution/reworking of approximately $6.5 \times 10^6 \text{ m}^3$ within the Stanley River to a distance of approximately 2 km downstream of the dam site, and about $4.5 \times 10^6 \text{ m}^3$ resting on the dam material above the lake level on the northern flank of the valley (Map 1). The catchment area above the point of blockage is 33 km^2 and receives on average 3,700mm of precipitation per year (*pers comm.* Martin Doyle, Tasman District Council, 2003).

The lake is characterised by dead tree stumps that protrude several meters above the lake level (which changes with seasonal lake level variation) and covers about 75% of the lake surface area (Fig 4.2). This suggests a rather uniform, slightly undulating lake bathymetry from approximately upstream of the three islands within the lake (Map 1). The deepest section of the lake is between the islands and the dam material, showing a maximum depth of 20m (Stocker, 1997).

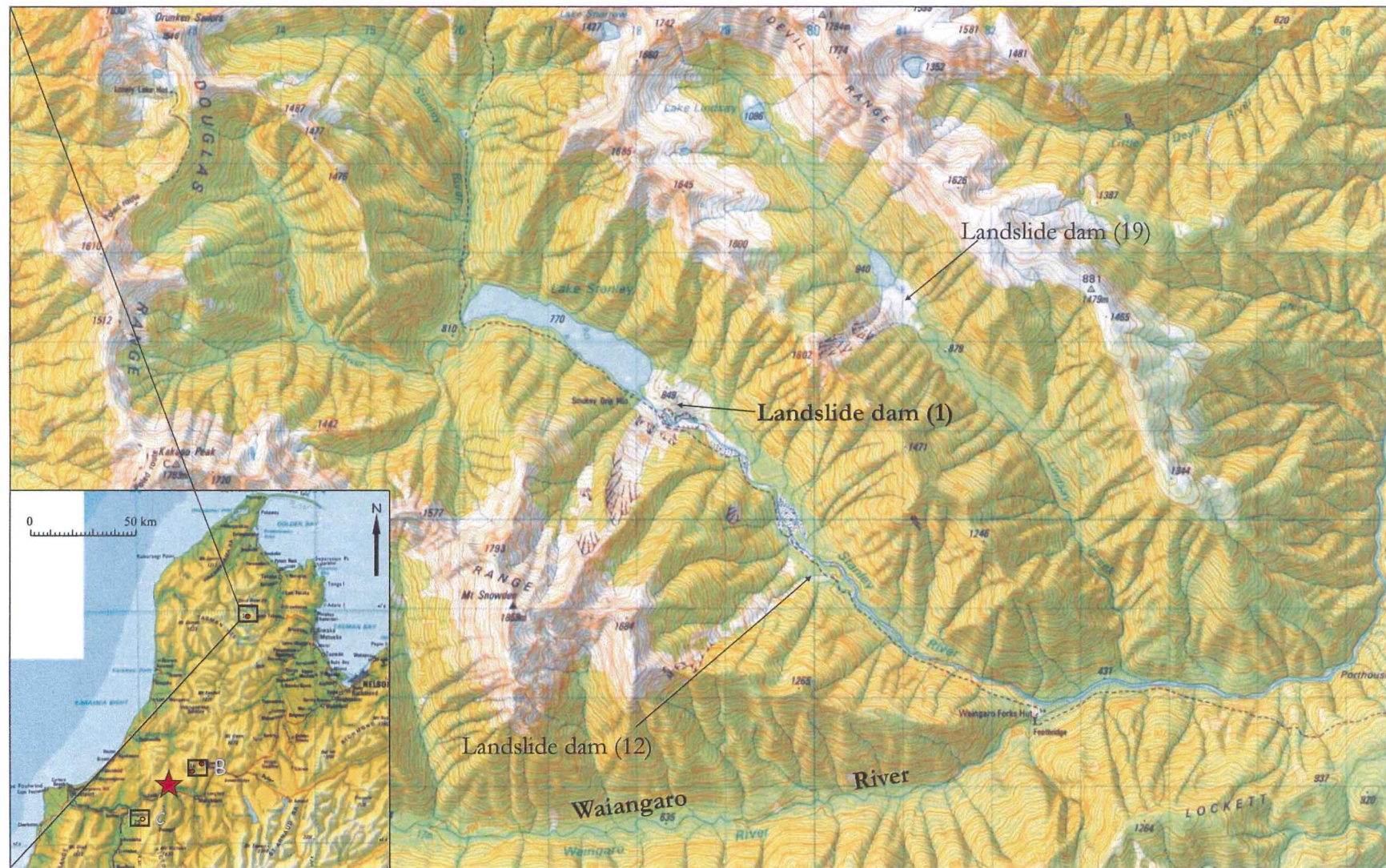


Fig. 4.1. Location map of Lake Stanley landslide dam (1). Lindsay (19) and Lower Stanley landslide dams are also visible in the Lindsay and Stanley Rivers respectively. B and C (inset) illustrate the locations of Lake Matiri/Rain Peak and Ram Creek landslide dams respectively.



Fig 4.2. View of Lake Stanley looking northeast at location 2 (engineering geological map) with the landslide dam (ld) material in the background. The average lake elevation is 770 m.a.s.l. The brown staining on the tree stumps indicates a lake level higher than present caused by either seasonal variation (location 1 Map 1) (Photo source: D Nottage; photo taken 13.3.1997, person unknown).



Fig 4.3. Aerial oblique photograph of Lake Stanley dam-forming landslide looking southwest. The landslide is divided into three zones displaying contrasting lithological composition and temporal activation. Zone I is the main source of landslide debris for the pre-1929 landslide, 1929 landslide, and landsliding between 1929 and 1968. The most recent landslide was from Zone II in 1994 and is clearly distinguished in the photo. River drains from right to left (photo taken by T. Nash December 2002).

Two main reports have been initiated by the Tasman District Council to assess the current state of Lake Stanley. Muller (1997) detailed the geology, interpreted the geomorphologic setting and outlined some probable future trends of the landslide. Stocker (1997) conducted a hazard assessment of Lake Stanley landslide dam, outlining the impacts and likelihood of further landslides into the lake and onto the existing dam. Both reports concluded from qualitative investigations that the dam is relatively stable, and noted that future landslides from the southern valley wall has the potential re-dam and further raise the lake level.

Field reconnaissance was carried out as part of this study in February 2003 inspecting the dam, landslide, spillway and reworked material downstream of the dam. Aerial oblique photographs were taken of the landslide, lake and dam site in December 2002 and February 2003. Documentation of the landslide prior to the aforementioned fieldwork is dominated by oblique aerial photographs of the dam and lake by L. Homer (IGNS various years). The only documented report with associated field reconnaissance of Lake Stanley, was carried out in 1997 by M. Muller in 'Landslides at Lake Stanley', the focus being on the geological nature of the surrounding rock masses and descriptions of the 1994 landslide.

4.2.2 GEOLOGICAL SETTING

The material comprising the dam is from the Takaka Terrane, which comprises volcanogenic sedimentary rocks, sheet lavas and argillitic porphyry rocks from the Devil River Volcanics Formation of Devonian age (Munker and Cooper, 1999). The internally highly disrupted Takaka Terrane is composed of at least 13 north-south trending fault-bounded slices (Rattenbury *et al.*, 1998), and has been tectonically deformed in at least four major episodes. Most Takaka Terrane units show brittle deformation and are weakly metamorphosed (Munker and Cooper, 1999). Shallow (< 15 km deep) earthquake epicentres have been located in the area in historical times, but shaking intensities of MM7 or greater have occurred at least six times in the past 150 years from earthquakes sourced within 200km of the dam site (Rattenbury *et al.*, (compilers) 1998).

The cross sectional valley morphology is U-shaped (Map 1) suggesting significant glaciation from the last glaciation c. 18,000 years ago. Schulmeister *et al.* (2001) suggest that there have been at least two, and as many as four phases of glaciation in the area during the last glaciation.

4.3 LANDSLIDE SOURCE AREA CHARACTERISTICS

Landsliding at Lake Stanley is comprised of a succession of landslides (described in detail in section 4.4) that can be generally described as a rock avalanches with a total initial (in-situ) volume for all landsliding of $18 \times 10^6 \text{ m}^3$, total rupture length of 1,150m, total width of 360m, total depth of 50m, head elevation of 1,400 m.a.s.l., and toe elevation of 700 m.a.s.l. (Map 1). The landslides have developed in rocks from the 510 Ma Devil River Volcanics Group, and in particular, the Benson Volcanics, described as basalt and basaltic andesite, and volcanoclastic deposits with andesite, rhyolite and dacite intrusives (Rattenbury *et al.*, 1998). The rock mass properties of the source rock are highly variable throughout the landslide complex, however they are generally highly fragmented as a result of their tectonic history and age.

The landslide complex is divided into 3 main zones (Fig 4.3) that correspond to spatially and temporally variable landslide events, landslide types and source rock characteristics. The source rock characteristics for each zone are discussed next followed by the temporal distribution of landsliding at Lake Stanley.

4.3.1 ZONE I

4.3.1.1 Landslide characteristics

Zone I extends from the head of the slide at 1,430 m.a.s.l., to a break in slope at about 1,050 m.a.s.l. (Map 1 and Fig 4.3), with an average width of 350m, a maximum depth of 50m from the inferred original topographic profile. Zone I has contributed between 50 and 60% of the overall landslide volume. Its average slope is 35° , with scree covering the majority of the failure surface at its angle of repose of about 32° , and it is comprised of strong to very strong slightly weathered angular volcanogenic rock material that is easily mobilised when disturbed.

The geological composition of Zone I consists of thinly bedded (200mm thick) volcanoclastic, fine-grained sedimentary rocks that strike north south and steeply dip to the east $> 70^\circ$. Structurally, the source rock is highly variable according to outcropping rocks from the eastern and western lateral margins of the landslide. These rocks are separated by a lithological or structural boundary (i.e. a fault) with a similar trend to the bedding of

outcropping rocks on the western lateral margin of the landslide (Zone I) (Map 1, red dashed line).

The mechanism of landsliding in Zone I is based on the outcropping rock mass characteristics exposed in the eastern lateral margin of the landslide that display planar slickensided joints sets (Fig 4.4). Failure on these highly persistent ($> 20\text{m}$) joint surfaces is inferred to be the main failure mechanism for Zone I.

Zone I landslide failure surface is concave based on profiles drawn from 1:50,000 topographical data, which are probably only accurate to $\pm 10\text{m}$ (Map 1). The failure surface is estimated to be a maximum of approximately 40–50m below the origin ground surface at the centre of the slide complex.

4.3.1.2 Head and Eastern lateral margin rock mass characteristics

The same outcropping rock is exposed in the head of the landslide and eastern margin. This rock mass consists of volcanoclastic sedimentary rocks with very close to very wide (5–2,000mm) defect spacing, low to very high (0.5 - $> 10\text{m}$) defect persistence, and an average unit block size ranging between very small ($< 10\text{mm}$) and very large ($> 1000\text{mm}$) (Fig 4.4).

4.3.1.3 Western lateral margin rock mass characteristics

The western lateral margin exposes highly jointed volcanoclastic bedrock rock mass with extremely close to close defect spacing ($< 100\text{mm}$), very low to low defect persistence ($< 2\text{m}$), and a very small to small average unit block size ($< 10\text{mm}$ equivalent cube side) (Fig 4.5). Rock material shed from this margin is moderately weathered, moderately strong to strong; brownish blue massive volcanically derived sedimentary rock, which differs slightly from the stronger and less weathered landslide head and eastern margin rocks.

4.3.2 ZONE II

Zone II extends from 1,050 m.a.s.l. to a break in slope at 850 m.a.s.l. (Fig 4.3), with an average slope angle of 24° , width of 400m and an estimated depth to the failure plane from the original ground surface of 25m (Map 1). The rock type in this zone contrasts with that in Zone I and is thought to be an intrusive igneous body, possibly a sill that is characterised by planar failure on a joint set dipping at 24° (dip slope) with a northerly dip-direction (Fig 4.6).



Fig 4.4. Major joint sets dipping to the northwest at $\sim 45\text{-}50^\circ$ from the eastern lateral margin rock mass Zone I. Joints are smooth, clean and planar. Bedding at this location is sub vertical trending from left to right of the photo in volcaniclastic sedimentary rocks. Photo looking southeast at location 2 Map 1. Rock hammer circled for scale (Photo taken February 2003).

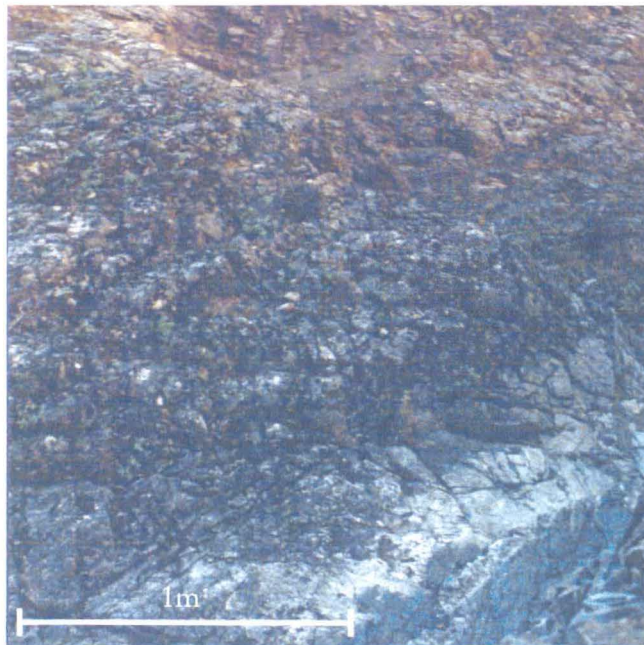


Fig 4.5. Closely jointed volcaniclastic sedimentary rock mass exposed in the upper western lateral margin of Zone I (location 3 Map 1).

The rock mass displays close to wide (25-500mm) defect spacing, low to very high 0.5 > 10m) defect persistence, an average unit block size between small and medium (10-500mm equivalent cube side) and is massive with no bedding present. The joints are closed with no infilling material, very planar and display a smooth, slightly slickensided surface. The dominant joint set (defect persistence > 30m) dips at 20° to the northeast.

Landsliding from Zone II is inferred to have occurred on the planar surface exposed along the slope, based on its rock mass characteristics (Fig 4.6). The majority of this planar surface is covered in landslide debris from Zone I up to and greater than 5 m thick. Current surface drainage has formed deep gullies that have eroded the colluvium deposited from Zone I down to the planar failure surface.

4.3.2.1 Zone III

Zone III is defined from the base of zone II (850 m.a.s.l.) to the onset of landslide material associated with the dam at 770 m.a.s.l., with an average slope angle of 32° (Fig 4.3). Zone III has identical rock mass characteristics and lithology (massive igneous intrusive) to that in Zone II, the difference being the joint set that controls failure (Fig 4.7). The main joint sets in Zone III have both a northeast-southwest strike, and a southeast northwest strike and dip between 30 and 80° (Map 1). Bedding is evident near the eastern lateral margin of zone III showing similar orientation to that at the head of the slide (70/135° dip/dip direction). The surface is smooth and slightly slickensided, and is devoid of significant volumes of debris. Vertical shear zones (?) of fractured rock up to 2m wide striking north-south are common throughout the massive rock mass of Zone III producing interlocked angular rock fragments but their presence is not thought to significantly affect the overall rock mass strength.

4.4 TIMING OF LANDSLIDING

A large landslide of unknown volume occurred because of ground accelerations from the 1929 Murchison earthquake. This landslide dammed the Stanley River and formed the present Lake Stanley. Since then there have been at least two further landslide events from the 1929 landslide complex. Lake bathymetry, landslide deposits, and personal communication with local residents indicates that landsliding occurred prior to the aforementioned events. These landslides are summarised as follows.



Fig 4.6. Planar joint surface at the base of zone II looking southwest towards the head of the slide (location 4 Map 1). Joint surface is smooth and planar; its lithotype is an intrusive igneous sill. Note the large amount of debris still on the planar surface left of centre photo. Erosion of the debris on the plane at this point is via a series of gullies that drain the landslide. Strike and dip of the failure surface is shown (photo taken February 2003).



Fig 4.7. Typical planar joint surface in Zone III comprising the intrusive sill as in Zone II . Note the absence of debris due to the steepness (30 degree) dip of the joint surface (location 5 Map 1)(Photo taken 13.3.1997).

4.4.1 PRE-1929 LANDSLIDING

The current vegetation pattern on the dam material consisting of at least three different tree ages, indicates several landslide depositional events (Fig 4.8, Stands A, B, and C). The age of the trees in Stand A (Fig 4.8) is unknown, however they represent the oldest stand of trees and are located on the opposite side of the valley to the landslide source (Section B-B' Map 1). These trees correspond to landsliding prior to 1929 (the date of landsliding and volumes involved are unknown). Prior to 1929, farmers in the district were reported to 'drive cattle up the Stanley (River) to graze on grassy flats' (*pers comm.*, Doug Nottage, 2003). The formation of the grassy flats suggests the presence of a pre-1929 structure blocking the Stanley River and forming a smaller lake than that of today, which may have 1) infilled with sediment allowing the cultivation of grass suggesting a relatively long period of damming; or 2) the gradual erosion of the dam material over time would have lowered the crest height, and also the lake level, allowing the establishment of the grassy flats seen prior to 1929. The later is favoured due to the estimated low sediment yield (actual sedimentation yield is unknown). Map 1 shows an area immediately upstream of the dam where no trees protrude from the current lake surface, which is inferred to be the location of the 'grassy flats'. Grazing cattle on the 'grassy flats' was reported to have ceased following the 1929 Murchison Earthquake, which triggered a large landslide that forms the current Lake Stanley (*pers comm.*, Doug Nottage, 2003).

The exact source for this landsliding is unknown, however scarring above the head of the current landslide (Fig 4.3) suggests the source was Zone I.

4.4.2 1929 LANDSLIDE

The Murchison earthquake in June 1929 triggered a landslide from Zone I and II (Map 1 and Fig 4.3) that dammed the Stanley River forming the current Lake Stanley based on historical evidence (*pers comm.*, D. Nottage, 2003), published and unpublished reports (Adams, 1981 b; Muller, 1997; Stocker, 1997) and physical evidence from the landslide source area and valley floor (field reconnaissance, this study). The dimensions of the 1929 landslide are not known, however vegetation regrowth on the dam surface in Stand B (Fig 4.8) corresponds to a landslide in 1929 with a volume sufficient enough to reach the opposite side of the valley and dam the Stanley River to its current level.

Established vegetation around the spillway is similar in density to Stand B vegetation suggesting the lake level may not have changed significantly since lake level stabilisation following the 1929 landslide (Fig 4.8).

4.4.3 1929 – 1968 LANDSLIDE

Further landsliding is apparent post 1929 and prior to aerial photography taken in 1968, based on vegetation regrowth (Stand C, Fig 4.8) that is less dense than the 1929 vegetation regrowth and covers the majority of the dam surface. Little is known about this landslide regarding the dimensions, exact timing and its source area (i.e. landslide Zone I, II or III).

4.4.4 1994 LANDSLIDE

Physical evidence (field reconnaissance including aerial oblique photographs, this study), unpublished reports (Muller, 1997; Stocker, 1997), and personal communication (D. Nottage, 2003) suggest that the formation of the most recent landslide at Lake Stanley was in 1994 (Map 1, Fig 4.3). The landslide had a volume of $250,000 \text{ m}^3$, length of 500m, width of 200m and a rupture depth of between 10 and 20m from inside the original landslide boundary in Zone II (Map 1 and Fig 4.3). The landslide is described as a rock avalanche comprising of a combination of loose landslide (colluvium) deposits resting on the planar Zone II failure surface described earlier, and bedrock from Zone II igneous intrusive rock mass; the triggering mechanism of the material is unknown. Debris from the landslide came to rest in the spillway of the dam and blocked it to an estimated height of 10m above the base of the spillway prior to this landslide, and up the opposite side of the spillway wall, destroying established vegetation on the dam surface (Fig 4.9) (the effects on drainage are discussed in section 4.6.1.2). Vegetation disruption is evident in Fig 4.8 as Stand D, which illustrates the extent of the landslide in 1994.

4.5 LANDSLIDE DAM CHARACTERISTICS

4.5.1 GENERAL DESCRIPTION/DIMENSIONS

Lake Stanley Landslide dam has an estimated total volume of $12.5 \times 10^6 \text{ m}^3$ (material below the lake level, based on volume definition Appendix F), a crest length of 500m and a minimum crest height above the original valley floor of 70m (Map 1).



Fig 4.8. View of the dam material looking north illustrating zones within the vegetation that define landslide events. Stand A is the oldest vegetation band associated with landsliding prior to 1929, Stand B correlates with the 1929 landslide, Stand C correlates with a landslide between 1929 and 1968, and Stand D correlates with landsliding in 1994. White arrow represents 1994 landslide movement direction.



Fig 4.9. View of the landslide complex from the dam material looking south east illustrating the damaged tree resulting from a landslide in 1994 (location 6 Map 1). Arrow represents landslide movement direction. (Photo T. Nash February 2003)

The average downstream dam face slope angle is 18° with an upstream dam face slope angle of 10° based on 20m topographic data. The lake drains via an eroded but stabilised natural spillway at the base of the landslide on the true left hand side of the valley, at an elevation of 770 m.a.s.l. (Map 1), which has cut an average slope angle of 5° through the dam material. The dam impounds Lake Stanley to a depth of 20m (Muller, 1997), with an average width of 360m, length of 2,190m and an estimated volume of $6.5 \times 10^6 \text{ m}^3$ (Map 1).

4.5.2 DAM MATERIAL

The internal composition of the dam is unknown, as no subsurface investigations have been carried out as part of this study or any previous investigations. Internal inspection of the dam material is achieved through the exposed slopes of the spillway, and gives the only indication of its internal characteristics. Any zoning that may exist internally cannot be observed. It is therefore assumed that the material exposed in the spillway walls is generally representative of the entire landslide dam mass.

Rock material comprising the dam is a mixture of massive igneous intrusive rock from the sills in Zone II and III, and the volcanoclastic sedimentary rocks near the head of the slide in Zone I. The igneous sill rock mass is a moderately weathered, very strong, bluish green, massive, medium to coarse crystalline igneous rock. The volcanoclastic sedimentary rocks from Zone I are moderately weathered, very strong, bluish grey, layered volcanoclastic sedimentary rocks. The dam material is block supported (coarser particles forming the dam are in contact with each other, and the fine matrix is present at an interstitial level (Casagli *et al.*, 2003)), poorly sorted and is dominated by very angular material ranging in size from less than 5mm to greater than 5m, with an average block size (D_{50}) of 250mm (Fig 4.10). Slight variation from the above description within the 1994 landslide deposits is evident, which shows a smaller block size (100-200mm), and is intermediate between matrix support (the coarser particles forming the dam are scattered inside a prevailing fine matrix, as they are not in contact with each other), and block supported as described above. The weathering and strength of the 1994 deposits remain similar to the original dam material.



Fig 4.10. A and B. Illustration of the rock material exposed in the spillway walls. This is considered representative of the material comprising Lake Stanley landslide dam. The blocks are in contact with each other and a fine grained matrix is present at an interstitial level. The photographs are taken from a similar area in the spillway wall (location 7, Map 1). Notebook length is 180mm. (Photo taken February, 2003

4.6 DRAINAGE OF LAKE STANLEY

Drainage of Lake Stanley is via the formation of a natural spillway, seepage through the dam material and direct evaporation from the lake surface. The proportion of drainage from the three methods varies seasonally, however overtopping at the minimum dam crest height is the main drainage mechanism. The spillway is divided and discussed in the next two sections based on the amount of erosion occurring currently and since formation.

4.6.1 SPILLWAY CHARACTERISTICS

4.6.1.1 Section A

This section extends downstream from the lake edge at the point of spilling for approximately 230m, with an average gradient of 3° (Map 1). Large volcanoclastic sedimentary and igneous sill rock material up to 5m in diameter armour this section of the spillway and lack any material finer than about 100mm in diameter. The material is moderately weathered, very strong and is intermediate between sub-angular and sub-rounded. Photographs taken of this spillway section in 1997 and 2003 show blocks that have not moved in 6 years of overtopping (Fig 4.11 A and B) and flow in the spillway. Rounding of the spillway blocks combined with the lack of disturbance at the point of overtopping and the maturity of vegetation around Section A of the spillway (described earlier), suggests that the lake has remained at its current level since it stabilised some time after initial overtopping. The flow over Section A is seasonally highly variable (Fig 4.11 A and B); during field reconnaissance in February 2003 there was very little flow in the spillway (< 10 l/s) (Fig 4.11 A), which disappeared completely 20m downstream of the lake edge into the dam material; flow was not observed in the remaining part of Section A (Map 1).

There is no evidence to suggest the spillway Section A is actively eroding, nor is there evidence to suggest the likely erosion of this section from overtopping in the near future.

4.6.1.2 Section B

Spillway Section B extends from the end of Section A (Map 1) for approximately 550m to the downstream limit of landslide dam material, with an average gradient of 5° , average width at the spillway base of 40m, width at the spillway top of 80m and a depth to the floor of the spillway of 35m (Map 1 and Fig 4.12).



Fig 4.11. **A.** View of the lake outlet looking northwest towards the Lake Stanley (location 8 Map 1). The length of the spillway at point of overtopping is $\sim 10\text{m}$. The height of flood debris above the base of the overflow channel is $\sim 1.5\text{m}$. Note the dead tree stumps protruding from the lake surface (Photo taken February 2003). **B.** View of the spillway during higher flow conditions. The photo is taken from a similar position to A and taken in 1997 (source D. Nottage). The arrow indicates the presence of a block to the side of the main flow that is present in both photos. Some of the blocks within the spillway have moved since the 1997 photo, however generally little has changed.

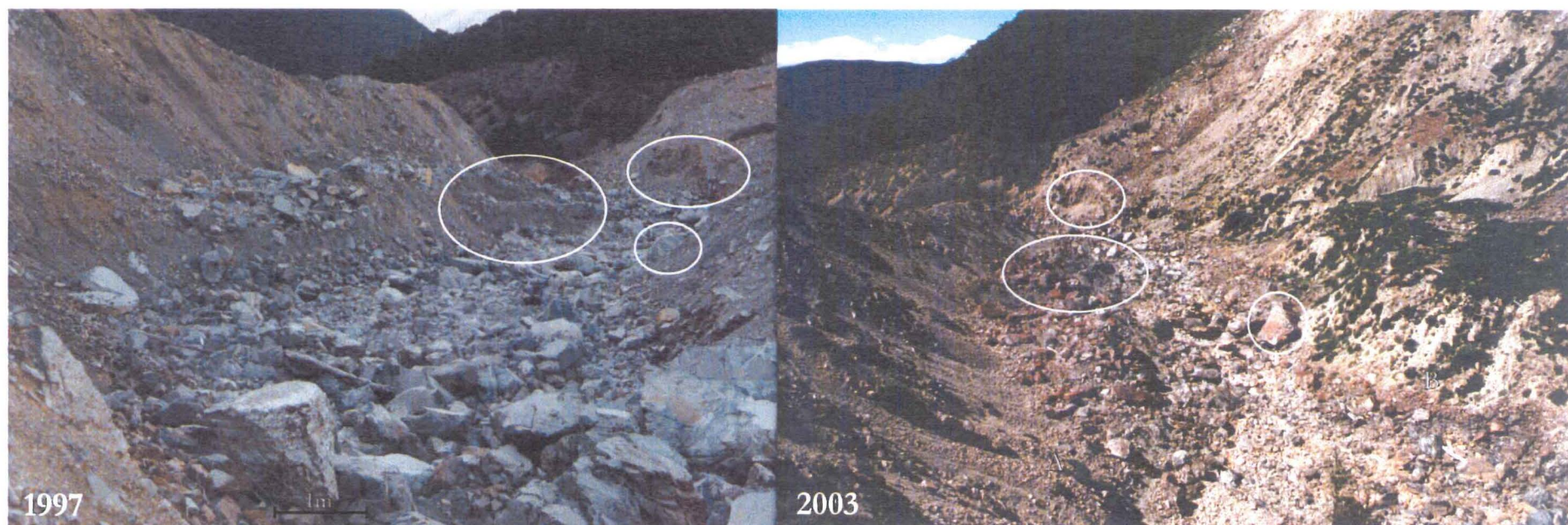


Fig 4.12. View of the spillway Section B looking downstream at location 8 Map 1 for both photos. The left photo was taken in 1997, and the right photo was taken during field reconnaissance for this study in 2003. The circles highlight three features that have been preserved in the spillway since 1997, suggesting limited erosion of Section B. The width of the spillway floor is about 40m.

Large (2-4m diameter), angular, very strong, slightly to slightly weathered blocks of volcanoclastic sedimentary and igneous sill rocks line Section B spillway (Fig 4.12). Section B is characterised by the active erosion of the spillway walls, which are at their angle of repose between 30 and 40°.

The relative current stability of Section B is observed by comparing a photo of the spillway taken in 1997 to one taken during field reconnaissance in 2003, which shows several large boulders that have not moved within 6 years of the 1997 photo (Fig 4.12). This also indicates that active erosion may be limited to large overflows caused by extreme rainfall events. Section B was also exposed to further debris input from the 1994 landslide, which blocked the spillway to a depth of 10m and is likely to have temporarily impounded water behind it. This water later overtopped the debris causing erosion and redeposition of the material up to 1km downstream giving the spillway its current shape.

At the time of field reconnaissance in February 2003, flow in the spillway was almost non-existent, with most flow occurring beneath the surface, which often exited and re-entered subsurface flow along the length of the spillway (Map 1). Flow (at an unknown rate) was observed over 80% of the entire spillway during a reconnaissance flight over the dam in December 2002 suggesting a high seasonal variation in flow through the spillway.

The long term development of Section B is one of continual erosion from the walls, base and in particular, erosion of the upstream end of Section B (nick point retreat), however, given the armouring from the large blocks in the spillway, erosion is restricted to high water flows generated during extreme rainfall events.

4.7 LANDSLIDE DAM STABILITY ASSESSMENT

4.7.1 GENERAL STABILITY

Lake Stanley is currently regarded as being stable (S) based on the terminology presented in Chapter Three. However, a cross section of the dam perpendicular to the valley axis produced from topographic 20m contour data suggests the instability of the dam immediately following its formation in 1929 (Map 1). Erosion of dam crest has occurred post dam-formation perhaps upon first overtopping of the crest or during the first extreme rainfall event, which lowered the lake level an unknown amount to its current elevation of 770 m.a.s.l. (Map 1). There is no record of catastrophic flooding downstream of the dam

since its formation in 1929 however, based on the maturity of the trees around the lake outlet, it is likely that erosion of the dam material would have occurred shortly after formation to allow the growth seen today.

The maturity of the lake outlet vegetation and slight rounding of the blocks armouring the spillway, suggest the lack of active erosion at this point (spillway Section A) since stabilisation post-formation in 1929. Contrastingly, the actively eroding nature of the spillway Section B indicates a non-equilibrium state but this thought to be attributed to a recent landslide (1994) which deposited material into and blocked the spillway. There has been little, if any, erosion of the spillway Section B since 1997 suggesting equilibrium may have been reached or that there have been no extreme rainfall events in this time.

The rock material comprising the dam is mechanically very resistant to internal erosion from flowing water due to its characteristics such as very high strength, moderate weathering and relatively large D_{50} of 250mm giving high intact strengths. A lack of fine dam material, and its clast-supported nature, resist internal piping erosion from seepage evident from the clear sediment-free groundwater exits via springs along the spillway during low flow conditions (Section B, Map 1). The rate and volume of seepage occurring through the spillway is unknown, however it is likely to be seasonally and climatically highly variable.

4.7.2 GEOMORPHIC INDEX ANALYSIS

Geomorphic indices that predict the ‘evolution’ of a landslide dam (termed post-formation development, this study) are applied to Lake Stanley landslide dam based on the current dam, lake and catchment conditions to assess the stability of the dam in its current state (Table 4.1). The application of the indices in assessing the stability of Lake Stanley landslide dam immediately post-formation is not considered here because the dimensions are unknown. However, by increasing the height of the dam from 70 to 100m above the original valley floor and increasing the dam and lake volume accordingly, the index values do not change significantly. This suggests that the present dimensions of Lake Stanley can be used to assess the dam stability immediately following formation and can represent possible future re-damming events at the dam site.

Table 4.1. Calculated index values for Lake Stanley (No. 1) landslide dam. Stable, unstable and uncertain ranges represent the domain boundaries allocated by Casagli and Ermini (1999). The original dimensions are estimated from Map 1 profile perpendicular to flow and are considered accurate to $\pm 30\%$.

Index	Calculated Value	Stable range	Unstable range	Uncertain range
Original Estimated Dimensions				
Impoundment Index (I_i) [V_d/V_l]	0.01	>0	n/a	<0
Blockage Index (BI) [V_d/A_c]	5.7	>4	<5	4 - 5
Dimensionless Blockage Index (DBI) $A_c * H_d/V_d$	2.26	<2.75	>3.08	2.75 - 3.08
Present Dimensions				
Impoundment Index (I_i) [V_d/V_l]	0.3	>0	n/a	<0
Blockage Index (BI) [V_d/A_c]	5.6	>4	<5	4 - 5
Dimensionless Blockage Index (DBI) $A_c * H_d/V_d$	2.3	<2.75	>3.08	2.75 - 3.08

4.7.3 PARAMETERS INFLUENCING STABILITY

From Table 4.1, the Impoundment Index (I_i), Blockage Index (BI) and Dimensionless Blockage Index (DBI) predict the dam to be stable given its present dimensions that agrees with its current dam status of stable (S) (from Chapter 3). This indicates that the parameters used in the three indices may represent the most influential parameters affecting the stability of this dam. These parameters are discussed as follows:

- Dam volume parameter has a direct influence on the BI and DBI values because of the relatively small catchment size (33 km^2) above Lake Stanley Landslide dam. From a physical point of view, the large dam volume ($12.5 \times 10^6 \text{ m}^3$) generates a higher resistance to flow past the point of blockage via seepage and overtopping, and provides some degree of protection from any failure mechanism. This parameter indirectly represents the geometry of the dam, in which a large dam corresponds to a wide (valley parallel) distribution.
- Catchment area above the point of blockage at Stanley is relatively small (33 km^2) compared to the volume of material resisting flow generated by the catchment. Flow velocities at the dam site are thus not sufficient to initiate erosion of dam material.
- Dam height indirectly represents the block size of the dam material (blockiness). A higher dam height corresponds to a larger average block size, which is more resistant to seepage and overtopping erosion than dams comprised of smaller blocks that correspond to a smaller dam height.

- The volume of Lake Stanley is approximately 50% less than the total dam volume that is resisting erosion, hence the positive I_i value for Lake Stanley, which predicts stability. This is based on the premise that the lake volume reflects the (relative) potential energy of the stored water and its ability to erode the dam material. Therefore, a (relatively) small lake volume compared to dam volume will enhance stability.

4.8 FUTURE DEVELOPMENT

4.8.1 LANDSLIDES ONTO THE DAM

There is a high possibility of further landsliding onto the current dam material, which would subsequently raise the crest and lake levels, based on historical landslide occurrence, investigations from this study, and rock mass characteristics of the source rock. Zone I is the likely source for future landsliding (Map 1) with the enlargement of the eastern and, in particular, the western lateral margins.

Insufficient structural data exists for kinematic analysis of the western margin rock mass to assess if it is possible for planar, wedge or toppling failure to occur. The orientations of the main joint sets for the eastern margin rock mass are known and can therefore be assessed for kinematic stability.

Fig 4.13 shows the equal area stereographic projection of five joints from the eastern lateral margin rock mass representing their dip and dip direction to assess its kinematic behaviour. The results show that planar failure is possible for one joint set, which satisfies all three structural conditions: 1) defect dip direction $\pm 20^\circ$ of the slope dip direction; 2) dip of the defect is less than the dip of the slope (defect daylights); and 3) dip of the defect is greater than the friction angle of the defect plane (conservatively estimated to be 28°). One other defect plane meets the requirements of 2 and 3, however does not daylight the slope, which dips at 55° . It is important to note that the slope does locally dip $> 55^\circ$, which may allow kinematically, failure to occur on this defect.

Wedge failure analysis from the eastern margin joint and bedding defects suggests that it is not kinematically possible for this type of failure to occur in the current state (Fig 4.13).

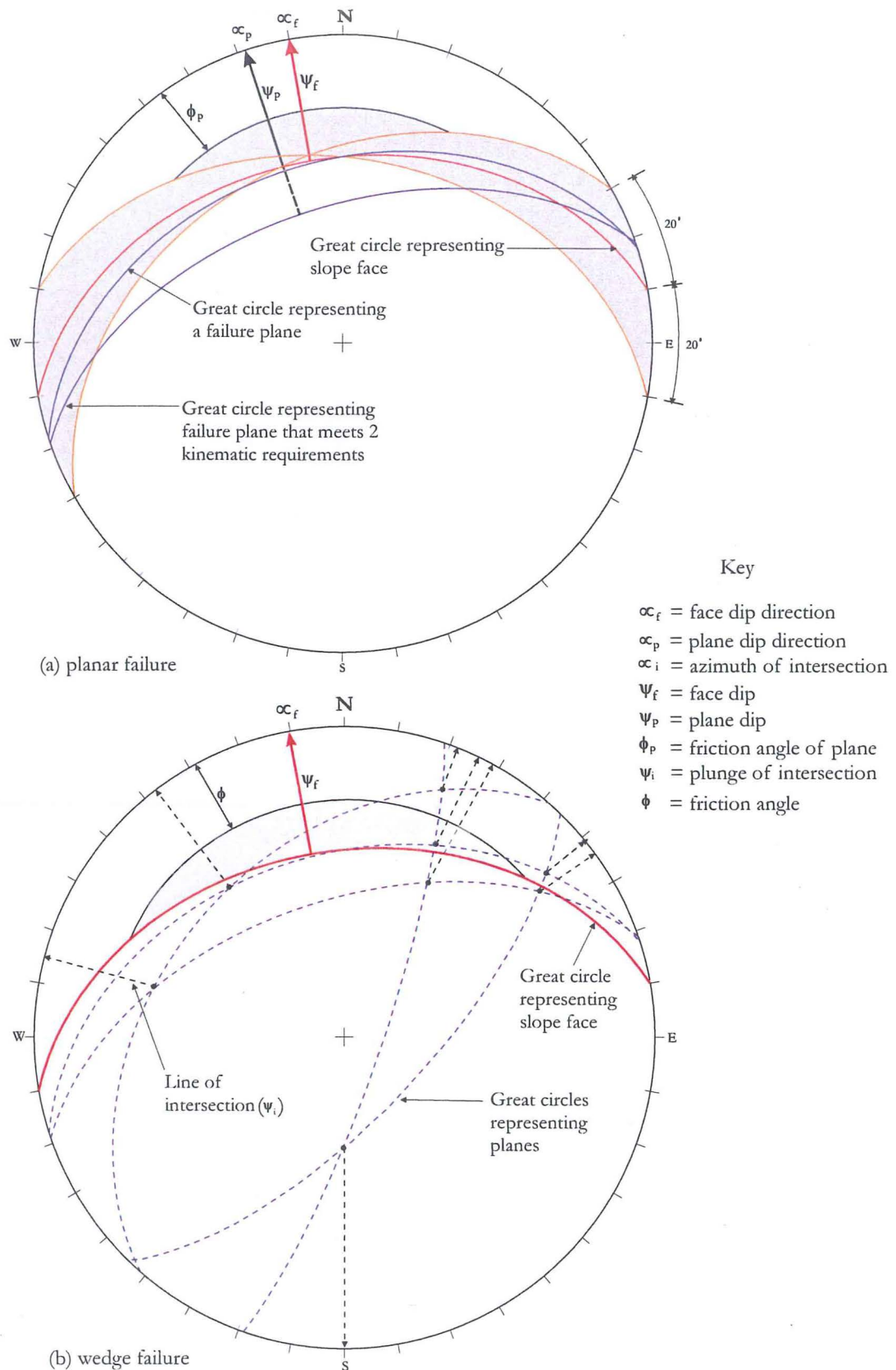


Fig 4.13. Stereographic projection for kinematic analysis of wedge and planar failure in Zone I rocks at Lake Stanley upper eastern lateral margin. Results show (a) planar failure is kinematically possible, and (b) wedge failure is not kinematically possible based on the limited number of defects used for the analysis.

A major cause of concern is a wedge of rock between the landslide complex and the stream immediately upstream of the landslide with a potential in-situ volume of between 5 and $7 \times 10^6 \text{ m}^3$; the material is currently stable lying between 250 and 700m above the lake level of 770 m.a.s.l. (Map 1). Displacement of this mass, depending on movement direction, could block the spillway, raising the crest height and/or enter the deepest section of the lake (near the dam) displacing reservoir water.

4.8.1.1 Potential for dam failure from further landsliding

As an example, if the dam crest was raised and consequently, the lake level by 40m from the mobilisation of the wedge of rock described above, the dam volume could be increased to about $17 \times 10^6 \text{ m}^3$ and the lake volume increased to between 20 and $30 \times 10^6 \text{ m}^3$. I_s , BI and DBI calculations based on the above scenario, give values of -0.1 (unstable), 5.7 (stable), and 2.1 (stable) respectively suggesting general dam stability.

Additional landsliding from this western wedge of material onto the existing may result in a relatively low chance of resisting overtopping erosion. Rock mass characteristics of outcropping rock from the landslide's western lateral margin (Zone I) are highly jointed and have a very small to small average unit block size ($< 10\text{mm}$ equivalent cube side), which is likely to produce landslide deposits with a relatively small D_{50} . The inability of these deposits to resist erosion is based on the 1994 landslide into the spillway of the dam (Map 1), which eroded upon overtopping owing to its relatively small ($100\text{-}200\text{mm}$) D_{50} . The higher erosivity of landslide dam material displaying a smaller D_{50} is not represented by any existing geomorphic index, therefore the accuracy of the post-formation development predicted for Lake Stanley dam, if the crest is raised by further landsliding, is cautioned.

4.8.2 LANDSLIDES INTO THE LAKE

Aerial photographic analysis of the reservoir slopes shows minor active gullying on the northern and southern slopes, producing small ($< 500 \text{ m}^2$) deltas into the lake from several small tributaries (Map 1). Major active deep-seated landslides, such as Lake Stanley landslide, are absent on the reservoir slopes, which further supports the presence of a structural control on the Lake Stanley landslide formation such as the propagation of a fault through the centre of the landslide complex (Map 1). The formation of landslides on the northern valley wall is considered unlikely based on the absence of significant

landsliding throughout this valley section. There is evidence of a major paleo-landslide or slump on the southern valley wall in the middle section of the lake (Map 1). Its surface is characterised by hummocky topography and minor head scarp preservation and is not thought to be currently active.

4.9 FURTHER WORK

Further work is required to accurately assess the recurrence of landslide events using dendrochronology, as an example, to date trees on the dam material opposite the landslide source. The existence of a terrace on the true left of the valley floor immediately downstream of the dam (Map 1) may indicate possible breaching events, or gradual redistribution of the dam material over time prior to the 1929 event. Aerial photographic evidence suggests that its origin is fluvioglacial by showing similar morphology to adjacent glaciated valleys (e.g. Lindsay, Waingaro). However, there is insufficient field evidence to suggest the origin of the terrace, hindered also because the lake covers the possible continuation of the terrace upstream of the dam. The source of the terrace is of particular importance from a hazard perspective in understanding the post-formation development of an impoundment pre-1929, therefore its origin should be determined to differentiate between outburst flood deposits and fluvioglacial deposits. More structural data for the rock mass on the western lateral margin rocks is needed to assess the likelihood for further landsliding. Monitoring of the rate of nick point retreat (lake ward erosion of dam material) within the spillway is recommended to assess erosion rates in the spillway of the dam.

4.10 SYNTHESIS

- Damming of the Stanley River has occurred multiple times in the recent past with at least two known major damming events, one prior to 1929, and the second during the 1929 Murchison Earthquake.
- Since the 1929 landslide, there have been at least two major landslides from within the 1929 landslide complex, and at least one of them is thought to have temporarily blocked the dam spillway before breaching.

- Cross section of the dam perpendicular to valley axis suggest the erosion of dam material following initial overtopping; there is insufficient evidence to accurately determine these original dimensions.
- Section A of the spillway (Map1) has not been subjected to erosion since lake stabilisation after formation.
- Section B of the spillway (Map 1) has undergone erosion in the recent past (related to the 1994 landslide). Photographic evidence suggests that this erosion of material has slowed considerably and may be restricted to high flow events.
- Outcropping rock mass characteristics in the source area and historical evidence suggests the strong possibility of further landsliding especially from the section of rock between the western lateral landslide scarp and the stream immediately upstream of the point of blockage.
- The rock material comprising the dam favours stability by demonstrating very high strength, slight to moderate weathering, and a relatively large average block size of 250mm in diameter, which resists erosion by overtopping and internal erosion by seepage.
- The application of the I_i , BI and DBI to assess the stability of the dam suggests the dam is stable based on the current dam lake and catchment dimensions.
- The parameters used in the indices, in particular the BI and DBI , represent the influential parameters of the dam, namely the relatively small catchment size and relatively large dam volume.
- The rock material comprising the dam is highly resistant to overtopping and seepage erosion due to its high strength, D_{50} of 250mm, and armouring of the spillway but these parameters are not directly represented in any of the indices that predict the landslide dam stability.

Chapter 5

LANDSLIDE DAM CASE STUDIES

5.1 INTRODUCTION

From the discussions presented in Chapter Three it is clear that parameters other than those defined by geomorphic indices influence, and in some cases control, the post-formation development of a landslide dam. Chapter Four provided a detailed discussion on the formation of Lake Stanley landslide dam and some reasons why its post-formation development was correctly predicted using geomorphic indices. Chapter Five continues this detailed analysis; however, it includes three landslide dams whose actual post-formation development differs from that predicted using geomorphic indices, and discusses the reasons why.

This chapter is divided into four sections. Sections 5.2, 5.3 and 5.4 detail the formation and failure (if applicable) of Ram Creek (No. 25), Rain Peak (No.16) and Lake Matiri (No. 5) landslide dams giving reasons for their incorrect prediction using geomorphic indices. The final section (5.5) synthesises sections 5.2 - 5.4 and presents the primary reasons why the geomorphic indices did not predict the actual post-formation development for these dams.

Therefore, the aims of this chapter are to:

- Provide an account of landslide dam formation and failure (if applicable);
- Evaluate the application of the Impoundment Index (I_i), Blockage Index (BI) and the Dimensionless Blockage Index (DBI) proposed by Casagli and Ermini (1999) and Ermini and Casagli (2003); and
- Discuss the primary influences on the stability of the landslide dams.

5.2 RAM CREEK LANDSLIDE DAM

5.2.1 INTRODUCTION

Ram Creek landslide dam is located 7km east of Inangahua Junction at the foot of the Brunner Range (Fig 5.1). Ram Creek is a tributary of Dee Creek, which joins the westwards draining Buller River approximately 5.5km below the dam site.

The M 7.2 1968 Inangahua Earthquake mobilised about $4.4 \times 10^6 \text{ m}^3$ of material as a translational landslide that dammed Ram Creek with an estimated volume of $2.8 \times 10^6 \text{ m}^3$ of landslide debris (dam volume); the remaining landslide material does not impede the drainage. The lake that formed behind the dam did not overtop the crest of the dam until its failure, almost 13 years after its formation on the 29th of April 1981, with a maximum lake volume of stored water prior to failure between 0.9 and $1.1 \times 10^6 \text{ m}^3$. Failure of the dam by overtopping was catastrophic. It released the entire lake volume and created a flood wave, which damaged bridges, roads and farmland downstream of the dam. The drainage basin area above the point of blockage is relatively small at 4.5 km^2 and, on average, receives 2,300mm of precipitation per year (*pers comm.*, K. Walter, NIWA, 2003).

The landslide dam is located within an up-faulted block of largely granitic rocks of the Brunner Range belonging to the Karamea Granite Suite, which range in age from mid Palaeozoic to Cretaceous. The landslide complex formed in rocks classified as Dunphy Granite, a subsidiary pluton within the Karamea Granite, described as a coarse-crystalline white or light grey muscovite granite with large megacrysts of potash feldspar (Nathan, 1978). Possibly the most important structure affecting the landslide source rock mass is the northeast-southwest trending east-dipping Lyell Fault less than 1km to the west of the dam site (Map 2), upon which surface rupturing occurred less than 5km southwest of the dam site from the Inangahua Earthquake in 1968 (Yeats, 2000).

5.2.1.1 Previous work

The formation of the landslide dam following the 1968 Inangahua earthquake was recorded by Simon Nathan as part of a regional geological mapping project between 1968 and 1970, and the head scarp of the landslide was shown on the subsequently published geological map (Nathan, 1978). An M.Sc thesis by Inwood (1997) reported on the aftermath of the dam failure and gave some estimates of dam, lake and landslide dimensions.



Fig. 5.1. Location of Ram Creek landslide dam and lake (pre failure). Arrow represents landslide movement direction. A and B in inset illustrate location of Lake Stanley and Lake Matiri/Rain Peak respectively. Yellow star is the location of the 1986 Inangahua Earthquake that triggered the dam-forming landslide.

Personal communication with Simon Nathan and Warren Inwood, a local farmer who witnessed the outburst flood 5 km downstream of the dam, provided information regarding the state of the dam prior to failure and photographs of the resulting flood deposits and dam site within a year of dam failure.

Field reconnaissance was carried out in March 2002 and February 2003; the latter was accompanied with aerial reconnaissance to document the present state of the landslide dam complex (Fig 5.2). Detailed engineering geological mapping of the landslide and dam complex was completed in February 2003 at 1:5,000 (Map 2) which is the only known detailed map of the landslide and dam complex since its formation.

5.2.2 LANDSLIDE AND SOURCE AREA CHARACTERISTICS

Aerial photographic evidence suggests landsliding at this site was absent prior to 1968 (NZAM 1:16,000; Run 1461, photos 35/36, flown 1948). The 1968 Inangahua earthquake triggered a mass movement 500m long, 425m wide, 40m deep and $\sim 4.5 \times 10^6 \text{ m}^3$ in volume (Map 2); its movement is best described as an extremely rapid rock avalanche. The elevation between the head and toe of the slide is 380m with an average slope of 20° and a slide direction of 225° (Map 2).

Aerial photography shows the slide had a run out zone of about 700m from its western lateral margin (NZAM 1:59,400; Run SN3777, photos H9, 10, and 11; flown 25/11/1974), suggesting either the disintegration of the landslide mass into a rock avalanche upon mobilisation, and/or highly saturated ground conditions prior to the earthquake. Landsliding extends headward of the primary landslide with several shallow ($< 4 \text{ m}$ deep) landslides activated in conjunction with the main slide (Map 2). One small slide to the north of the main landslide is currently shedding material from its source, although this has not contributed to the volume of material damming Ram Creek. There is evidence for a deep-seated landslide to the east of the main slide (Map 2), which is in the early stages of development, but it is inferred to be of similar scale and mechanism to that of the Ram Creek Dam-forming landslide of 1968.

5.2.2.1 Landslide source

The source rock mass quality is highly variable but can generally be described as closely fractured, very close to close (5-100mm) defect spacing, moderate (5-10m) persistence, and a small (10-100mm cube side) average unit block size, micaceous granite displaying a

deep weathering profile (Fig 5.3). The fracturing of the rock mass in the source area is so intense that representative structural data could not be acquired. It is important to note that gullying at this location has exposed the bedrock and may have contributed to the rock mass deterioration by exposing the mass and augmenting the weathering process. Nevertheless, the rock mass characteristics described at this location are considered to generally represent the entire source rock mass.

5.2.3 LANDSLIDE DAM CHARACTERISTICS

5.2.3.1 General description/dimensions

Material comprising the dam is well displayed in the breach sidewalls due to limited vegetation regrowth since dam failure in 1981, and local failures on the breach wall slopes (Fig 5.3, 5.4). These material characteristics are therefore considered very representative of the overall material comprising the dam. The average slope of the downstream dam face prior to breaching was 14° (1 on 4), with the slope of the upstream face inferred to be steeper, averaging about 20° (1 on 2.7) based on the profiles produced from 20m topographical data that are probably only accurate to $\pm 10\text{m}$ (Map 2). The dam crest length prior to breaching was 550m, with a maximum height above the original valley floor of 40m (based on 20m contour data), giving a total dam volume of approximately $2.8 \times 10^6 \text{ m}^3$.

Currently, active landsliding within the dam complex is restricted to the southern side of the valley; a small landslide ($< 5 \text{ m}^3$ in volume) at this location was witnessed during field reconnaissance in February 2003. The breach sidewalls are deeply incised by numerous gullying, notably more so on the steeper southern (northern facing) wall, which has an average slope between 40 and 45° . The northern (southern facing) wall has an average slope angle between 30 and 35° .

5.2.3.2 Dam material

The granite rock material comprising the dam is angular to sub angular, moderately to highly weathered, moderately strong to strong bluish brown, massive and medium to coarsely crystalline (Fig 5.4). The dam material is described as poorly sorted displaying grain sizes ranging from $< 1\text{mm}$ to 1m in diameter with an estimated D_{50} of 70 mm .



Fig 5.2. Aerial oblique of Ram Creek landslide dam looking east. The landslide (l) was triggered by the 1968 Inangahua earthquake forming a landslide dam (ld) and impounding a lake (la). The landslide overtopped eroding a v-shaped notch into the dam material discussed in the text as the breached section (b). Note the relative lack of vegetation in the breached section of the dam. (Photo taken February, 2003).

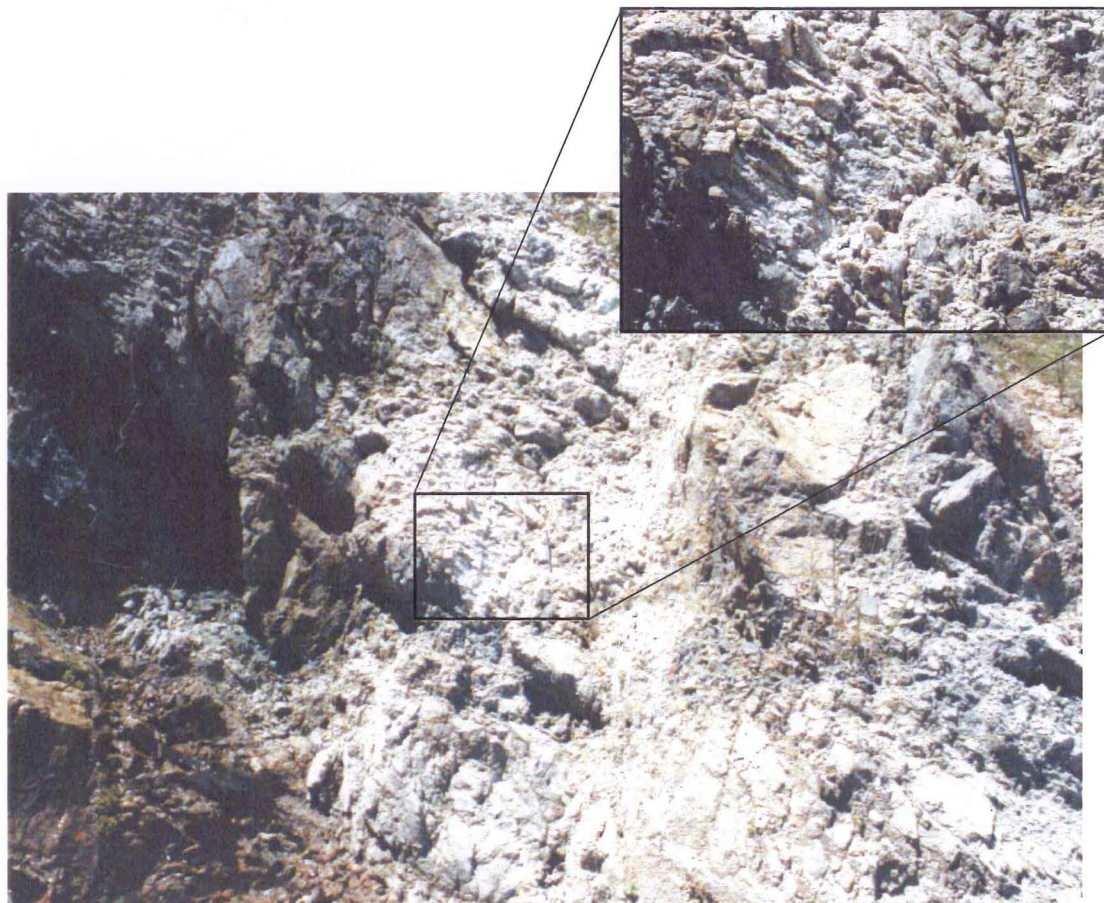


Fig 5.3. Location 1 (Map 2) illustrating the source rock mass characteristics. Note the deep weathering profile of the granite indicated by the intense discoloration within the mass. The highly fractured nature of the mass makes it difficult to obtain representative structural data for kinematic analysis of the landslide. The inset details the rock mass and shows the presence of extensive potash feldspar zones within the granite.

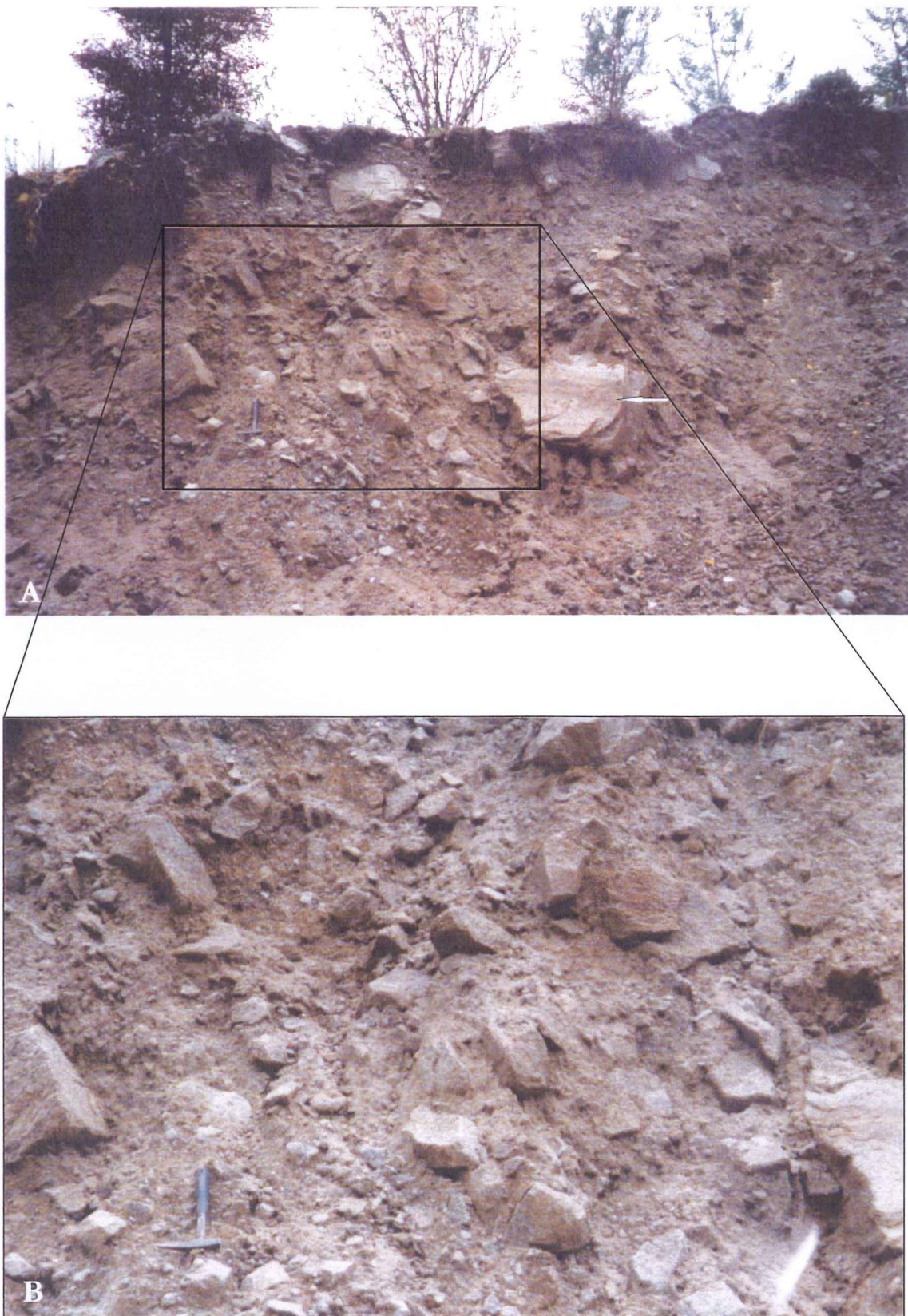


Fig 5.4. Location 2 (Map 2) illustrating the dam material comprising the landslide dam, which is considered representative of the entire dam mass. The arrow (A) shows the largest size clast of 1m in diameter and an estimated D_{50} of 70mm (B). See text for a detailed description of the rock material properties (photo taken April, 2002).

The dam material is generally grain-supported because coarser particles forming the dam are in contact with each other and the fine matrix is present at an interstitial level (Fig 5.4); refer also Casagli *et al.*, 2003. In some areas along the breach sidewall, larger (50-100mm) clasts float in a fine-grained, predominantly sand-sized (1-5 mm diameter) matrix and are not in contact with each other (termed matrix supported); overall, the dam material is described as grain or block supported.

5.2.4 FAILURE OF THE DAM

5.2.4.1 Dam and lake status between 1968 and 1981

Prior to 1968, there was no evidence of major landsliding at the dam site (based on aerial photography). The formation of the Ram Creek landslide dam occurred as a single event resulting from ground accelerations caused by the M_s 7.2 Inangahua earthquake on the 23rd of May 1968. The landslide blocked the flow of Ram Creek, creating an unnamed lake behind it that stabilised at an unknown level below the crest of the dam for almost 13 years until its failure in 1981 (*pers comm.*, S. Nathan, IGNS, 2003).

The volume of water and the height of the lake behind the dam between formation in May 1968 and failure in 1981 are unknown. Personal communication with local farmers suggest the lake level had stabilised well below the minimum crest height (unknown distance below) when visited one year after formation, suggesting that the evaporation and seepage through abutment rock and dam debris was equal to the stream input from the relatively small catchment of 4.5 km². This stabilisation is also evident on aerial photographs (NZAM 1:59,400; run SN3777, photos H9, 10, and 11; flown 25/11/1974), and shows no spillway development. There is no evidence of springs downstream of the dam either, however their presence is almost certain given that no natural spillway had formed. There is also no evidence suggesting the dam had ever overtopped the minimum crest level before breaching in 1981.

5.2.4.2 Antecedent rainfall and breaching

Rainfall between 1968 and 1981 averaged 2,208 mm per year or 184 mm per month and a maximum monthly rainfall of 452 mm was recorded in April 1974 at a rain gauge located at Inangahua Junction (7 km west of the dam site). During the week prior to its failure on the 29th of April 1981, 'heavy rain' occurred on the West Coast (S. Nathan, unpublished manuscript, 2001), which may have increased the lake level above its normal seasonal

range. Around Inangahua, rainfall was heavy but variable, with two rain gauges 5km apart recording 50 and 200mm in a few hours (S. Nathan, unpublished manuscript, 2001). On the 29th of April 1981, the dam burst catastrophically from overtopping of the dam, which released the impounded water behind the lake.

The dam burst was not observed, but the ensuing flood was recorded in late afternoon at the SH6 Bridge across Dee Creek, 5km downstream of the dam. It arrived in pulses of flood waves, some over 2m high, depositing about 2m of debris over 25 hectares (250,000 m²) of grazing land immediately upstream of the Dee Creek bridge, which was itself washed away by two pulses of flood water (Benn, 1990; S. Nathan, unpublished manuscript, 2001) (Fig 5.5).



Fig 5.5. Flood debris 5.5km downstream of the dam resulting from the breach of Ram Creek landslide dam on the 29th April 1981 (Location 3, Fig 5.1). The flood wave destroyed the SH6 bridge across Dee Creek (of which Ram Creek is a tributary of) and buried the road under 3 to 4m of logs and debris. Note the trucks in the background (arrow) for scale. (Photo source Inwood, 1997).

It is inferred that overtopping of the dam crest by the impounded water caused the catastrophic erosion of approximately $1 \times 10^6 \text{ m}^3$ of dam material in a v-shaped breach 100m wide at its top, 500m long and 40m deep (Map 2 and Fig 5.6).



Fig 5.6. Location 3 (Map 2) looking west illustrating the breached section for the landslide dam following failure. Note the absence of large boulders at the base of the breach and the side walls. Outwash terraces are also present downstream of the dam (arrow) (photo source S. Nathan; 21/1/1983)



Fig 5.7. Location 5 (Map 2) about 1km downstream of the dam showing > 2m of aggradation from the breaching and failure of the Ram Creek landslide dam. Rock hammer circled for scale. (Photo taken February 2003)

This material was subsequently redistributed up to 5.5km downstream of the dam site, although most aggradation occurred immediately downstream of the dam (Fig 5.7). The lake level is estimated to have dropped by about 30m, releasing between 0.9 and 1.1×10^6 m^3 of water over a short period (S. Nathan, unpublished manuscript, 2001).

Current activity at the dam site, 22 years after breaching, is restricted to gullying at the head of the landslide and minor slope failures within the breached section of the dam. Flow over the breached dam section is overland, with little sub surface flow; large (between 1-2 m) blocks now line the base of the breached section.

5.2.4.3 Breach outflow

Estimations of the peak discharge immediately downstream of the dam following breaching are estimated using empirically derived regression relationships and dimensionless analysis, which gave an estimated peak discharge immediately downstream of the dam of about $1000 \text{ m}^3/\text{s}$. This can be compared to the mean annual flood and the 5-year flood in the Buller River of 4,894, and 5,963 m^3/s , respectively (*pers comm.*, Martin Doyle, Tasman District Council, 2003) and a maximum flow recorded in 1950, of 12,459 m^3/s (Benn, 1990).

At 7.00pm on the 29th of April 1981 four hours after Dee Creek was washed out by a flood wave from the failure of Ram Creek landslide dam, a peak discharge of $4,335 \text{ m}^3/\text{s}$ was recorded in the Buller River, approximately 22 km downstream of the Dee Creek confluence with the Buller (Benn, 1990). This may be related to the breaching of the Ram Creek landslide dam.

5.2.5 PARAMETERS AFFECTING DAM STABILITY

5.2.5.1 Geomorphic Index analysis

Geomorphic indices used to predict the post-formation development of ram Creek landslide dam give the following results (Table 5.1):

Table 5.1. Calculated index values for Ram Creek (No. 25) landslide dam. Stable, unstable and uncertain ranges represent the domain boundaries allocated by Casagli and Ermini (1999).

Index	Calculated Value	Stable range	Unstable range	Uncertain range
Impoundment Index (I_i) [V_d/V_t]	0.4	> 0	n/a	< 0
Blockage Index (BI) [V_d/A_c]	5.8	> 4	< 5	4 - 5
Dimensionless Blockage Index (DBI) [$A_c \cdot H_d/V_d$]	1.8	< 2.75	> 3.08	2.75 - 3.08

Analysis of the stability of Ram Creek is based on estimations from engineering geological plan and section maps (Map 2) of the lake and dam dimensions prior to breaching. Table 5.1 indicates that all three geomorphic indices predict Ram Creek landslide dam to be stable based on a combination of the dam volume, lake volume, dam height and catchment area above the point of blockage, prior to dam failure. This contrasts with the actual post-formation development of the landslide dam, which is described as completely failed (CF), this thesis. The indices did correctly forecast the short-term (< 15 year) post-formation development of the dam but failed to predict the catastrophic breaching of the dam 13 years post-formation.

5.2.5.2 Additional factors affecting stability

The primary cause of dam failure is the dam material's inability to resist erosion from overtopping of the impoundment, which is attributed to the small (D_{50} of 70 mm) grain size comprising the dam, and the relatively low strength and moderate to high weathering status of the rock material. The contrast between the actual dam status to that predicted by the indices, suggests that additional parameters such as the characteristics of the rock material comprising the dam and rainfall intensity in the catchment, have influenced the post-formation development of Ram Creek landslide dam.

The slope of the downstream face of the dam is 14° , 5° steeper than the average slope for non-failed dams. This increases the velocity and erosivity of overtopping waters reducing the dam's stability. The *DBI* does consider this parameter indirectly by using the dam height, which is thought to control the steepness of the dam faces (Ermini and Casagli, 2003); however, its *DBI* value of 1.8 is well below the unstable domain of > 3.08 .

Based on the relatively small catchment size of 4.5 km^2 , Ram Creek should not have failed when using the three geomorphic indices to predict post-formation development. This parameter has a heavy weighting on the final index value when clearly additional factors such as the small (70 mm) D_{50} , have a large influence on the resistance to overtopping erosion and hence stability. The indices do not consider directly or indirectly, the importance of rainfall intensity in the catchment area, which is also a clear contributing factor in the failure of Ram Creek landslide dam. Even with this particularly small catchment, high rainfall intensity (e.g. monthly average rainfall in 24 hours) produces a relatively large runoff, which has, in the case of Ram Creek, compromised the stability of

the dam by allowing higher flows to catastrophically erode the highly erodible dam material.

The fact that the dam failed catastrophically almost 13 years after formation is uncharacteristic of landslide dams as indicated by Schuster (1986), who argues that only c.10% of dams last ≥ 1 year after formation. This short-term stability of Ram Creek landslide dam is therefore attributed to the dam's ability to stabilise the impounded lake below the minimum crest height preventing overtopping and erosion of dam material (via seepage/evaporation). This is also a function of the relatively small runoff from a small (4.5 km²) catchment, which is the basis for the *BI* and *DBI* values. The indices cannot predict the erosivity of the dam material if or when overtopping occurs; hence, the correct short-term prediction until overtopping occurred some 13 years later. Antecedent rainfall in the week prior to failure is thought to have reduced the storage capacity available at the time if the intense rainstorm that finally overtopped the dam.

5.2.6 FUTURE DEVELOPMENT

Breaching of the dam in 1981 has reduced the lake to a small (30 m²) area of slightly swampy ground immediately upstream of the original dam. Further landsliding is possible from the obvious ridge directly upstream of the original landslide and has the potential to re-dam Ram Creek on a similar scale as the 1968-81 landslide dam. Further landsliding from the breached walls through the landslide debris will continue to reduce the slope angle, however the potential for re-damming from these slopes is minimal given that they have stabilised at their angle of repose. Gullying of the breach walls will continue to degrade and reduce the slope angle.

5.2.7 RAM CREEK SYNTHESIS

- The Inangahua earthquake in May 1968 triggered a landslide in highly jointed, deeply weathered granite that blocked Ram Creek, forming a natural dam and impounding a lake.
- Drainage of the lake occurred via seepage through the dam material and abutments, and evaporation. The formation of a natural spillway did not occur for a period of 13 years prior to catastrophic breaching in April 1981.

- Dam failure in April 1981, released the entire impoundment volume catastrophically producing an estimated maximum flow of $1,000 \text{ m}^3/\text{s}$ downstream of the dam.
- Dam stability analysis using three geomorphic indices correctly forecasted the short-term (< 13 year) dam stability, however failed to predict the catastrophic dam failure 13 years after formation.
- The primary cause of failure is the small (70 mm) D_{50} of the material comprising the dam and its inability to resist erosion from overtopping of the impoundment triggered by an extreme rainfall event and exacerbated by antecedent rainfall.
- The I_i , BI and DBI predicted Ram Creek landslide dam to be stable, which was correct in the short term (< 13 years) but not correct on the long term. This is attributed to the parameters used in the indices, which do not adequately represent additional influential parameters such as D_{50} , strength of dam material, and rainfall intensity.

5.3 RAIN PEAK LANDSLIDE DAM

5.3.1 INTRODUCTION

Rain Peak landslide dam is located in an unnamed tributary of the West Branch Matiri River, which in turn forms a tributary of the south flowing Matiri River (Fig 5.8). The Matiri River, situated in the southern part of the Kahurangi National Park, South Island, joins the west flowing Buller River approximately 12km south of the West Branch Matiri River confluence.

Rain Peak landslide dam was formed by a $3.8 \times 10^6 \text{ m}^3$ translational landslide, which was triggered by the $M_s 7.8$ 1929 Murchison earthquake. Approximately $1.0 \times 10^6 \text{ m}^3$ of the landslide material produced a dam, impounding a maximum of $\sim 300\,000 \text{ m}^3$ of water. The dam has since failed (Fig 5.9), giving it a dam status of completely failed (CF), which contrasts with that predicted by the geomorphic indices. The drainage basin area (catchment size) at the point of blockage is relatively small (3.5 km^2), and receives on average 2585mm of precipitation.

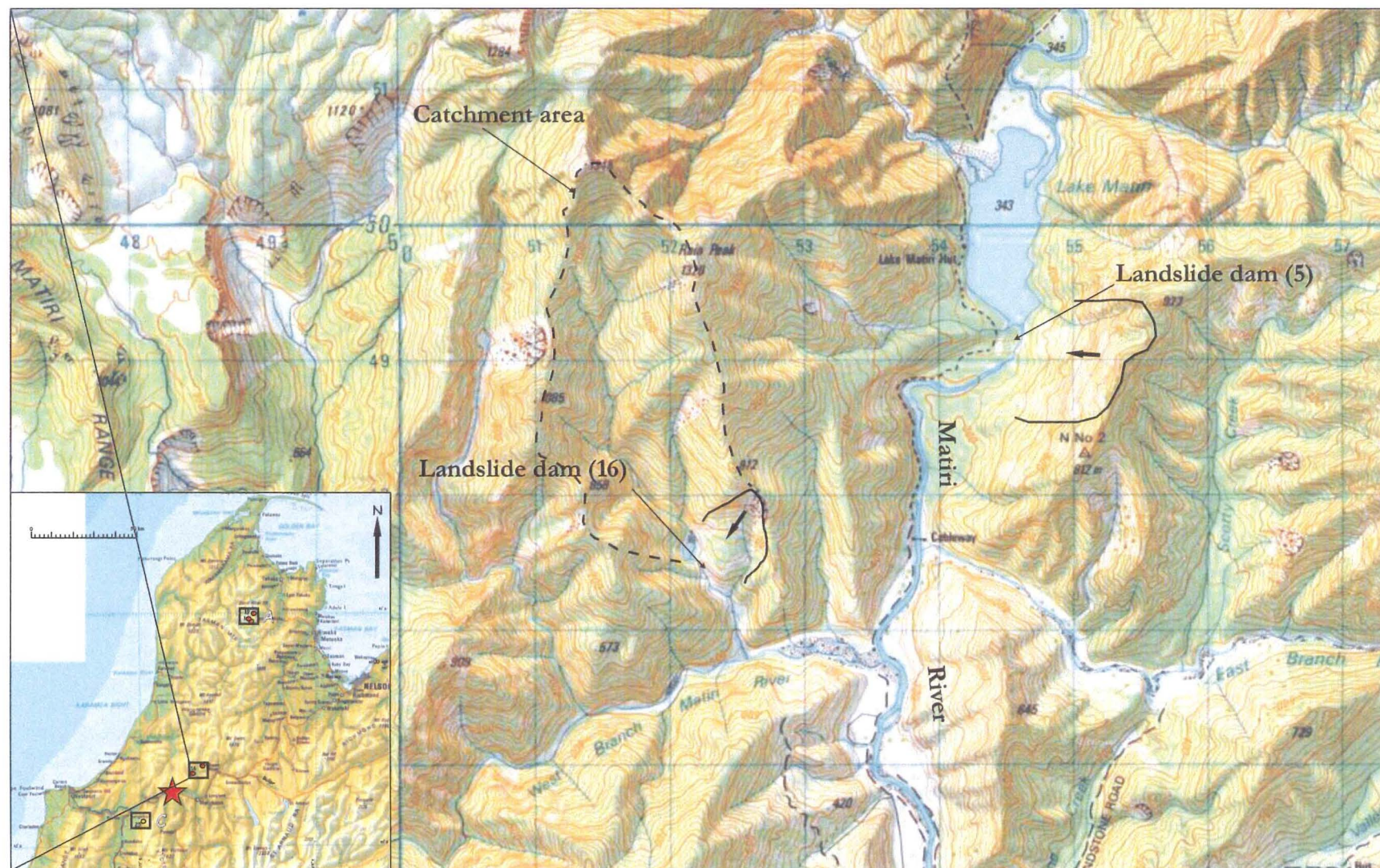


Fig. 5.8. Location map of Lake Matiri (5) and Rain Peak (16) landslide dams. Black arrows show landslide movement direction. A and C (inset) illustrate the locations of Lake Stanley and Ram Creek landslide dams respectively; start locates the 1929 Murchison earthquake epicentre.

The Rain Peak landslide developed in extensively hydrothermally altered Devonian granite (Suggate, 1984). These rocks are truncated to the east by the east-dipping, northeast trending Maunga Fault, which is inferred to be located ~ 200m east of the landslide head scarp (Map 3).

This study constitutes the first detailed analysis of the Rain Peak landslide dam since formation c.74 years ago. Prior to this study, investigations had been limited to acknowledgment of a landslide and associated lake on the 1:50 000 S M29 AC – Mangles Valley Geological Map of New Zealand (Suggate, 1984). Hancox *et. al.* (2002) describes the dam attributes and location, and recognised the dam as triggered by the 1929 Murchison earthquake.

The aims of this section are to:

- Provide an account of the formation and failure of the Rain Peak landslide dam;
- Evaluate the applicability of the Casagli and Ermini (1999) and Ermini and Casagli (2003) geomorphic indices to assess its stability; and
- Comment on additional dam parameters influencing stability.

Rain Peak landslide dam field reconnaissance was carried out in April 2002 and February 2003, detailing the dam and landslide complex and allowing the production of an engineering geological map and sections (Map 3). Field reconnaissance was augmented by aerial inspection and oblique photography (Fig 5.9).

5.3.2 LANDSLIDE AND SOURCE AREA CHARACTERISTICS

The Rain Peak landslide occurred in massive fine-grained muscovite-biotite granite (Suggate, 1984) and is interpreted as a very rapid translational slide having a rupture length of 480m, width of 440m, and a depth to failure surface of 35m. These dimensions extend from the head of the slide at 675 m.a.s.l. to the toe at 400 m.a.s.l., forming a failure surface at an angle of 20° with a runout direction to the southwest (Map 3).

5.3.2.1 Landslide source

Rock mass characteristics of the landslide source area could not be described due to inaccessibility of the landslide. Outcropping rock mass characteristics upstream and downstream of the dam (location 1 and 2, Map 3) are used to infer the landslide source rock mass, which are described as massive, extremely wide defect spacing, very high defect

persistence producing a very large average unit block size, and a low weathering profile. The joints are clean, close and planar to slightly wavy.

Active landsliding is restricted to gullying of the breach sidewalls and surficial landsliding upstream of the dam around the original lake perimeter (Map 3). Breach sidewalls are highly unstable and have a variable thickness of colluvium covering the surface particularly at the base of the valley with the development of extensive debris cones (Fig 5.10).

5.3.2.2 Landslide deposits

The landslide can be divided into two main zones based on the type of movement and the rock material characteristics of the slide debris, as follows:

Zone I is characterised by intact granite mass that has been translated down the failure surface very rapidly, and constitutes the majority of the landslide (Map 3). The rapid mobilisation of this mass is inferred based on aerial oblique and stereo pair photographs, volumetric analysis and vegetation patterns. Zone I rock material is well exposed in the breached section of the dam, however, difficulties involved in analysing this material makes it impossible to sample or describe. Zone I rock material displays bedrock characteristics when observed from the valley floor, and can easily be mistaken as such.

Zone II shows contrasting movement to Zone I (Map 3). Zone II landslide material is massive, well-graded and angular, with a maximum clast size of 300mm and minimum of < 1mm. There are numerous dead trees throughout, characteristic of rock avalanche deposits (Fig 5.11). Zone II rock material is described as moderately to highly weathered, moderately strong, bluish brown, massive, granite. Zone II material is deposited up to 1km downstream of the lake but is also present upstream of the dam and zone I (Map 3 and Fig 5.11).

5.3.3 LANDSLIDE DAM CHARACTERISTICS

5.3.3.1 General description/dimensions

Dam and lake dimensions prior to failure have been estimated based on profiles perpendicular and parallel to the valley axis, which are drawn from 20m topographical data, and are considered accurate to $\pm 10\text{m}$ (Map 3).



Fig 5.9. Oblique aerial stereo pairs of Rain Peak landslide dam post-failure looking north-northwest. Note the similarities of the v-shaped breached section (centre of photo) of the dam here with Ram Creek breached section (Fig 5.2). The image also shows the landslide source (ls) and outwash deposits (ow) downstream of the dam. (Photos taken February 2003).



Fig 5.10. View looking southeast in the direction of flow (location 3, Map 3) at the breached section of the dam (b). Landslide direction is from left to right. The top of zone II (arrow) is ~ 45m above the breach floor. Note the debris cones (dc) development at the base of the true left breach wall. (Photo taken April 2002).



Fig 5.11. Stratified sediments (ss) 700m downstream of the Rain Peak lake (location 4, Map 3) overlying massive landslide deposits (ld) from movement in zone II. Note the logs protruding from the slope (arrow) within the landslide deposit. Active erosion of the terrace is evident with the build up of debris at the base of the slope. Note also the lack of large boulders within the landslide/outwash deposits and the regrowth on the outwash debris. Height of the terrace above the valley floor is ~ 4m. (Photo looking southeast taken February, 2003).

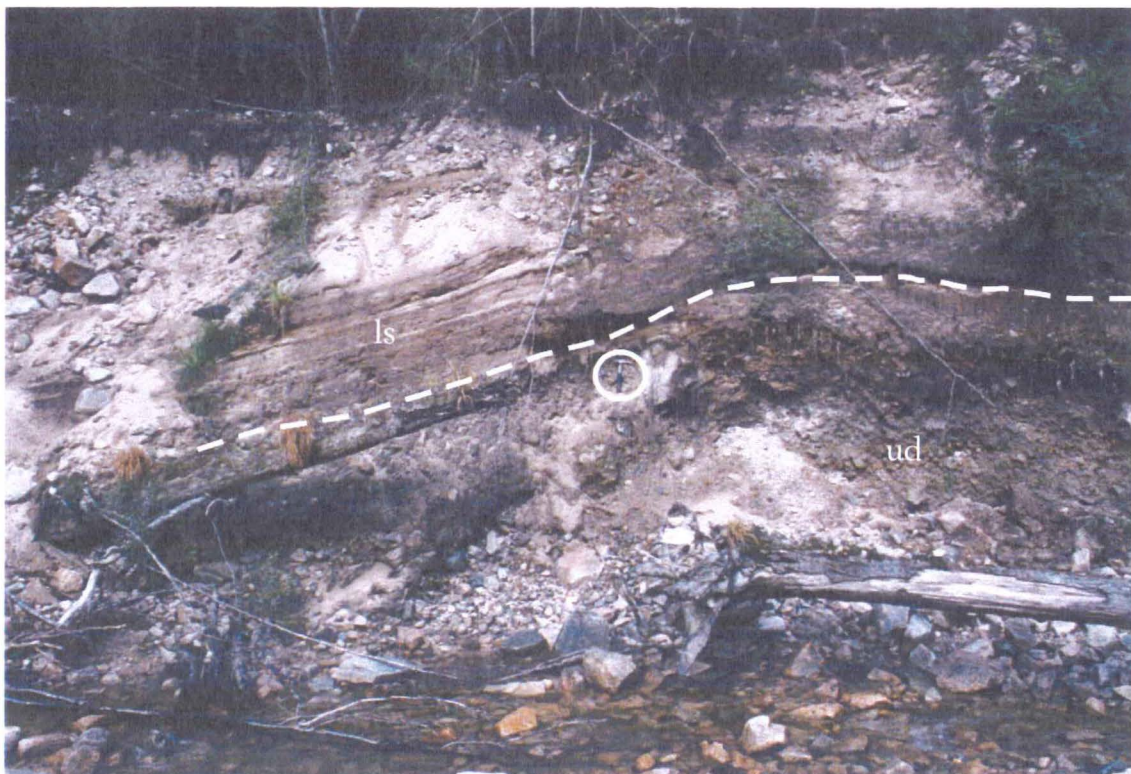


Fig 5.12. Finely laminated lake sediments (ls) at location 5 (Map 3) overlying undifferentiated deposits (ud) inferred to be stream alluvium. Note the large block to the right of the hammer (circled) measuring 400mm in diameter. Large clasts like this are absent within the finely laminated lake sediments (above dashed line) (photo taken February, 2003).

Prior to breaching, the dam faces had an average downstream slope of 13° , an upstream slope of 9° a crest length of 140m, and an average height above the original valley floor of 30m, giving a total dam volume of $\sim 1.0 \times 10^6 \text{ m}^3$. Zone I rock material comprises about 85% of the dam volume, while zone II contributes the remaining 15% to the overall dam volume (Map 3).

5.3.3.2 Dam material

Remnant original dam material is found on the true right breach sidewall and is considered in this study to represent the original composition of the dam (Fig 5.10). Erosion of dam material following breaching means that a direct analysis of the actual material comprising the dam cannot be obtained. However, the representative material is described as:

- highly weathered, moderately strong, brownish grey, massive granite, moderately graded, predominantly grain supported (coarser particles forming the dam are in contact with each other and the fine matrix is present at an interstitial level), angular granite. The maximum clast size observed was 1.5m and a minimum of $< 5 \text{ mm}$. Average grain or block size comprising the dam is estimated to be 60mm.

5.3.4 FAILURE OF THE DAM

Exact timing of the Rain Peak landslide dam formation and failure is unknown. As previously mentioned, it is assumed the landslide was triggered by the ground accelerations produced by the 1929 Murchison earthquake. This is based on tree growth within the slide complex, which is similar to tree growth on other landslides in the area known to have formed from the earthquake. Hancox *et al.* (2002) also cite the dam as being formed from the 1929 Murchison earthquake; however, there are no known studies or observations directly linking this landslide with this earthquake, or any studies or observations regarding its failure.

5.3.4.1 Dam status between 1929 and 1977

Little is known about the dam and lake characteristics prior to the earliest known aerial photography in 1977, which shows an impounded lake. Its dimensions are used as the pre-failure (maximum) lake dimensions in the following section (Map 3).

5.3.4.2 Dam status post- 1977

Field reconnaissance in 2002 and 2003 indicated the lake has drained to its current volume of about 2000 m³ (~ 1% of the original lake volume) since 1977 by eroding and redistributing about 0.5 x 10⁶ m³ of dam material (half of the total dam volume) in a v-shaped notch up to 1km downstream of the lake (Map 3 and Fig 5.10). Existence of an impoundment larger than the present lake is based on geological deposits, vegetation patterns, and aerial photography, suggesting a maximum stabilised lake volume of 150,000 m³, length 230m, width 100m and a depth of 20m (Map 3).

Original lake dimensions (1977 lake levels) are based on the presence of laminated lake sediments, several meters thick, overlying a well sorted undifferentiated deposit inferred to be stream alluvium (Fig 5.12), which are preserved at two locations around the periphery of the original lake (locations 5 and 6, Map 3). This allows an estimate of the maximum lake dimensions prior to dam failure. Variation in vegetation upstream of the dam show a change from well-established forested slopes to immature shrubs and grasses below a horizontal line upstream of the dam at the inferred original lake level of 420 m.a.s.l. and represents growth since dam failure (Fig 5.13).

The dam is thought to have failed catastrophically, based on a landslide on the western valley wall near the downstream limit of the original lake. This is inferred to have been initiated by the rapid drawdown of the lake following dam failure by increasing the pore pressure within the rock mass (Map 3, Fig 5.14).

The presence of stratified sediments 600m downstream of the dam, displaying characteristics of dam breach outwash deposits, further support lake drainage through catastrophic dam failure (location 4, Map 3 and Fig 5.11). These outwash deposits overly 2-3m of zone II landslide debris and are currently about 4 m above the present stream level. Vegetation on the outwash surface although undated, is probably < 20 years old and shows similarities to the vegetation density and type below the original lake level. This implies that failure has occurred within the last 20 yrs.

Aerial photography taken in 1977 (NZAM; SN 5041 E1/2) indicates the development of an eroded spillway over the dam crest, allowing the lake with the above dimensions to drain via overtopping. Total erosion of the remaining dam material via draining of the lake has occurred post 1977.

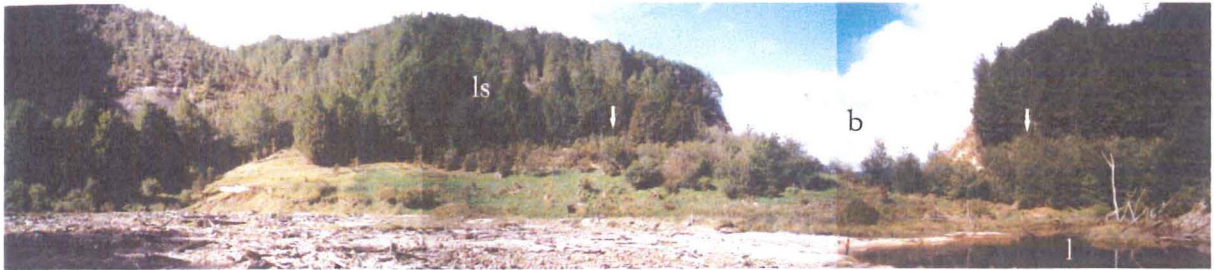


Fig 5.13. Panoramic view illustrating the present lake (l), breached section of the dam (b), landslide deposits (ls) and original lake level (vertical arrows). Photo position location 7 (Map 3) looking southeast. Horizontal arrow locates fine-medium grained stratified lake sediments. Note person at edge of lake for scale.



Fig 5.14. Photograph looking southwest at the Rain Peak dam and lake complex post failure (location 8, Map 3) illustrating the breached dam section (b), landslide (triggered by rapid lake drawdown) (dl), the present lake (l) and lake sediments from the original lake prior to breaching. The arrows indicate the original lake level prior to breaching. Dam forming landslide movement direction from top left of the photograph. Stream flow is from right to left (black arrow) (Photo taken April, 2002).

Peak discharges immediately downstream of the dam following catastrophic dam failure are estimated using empirical regression equations based on lake area, volume and depth giving an average peak discharge of $\sim 400 \text{ m}^3/\text{s}$ (Manville, 2001). Dimensionless analysis is a more sophisticated method to predict peak discharges based on the excess lake volume, breach depth and dam height, which give a peak discharge of about $600 \text{ m}^3/\text{s}$.

5.3.5 PARAMETERS AFFECTING DAM STABILITY

5.3.5.1 Geomorphic Index analysis

Geomorphic indices predicting the post-formation development of Rain Peak landslide dam give the following results (Table 5.2):

Table 5.2. Calculated index values for Rain Peak (No. 16) landslide dam. Stable, unstable and uncertain ranges represent the domain boundaries allocated by Casagli and Ermini (1999).

Index	Calculated Value	Stable range	Unstable range	Uncertain range
Impoundment Index (I_i) [V_d/V_l]	0.52	>0	n/a	<0
Blockage Index (BI) [V_d/A_c]	5.5	>4	<5	4 - 5
Dimensionless Blockage Index (DBI) [$A_c \cdot H_d/V_d$]	2	<2.75	>3.08	2.75 - 3.08

Clearly all three geomorphic indices predict Rain Peak landslide dam to be stable based on a combination of lake volume, dam volume, dam height and catchment area (dimensions prior to failure) where obviously its actual post-formation development is complete dam removal and lake drainage over a period of about 40 years giving a current dam status of completely failed (CF). As with the Ram Creek landslide dam, the indices may have predicted the short-term development correctly but failed to predict the long-term development of this dam.

5.3.5.2 Additional factors affecting stability

Parameters used in the above indices are shown to influence the development of a dam. However, the contrast between the actual dam status to that predicted by the indices suggests that parameters other than those used influence the post-formation development of Rain Peak landslide dam, such as the small average unit block size and rainfall intensity in the catchment.

Rain Peak dam material is described as highly weathered, moderately strong and a small (D_{50} of 60mm) average grain size, typical of failed dams in the dataset. The D_{50} size if

60mm comprising the dam is thought to be the main factor in the inability of Rain Peak landslide dams to resist erosion from overtopping through the absence of large coherent blocks needed to armour the spillway against overtopping erosion. This contradicts with the highly stable Lake Matiri spillway that is lined with blocks 4m in diameter.

The moderate weathering of the dam material has reduced its strength, which in turn reduces the ability of this material to resist overtopping erosion by lowering its durability. The slope of the downstream face of the dam is 13° , which is 5° steeper than the average slope for the analysed non-failed dams in this study. As a result, the slope increases the velocity and erosivity of the overtopping waters and is therefore considered an important parameter influencing stability. The *DBI* does consider this parameter indirectly by using the dam height, which is thought to control the steepness of the dam faces (Ermini and Casagli, 2003); however, its *DBI* value of 2.0 is still well below the unstable domain of > 3.08 .

All three indices fail to consider the influence of the variables outlined above when predicting the development of the dams post-failure. As with Ram Creek landslide dam, the relatively small catchment size of 3.5 km^2 generates too much control on the prediction of post-formation development using the *BI* and *DBI*. Even with this particularly small catchment, high rainfall intensity will produce a relatively large runoff, which could compromise the stability of a dam and is the likely case with Rain Peak; parameters used in the three indices cannot represent this rainfall intensity.

The dam's relative stability for approximately 40 years is primarily due to the small catchment above the point of blockage, which generates small flows, lowering the ability of overtopping water to entrain sediment and erode dam material. The primary cause of catastrophic failure occurring 40 years after formation is attributed to nick-point retreat in the spillway, similar to the Lake Stanley spillway, which reduces the total amount of material available to resist overtopping erosion. This allows higher flows produced by extreme rainfall events to catastrophically erode the highly erodible dam material.

5.3.6 FUTURE DEVELOPMENT

Continual down cutting of the riverbed is likely to occur throughout the stream length, between the lake and the confluence with the West Branch Matiri River. This, combined with the high slope gradient and high erodibility of the material comprising the breach side

walls and, in particular, the true left wall may cause further landsliding from this section in the valley (Fig 5.10). The continual erosion of the breach sidewalls is attributed to the undercutting of the fine-grained rock material comprising the zone I debris (breach sidewalls) by the stream. The volumes involved in further landsliding at this location are not considered significant to re-dam the stream.

5.3.7 RAIN PEAK SYNTHESIS

- The Murchison earthquake of 1929 is assumed to have triggered a landslide that blocked a tributary of the West Branch Matiri River, impounding a lake that subsequently drained episodically from lowering of the dam
- Failure since 1977 is thought to have occurred catastrophically within the last 20 years, based on aerial photographs and regrowth on outwash deposits downstream of the dam and below the original lake level upstream of the dam
- It is estimated that this catastrophic failure released 99% of the lake volume over about 15 minutes (dimensionless analysis, V. Manville, 2001) with a peak flow between 400 – 600 m³/s
- Post-formation dam development using three geomorphic indices suggest the dam should have remained stable
- Relatively small D_{50} and low durability of material comprising Rain Peak dam, rainfall intensity and steep valley gradient decrease the stability of the dam; nevertheless, these parameters are not included in the I_i , BI and DBI to predict the post-formation development of Rain Peak landslide dam.

5.4 LAKE MATIRI LANDSLIDE DAM

5.4.1 INTRODUCTION

Lake Matiri (No. 5 in landslide database) is located 16 km north of Murchison township within the Matiri valley and in the southern part of the Kahurangi National Park. It drains south to the confluence with the Buller River, 13km downstream of the lake (Fig 5.8), and has an extensive catchment above the point of blockage.

Lake Matiri landslide dam has formed from a series of prehistoric landslides dated at about 300 yrs B.P (Adams, 1981 a) in steeply dipping, bedded, indurated Tertiary sandstones on the eastern valley wall. Further landsliding occurred in 1929 following the Ms 7.8 Murchison earthquake and slightly raised the lake level. The total volume of material from all landsliding is $12 \times 10^6 \text{ m}^3$, of which $3.1 \times 10^6 \text{ m}^3$ has contributed to a landslide dam with a crest length of 380m and a 35m height above the original valley floor.

Lake Matiri drains via overtopping at a minimum crest height of 340 m.a.s.l., giving the lake a volume of nearly $6 \times 10^6 \text{ m}^3$ and a length, width and depth of 1,350m, 420m and 30m respectively, and is described as highly stable (HS). Application of geomorphic indices to assess the post formation development of Lake Matiri suggests the dam should be unstable, which contradicts the actual post-formation development.

The Matiri valley has been glaciated and displays the characteristic u-shape morphology. The catchment area upstream of the point of blockage is 160 km^2 , and receives on average 2.8m of precipitation per year producing an average flow at the lake's outlet of $10.5 \text{ m}^3/\text{s}$ (*pers comm.*, K. Walter, NIWA, 2003). The dam is classified as type III based on the geomorphologic classification of landslide dams by Costa and Schuster (1988).

Lake Matiri has been identified as a potential site for hydroelectric generation. Investigations prior to this study relating to the dam's suitability comprised several geotechnical feasibility reports by Tonkin and Taylor in 1994, and New Zealand Energy Limited in 2001 (*pers comm.*, David Inch, New Zealand Energy Ltd, 2003). The last report identifies the Lake Matiri Hydro-electric Project Scheme as being geotechnically feasible.

The aims of this section are to:

- Provide an account of the formation and failure of the Lake Matiri landslide dam;
- Evaluate the applicability of the Casagli and Ermini (1999) and Ermini and Casagli (2003) geomorphic indices to assess stability; and
- Comment on additional parameters influencing dam stability

Lake Matiri landslide dam field reconnaissance was carried out in April 2002 and February 2003 with mapping of the dam and landslide complex allowing the production of an engineering geological map and sections (Map 4). Field reconnaissance was augmented by oblique aerial photography on the above dates (Fig 5.15).



Fig. 5.15. Oblique areal photograph of Lake Matiri landslide dam (ld) looking southeast. Matiri River (mr) enters the top left of the lake, while Bay Creek (bc) tributary enters the top right, both forming large deltas that are slowly filling Lake Matiri. Landsliding (ls) from the eastern valley wall has formed the dam. Note the ridge protruding into the valley at right angles to flow enhancing the stability of the dam. .



Fig. 5.16. Photo looking east at the steeply dipping ($> 60^\circ$) calcareous sandstone landslide source area. The slickensided planar nature of the bedding plane is evident in the photo as vertical lineations running the length of the slope. This indicates movement has occurred on the bedding surface in the past. Photo taken in February 2003 (Location 1, Map 4).

5.4.2 HISTORICAL ACCOUNT OF DAMMING

The formation of Lake Matiri occurred ~ 300 yrs ago from landsliding on the eastern valley wall damming the Matiri River. This age is based on radiocarbon dating of small branches within deposits downstream of the dam (Adams, 1981 a), and the maturity of trees on the dam surface, particularly opposite the landslide source, is consistent with such an age. The triggering mechanism for the original dam-forming landslide (300yrs B.P.) is unknown. Adams (1981 a, b) suggests the original dam forming landslide may have been seismic in origin, but cautions this inference.

Henderson (1937) reports on lake dimensions prior to 1929, suggesting that it was 1200m long, 500m wide, 22 meters deep and covered an area of 600 000 m². Comparison of current lake dimensions to those of Henderson (1937) show little variation suggesting the increase in lake elevation was not significant. Extending deltas into the lake have formed upstream of the dam again indicating the dam and lake have existed for some time (Fig 5.21) and have reduced the area and volume of the lake. Henderson (1937) confirmed landsliding from the eastern valley wall caused by ground accelerations from the 1929 Murchison earthquake. Vegetation regrowth makes recognition and analysis of the 1929 slide difficult, and as a result, little is known about the actual volumes involved. Oblique aerial photographs taken in 2002 and 2003 and field reconnaissance indicate the likely extent of landsliding in 1929 (Map 4).

Adams (1981 a, b) identified material up to 2.5km downstream of the dam as 'mudflow deposits' from the overtopping of the dam soon after its formation at 290 ± 60 yr B.P. Breaching of a dam larger than the present dam would generally cause catastrophic flooding and aggradation more than 2.5 km downstream of the dam site. However, no aggradation from a breaching event is recorded downstream of the 'mudflow' deposits described by Adams (1981 a, b). These 'mudflow' deposits (Map 4) are likely to date landsliding from the eastern valley wall around 290 ± 60 yr B.P at the same time Lake Matiri was first formed, possibly from the same laterally extensive landslide source area. Once dam overtopping occurred, the Matiri River was forced to the opposite (western) side of the valley, gradually downcutting into the undifferentiated 'mudflow' or 'outwash' deposits downstream of the dam to a depth of about 10m (Map 4).

5.4.3 LANDSLIDE SOURCE AND DEPOSIT CHARACTERISTICS

Undercutting of the eastern slope by the Matiri River, which was forced against the valley wall by a ridge protruding into the valley at right angles (glacial origin?) has caused the initial landsliding (Map 4). Undercutting at this location removed toe support for the steeply dipping ($> 60^\circ$) sedimentary rocks, allowing planar failure to occur on the many slickensided smooth bedding surfaces (Map 4 and 5.16).

Lake Matiri landslide is described as an extremely rapid, reactivated, widening, successive, translational landslide with a total landslide volume of $12 \times 10^6 \text{ m}^3$. The landslide source area is characterised by 10 m thick Tertiary marine sandstone beds that dip between 60 and 70° into the valley floor and has a head elevation of 900 m.a.s.l, which is approximately 500m above the current lake level (Map 4).

Landslide material is described as moderately weathered, strong, greyish brown, coarsely layered, medium-grained sandstone. The average clast size is 2m, max of 20m and has an unknown minimum clast size. Source rock mass characteristics are based on a small outcrop at the base of the slide, which can be described as having very wide (500-2000mm) defect spacing, very high ($> 10\text{m}$) defect persistence and a very large ($> 1.0 \text{ m}^3$) average unit block size. Landslide deposits

5.4.4 LANDSLIDE DAM CHARACTERISTICS

5.4.4.1 General description/dimensions

Lake Matiri landslide dam has an estimated volume of $3.1 \times 10^6 \text{ m}^3$ (material below the lake level; based on definition Appendix F), a crest length of 380m and a crest height of 35m above the original valley floor (Map 4). The slope of the downstream and upstream dam face is relatively shallow at 7 and 5.5° respectively, based on profiles produced from 20m topographical data that are probably only accurate to $\pm 10\text{m}$ (Map 4).

The dam has a geomorphic classification of type III (Costa and Schuster, 1988) with a basal length of 550m, with the landslide material covering about 1.5 km of the valley floor (Map 4).

Overtopping of the dam crest via three natural spillways is the main mechanism draining the lake (Map 4 and 5.17), however, seepage through the dam material may account for as much as 5% (?) of impoundment drainage.



Fig. 5.17. Photo at the dam crest looking south at the main spillway. This photo was taken in April 2002 showing a moderate flow over the crest into the main spillway. Note the large boulders are up to 4m in diameter. (Person for scale indicated by the arrow in the middle right of the photo). The fine debris in the foreground is from a tributary that flows over the dam material from the west at right angles to the flow of the Matiri River (Location 4, Map 4).



Fig 5.18. View of the main spillway looking southwest at a position distal to the landslide source. Flow rate at time of photograph (February, 2003) is 0.3m lower than flows observed in April 2002. High flows are evident based on the debris deposited up to 2m above the average lake level (arrow). Note the large sandstone boulders in the left of the image. The smaller blocks in the foreground are from a small tributary entering from the right of the image (Location 4, Map 4).

Lake volume and hence flow over the dam crest is seasonally variable with higher flows recorded in winter where the inflow into the lake is a lot higher than in the dryer summer months, which corresponds to lower flows over the dam crest. The seasonal variation was demonstrated during field reconnaissance in April 2002 and February 2003 with the lake level about 300mm lower in February than in April the previous year (Fig 5.18). The lower lake level in February corresponded to a lower flow of water over the dam crest and in the spillway on the downstream dam face. Fig 5.18 illustrates flood debris 2m above the average lake level demonstrating the ability of the dam to resist high flood flows over the crest and on the downstream dam face. A flow gage at the lake outlet between 1979 and 1993 (site 93214; NZMG 2454500:5949200; *pers comm.*, K. Walter, NIWA, 2003) measured a maximum flow of $37 \text{ m}^3/\text{s}$ in September 1980 which again demonstrates the high flows that must occur during flood events.

5.4.5 DAM MATERIAL

The dam material is described as:

- Moderately weathered, strong, greyish brown, massive calcareous sandstone, moderately well sorted, block supported and sub angular. The maximum block size observed was 20 m in diameter (800 m^3), and a minimum of 0.2 m. Average block size (D_{50}) comprising the dam is inferred to be between 2 and 4 m based on the exterior blocks on the dam surface (Fig 5.19). There have been no subsurface investigations on Lake Matiri therefore the exact size and characteristics of the blocks comprising the dams interior is unknown.

All three spillways on the downstream dam face display heavy armouring by large ($> 4 \text{ m}$) rounded blocks as described above, with several additional ephemeral spillways also displaying heavy armouring (Fig 5.19). Flow was present in the primary channel during field reconnaissance in April 2002 and February 2003, but several of the secondary flood channels were not occupied during this field reconnaissance. (Map 4 and Fig 5.17, 5.19).



Fig 5.19. A. Photograph of blocks lining the spillway on the downstream face of the dam, location 3 Map 4. The maximum size of the blocks in the photo is 4m in diameter. Rock hammer circled for scale. B. View of the spillway on the downstream face of the dam looking southeast location 3, Map 4. Note the surface flow has increased slightly from the previous photo indicating less subsurface flow is occurring. Block sizes are still large with a maximum in this photo of 4m in diameter. Note also, the well established vegetation on the dam material to the sides of the spillway.

5.4.6 PARAMETERS AFFECTING DAM STABILITY

5.4.6.1 Geomorphic Index analysis

Geomorphic indices predicting the post-formation development of Lake Matiri landslide dam give the following results (Table 5.3) based on the current lake and dam characteristics assuming that little (if any) modification of the dam has occurred since formation 300 years ago.

Table 5.3. Calculated index values for Lake Matiri (No. 5) landslide dam. Stable, unstable and uncertain ranges represent the domain boundaries allocated by Casagli and Ermini, 1999, and Ermini and Casagli, 2003.

Index	Calculated Value	Stable range	Unstable range	Uncertain range
Impoundment Index (I_i) [V_d/V_l]	-0.3	>0	n/a	<0
Blockage Index (BI) [V_d/A_c]	4.3	>4	<5	4 - 5
Dimensionless Blockage Index (DBI) [$A_c \cdot H_d/V_d$]	3.3	<2.75	>3.08	2.75 - 3.08

From Table 5.3, the I_i and DBI predict Lake Matiri landslide dam to be unstable using a combination of lake volume, dam volume, catchment area, and the height of the dam above the original valley floor. The dam lies in the uncertain domain when applied to the BI , which uses dam volume and catchment area to predict its post-formation development.

Clearly, Lake Matiri does not display characteristics of an unstable dam (as defined by the geomorphic indices of Casagli and Ermini, 1999 and Ermini and Casagli, 2003) yet has a dam status of highly stable (HS) using the classification proposed in this study (Chapter Three). This suggests that the four parameters used by the indices do not adequately represent the major parameters that are influencing the post-formation development of Lake Matiri landslide dam.

5.4.6.2 Additional factors influencing stability

The primary factor contributing to the stability of Lake Matiri landslide dam is the very large (> 4 m) strong blocks lining all three spillways, and potentially comprising the entire mass of the dam. This allows overtopping of the dam crest and seepage through the dam without causing external or internal erosion.

The valley morphology influences the post-formation development of Lake Matiri landslide dam via the ridge of Tertiary sediments protruding into the valley at right angles to flow effectively reducing the valley width from 500 to 200 m. Its presence stops the

diversion of the Matiri River around the landslide debris opposite to the landslide source and ties into the dam structure.

The relatively low gradient of the Matiri River (1.5°) may have also reduced the potential energy available to erode the dam material relative to the gradient of the two failed dams (Ram Creek and Rain Peak) of 8.5° and 9° . Lake Matiri landslide dam's downstream face of 7° is also low relative to these two failed dams, which have angles of 14° and 13° , effectively lowering the velocity and erosivity of the overtopping water and thus increasing its stability.

Clearly, the post-formation development of Lake Matiri landslide dam is not adequately represented by the parameters used in the I_i , BI or DBI namely dam volume, dam height, lake volume and catchment area which do not account for the additional influential parameters such as the large D_{50} (2m) block size resisting erosion. Using the dam volume and catchment area (BI), Lake Matiri lies in the uncertain domain. However when the dam height is included using the DBI , the index predicts the dam to be unstable based on the Ermini and Casagli (2003) argument that the higher the dam crest is above the original valley floor, the higher the velocities and erosivity of overtopping water, hence instability. The indices, particularly the DBI , do not account for the large block size armouring the spillway, which resists the high velocity and erosivity from overtopping.

Empirical regression relationships developed to calculate the peak discharge from a landslide dam upon failure are applied to the current dam and lake dimensions of Lake Matiri to assess the potential flood hazard should catastrophic dam fail occur. This method estimates an average peak discharge of $1,500 \pm 551 \text{ m}^3/\text{s}$ immediately downstream of the dam (Manville, 2001). Using parametric relationships that consider the breach geometry when estimating the peak discharge immediately downstream approximate a peak discharge of $12,000 \text{ m}^3/\text{s}$, a mean breach width through the dam of 94 m, and a development time of 35 minutes (Manville, 2001).

5.4.7 FUTURE DEVELOPMENT

Based on the dam material's high resistance to erosion from overtopping and seepage, even during high flows (refer Fig 5.18), the future performance of the dam in resisting erosion both internally and externally, is not likely to change in the foreseeable future and suggests relative long-term stability even under future severe events (N.B. 1929 earthquake did not

cause dam failure). Sedimentation from delta growth especially from Bay Creek (Map 4 and Fig 5.15) will continue to fill the lake; however, the rate of sedimentation is unknown.

Further landsliding from the eastern valley wall is possible given the steeply dipping nature of the rock mass (Map 4). It should be noted that the undercutting of the slope by the Matiri River has ceased due to dam formation. Upstream of the dam, the eastern slopes bordering the lake display thick-bedded sandstone dipping steeply ($> 60^\circ$) into the valley, which if they were to fail, could potentially create an overtopping flood wave that may undermine the stability of the dam. However, undercutting of these slopes by the Matiri River has not occurred suggesting relative long-term stability of both the dam and lake.

5.4.8 LAKE MATIRI SYNTHESIS

- Lake Matiri formed 300 yrs ago from a landslide that blocked the Matiri River to a height of 35m above the original valley floor
- The reactivation of landsliding from the Murchison earthquake in 1929 deposited more material on the dam and raised the lake level by an unknown but small amount
- Drainage of the lake is via naturally formed spillways over the dam, which are heavily armoured by large blocks > 4 m in diameter, and seepage through the highly permeable dam material
- The stability of the dam is attributed to the dam material's large block size and relatively high strength and durability (no swelling or slaking due to the calcareous cement; rate of solutioning of CO_3 is too slow to affect strength), which resist erosion from internal piping and overtopping of the reservoir water.
- When using a combination of the lake volume, dam volume, dam height and catchment area, the I_i and DBI geomorphic indices predict the dam to be unstable. Lake Matiri landslide dam lies in the uncertain domain when using the $BI (V_d/A_b)$.
- Clearly, the parameters used in the geomorphic indices do not solely control the post-formation development of Lake Matiri landslide dam, and fail to incorporate the dam material characteristics that are shown to increase its ability to resist erosion in this situation.

5.5 CHAPTER 5 SYNTHESIS

- Detailed assessment of two failed dams (Rain Peak, No. 16; and Ram Creek, No.25) and two non-failed dams (Lake Stanley, No. 1; and Lake Matiri, No. 5) was carried out to evaluate in greater detail additional parameters that influence or control the post-formation development of a dam. The two failed dams did so catastrophically, while the two non-failed dams potentially pose a risk to downstream settlements and infrastructure.
- The post-formation development of one dam (Lake Stanley) is correctly predicted using current geomorphic indices, while the remaining three (Lake Matiri, Rain Peak and Ram Creek) are incorrectly predicted using the geomorphic indices defined by Casagli and Ermini (1999) and Ermini and Casagli (2003).
- Dam material characteristics were shown to strongly influence the post-formation development of the landslide dams studied. In particular, the block size of the dam material has a major influence on post-formation development with larger average block sizes ($> \sim 250\text{mm}$) corresponding to relative stability, while dams comprising smaller ($< \sim 100\text{mm}$) average block size are easily eroded and hence potentially unstable. Between these limits, (100-250) failure depends on the maximum block size and the nature of support (i.e. block or matrix supported).
- Rainfall duration influences the post-formation development of the landslide dams studied by providing higher flows that entrain (finer-grained) dam material upon breaching or overtopping, causing catastrophic failure.

Chapter 6

POST-FORMATION LANDSLIDE DAM DEVELOPMENT

6.1 INTRODUCTION

The post-formation development of a landslide dam is influenced by a combination of dam, lake and catchment parameters. Parameter influence was recognised by Casagli and Ermini (1999), who developed two indices to predict the evolution (termed ‘post-formation development’ this study) of a landslide dam using a combination of the dam volume, lake volume and catchment area. These were the Impoundment Index (I_i) and the Blockage Index (BI), and subsequently a third index (the DBI) was introduced by Ermini and Casagli (2003). This was an attempt to improve the BI by incorporating a fourth parameter, the dam height, which they recognised as also influential in the post-formation development of a dam.

Casagli and Ermini (1999) propose the use of the I_i as a tool to assess the stability of a newly formed dam, while the BI and DBI can be used as a method of preliminary forecasting a landslide dam’s long-term post-formation development. Application of the three indices to determine their ability to predicting the post-formation development of selected large ($> 100,000 \text{ m}^3$) landslide dams from a geographically similar region of the South Island, New Zealand (Murchison dataset), gave mixed results (Chapter Three). The BI was the most accurate, correctly predicting the actual development for 19 of 22 (86%) landslide dams in the Murchison dataset. Applying the DBI to 21 landslide dams from the Murchison dataset correctly predicted the post-formation development for 17 (81%), but when applying the I_i to 19 dams from the same study, the correct post-formation development was only forecasted for 11 landslide dams (58%).

Reasons for the indices not predicting the actual post-formation development for all the dams analysed are attributed to the inability of the parameters used in the respective indices to represent additional parameters that are known to influence the dam stability. Analysis in Chapters Three, Four and Five suggest that block size, intact rock strength, matrix/block ratio and rainfall/runoff relationships are additional dam parameters influencing the development of a landslide dam.

The aims of chapter six are therefore to:

- Review more fully the parameters used in the I_i , BI and DBI to outline problems with using these indices to predict post-formation landslide dam development;
- Attempt to modify the DBI by incorporating other factors which are believed to influence dam stability;
- Apply a modified DBI ($MDBI$) to five selected dams that represent a range of post-formation development; and
- Assess the applicability of the $MDBI$ and assess the applicability of using geomorphic indices in general to predict the post-formation development of a landslide dam.

6.2 IMPOUNDMENT INDEX (I_i)

Casagli and Ermini (1999) proposed an impoundment index (I_i), which uses landslide dam volume (V_d) and the impounded lake volume (V_l) to predict the post-formation development of the dam, in particular newly formed dams. Their equation takes the form:

$$I_i = \log\left(\frac{V_d}{V_l}\right)$$

where both parameters are in m^3 and the index itself is dimensionless.

Exact dimensions used to quantify the lake and dam volume are not given by Casagli and Ermini (1999), therefore the inferred meanings follow the terminology presented in this thesis (Chapter Three). Dam volume is thus the volume of material below the height of the spillway (or minimum crest height if the lake does not overtop the dam), and the lake volume is the volume of water stored upstream of the dam below the minimum crest height. Both attributes are relatively hard to estimate due to the assumptions of valley

dimensions prior to formation and the amount of lake infilling due to sedimentation; however they are both considered by Casagli and Ermini (1999) to influence the development of a landslide dam. Casagli and Ermini argue that the larger the lake volume, the more water there is available to erode landslide dam material, and the smaller the dam volume, the less material there is available to resist overtopping and seepage erosion produced by an impounded lake. Hence, their hypothesis is that if the dam volume is greater than the volume of the impounded lake ($I_i > 0$) the dam remains ‘stable’, otherwise failure is likely to occur.

Casagli and Ermini (1999) applied I_i to about 18 landslide dams from the Northern Apennines, Italy to test their hypothesis (Fig 6.1 a). By plotting the dam volume against the lake volume they were able to divide existing, filled and dams displaying slow erosion (collectively termed ‘stable’ dams by Casagli and Ermini, 1999) from dams displaying complete failure (termed failed dams by Casagli and Ermini, 1999) by the line $I_i = 0$ (i.e. $V_d = V_l$). All 13 dams defined as stable had an $I_i > 0$ ($V_d > V_l$), while three of four dams defined as failed had an $I_i < 0$ ($V_l > V_d$). Therefore, using the $I_i = 0$ boundary, the actual post-formation development was correctly shown in 17 of the 18 dams (94%) used in the Casagli and Ermini (1999) study, which clearly supports their hypothesis. However, the age and reliability of the dams used in their study is not known, which may have influenced the results, and they did identify one dam, which should have been stable but failed by piping erosion because of seepage.

To test the applicability of I_i to dams in a geographically similar region, it was applied to 19 landslide dams from the Murchison dataset where the dam and lake volumes could be estimated (Fig 6.1 b). The index predicted the correct post-formation development for 11 dams (58%). However, the actual post-formation development for the remaining eight landslide dams was different to that predicted by the I_i . This low success rate when using the I_i on dams in the Murchison dataset is attributed to the inability of the dam and lake volume to represent other parameters that have a greater influence on the post-formation development.

As an example, Lake Matiri has a lake volume twice that of the dam impounding it and is therefore considered unstable using the I_i . However, it is described in this study as HS (highly stable) because of the resistance of large ($\sim 4\text{m}$ or $> 64\text{ m}^3$) strong sandstone blocks comprising the dam against overtopping and seepage erosion.

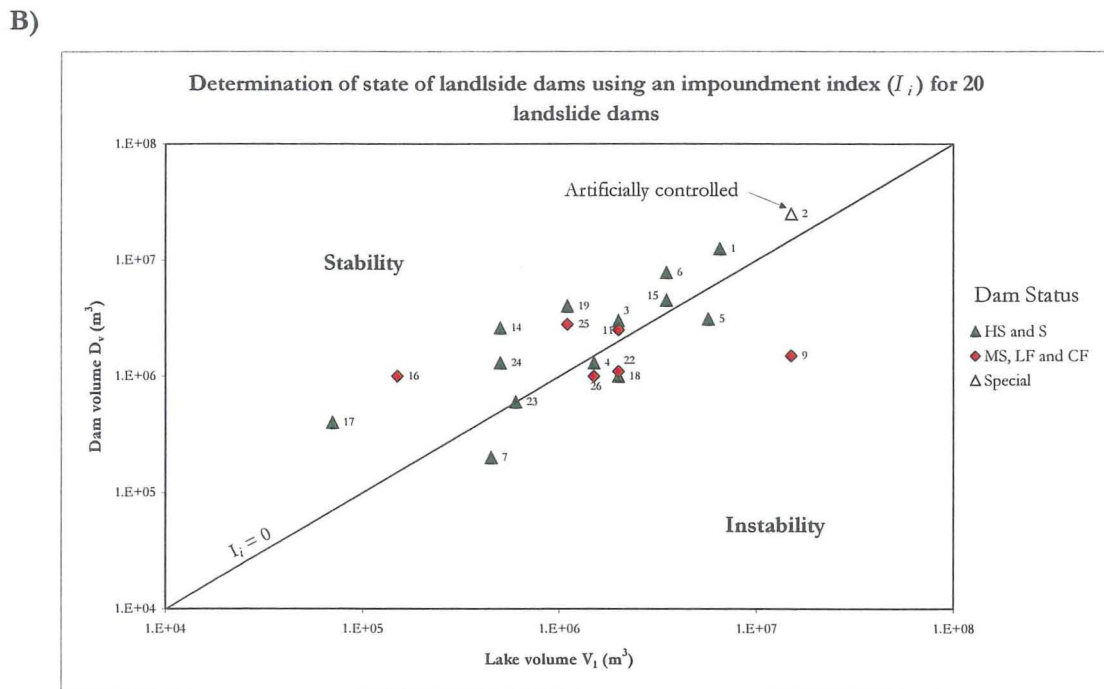
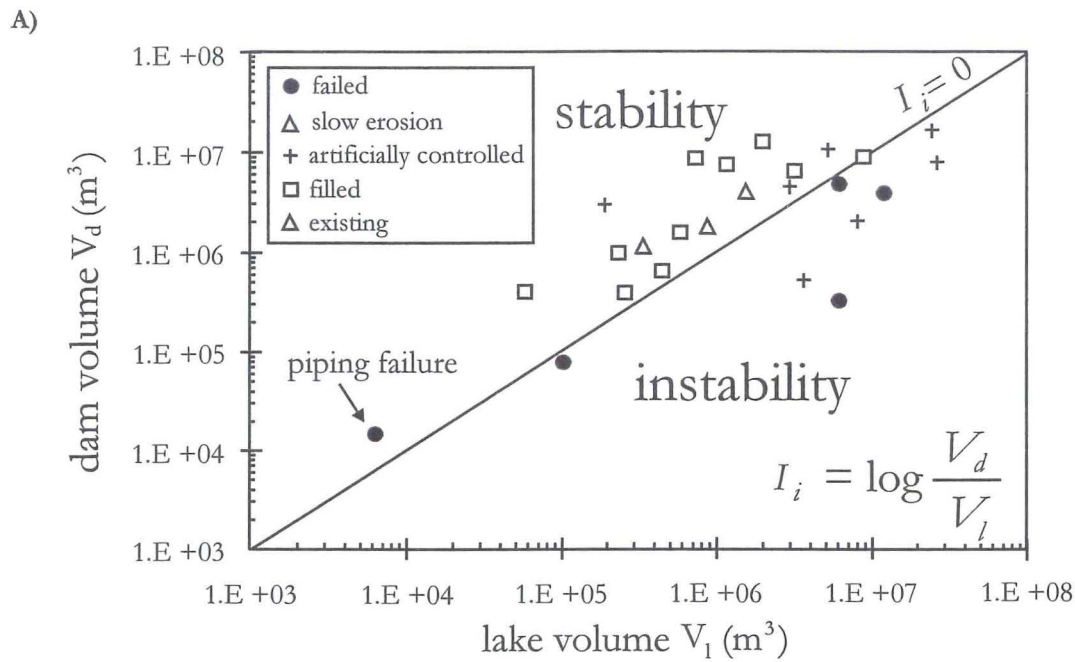


Fig 6.1. (A) Application of the I_i to 18 landslide dams (Casagli and Ermini, 1999) from the Northern Apennines, Italy. The plot of dam volume vs. lake volume indicates 16 of 17 dams fit in the correct stability domain. (B) Application of the I_i to 20 dams from the Murchison dataset. Dams described as highly stable (HS) and stable (S) from this study are collectively termed stable, while dams described as marginally stable (MS), largely failed (LF) and completely failed (CF) are collectively termed unstable dams. 11 of the 19 stable and unstable dams fit into the correct stability domain. The Matakitaki dam (No. 2) has been artificially controlled and is not used in the analysis.

Lake and dam volume used in the I_i calculations does not represent the influence of the very large block size on stability, which is a significant factor at Lake Matiri.

The opposite is true when applied to Ram Creek, which is considered stable using the I_i yet its actual status is completely failed (CF). Again, a major contributing factor to the failure of Ram Creek landslide dam is the inability of the relatively fine dam material ($D_{50} \leq 70\text{mm}$) to resist erosion from overtopping; this particle size influence cannot be represented using the dam and lake volume parameters present in the I_i . In addition, the erosivity and velocity of an overtopping flow is largely controlled by the steepness of the downstream face of a dam, which relates to the dam height/footprint length ratio. The influence of this parameter on Lake Matiri and Ram Creek landslide dams cannot be represented by the dam or lake volume, but is clearly important in both cases (Chapter 5, Section 5.2.3.2).

In conclusion, the relatively simplistic I_i uses lake and dam volume parameters that fail to represent additional important dam attributes such as block size and the steepness of the downstream dam face when applied to selected dams from the Murchison dataset. This explains the relatively low (58%) success rate of the I_i as opposed to the Casagli and Ermini (1999) study, which predicted 94% of the actual post-formation development correctly. However, the index may still have some applicability for an initial assessment of a recently formed landslide dam for emergency management purposes.

6.3 BLOCKAGE INDEX (BI)

Casagli and Ermini (1999) proposed a blockage index (BI) to predict the post-formation development of a dam, using dam volume (V_d expressed in m^3) and the watershed area (A_b , termed catchment area this study and expressed in km^2) above the point of blockage. This is defined as:

$$BI = \log\left(\frac{V_d}{A_b}\right)$$

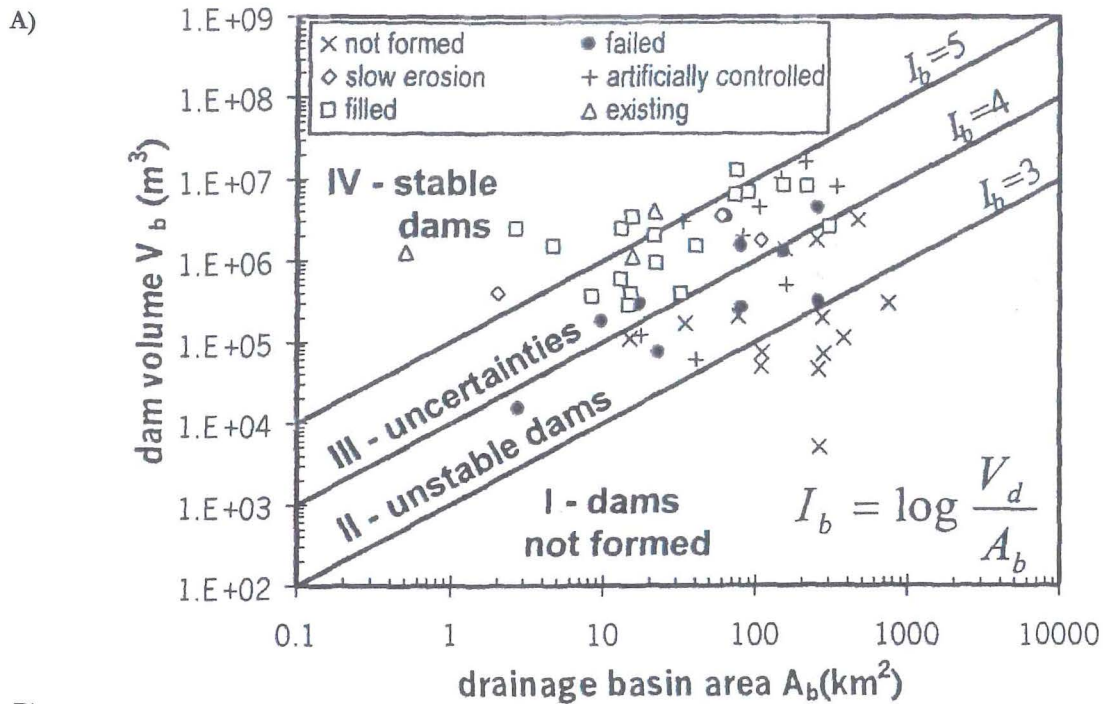
The BI uses the catchment area, as opposed to the lake volume, which Casagli and Ermini (1999) suggest represents the river discharge and valley width. Investigations from the Murchison study show catchment area also represents the stream/river gradient at the point of blockage because higher stream/river gradients are normally associated with smaller

catchments in mountainous terrain near the head of a tributary. Lower gradient rivers, such as the Buller River, South Island, New Zealand, are characterised by high flows generated by large catchment areas.

Swanson *et al.* (1985) proposed that in general, small landslides entering large channels with a large catchment area produce dams with short lifetimes, and that landslides which are large relative to the channel and valley floor receiving the deposits (e.g. associated with small catchments) are more likely to produce dams with long lifetimes. However, because the landslide dam volume is generally smaller than total landslide volume, Casagli and Ermini (1999) use the ratio of dam volume over the catchment area above the point of blockage to predict the post-formation development of a dam, as defined by the *BI*. Like Swanson *et al.* (1986), Casagli and Ermini hypothesise the larger the catchment area the lower the stability, and the smaller the catchment area the higher the stability of a landslide dam.

Casagli and Ermini (1999) applied the *BI* to c.60 landslide dams from the Northern Apennines, Italy to define stable, unstable, dams not formed, and uncertain domains. By graphing dam volume, defined as the volume to the minimum crest height, against catchment area above the point of blockage on a bi-logarithmic plot they were able to divide existing, filled and dams displaying slow erosion (collectively termed 'stable' dams) from dams displaying complete failure (termed 'failed' dams) (Fig 6.2a). All 10 dams classified as 'failed' had a $BI < 5$ (large catchment area relative to dam volume), and all 24 dams classed as 'stable' had a $BI > 4$ (small catchment area relative to dam volume). Dams having not formed (partial blockage, channel deviation erosion of the landslide toe, in which the formation of a complete dam is prevented, Casagli and Ermini, 1999) all have a $BI < 4$. 'Dams not forming' is not considered in the Murchison study because a landslide that does not block a stream or river to form a lake of some description is not strictly a landslide dam. The fourth domain defines the overlap between stable and unstable dams having *BI* values between four and five, and is termed uncertain in which 15 stable and five failed dams plot in the Casagli and Ermini (1999) study (Fig 6.2a).

All the dams used by Casagli and Ermini (1999) to test the *BI* fitted into their correct domain.



B)

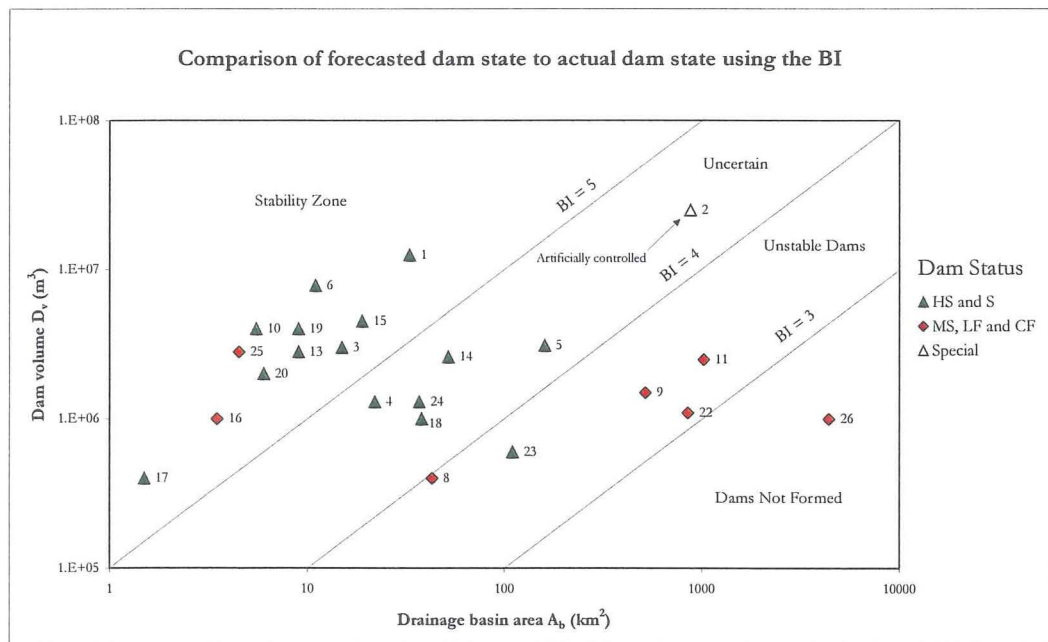


Fig 6.2. (A) Application of the BI to c.60 landslide dams from the Northern Apennines, Italy (Casagli and Ermini, 1999). The plot allows the definition of stable, unstable, uncertain and dams not formed domains. (B) Application of the BI to 23 dams from the Murchison dataset. Dams described as highly stable (HS) and stable (S) from this study are collectively termed stable, while dams described as marginally stable (MS), largely failed (LF) or completely failed (CF) are collectively termed unstable dams. 19 of the 22 stable and unstable dams excluding Matakita (No. 2) which was artificially controlled, fit into the correct stability domain giving an accuracy of 86%.

The age and reliability of their dataset is not known, however, there is an indication that dams forming and failing several hundred years ago were included in their study, thus reduce the reliability of their observations and calculated dam attributes such as dam volume for example.

To test the applicability of the *BI* to dams from a geographically similar region, it was applied to 22 landslide dams from the Murchison dataset where the dam volume could be estimated (Fig 6.2b). Based on the status of the individual dams (i.e. HS, S, MS, LF and CF, Chapter Three) the *BI* correctly predicted the actual post-formation development for 19 dams (86%), with the actual development for the remaining three dams not correctly predicted. This relatively high success rate is attributed to the large influence the catchment area has on the ability of dam material to resist erosion. In general, a large catchment area at the point of blockage corresponds to a larger flow and hence more erosion power especially at overtopping. The opposite is true for dams with small catchments, which generally have a lower flow and therefore less power to erode the dam material.

The relatively small catchment area of 4.5 km² and 3.5 km² associated with Ram Creek (No. 25) and Rain Peak (No. 16) landslide dams, respectively, give *BI* values of 5.8 and 5.5 indicating both dams to be stable. However, Ram Creek failed catastrophically almost 13 years after formation when the lake overtopped the dam crest for the first time, and Rain Peak about 50 years after its formation, clearly indicating the incorrect dam development forecasted by the *BI*. Both dams were characterised by having very small average block sizes (60 – 70mm diameter) not capable of resisting erosion from overtopping, and also steep stream gradients at the point of blockage. The ability of the *BI* to predict the short term (< 10 year) dam development for Ram Creek and Rain Peak landslide dams is based on the small amount of water available at the point of blockage (a function of the small catchment size), which approximated the amount of seepage through the dam and evaporation from the lake surface. However, the catchment area fails to represent the likely intensity of rainfall during an extreme event, which was for Ram Creek and Rain Peak what caused the impoundments to overtop and erode the highly erodible dam material. This aspect cannot be represented by the *BI*, despite its obvious usefulness for short-term stability assessment.

The high accuracy of 86% when applying the *BI* to dams in the Murchison dataset, is attributed to either 1) the ability of the catchment area to represent other parameters that influence dam stability, such as river gradient, river flow and stream power; or 2) the

influence of catchment size may be so great that it overrides other controlling parameters like block size and the slope of a dam's downstream face. The latter (2) is considered true for dams with high ($> 1000 \text{ km}^2$) catchment areas such as the Buller (No. 26) and the Maruia (No. 11) landslide dams, while the opposite effect is observed for dams with relatively small ($< 5 \text{ km}^2$) catchments.

6.4 DIMENSIONLESS BLOCKAGE INDEX (*DBI*)

Ermini and Casagli (2003) proposed a dimensionless blockage index (*DBI*), that uses the same parameters as the *BI*, but includes the dam height (H_d) which is assumed to define the height of the minimum dam crest or lake level from the original valley floor, in an attempt to improve the *BI* to predict the post-formation development of a landslide dam. Their equation takes the form:

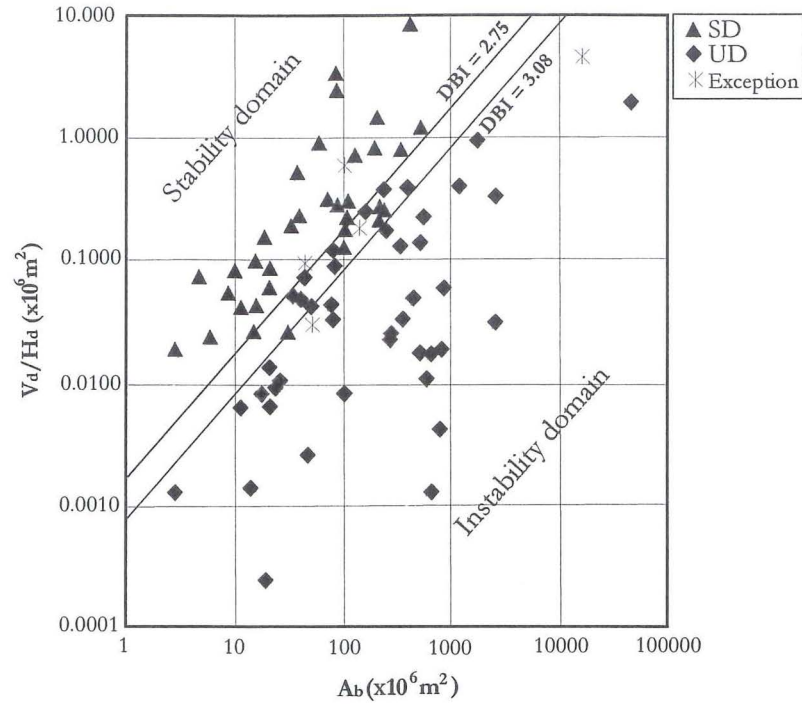
$$DBI = \log\left(\frac{A_b \times H_d}{V_d}\right)$$

where the A_b is in m^2 , H_d in m and V_d in m^3 , with the index itself dimensionless. The A_b and V_d parameters are described as for the *BI*, and H_d as above, however it is noted that the dam height parameter is not defined by Ermini and Casagli (2003).

Ermini and Casagli (2003) include the dam height on the premise that it controls the steepness of the dam slope downstream, and consequently the velocity and erosivity of overtopping lake water. For dams subjected to piping erosion, the dam height controls the position of the water table through a dam and, in particular, the hydraulic gradient. Therefore, the greater the dam height, the higher the potential for dam failure, and the smaller the dam height the lower the risk of dam failure. Dam volume and catchment area influence the stability of a dam as previously discussed; their importance in influencing the post-formation development is recognised, hence their inclusion in the *DBI*.

To test the *DBI*, Ermini and Casagli (2003) applied 84 landslide dam cases from different geographic regions worldwide to define stable (remained stable and has not encountered a breach thus still impounding an existing or relict lake; $DBI < 2.75$); unstable (dam that has undergone erosion or collapse leading to a catastrophic breach, with the subsequent release of the impounded water; $DBI > 3.08$); and uncertain (DBI between 2.75 – 3.08) domains based on the dam's observed post-formation development (Fig 6.3a).

A)



B)

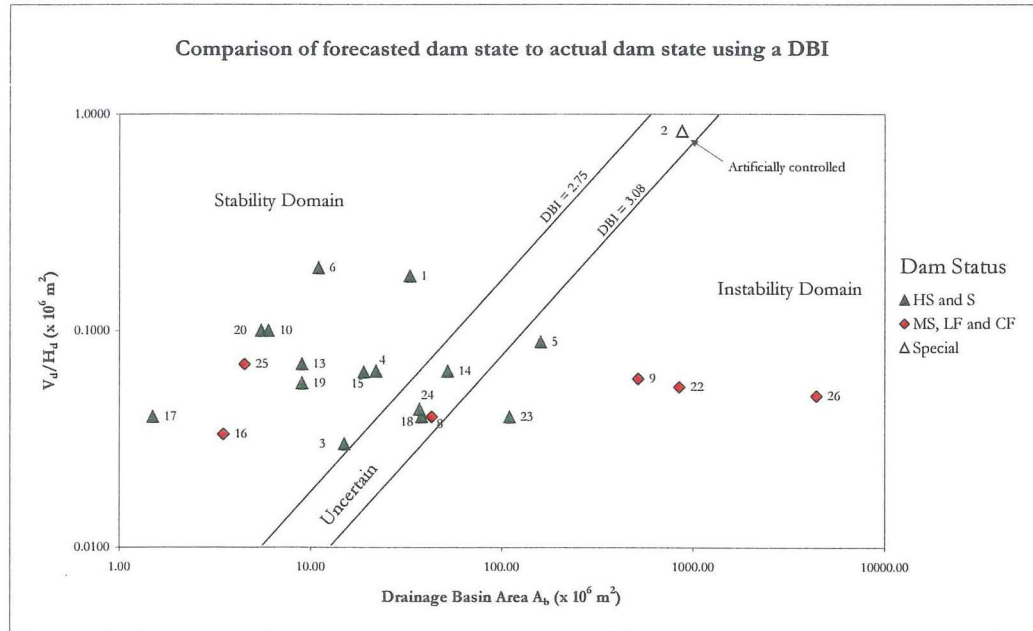


Fig 6.3. (A) Application of the *DBI* to 84 landslide dams worldwide (Ermini and Casagli, 2003). The dams allow the definition of stable, unstable and uncertain domains. (B) Application of the *DBI* to 22 landslide dams from the Murchison dataset. Dams described as highly stable (HS) or stable (S) in the Murchison study are collectively termed stable, while dams described as moderately stable (MS), largely failed (LF) or completely failed (CF (completely failed)) are collectively termed unstable dams. 17 of 21 stable and unstable dams, excluding the artificially controlled Matakkitaki (No. 2) dam, fit into the correct stability domain showing a *DBI* accuracy of 81%.

The Ermini and Casagli (2003) study showed 35 of the 37 stable landslide dams had a *DBI* < 3.08 and 44 of the 47 unstable dams having *DBI* > 2.75 . Therefore, the *DBI* predicted the correct post-formation development for 94% of the dams, and only incorrect development for the remaining 6%, thus supporting the inclusion of the dam height parameter in the *DBI*.

The reliability of the data used in the Ermini and Casagli (2003) study is unknown, however based on the spatial, temporal and physical variability in quantification of dam and catchment parameters, there are likely to be errors or assumptions. The 6% of the dams showing development opposite to that predicted by the *DBI* are interpreted as ‘exceptions’ to a ‘common’ landslide dam behaviour by Ermini and Casagli (2003) based on the following:

- Rapid rise in lake level causing overtopping (two dams), and failure upon first overtopping as a result of the high ($> 5\text{m a}^{-1}$) rainfall (one dam).
- Seepage through the dam stabilised the lake at a level below the minimum crest height (one dam), and huge rock blocks (unknown diameter) prevented failure from overtopping and piping erosion (one dam).

To test the applicability of the *DBI* in a geographically similar area it was used on 22 landslide dams from the Murchison study where dam volume, dam height and catchment area could be calculated (Fig 6.3b). The index predicted the correct post-formation development for 17 landslide dams (81%) and the incorrect development for the remaining four (19%), suggesting that the *DBI* (like the *BI*) can be applied to the dams from the Murchison dataset to predict the post-formation dam development. (The Matakita landslide dam was not included in the analysis as it was artificially controlled).

Similarities exist between the Ermini and Casagli (2003) study and the Murchison *DBI* study through the incorrect prediction of actual post-formation development for several dams. However, it is suggested here that the inaccuracies are not exceptions to common landslide dam behaviour, but reflect the highly variable nature of landslide dams, which cannot be simply represented by the three *DBI* parameters.

Parameters influencing the 19% of dams incorrectly predicted by the *DBI* include:

- small ($< 70\text{mm}$) average block size and low strength dam material supplying little resistance to overtopping erosion;

- high rainfall intensity causing overtopping in the case of small catchment areas; and
- large ($> 4\text{m}$), strong blocks comprising the dam material, provides resistance to overtopping erosion

In summary, the *DBI* predicted a similar percentage of the actual post-formation development for dams in the Murchison study as the *BI*, and the addition of the dam height did not significantly improve the accuracy of the index. However, the application of the *DBI* to the relatively small dataset in the Murchison study, and the difficulties involved in estimating the dam height, may have influenced the resulting *DBI* calculations. The correct prediction for 81% of the dams in the Murchison study is still a good correlation and therefore could be used for an initial assessment of a recently formed landslide dam.

6.5 DEVELOPMENT OF A MODIFIED *DBI* (*MDBI*)

6.5.1 BACKGROUND

Landslide dam longevity is controlled by a number of parameters that are spatially and temporally variable, and which influence the ability of the blockage material to resist erosion typically from overtopping of the dam crest and occasionally by piping through the dam material. The representation of these influencing parameters through several major parameters comprising the I_i , *BI* and *DBI* shows in general a good correlation, with relatively high accuracy as previously discussed. However, it is also evident from the application of the indices to the Murchison dataset that several other parameters are very important in controlling the post-formation development of a landslide dam that cannot be represented by the parameters used in the indices. Therefore, the aims of this section are to:

- Summarise parameters that influence the post-formation development of a landslide dam;
- Attempt to modify the most recent *DBI* to include other parameters considered important in controlling a landslide dam's post-formation development;
- Present a modified dimensionless index (*MDBI*) which incorporates other important parameters; and
- Apply the *MDBI* to the 4 dams investigated in detail from the Murchison dataset, and to one landslide dam that formed and failed in 1999.

6.5.2 *MDBI* DEVELOPMENT

Selection of parameters to be used in the *MDBI* follow previous discussions based on results from the application of landslide dams in the Murchison dataset. The parameters used, the reasons for their incorporation, and additional representative parameters are summarised in Table 6.1 followed by a brief discussion on how the *DBI* was modified to form the *MDBI*.

Table 6.1. Parameters used in the proposed *MDBI* summarising reasons for their inclusion and a brief description of each parameter.

Parameter	Brief description	Represented parameters
Catchment area (A_c)	Area of the watershed or catchment above the point of blockage (m^2).	Represents river discharge, erosivity of the river, valley shape, valley width, gradient of the river and rate of inflow into lake.
Lake area (A_l)	Surface area of the impounded water upstream of dam at crest level (m^2).	Indirect measure of lake volume, which controls the amount of water available to erode dam material.
Footprint length (L_f)	Valley parallel length of the landslide dam's base at the spillway or at low point in crest level if not overtopped (m).	Combined with dam height it represents the cross sectional area of a landslide dam, which effects resistance to overtopping erosion.
Dam height (H_d)	Height from the valley floor to the minimum dam crest level (m).	Slope of the downstream dam face, velocity and erosivity of overtopping water, dam cross sectional area, dam material blockiness, dam size/geometry.
Dam volume (V_d)	Amount of material effectively resisting flow in river to dam crest (m^3).	Amount of material available to resist erosion from overtopping or seepage, dam self weight.
Mean block volume (V_b)	Volume of mean individual block (D_{50}) forming dam (m^3).	strength of the dam material, relative permeability of dam material, ability to resist overtopping erosion and represents the self armouring ability of a dam.

From the parameters listed in Table 6.1 the *MDBI* is defined as:

$$MDBI = \log \left(\left(\frac{A_c}{A_l} \right) \times \left(\frac{H_d}{L_f} \right) \times \left(\frac{V_d}{V_b} \right) \right) \quad \text{Equation 6.1}$$

where A_c is the catchment area (m^2), A_l is the lake area (m^2), H_d is the height of the dam (m), L_f is the length of the dam footprint at the lowest point in the dam crest (m), V_d is the volume of the dam (m^3), and V_b is the volume of the mean block size forming the dam (cubic of the D_{50} expressed in m^3). The index itself is dimensionless, as is each of the component parameters.

In a benchmark paper by Schuster and Costa (1986) two factors, among others, were identified as important in the timing and magnitude of a dam failure, these being the rate of inflow into the impoundment and the size and depth of the impoundment, a fact also supported by the Murchison, Casagli and Ermini (1999), and Ermini and Casagli (2003) studies. The rate of inflow into an impoundment is represented by A_c , while the size and

depth of an impoundment is represented by the A_l parameter, and both are incorporated in the *MDBI* through the ratio A_c/A_l (Equation 6.1). In general, a larger catchment area corresponds to 1) larger flows at the point of blockage, giving the river higher erosive potential; and 2) a lower valley gradient, which corresponds to a larger lake volume and a higher potential energy available to erode dam material. Lake area is a relatively easy parameter to quantify either in a current state of overtopping, or prior to lake filling by using the minimum crest level contour as the approximate maximum lake area upon later overtopping. Lake area is considered to broadly represent the lake volume, and has therefore been used as a proxy for lake volume in the *MDBI*. From this it is therefore expected that a dam with a larger A_c/A_l ratio will fail relative to a dam with a smaller A_c/A_l ratio, but clearly this parameter on its own cannot define long term behaviour of a landslide dam.

Dam size and geometry was identified by Schuster and Costa (1986) as influencing the degree of protection against rapid erosion (failure) of landslide dams, a fact also supported by the Murchison, Casagli and Ermini (1999), and Ermini and Casagli (2003) studies. Representation of landslide dam morphology in the *MDBI* is via the H_d/L_f ratio (Equation 6.1), where the dam height represents indirectly: 1) the nature of the materials forming the landslide dam such as the proportion of larger blocks and the slope of the downstream dam face; and 2) the erosivity and velocity (gradient) of overtopping waters on the downstream face. When combined with the dam footprint length at the spillway / minimum crest height position (H_d / L_f), the ratio represents the cross sectional area of the dam at its low point, which relates to the amount of material available to resist erosion from overtopping and seepage. In general the higher the H_d / L_f ratio the steeper the dam face and the higher the velocity and erosivity of overtopping water, which is commonly associated with failed dams. In addition, a higher H_d / L_f ratio produces a steeper hydraulic gradient through the dam, also favouring dam failure.

Schuster and Costa (1986) also recognise dam material characteristics as influencing the ability to resist erosion, either at the surface of the dam as the impoundment overtops or internally due to seepage. The importance of dam material characteristics, such as grading and block size, is recognised and highlighted in Chapters Three, Four and Five, and in the studies by Casagli and Ermini (1999) and Ermini and Casagli (2003). They are represented in the *MDBI* by the V_d/V_b ratio (Equation 6.1), where V_d directly measures the size of the dam, with larger volumes corresponding to larger dam dimensions that provide a higher

degree of protection against failure by any mechanism. Dam material characteristics such as the material's intact strength and weathering, ability to resist internal erosion through seepage and surface erosion by overtopping, are proven in the Murchison study to strongly influence post-formation development. These are indirectly represented in the *MDBI* by the V_b , whereby the smaller the average block size of the dam material (cube of the D_{50}) the higher the amount of fines which makes the dam less resistant to erosion during later overtopping, while the opposite effect is observed for dams comprising a large block size. The additional dam material characteristics may or may not be reliably represented by the V_b , such as minimum block size, ratio of fine to coarse material (grading), and matrix or block support. However, the higher the V_d/V_b ratio the more susceptible the dam is to erosion by overtopping or piping indicating instability, whereas the smaller the ratio the more resistant the dam material will be to erosion, thus indicating relative stability.

6.5.3 *MDBI* APPLICATION TO SELECTED DAMS

6.5.3.1 Approach used

To test the applicability of the *MDBI*, it was applied to:

- Lake Stanley (No. 1) which is defined as stable (S) in this study being an example of a dam showing gradual erosion of the dam crest over time but essentially stable;
- Lake Matiri (No. 5) which is defined within this study as highly stable (HS) and it is a good example of a dam that has undergone little erosion of the crest since emplacement;
- Rain Peak (No. 16) which is defined as completely failed (CF) in this study, having downcut episodically over a 50 year period post-formation;
- Ram Creek (No. 25) which is defined also as completely failed (CF) in this study, and which breached catastrophically 13 years after formation upon first overtopping;
- Poerua which formed and failed in 1999 and which is a good example of a dam that has failed within one week of formation (N.B. not included in the Murchison dataset, see section 6.5.3.2).

Reasons why these five dams have been selected to test the applicability of the *MDBI* as opposed to the remaining dams in the Murchison dataset are:

- They represent the entire range of post-formation dam development from high longevity and low erosion of dam material (Lake Matiri landslide dam), to low longevity and high erosion of dam material (Poerua landslide dam);
- All necessary parameters required for the *MDBI* are known; and
- There is a good knowledge of each dam's post-formation history.

Parameter values used for each of the above dams to calculate the *MDBI* (Equation 6.1) are summarised in Table 6.2.

Table 6.2. Data used to calculate the *MDBI* for four landslide dams from the Murchison dataset and the Poerua landslide dam, an example of a dam with very low longevity but is not included in the Murchison dataset.

Dam No.	Landslide Dam Name	A_c ($\times 10^6 \text{ m}^2$)	A_l ($\times 10^3 \text{ m}^2$)	H_d (m)	L_f (m)	V_d ($\times 10^6 \text{ m}^3$)	V_b (m^3)
5	Lake Matiri	160	470	35	530	3.1	8
1	Lake Stanley	33	770	20	900	12.5	1.56×10^{-2}
16	Rain Peak	3.5	15	30	320	1	3.43×10^{-4}
25	Ram Creek	4.5	40	40	650	2.8	3.43×10^{-4}
*	Poerua	44	300	80	650	10	2.16×10^{-7}

6.5.3.2 Poerua landslide dam

On the 6th of October 1999 between $10\text{--}15 \times 10^6 \text{ m}^3$ of schist and colluvium fell almost 1800m into the Poerua River on the West Coast of the South Island, forming a dam $\sim 10 \times 10^6 \text{ m}^3$ in volume, 85m high with a crest length of 450m, and a footprint length of 650m (Hancox et al., 1999). Dam material consisted of boulders up to 4m in diameter; however the average block size diameter (D_{50}) was $\sim 6\text{mm}$ (*pers comm.*, T.Davies, 2003) or $\sim 2.16 \times 10^{-7} \text{ m}^3$. The landslide mass impounded a lake 1200m long and 80m deep, with an estimated volume of $5\text{--}7 \times 10^6 \text{ m}^3$ (Hancox et al., 1999). Overtopping of the lake occurred almost 24 hours after formation, however rapid downcutting did not occur until the 12th of October 1999, 6 days after initial overtopping, during a storm in which at least 80mm of rain fell overnight. This reduced the lake to $\sim 25\%$ of the original volume and eroded a 300m long v-shaped channel through the dam in a short period of time (Hancox et al., 1999). The resulting flood peaked between 500 and $1000 \text{ m}^3 \text{ s}^{-1}$ $\sim 8\text{km}$ downstream of the dam, causing major aggradation but no loss of life.

6.5.3.3 Application of the *MDBI*

Table 6.3 summarises the predicted development for the five dams based on index values obtained from the I_i , BI and DBI , as opposed to their actual development, and the $MDBI$ values are also given.

Table 6.3. Summary of results from application of the I_i , BI , DBI and $MDBI$ indices on four dams from the Murchison dataset and one recent landslide dam not included in the dataset (* Poerua landslide dam; see text for details). The predicted post-formation development is indicated for each dam using the I_i , BI and DBI based on its calculated index value.

Dam No.	Landslide Dam Name	Actual Dam Status (this study)	I_i	*(failed) ✓(stable)	BI	*(failed) ✓(stable)	DBI	*(failed) ✓(stable)	$MDBI$ value
5	Lake Matiri	HS	-0.30	✗	4.30	✗	3.30	✗	6.94
1	Lake Stanley	S	0.30	✓	5.60	✓	2.30	✓	8.90
16	Rain Peak	CF	0.40	✓	5.80	✓	1.80	✓	10.75
25	Ram Creek	CF	0.52	✓	5.50	✓	2.00	✓	10.80
*	Poerua	LF	0.22	✓	5.30	✓	2.51	✓	14.90

As shown in Table 6.3, the I_i , BI , and DBI indices all predict the opposite post-formation development to the five dams actual observed development for reasons previously discussed in sections 6.2 – 6.4.

However, the calculated $MDBI$ values for the five landslide dams show 3 that were characterised in this study as either completely failed (CF) or largely failed (LF) have a significantly higher $MDBI$ value (> 10) than the two dams characterised as HS and S (< 10). Therefore, by using the $MDBI = 10$ the five dams can be divided into two classes based on their observed actual post-formation development describing;

- 1) $MDBI > 10$; higher probability that catastrophic failure will occur (generally upon first overtopping; loosely termed ‘unstable’); and
- 2) $MDBI < 10$; a lower probability that catastrophic failure will occur, however gradual erosion and self-armouring may occur over time for dams (termed ‘stable’).

Refinement of the above two classes into 4 domains to further define the likely post-formation development of a landslide dam is proposed below; the application of a larger dataset is required to justify the following domains, as the influence of the relatively small dataset of five dams used here is acknowledged (Fig 6.4).

- **Domain 1:** ($MDBI < 8$) high resistance to erosion from overtopping and seepage;

- **Domain 2:** ($MDBI$ 8 – 10) gradual erosion of the dam material over time lower the lake volume and dam crest level;
- **Domain 3:** ($MDBI$ 10 – 12) erosion of dam material upon first overtopping draining all or part of the impoundment through one or more catastrophic events;
- **Domain 4:** ($MDBI > 12$) failure of dam upon or shortly after first overtopping of the impoundment, typically catastrophically;

Domains 1 to 4 are graphically illustrated in Fig 6.4 by plotting $(A_c \times H_d \times V_d)$ vs. $(A_l \times L_f \times V_b)$.

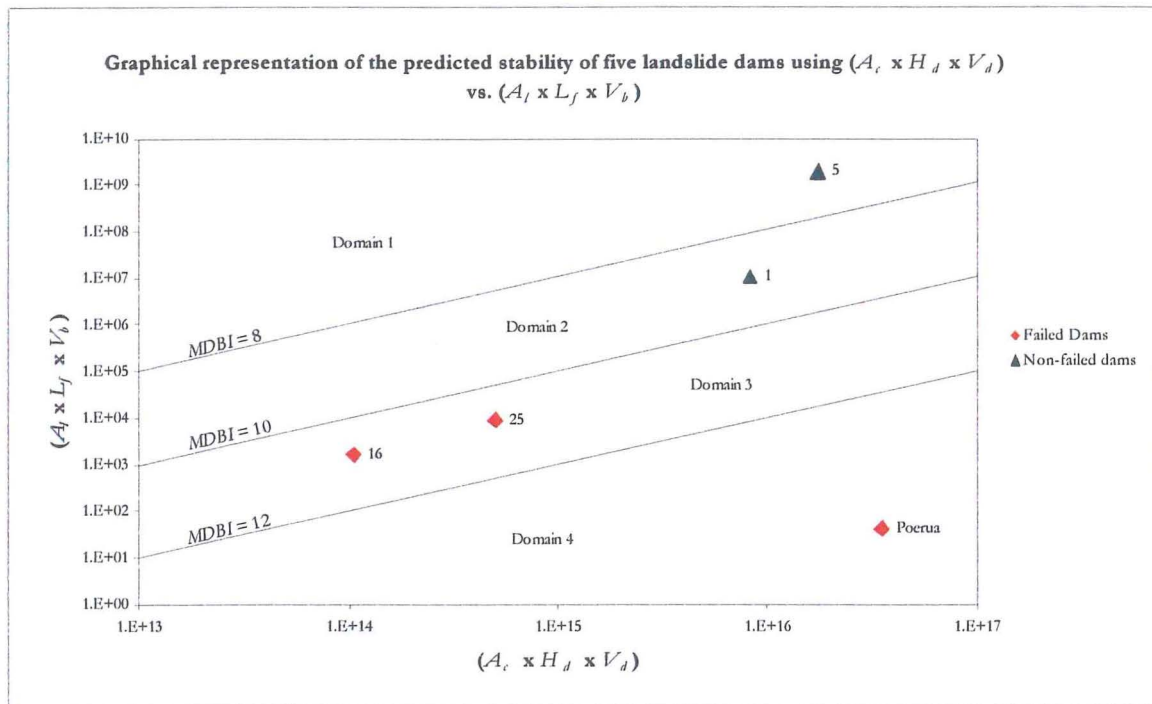


Fig 6.4. Graphical representation of $MDBI$ values for five landslide dams, which are generally divided into unstable ($MDBI > 10$) and stable ($MDBI < 10$) fields, and further refined into four domains as discussed in text. Fields and domains are based on the actual post-formation development of the dams used to test the $MDBI$.

6.5.4 ASPECTS OF THE $MDBI$ CONTRIBUTING TO BETTER CORRELATION

The $MDBI$ appears to better identify boundaries between failed and non-failed dams by extending the BI and DBI to incorporate L_f and V_b parameters, which are known to be important controls. Analysis of the $MDBI$'s three component ratios for the five applied dams show the V_d/V_b ratio, which ranges from 3.9×10^5 for a stable dam to 4.6×10^{13} for an unstable dam, to be the dominant control in the final index value (Table 6.4). In addition, this ratio alone differentiates between failed and non-failed dams because of the

high weighting imposed by the average block size, which is generally several orders of magnitude smaller than the dam volume. The high influence of the block size is justified from previous discussions indicating the association of a small average block size with a higher probability of failure upon first overtopping due to the higher erosive potential of the dam materials. The A_c/A_l ratio shows little variation in the five sampled dams (Table 6.4), indicating this ratio used alone cannot differentiate between failed and non-failed dams. Likewise, the H_d/L_f ratio does not differentiate between failed and non-failed dams (Table 6.4), although the higher ratios are associated with 2 of the 3 failed dams (Rain Peak and Poerua). However, the combination of the three ratios in forming the *MDBI* value do differentiate between failed and non-failed dams based on its application of this limited dataset.

Table 6.4. Summary of the individual *MDBI* index ratios used for the five applied dams demonstrating the variation and weighting of each ratio to the final *MDBI* value.

Dam No.	Landslide Dam Name	(A_c/A_l)	(H_d/L_f)	(V_d/V_b)	Actual Dam Status	Comments
5	Lake Matiri	340	0.066	3.8×10^5	HS	Large D_{50} ; heavily armoured spillway
1	Lake Stanley	43	0.022	8.0×10^8	S	Large dam volume; armoured spillway
16	Rain Peak	233	0.094	2.9×10^9	CF	Small D_{50} ; very small catchment
25	Ram Creek	113	0.062	8.2×10^9	CF	Small D_{50} ; small catchment
*	Poerua	147	0.123	4.6×10^{13}	LF	Extremely small D_{50} ; large catchment

Whilst further data are needed to confirm the above analysis, it would appear that the *MDBI* may be a useful tool in predicting a landslide dam's post-formation development as defined by the domain selection in Figure 6.4 and the following:

- *Domain 1*: dam resists erosion from overtopping; a very low probability catastrophic dam failure will occur;
- *Domain 2*: stabilisation of the dam crest level with gradual erosion of the dam crest level and lowering of the lake; a moderate probability of catastrophic dam failure;
- *Domain 3*: a high probability erosion of dam crest following first overtopping will be catastrophic releasing all or part of the lake volume;
- *Domain 4*: the highest probability catastrophic dam failure will occur upon first overtopping releasing all or part of the lake volume.

The findings in Chapters Three, Four, Five and parts of Chapter six suggest the large number of variables associated with landslide dams means that no index value can adequately predict post-formation dam development. The *MDBI*, does however, appear to be a significant improvement on current indices that predict the post-formation development by introducing V_b , which is known to be critical.

Additional parameters shown to influence a dams development that are not incorporated in the *MDBI*, suggestions for further refinement of the *MDBI*, and problems encountered with its formulation are as follows:

- Rainfall intensity within the catchment area controls the ability of the lake to absorb the variations of flow into the impoundment. For dams with a pre-existing spillway, higher rainfall intensity corresponds to a higher inflow into the impoundment, which can increase the flow in the spillway above the critical velocity necessary for erosion and entrainment (e.g. Poerua landslide dam). For dams where the impoundment has stabilised below the minimum crest height, a high intensity rainfall event may cause the impoundment to overtop for the first time, causing catastrophic erosion of the dam material (e.g. Ram Creek landslide dam);
- The timing of failure cannot be predicted using the *MDBI* or any existing index;
- The heavy influence on the *MDBI* value from the V_d/V_b ratio may override other more important parameters, influencing a dams post-formation development; and
- The variation in particle size (grading) and the grain-to-grain support (grain or matrix support) of landslide dam material is also a major influence in the development of a dam. The incorporation/substitution of the V_b (D_{50}) in the *MDBI* with the coefficient of uniformity ($C_u = D_{60}/D_{10}$), may for example, better represent the grading and support parameters.

6.6 SYNTHESIS

- The accuracy of indices in predicting a dam's post-formation development is controlled by the parameters used in the respective index, and their ability to represent either directly or indirectly additional parameters that are known to influence a dam's development.

-
- Incorporating V_b and L_f to the DBI to form the $MDBI$ appears to better identify boundaries between failed and non-failed dams when applied to the 5 landslide dams by correctly incorporating a significant weighting on median particle size (D_{50}) of the dam material.
 - Of the 5 dams investigated, the dams that are known to have failed are characterised by having a $MDBI$ of > 10 , while dams described as non-failed are characterised by having a $MDBI < 10$.
 - Application of 5 selected landslide dams that represent a wide range of development, to the current indices predicts a development opposite to their actual post-formation development, and these have been subjected to further evaluation .
 - Application of existing indices on landslide dams from the Murchison study is generally good, with the BI and DBI predicting the correct development for over 80% of the dams investigated. The I_i , however, only predicted the correct development for $\sim 50\%$ of dams investigated, and was the worst of the existing indices.
 - The $MDBI$ may be a useful tool for initial hazard assessment for newly formed landslide dams through definition of 4 domains based on the $MDBI$ values for the five dams.
 - The application of a larger dataset is needed to further refine and test the accuracy of the $MDBI$.
 - The heavy influence of the V_d/V_b ratio on the $MDBI$ value needs further investigation. The D_{60}/D_{10} dam material ratio may be a possible surrogate.

Chapter 7

SUMMARY & CONCLUSIONS

7.1 PROJECT AIMS AND METHODS

The main aims of this study have been:

- To review available literature on landslide dam formation and failure;
- To develop a database of large landslide dams in the northern part of the South Island;
- To analyse results in terms of currently published geomorphic indices; and
- To develop a revised geomorphic index that better predicts dam development over time.

All these objectives were achieved. By reviewing all available literature on landslide dams, it was possible to identify shortcomings in the current understanding of landslide dam longevity. A database of 26 failed and non-failed landslide dams ('Murchison dataset'), formed in the northern part of the South Island, New Zealand, was developed from field investigations, detailed mapping and review of existing literature. Analysis was achieved by standardising and defining the landslide dam terminology used, distinguishing failed dams from non-failed dams, and assessing the parameters common to both. The application of existing geomorphic indices that predict a landslide dam's post-formation development were tested with the Murchison dataset. From this analysis, detailed assessment was carried out of one dam, which agreed with the forecasted post-formation development, and three that had a different post-formation development to that predicted. This led to the development of a revised geomorphic index that better predicts dam development over time by using five landslide dams that represent a wide range of post-formation development.

7.2 LANDSLIDE DAM DATASET

7.2.1 MURCHISON & INANGAHUA EARTHQUAKES

- The M 7.8 Murchison earthquake of 1929 produced innumerable landslides and formed hundreds of landslide dams, of which 24 of the largest ($> 100,000 \text{ m}^3$) were used to form a dataset of landslide dams in northwest Nelson.
- The M_s 7.2 Inangahua earthquake in 1968 produced many landslides also, and a number of them formed landslide dams, of which two of the largest ($> 100,000 \text{ m}^3$) that formed are included in the Murchison dataset.

7.2.2 DATABASE CONSTRUCTION

- Dam-forming source landslide, dam, lake and catchment characteristics are all parameters considered important in characterising a landslide dam, and are included in the dataset. These parameters are subdivided into both dam-forming landslide and landslide dam parameters.
- Dam-forming landslide parameters include source dimensions, engineering geological descriptions of landslide deposits, source rock and landslide classification, and causes of landsliding (Appendix F).
- Dam, lake and catchment parameters include the original and present dam dimensions, material comprising the dam such as grading, breach characteristics (if applicable), lake and catchment characteristics, and deaths/damage resulting from a dam breach or dam-forming landslide event.
- Acquisition of data relating to the landslide dams in the dataset was achieved through literature review, field and aerial reconnaissance, and engineering geological mapping. Parameters relating to each dam in the Murchison dataset are recorded on two Excel datasheets and one A4 schematic map (Appendix A), giving a total of 26 entries (Appendix B).

7.2.3 ANALYSIS OF MURCHISON DATASET

- Stable and unstable terminology used to classify the current state of a landslide dam is subdivided into five sections defined as the dam status in this thesis because landslide dams in the Murchison dataset display a wide range of post-formation development.

The dam status is based on the amount of material eroded from the original dam volume since formation termed the degree of modification (DOM). The dam status is divided into highly stable (HS; DOM < 10%), stable (S; DOM 10-35%), marginally stable (MS; DOM 35-65%), largely failed (LF; DOM 65-90%) and completely failed (CF; DOM > 90%). For comparative reasons, a 'stable' dam from the Murchison dataset refers to landslide dams with a dam status of HS or S, while a 'failed' landslide dam refers to a landslide dam with a dam status of MS, LF or CF, which typically show episodic or catastrophic release of the impounded water.

- One of the most influential parameters in the post-formation development of landslide dams in the Murchison dataset is the dam-forming landslide volume, with non-failed dams showing a larger average in-situ dam-forming landslide volume ($6.8 \times 10^6 \text{ m}^3$) than failed dams ($3.4 \times 10^6 \text{ m}^3$).
- The catchment area above the point of blockage is a significant parameter affecting the post-formation development of a landslide dam. Failed dams in the dataset have an average catchment area of 861 km^2 , while non-failed dams have an average catchment area of 79 km^2 . From this, it is shown that there is a clear link between catchment size and discharge at the point of blockage, which controls the rate of inflow into the impoundment, overall erosivity of the river and the shape of the valley, thus controlling the post-formation development of a landslide dam.
- Other parameters influencing the post-formation development of landslide dams in the Murchison dataset include the dam-forming landslide's source rock mass and material characteristics. Highly weathered and low strength rock material and closely spaced, low persistence and small defect unit block sizes are all associated with failed dams in the dataset.
- The average block size (D_{50}) influences the post-formation development of the landslide dams. The mean block size for failed dams in the dataset is 300mm, while the mean block size for a non-failed dam is 500mm.
- Dam dimensions affect the post-formation development of the landslide dams. Non-failed dams are characterised by a higher (pre-failure) crest height (42m for non-failed, 24m for failed), larger dam volume ($4.5 \times 10^6 \text{ m}^3$ for non-failed; $1.5 \times 10^6 \text{ m}^3$ for failed dams), and higher upstream and downstream slope of the dam face (8° for non-failed, $\sim 12^\circ$ for failed dams).

- Lake volume has some control on the post-formation development of the landslide dams, with the average original lake volume for failed dams of $3.9 \times 10^6 \text{ m}^3$ while non-failed dams have an average original lake volume of $1.8 \times 10^6 \text{ m}^3$.
- Rock type is not found to significantly influence the post-formation development of landslide dams in the Murchison dataset, unit rock block size being far more significant in terms of resisting erosion accompanying downcutting.
- There is a low correlation among 1) the type of landslide movement, state of landslide activity (timing of movements); 2) distribution of landslide activity (distribution of movement in the landslide); 3) style of landslide activity (how different movements contribute to landslide mass), and the post-formation development of landslide dams in the Murchison dataset.
- All dams that drain by overtopping of the impoundment and have not catastrophically failed show gradual erosion of the dam material, and subsequent lowering of the dam crest/lake level.

7.2.4 GEOMORPHIC INDICES

- Geomorphic indices use a combination of dam volume, dam height, lake volume and catchment area above the point of blockage to predict the post-formation development of a landslide dam. The geomorphic indices analysed here include the Impoundment Index (I_i), Blockage Index (BI), and a Dimensionless Blockage Index (DBI) as developed by Casagli and Ermini (1999) and Ermini and Casagli (2003).
- In order to forecast the post-formation development of dams in the Murchison dataset, the I_i was applied to 19 landslide dams where original lake and dam volumes were known. This index predicted the correct post-formation development for 11 of the 19 landslide dams (58%) based on the lake and dam volume parameters. This poor correlation is interpreted as being related to the inability of the two parameters alone (both dam and lake volume) used by the index to adequately represent the strong influence that additional parameters have on a dam's post-formation development.
- The BI , when applied to 22 landslide dams from the Murchison dataset, predicted the correct post-formation development for 19 dams (86%) using the dam volume and catchment area above the point of blockage parameters. This indicates that the parameters used in the BI represent two of the most significant parameters that

influence the post-formation development of a landslide dam. However, this index does not consider, for example, the material comprising a landslide dam and its ability to resist erosion from overtopping or seepage through the dam, which were found from this study to also highly influence the post-formation development of a dam.

- Addition of the dam height parameter to the parameters used in the *BI* forms the *DBI*, which is the most recent index. Application of the *DBI* to 21 landslide dams from the Murchison dataset predicted the correct post-formation development for 17 dams (81%). This suggests that the addition of the dam height does not increase the accuracy of this index relative to the *BI*, although 81% correct prediction is still considered to be a good correlation.
- It is clear from the application of the above indices that additional parameters other than those used in existing indices influence the post-formation of a landslide dam such as a landslide dam's height to length ratio, the average block size comprising the dam, and rainfall duration.

7.3 DETAILED INVESTIGATION

7.3.1 SELECTION CRITERIA

- Detailed assessment of two failed dams (Rain Peak, No. 16; and Ram Creek, No. 25) and two non-failed dams (Lake Stanley, No. 1; and Lake Matiri, No. 5) was carried out to evaluate in greater detail additional parameters that influence or control the post-formation development of a dam. The two failed dams did so catastrophically, while the two non-failed dams potentially pose a risk to downstream settlements and infrastructure.
- The post-formation development of one dam (Lake Stanley) is correctly predicted using current geomorphic indices, while the remaining three (Lake Matiri, Rain Peak and Ram Creek) are incorrectly predicted using the geomorphic indices defined by Casagli and Ermini (1999) and Ermini and Casagli (2003).

7.3.2 LAKE STANLEY LANDSLIDE DAM

- Lake Stanley landslide dam has a total dam volume of $12.5 \times 10^6 \text{ m}^3$ and impounds $6.5 \times 10^6 \text{ m}^3$ of water at 770 m.a.s.l. forming Lake Stanley, which drains via overtopping through an incised but armoured spillway. A landslide triggered by the 1929

Murchison earthquake caused the formation of the current lake. Landsliding within the 1929 landslide source complex has occurred at least twice since that time, and at least once prior to 1929. The pre-1929 landslide dammed the Stanley River at the same location as the present dam; however, it had drained before the 1929 landslide event. The current dam material is moderately weathered, very strong, angular, well-graded volcanoclastic rock with a D_{50} of 250mm and a maximum block size of 5m.

- In its current state the landslide dam is stable, which agrees with the post-formation development predicted by all three geomorphic indices. The stability of the dam is attributed to its large dam volume relative to a small catchment size of 33 km², the ability of the dam material to resist erosion from overtopping and seepage, and armouring in the spillway by larger (> 3m diameter) blocks.
- Further landsliding at Lake Stanley is likely to occur based on the history and kinematics of the landslides at the point of current damming. This could increase the height of the current dam and raise the lake level, which has the potential to fail catastrophically given the likely small defect unit block size because of the closely fractured nature of the source rock mass. There is a lesser chance of landsliding into Lake Stanley and displacing the lake water, however there is evidence for potential landsliding on the southern slopes bordering the lake.

7.3.3 RAM CREEK LANDSLIDE DAM

- Ram Creek landslide dam had an original volume of $2.8 \times 10^6 \text{ m}^3$, and it formed from a landslide with a volume of $4.4 \times 10^6 \text{ m}^3$ that was triggered by the 1968 M_s 7.2 Inangahua earthquake. The dam impounded a lake, which did not overtop the dam crest until its failure in 1981 following a high duration rainstorm event. Overtopping of the dam crest caused the catastrophic release of the maximum lake volume of about $1.0 \times 10^6 \text{ m}^3$, which damaged infrastructure and inundated farmland for 6km downstream to its confluence with the Buller River.
- The dam material is angular, poorly sorted, moderately to highly weathered, moderately strong to strong granite, with a D_{50} of 70mm and a maximum block size of 1m in diameter and is intermediate between matrix and block supported
- Failure is attributed to the rapid erosion of the fine dam material following first overtopping of the impoundment.

- Application of the I_i , BI and DBI predict Ram Creek landslide dam to be stable based on the original dimensions, when clearly it is not. This incorrect prediction is based on the inability of the parameters used in the indices to represent the highly erodible nature of the fine-grained material comprising the landslide dam, as demonstrated by the small D_{50} , and the likely high rainfall duration.

7.3.4 RAIN PEAK LANDSLIDE DAM

- Rain Peak landslide dam had an original volume of $1.0 \times 10^6 \text{ m}^3$, and it formed from a landslide that was triggered by the 1929 Murchison earthquake, impounding a maximum of $300,000 \text{ m}^3$ of water before episodic overtopping caused failure in stages between 1977 and 2002, reducing the lake volume to $\sim 2,000 \text{ m}^3$. Drainage of the impoundment was via a spillway over the crest of the dam, allowing gradual erosion of dam material until complete failure occurred.
- The dam material is highly weathered, moderately strong massive granite that is block supported, with a maximum block size of 1.5m and a D_{50} of 60mm.
- Application of the I_i , BI and DBI predict Rain Peak landslide dam to be stable based on the original dimensions, when clearly it is not. As with Ram Creek, the incorrect prediction is based on the inability of the parameters used in the indices to represent the highly erodible nature of the material comprising the landslide dam, as demonstrated by the small D_{50} and the highly weathered, weak material comprising the dam.
- High rainfall duration in the small catchment above the dam (3.5 km^2) is likely to have initiated the episodic overtopping failure of the dam. Final catastrophic failure occurred > 40 yrs after formation because gradual erosion of the dam in the spillway reduced its capacity to resist high flows over its crest produced by high duration rainfall. Rainfall duration is not represented in the current indices.

7.3.5 LAKE MATIRI LANDSLIDE DAM

- Lake Matiri landslide dam was formed from a landslide in steeply dipping Tertiary sandstones about 300yrs ago based on C^{14} dating of plant material in landslide deposits (Adams 1981a). Further landsliding was triggered by the 1929 Murchison earthquake, the volume of which is unknown. The total dam volume is estimated at $3.1 \times 10^6 \text{ m}^3$, which currently impounds $6 \times 10^6 \text{ m}^3$ of water to form Lake Matiri. Drainage of the impoundment is via overtopping and seepage through the dam.

- Material comprising the dam is moderately weathered, strong, moderately well sorted, block supported calcareous sandstone, with a maximum block size of 20m and a D_{50} between 2 and 4m. In its current state the landslide dam is considered stable from catastrophic failure based on the lack of erosion of the dam crest since formation (< 2m).
- Application of the I_i , BI and DBI suggest the dam should have failed, but clearly, the dam has not. The incorrect prediction of Lake Matiri's post-formation development is due to the inability of the parameters used in the indices to represent the dam's large block size, which resists overtopping and seepage erosion. The valley morphology at the point of blockage is narrow because of a ridge that propagates into the valley at right angles to river flow.
- Further landsliding at Lake Matiri, particularly into the lake, is unlikely, as the Matiri River no longer undercuts the valley wall at the dam site or around the lake edge. It is therefore expected that the dam will continue to retain Lake Matiri for an indefinite period.

7.3.6 GENERAL CONCLUSIONS

- Dam material characteristics strongly influence the post-formation development of the landslide dams studied. In particular, the block size of the dam material is thought to have a major influence on post-formation development.
- Larger average block size of dam material ($> \sim 250\text{mm}$) correspond to relative stability, while dams comprising smaller ($< \sim 100\text{mm}$) average block size are easily eroded and hence potentially unstable. Between these limits (100-250) failure depends on the maximum block size and the nature of support (i.e. block or matrix supported).
- Rainfall duration influences the post-formation development of the landslide dams studied by providing higher flows that entrain (finer-grained) dam material upon breaching or overtopping, causing catastrophic failure.
- Dam geometry (upstream and downstream slope of the dam face) influences the stability of a landslide dam. Increasing the slope of the downstream face increases the velocity and erosivity of overtopping waters, and hence decreases stability. The steepness of the dam face is a function of the basal length of a dam (termed footprint

length, this study) and the height of the minimum crest level above the original valley floor.

7.4 MODIFIED DIMENSIONLESS BLOCKAGE INDEX (*MDBI*)

7.4.1 IMPORTANT ADDITIONAL PARAMETERS

- The representation of parameters that influence the post-formation development of a dam through the I_t , BI and DBI shows, in general, a good correlation, with better than 80% accuracy for the BI and DBI . Only the I_t was found in this study not to be a good predictor.
- Several other parameters are very important in controlling the post-formation development of a landslide dam that cannot be represented by the parameters used in the indices, such as the average block size of the dam material, downstream face angle of a dam (represented using dam height and dam footprint length) and rainfall duration.

7.4.2 FORMULATION OF THE *MDBI*

- A new geomorphic index, the Modified Dimensionless Index (*MDBI*), has been developed as part of this study. This index uses the four parameters identified as being influential in the post-formation development of a landslide dam used that are included in existing geomorphic indices. Two additional parameters, the average block size and the dam footprint length, are combined to form the *MDBI* which is given as:

$$MDBI = \log \left(\left(\frac{A_c}{A_l} \right) \times \left(\frac{H_d}{L_f} \right) \times \left(\frac{V_d}{V_b} \right) \right)$$

where A_c is the catchment area (m^2), A_l is the lake area (m^2), H_d is the height of the dam (m), L_f is the length of the dam footprint at the lowest point in the dam crest (m), V_d is the volume of the dam (m^3), and V_b is the volume of the mean block size forming the dam (cube of the D_{50} expressed in m^3). The index itself is dimensionless, as is each of the component parameters.

- The *MDBI* was applied to Lake Stanley (No. 1), Lake Matiri (No. 5), Rain Peak (No. 16), and Ram Creek (No. 25), which are all included in the Murchison dataset. The Poerua landslide dam was also included because it is a good example of a recent landslide dam in New Zealand that had failed within one week of formation.

- These five dams were selected because 1) they represent the entire range of post-formation dam development from high longevity and low erosion of dam material, to low longevity and high erosion of dam material; 2) all necessary parameters required for the *MDBI* are known; and 3) there is a good knowledge of each dam's post-formation history.

7.4.3 APPLICATION TO FIVE DAMS

7.4.3.1 Lake Stanley and Lake Matiri Landslide Dams

- Lake Stanley and Lake Matiri landslide dams have both stabilised at or below their original crest height following dam formation, and are currently considered to be stable. Application of the *MDBI* to the current dimensions of Lake Matiri landslide dam gives a value of 6.94, while application of this index to the current dimensions of Lake Stanley landslide dam gives a value of 8.90.

7.4.3.2 Rain Peak, Ram Creek

- Rain Peak and Ram Creek landslide dams have undergone substantial erosion via one or several catastrophic overtopping failure events; both are described as failed landslide dams, even though $< 5\%$ of the original lake volume remains.
- Applying the *MDBI* index to the original (pre-failure) dam dimensions of Rain Peak landslide dam gives a value of 10.75; applying it to Ram Creek landslide dam gives a value of 10.80.

7.4.3.3 Poerua Landslide Dam

- The original volume of the Poerua Landslide Dam was approximately $10 \times 10^6 \text{ m}^3$, which impounded a lake with a volume between 5 and $7 \times 10^6 \text{ m}^3$. The lake overtopped the dam 24 hours after formation without catastrophic failure; six days after initial overtopping the dam failed catastrophically during a rainstorm, reducing the lake to about 25% of its original volume.
- The dam material consisted of angular boulders of schist and colluvium with a maximum diameter of 4m, and an average diameter (D_{50}) of 6mm. Application of the *MDBI* yields a value of 14.90.

7.4.4 RESULTS FROM *MDBI* APPLICATION

- Calculated *MDBI* values for 3 dams defined as failed have a significantly higher *MDBI* value (> 10) than the two stable landslide dams, which have a *MDBI* value less than 10. Therefore, by using an *MDBI* value of 10 the five dams can be divided into two classes based on their observed actual post-formation development, with 1) $MDBI > 10$ indicating a higher probability that catastrophic failure will occur (generally upon first overtopping; loosely termed ‘unstable’); and 2) $MDBI < 10$ indicating a lower probability that catastrophic failure will occur, however gradual erosion and self-armouring may occur over time for such dams (termed ‘stable’).
- The V_d/V_b ratio is highly sensitive to variation in the average block size comprising a dam, which is a parameter shown to be a major influence in a dam’s stability. This ratio has the greatest influence in the *MDBI* value.

7.5 RECOMMENDATIONS FOR FURTHER RESEARCH

- It is recommended that a wider landslide dam dataset be applied to the *MDBI* to further test its accuracy, and to refine the parameters used both for short-term stability assessment following impoundment, and for longer-term prediction of post-formation dam (and lake) development.
- Rainfall duration and maximum block size of the dam material also require further evaluation. Refining the *MDBI* to include parameters such as D_{60}/D_{10} may provide better estimation of landslide dam development post-formation.
- It is clear from the Murchison study that the block size and grading (matrix or block support) of the landslide dam material exert significant influence on dam longevity and evolution, and this is reflected in the substantial weighting given to D_{50} in the *MDBI*.
- The *MDBI* appears to be a useful tool for initial hazard assessment for newly formed landslide dams through definition of four domains based on the *MDBI* values for the five dams.

REFERENCES

- Adams, J., (1981 a). Earthquake-dammed lakes in New Zealand. *Geology*, 9: 215-219.
- Adams, J., (1981 b). Earthquake-triggered landslides form lakes in new Zealand. *Earthquake Information Bulletin*, 13(6): 205-215.
- Anderson, H. and Webb, T., (1994). New Zealand Seismicity: patterns revealed by the upgraded National Seismograph Network. *New Zealand Journal of Geology and Geophysics*, 37: 477-493.
- Asanza, M., Schuster, R.L. and Ribadeneira, S., 1991. Landslide blockage of the Pisque River, northern Ecuador. Bell, D.H., editor, Landslides. Glissements de Terrain. Proceedings of the sixth international symposium 10-14 February 1992, Christchurch: 1229-1234.
- Bathurst, J.C. and Ashiq, M., (1998). Daybreak flood impact on mountain stream bed load transport after 13 years. *Earth Surface Processes and Landforms*, 23(7): 643-649.
- Bell, D.H. and Pettinga, J.R., (1983). Presentation of geological data. *Engineering for dams and canals*, I.R.Brown, editor, *Proceedings of the Technical Group*, 9(4(G)): I4.1-4.35.
- Bell, F.G., (1983). *Engineering Properties of Soils and Rocks (2nd ed.)*. London, Butterworths, 149 pp.
- Benn, J.L., (1990). A chronology of flooding on the West Coast, South Island, New Zealand 1846 - 1990, *West Coast Regional Council Report*.
- Benn, J.L., (1992). A review of earthquake hazards on the West Coast. *The West Coast Regional Council*, February 1992: 12-58.
- Berryman, K.R., (1980). Late Quaternary movement on the White Creek Fault, South Island, New Zealand. *New Zealand Journal of Geology and Geophysics*, 23(1): 93-101.

- Bishop, K.M., (2002). A long-runout landslide in southeastern California; block glide or rock avalanche? A suggested modification in the definition of a rock avalanche. *Geological Society of America*, 34(5): 93.
- Blikra, L.H. and Nemec, W., (1998). Postglacial colluvium in western Norway; depositional processes, facies and palaeoclimatic record. *Sedimentology*, 45(5): 909-959.
- Bommer, J.J. and Rodriguez, C.E., (2002). Earthquake-induced landslides in Central America. *Engineering Geology*, 63.
- Brown, M.C., (1976). *Difficult country: An informal history of Murchison*. Murchison Historical and Museum Society Inc., 262 pp.
- Canuti, P., Casagli, N. and Ermini, L., (1998). Inventory and analysis of landslide dams in the Northern Apennine as a model for induced flood hazard forecasting. In: K. Andah (Editor), *Managing Hydro-Geological Disasters in a vulnerable Environment*. CRN - GNDICI Publication 1900. CNR - GNDICI - UNESCO (IHP), Perugia, pp. 189-202.
- Casagli, N. and Ermini, L., (1999). Geomorphic analysis of landslide dams in the Northern Apennine. *Transactions, Japanese Geomorphological Union*, 20(3): 219-249.
- Casagli, N. and Ermini, L., (2000). Landslide dam management: from hazard source to environmental resource. In: K. Andah (Editor), *Water Resources Management in a Vulnerable Environment for Sustainable Development*. CRN - GNDICI Publication 2115 CNR - GNDICI - UNESCO (IHP), Perugia, pp. 209-219.
- Casagli, N., Ermini, L. and Rosati, G., (2003). Determining grain size distribution of the material composing landslide dams in the Northern Apennines: sampling and processing methods. *Engineering Geology*, 69: 83-97.
- Clague, J.J. and Evans, S.G., (1994). Formation and failure of natural dams in the Canadian Cordillera. *Geological Survey of Canada Bulletin*, 464: 35pp.
- Costa, J.E., (1985). Floods from dam failures, *United States Geological Survey, Open File Report 85-560*.
- Costa, J.E., (1988). Floods from dam failures. In: V.R. Baker, R.C. Kochel and P.C. Patton (Editors), *Flood Geomorphology*. John Wiley and Sons. Inc., pp. 439-69.
- Costa, J.E., (1991). Nature, mechanisms, and mitigation of the Val Pola landslide, Valtellina, Italy, 1987-1988. *Z Geomorph. N.F.*, 35(1): 15-38.
- Costa, J.E. and Schuster, R.L., (1988). The formation and failure of natural dams. *Geological Society of America Bulletin*, 100: 1054-1068.

- Costa, J.E. and Schuster, R.L., (1991). Documented historical landslide dams from around the world. *U.S. Geological Survey Open-File Report 91-239*: 486pp.
- Crozier, M.J., (1986). *Landslides: causes, consequences & environment* / Michael J. Crozier. Croom Helm.
- Crozier, M.J., Deimel, M.S. and Simon, J.S., (1995). Investigation of earthquake triggering for deep-seated landslides, Taranaki, New Zealand. *Quaternary International*, 25: 65-73.
- Cruden, D.M., (1991). A simple definition of a landslide. *Bulletin of the International Association of Engineering Geology* (43): 27-29.
- Cruden, D.M. and Varnes, D.J., (1996). Landslide types and processes. In: A.K. Turner and R.L. Schuster (Editors), *Landslides: Investigation and Mitigation special report 247*. National Academy Press, Washington, D.C.
- Dethier, D.P. and Reneau, S.L., (1996). Lacustrine chronology links Late-Pleistocene climate change and mass movements in northern New Mexico. *Geology*, 24(6): 539-542.
- Donadini, L. and Kunz, M., (2002). Laboratory model of the Poerua landslide dambreak in 1999 in Westland, New Zealand. Dissertation for the

Diploma in Environmental Engineering, *Thesis*, ETH-Zuerich, Switzerland, 36p + App pp.
- Dowrick, D.J., (1994). Damage and intensities in the magnitude 7.8 1929 Murchison, New Zealand, earthquake. *Bulletin of the New Zealand Society for Earthquake Engineering*, 27(3): 190-203.
- Eden, D.N. and Page, M.J., (1998). Paleoclimate implications of a storm erosion record from Holocene lake sediments, north Island, New Zealand. *Palaeogeography, Palaeoclimatology, Palaeoecology*, 139: 37-58.
- Eisbacher, G.H. and Clague, J.J., (1984). Destructive mass movements in high mountains; hazard and management. *Paper - Geological Survey of Canada*, 84-16: 228.
- Ermini, L. and Casagli, N., (2003). Prediction of the behaviour of landslide dams using a geomorphological dimensionless index. *Earth Surface Processes and Landforms*, 28: 31-47.
- Evans, S.G., (1986a). Landslide damming in the cordillera of western Canada. In: R.L. Schuster (Editor), *Landslide dams: Processes, risk and mitigation*. American Society of Civil Engineers, pp. 111-130.

- Evans, S.G., (1986b). The maximum discharge of outburst floods caused by the breaching of man-made and natural dams. *Canadian Geotechnical Journal*, 23(3): 385-387.
- Ferrar, H.T. and Grange, L.I., (1929). Geological Reconnaissance of the Murchison Earthquake Area. *New Zealand Journal of Science and Technology*, 11: 185-191.
- Francis, P., 1993. Volcanoes: a planetary perspective / Peter Francis. Oxford University Press.
- Fread, D.I., (1988). *BREACH - An erosion model for earthen dam failures*. Silver Spring, Maryland, National Weather Service, 29 pp.
- Fyfe, H.E., (1929). Movement on the white creek fault New Zealand, during the Murchison earthquake of 17th June 1929. *The New Zealand Journal of Science and Technology*, 11: 192-197.
- Grigg, J.R., (1947). *Murchison, New Zealand; How a settlement emerges from the bush*. R. Lucas and Son (Nelson Mail) Ltd. Nelson, New Zealand, 98 pp.
- Hancox, G., Perrin, N. and Dellow, G., (2002). Recent studies of historical earthquake - induced landsliding, ground damage, and MM intensity in New Zealand. *Bulletin of the New Zealand Society for Earthquake Engineering*, 35(2): 59-95.
- Hancox, G.T., McSaveney, M.J., Davies, T.R. and Hodgson, K., (1999). Mt Adams rock avalanche of 6 October 1999 and the subsequent formation and breaching of a large landslide dam in Poerua River, Westland, New Zealand. 99/19, *Institute of Geological and Nuclear Sciences*.
- Hancox, G.T. and Perrin, N., (1994). Green Lake landslide: a very large ancient rockslide in glaciated terrain, Fiordland, New Zealand, *Institute of Geological and Nuclear Sciences Science Report 93/18*, Lower Hutt.
- Hancox, G.T., Perrin, N. and Dellow, G., (1997). Earthquake - induced landsliding in New Zealand and implications for MM intensity and seismic hazard assessment, *Institute of Geological and Nuclear Sciences Science Report 43601B*.
- Hansen, D.E. and Morgan, R.L., (1986). Control of thistle Lake, Utah. In: R.L. Schuster (Editor), *Landslide dams; Processes, risk and mitigation*. American Society of Civil Engineers, pp. 84-97.
- Henderson, J., (1937). The west Nelson earthquake of 1929. *The New Zealand journal of Science and Technology*, 19(2): 65-144.
- Hewitt, K., (1998). Catastrophic landslides and their effects on the Upper Indus streams, Karakoram Himalaya, northern Pakistan. *Geomorphology*, 26: 47-80.

- IAEG, C.o.L., (1990). Suggested nomenclature for landslides. *Bulletin of the International Association of Engineering Geology*(41): 13-16.
- Inwood, K.S., (1997). Geological setting, gravity collapse and hazard assessment of the Kongahu Fault zone, Westport. Unpublished M.Sc. Thesis, University of Canterbury, New Zealand, 156 pp.
- ISDR, (2000). *USOI Landslide Dam and Lake Sarez*. United Nations, 115 pp.
- Johnston, M.R., (1974). Major landslides in the Upper Buller Gorge, southwest Nelson. *New Zealand Institute of Engineers transactions*, 1: 239-244.
- Kalser, B.N. and Fleming, R.W., (1986). The 1983 landslide dam at Thistle, Utah. In: R.L. Schuster (Editor), *Landslide dams: Processes, risk and mitigation*. American Society of Civil Engineers, pp. 59-83.
- Keefer, D.K., (1984). Landslides caused by earthquakes. *Geological Society of America Bulletin*, 95: 406-421.
- Kiersch, G.A., (1964). Vaiont reservoir disaster'. *Civil Engineering*, 34: 32-39.
- King, J., Loveday, I. and Schuster, R.L., (1989). The 1985 Bairaman landslide dam and resulting debris flow, Papua New Guinea. *Quarterly Journal of engineering Geology*, 22: 257-270.
- Kojan, E. and Hutchison, J.N., (1978). Mayunmarca rockslide and debris flow, Peru. In: B. Voight (Editor), *Rockslides and avalanches; 1, Natural phenomena*. Elsevier Sci. Publ. Co., Amsterdam, Netherlands, pp. 315-361.
- Korup, O., (2002). Recent research on landslide dams - a literature review with special attention to New Zealand. *Progress in Physical Geography*, 26(2): 206-235.
- Kramer, S.L., (1996). Geotechnical earthquake engineering. *Prentice-Hall civil engineering and engineering mechanics series*.
- Lensen, G.L. and Otway, (1971). Earthshift and post-earthshift deformation associated with the May 1968 Inangahua earthquake, New Zealand. *Recent Crustal Movements, Royal Society of New Zealand*, 9: 107-116.
- Lensen, G.L. and Suggate, R.P., (1968). Inangahua earthquake - Preliminary account of the geology. *Preliminary Reports on the New Zealand Department of Scientific and Industrial Research Bulletin*, 193: 17-36.
- Li, T., (1989). Landslides extent and economic significance in China. In: E.E. Brabb and B.L. Harrod (Editors), *Landslides. extent and economic significance. Proceedings*

- 28th International Geological Congress Symposium on Landslides, 17 July, Washington D.C. Rotterdam. Barkema, pp. 271-287.*
- Li, T., Schuster, R.L. and Jishan, W., (1986). Landslide dams in South - Central China. In: R.L. Schuster (Editor), *Landslide dams: Processes, risk and mitigation*. American Society of Civil Engineers, pp. 146-162.
- Macchione, F. and Sirangelo, B., (1988). Study of earth dam erosion due to overtopping. *Proceedings of the Technical Conference in Geneva organised by the World Meteorological Organisation, Nov. 1988: 212-219.*
- Manville, V., (2001). Techniques for evaluating the size of potential dam - break floods from natural dams. *Institute of Geological and Nuclear Sciences report 2001/28.*
- Meyer, W., Sabol, M.A. and Schuster, R.L., (1986). Landslide dammed lakes at Mount St. Helens, Washington. In: R.L. Schuster (Editor), *Landslide dams: processes, risk and mitigation*. American Society of Civil Engineers, pp. 21-41.
- Meyer, W., Schuster, R.L., Fellow, ASCE and Sabol, M.A., (1994). Potential for seepage erosion of landslide dam. *Journal of Geotechnical Engineering*, 120(7): 1211-1229.
- Muller, M., (1997). Landslides at Lake Stanley, *Unpublished Report for the Tasman District Council*, Nelson, New Zealand.
- Munker, C. and Cooper, R.A., (1999). The Cambrian arc complex of the Takaka Terrane, New Zealand: an integrated stratigraphical, paleontological and geochemical approach. *New Zealand Journal of Geology and Geophysics*, 42: 415-445.
- Nathan, S., 1978a. Sheets S31 and Pt S32 - Buller-Lyell. Geological map of New Zealand 1:63 360 NZGS.
- Nathan, S., (1978b). Tertiary rocks near the White Creek Fault, Upper Buller gorge, New Zealand. *Journal of the Royal Society of New Zealand*, 8(1): 5-15.
- Nicoletti, P.G. and Parise, M., (1994). Rock-avalanche and backwater-flooding hazards at Plati (S. Italy). *proceedings of the seventh international congress International Association of Engineering Geology*: 1391-1399.
- Nicoletti, P.G. and Scalzo, A., (1998). Ancient landslide-dammed lakes in southeastern Sicily and their presumable contribution to malaria development: a poorly known effect of local seismicity. *International Journal of Anthropology*, 13(3-4): 201-210.
- Nicoletti, P.G. and Sorriso-Valvo, M., (1991). Geomorphic controls of the shape and mobility of rock avalanches. *Bulletin of the Geological Society of America*, 103(10): 1365-1373.

- Ongley, M., (1932). Waikaremoana. *The New Zealand Journal of Science and Technology*, 14: 173-184.
- Pearce, A.J. and O'Loughlin, C.L., (1985). Landslides during a M7.7 earthquake: influence on geology and topography. *Geology*, 13: 855-858.
- Pearce, A.J. and Watson, A.J., (1986). Effects of earthquake - induced landslides on sediment budget and transport over a 50-year period. *Geology*, 14: 52-55.
- Perrin, N. and Hancox, G.T., (1992). Landslide - dammed lakes in New Zealand Preliminary studies on their distribution, causes and effects. *Bell, D.H., editor, Landslides. Glissements de Terrain. Proceedings of the sixth international symposium 10-14 February 1992, Christchurch*: 1457-66.
- Pettinga, J.R., (1997). *Present-day plate boundary tectonics of New Zealand; from oblique subduction to continental collision*. Terrane dynamics 97; international conference on Terrane geology; abstracts of papers presented, 136-139 pp.
- Philip, H. and Ritz, J.-F., (1999). Gigantic paleolandslide associated with active faulting along the Bogd fault (Gobi-Altay, Mongolia). *Geology*, 27(3): 211-214.
- Rattenbury, M.S., Cooper, R.A. and Johnston, M.R., (1998). Geology of the Nelson area, *Institute of Geological and Nuclear Sciences*, Lower Hutt, New Zealand.
- Rattenbury, M.S., Cooper, R.A. and Johnston, M.R., ((compilers) 1998). Geology of the Nelson area, *Institute of Geological and Nuclear Sciences*, Lower Hutt, New Zealand.
- Read, S.A.L., Beetham, R.D. and Riley, P.B., (1992). Lake Waikaremoana barrier - A large landslide dam in New Zealand. *Bell, D.H., editor, Landslides. Glissements de Terrain. Proceedings of the sixth international symposium 10-14 February 1992, Christchurch*, 2: 1481-1487.
- Reneau, S.L. and Dethier, D.P., (1996). Late Pleistocene landslide - dammed lakes along the Rio Grande, White Rock Canyon, New Mexico. *Geological Society of America Bulletin*, 108: 1492 - 1507.
- Riley, P.B., Meredith, A.S. and Lilley, P.B., (1993). Tunawaea landslide dam collapse; Physical and environmental consequences. *Proceedings of the IPENZ Annual conference, Hamilton, 1993*: 629-639.
- Riley, P.B. and Read, S.A.L., (1991). Lake Waikaremoana - present day stability of landslide barrier. *Bell, D.H., editor, Landslides. Glissements de Terrain. Proceedings of the sixth international symposium 10-14 February 1992, Christchurch*: 1249-56.

- Riley, P.B. and Read, S.A.L., (1992). Lake Waikaremoana - present day stability of landslide barrier. *Bell, D.H., editor, Landslides. Glissements de Terrain. Proceedings of the sixth international symposium 10-14 February 1992, Christchurch*: 1249-56.
- Sager, J.W. and Chambers, D.R., (1986). Design and construction of the Spirit Lake outlet tunnel, Mount St. Helens, Washington. In: R.L. Schuster (Editor), *Landslide dams: processes, risk and mitigation*. American Society of Civil Engineers, pp. 42-58.
- Schuster, R.L., (1985). Landslide dams in the western United States. *Proceedings of the 9th International Conference and Field Workshop on Landslides*: 411 - 418.
- Schuster, R.L., (1993). Landslide dams - A worldwide phenomenon. *Proceedings, Annual Symposium of the Japan landslide Society, kansai Branch, Osaka, April 27, 1993*: 1-23.
- Schuster, R.L., (1996). Slumgullion landslide dam and its effects on the Lake Fork. *Varnes, D.J., Savage, W.Z., editors, the Slumgullion Earth flow: A large - Scale natural Laboratory*, USGS Bulletin 2130.
- Schuster, R.L., (2000). Outburst debris-flows from failure of natural dams. *Proceedings of the second International Conference on Debris-Flow Hazard Mitigation/Taipei/Taiwan/16-18 August 2000*: 29-42.
- Schuster, R.L., Bucknam, R.C. and Mota, M.A., (2001). Stability assessment of a hurricane Mitch - induced landslide dam on the Rio La Lima, Sierra De Las Minus, eastern Guatemala. *USGS Open - File Report 01-120*: 1-7.
- Schuster, R.L. and Costa, J.E., (1986). A perspective on landslide dams. In: R.L. Schuster (Editor), *Landslide dams: processes, risk and mitigation*. American Society of Civil Engineers, pp. 1-20.
- Schuster, R.L., Wieckorek, G.F. and Hope, D.G., (1989). Landslide dams in Santa Cruz County, California, resulting from the earthquake. *U.S. Geological Survey Professional Paper 1551 - C*: 51-70.
- Seed, H.B., (1968). Landslides during earthquakes due to soil liquefaction. *American Society of Civil Engineers, Journal of the Soil Mechanics and Foundation Division Geotechnical Special Publication 3*, 94(SM5): 1053-1122.
- Shulmeister, J., McKay, R., Singer, C. and McLea, W., (2001). Glacial geology of the Cobb Valley, northwest Nelson. *New Zealand Journal of Geology and Geophysics*, 44: 47-54.
- Singh, V.P., (1996). Dam breach modelling technology. *Water Science and Technology Library*, 17(Chapter 2): 27-40.

- Speight, R., (1933). The Arthur's Pass earthquake of 9 March 1929. *The New Zealand journal of Science and Technology*, 15: 173-182.
- Stirling, M.W., McVerry, G.H. and Berryman, K.R., (2002). A new seismic hazard model for New Zealand. *Bulletin of the Seismological Society of America*, 92(5): 1878-1903.
- Stocker, R.V., (1997). Lake Stanley Dam Failure Investigation, *Envirotech Design Group*, Takaka.
- Suggate, R.P., 1984. Sheet M29 AC - Mangles Valley. Geological map of New Zealand 1:50 000. Department of Scientific and Industrial Research, Wellington, New Zealand.
- Swanson, F.J., Oyagi, N. and Tominaga, M., (1986). Landslide dams in Japan. In: R.L. Schuster (Editor), *Landslide dams: Processes, risk and mitigation*. American Society of Civil Engineers, pp. 131-145.
- Trauth, M.H., Alonso, R.A., Haselton, K.R., Hermanns, R.L. and Strecker, M.R., (2000). Climate change and mass movements in the NW Argentine Andes. *Earth and Planetary Science Letters*, 179: 243-256.
- Trauth, M.H. and Strecker, M.R., (1999). Formation of landslide - dammed lakes during a wet period between 40,000 and 25,000 yr B.P. in northwestern Argentina. *Palaeogeography, Palaeoclimatology, Palaeoecology*, 153: 277-287.
- Turner, A.K. and Schuster, R.L., (1996). *Landslides: Investigation and mitigation* / A.K. Turner, R.L. Schuster, editors. National Academy Press, 673 pp.
- Van Asch, T.W.J., Buma, J. and Van Beek, L.P.H., (1999). A view on some hydrological triggering systems in landslides. *Geomorphology*, 30: 25-32.
- Varnes, D.J., (1978). *Slope movement types and processes*. in Schuster, R.L., Kirizek, R.J. eds., *Landslides - Analysis and control*. National Academy of Sciences, Washington, D.C., Transportation Research Board Special Report 176, p. 11-33.
- Varnes, D.J., (1984). Landslide hazard zonation: a review of principles and practice. *United Nations Educational, Scientific and Cultural Organisation, Paris*: 61 pp.
- Walder, J.S. and O'Connor, J.E., (1997). Methods for predicting peak discharge of floods caused by failure of natural and constructed earthen dams. *Water Resources Research*, 33(10): 2337-2348.
- Wayne, W.J., (1999). The Alemania rockfall dam: A record of a Mid - Holocene earthquake and catastrophic flood in northwestern Argentina. *Geomorphology*, 27: 295-306.

- Webby, M.G. and Jennings, D.N., (1994). Analysis of dam break flood caused by failure of Tunawaea landslide dam. *IEAust Conference on Hydraulics in Civil Engineering 15-17 February, 1994, Brisbane, Australia*: 163-168.
- Yeats, R.S., (2000). The 1968 Inangahua, New Zealand, and 1994 Northridge, California, earthquakes: implications for northwest Nelson. *New Zealand Journal of Geology and Geophysics*, 43: 587-599.
- Yetton, M.D., (1998). Progress in understanding the paleoseismicity of the central and northern Alpine Fault, Westland, New Zealand. *New Zealand Journal of Geology and Geophysics*, 41(4): 475-483.
- Yetton, M.D., (2002). Paleoseismic investigation of the north and west Wairau sections of the Alpine Fault, South Island, New Zealand, *Earthquake Commission Research Report No. 99/353*, Christchurch.

Appendix A

Sample Landslide and Dam Datasheets

This Appendix contains an example of Casagli and Ermini (1999) datasheets for the landslide and dam, lake and catchment. Samples of the modified datasheets from the Murchison study are included with an example of the A4 schematic map that compliments each dam in the Murchison dataset.

DAM DEBRIS SOURCE AREA				
Reference number:		Reference name:		
Date of landslide:		NZMG coordinates for source centre:		
Subsequent major landslide failures:		Map edition/Scale:		
District in which landslide occurred <input type="radio"/> Tasman <input type="radio"/> Westland		Approx. elevation of landslide centre (m.s.l.):		
SOURCE DIMENSIONS ¹				
Rupture length (m)	Area (m ²):	Head elevation (m.s.l.):		
Rupture width (m):	Initial landslide volume (m ³):	Toe elevation (m.s.l.):		
Rupture depth (m):	Final landslide volume ² (m ³):	Travel angle/azimuth (°):		
GEOLOGY				
Geological description of source rock:				
Rock Material ³				Land use
Weathering:		Fabric:		<input type="radio"/> shrubs/bushland
Strength:		Rock name:		<input type="radio"/> forest (native)
Rock Mass ³				<input type="radio"/> forestation
Defect spacing:		Average unit block size:		<input type="radio"/> urban areas
Defect persistence:		Dip/direction of joint/strata (°):		<input type="radio"/> farmland
LANDSLIDE CLASSIFICATION ⁴				
DESCRIPTION OF INITIAL FAILURE		ACTIVITY		
Movement	Velocity	State	Landslide movement	Style
<input type="radio"/> fall	<input type="radio"/> very slow (< 1.6m/year)	<input type="radio"/> active	<input type="radio"/> advancing	<input type="radio"/> single
<input type="radio"/> rock avalanche	<input type="radio"/> slow (< 13m/month)	<input type="radio"/> reactivated	<input type="radio"/> retrogressive	<input type="radio"/> complex
<input type="radio"/> translational slide	<input type="radio"/> moderate (< 1.8m/h)	<input type="radio"/> suspended	<input type="radio"/> widening	<input type="radio"/> composite
<input type="radio"/> rotational slide	<input type="radio"/> rapid (< 3m/min)	<input type="radio"/> dormant	<input type="radio"/> enlarging	<input type="radio"/> multiple
<input type="radio"/> spread	<input type="radio"/> very rapid (< 5m/s)	<input type="radio"/> stabilised	<input type="radio"/> diminishing	<input type="radio"/> successive
<input type="radio"/> flow	<input type="radio"/> extremely rapid (> 5m/s)	<input type="radio"/> abandoned	<input type="radio"/> confined	
Acquisition of velocity information <input type="radio"/> observed <input type="radio"/> reported/published <input type="radio"/> personal account <input type="radio"/> inferred				
Material	General description of first movement and any subsequent movements:			
<input type="radio"/> rock				
<input type="radio"/> debris				
<input type="radio"/> earth				
LANDSLIDE CAUSE (S)				
Pre-existing geological controls:				
Triggering mechanisms:				
Subsequent failures:				
NOTES/REFERENCES				

¹ Refer to general plan view to locate measurement positions² Final volume of displaced debris estimated using a swell factor of 33% (Nicoletti & Sorrisio - Valvo 1991)³ Qualifying terms based on Bell and Pettinga (1983)⁴ Classification based on Cruden and Varnes (1996)

A-1. Illustration of the datasheet used in the inventory of 26 landslide dams in the Murchison study to record dam-forming landslide parameters.



Università degli Studi di Firenze - Dipartimento di Scienze della Terra

DATA-FORM FOR INVENTORY OF LANDSLIDE DAMS

GENERAL INFORMATION ON THE LANDSLIDE EVENT					
Compilation		Localisation		Hydrographic basin	
Inventory No.:		Region:		1° order:	
Date:		Province:		2° order:	
Reporter:		Municipality:		3° order:	
Affiliation:		Locality:		Date of landslide:	
Cartography			UTM Co-ordinates of landslide top		
Map edition:		East:		North:	
Scale:		Reference No.:			
LANDSLIDE MORPHOMETRY					
General data		Displaced mass		Surface of rupture	
Crown elevation Q_c (m)	Horizontal length L_h (m)	Length L_d (m):		Length L_r (m):	
Head elevation Q_h (m)	Height difference H (m)	Width W_d (m):		Width W_r (m):	
Toe elevation Q_t (m)	Travel angle β (°)	Depth D_d (m):		Depth D_r (m):	
Total length L (m)	Travel azimuth α (°)	Area A_d (m ²):		Area A_r (m ²):	
Center-line length L_c (m)	Total area A (m ²)	Final volume V_f (m ³):		Initial volume V_i (m ³):	
GEOLOGY			LAND USE		
Formation 1 Formation 2 Description			<input type="radio"/> urban areas <input type="radio"/> quarry area <input type="radio"/> abandoned area <input type="radio"/> bushes <input type="radio"/> riparian vegetation <input type="radio"/> rangelands <input type="radio"/> croplands <input type="radio"/> arborized croplands <input type="radio"/> specialised cultures <input type="radio"/> reforestation <input type="radio"/> coppice <input type="radio"/> wood		
1 2 Slope-strata relationship <input type="radio"/> horizontal strata <input type="radio"/> Aniscinal slope <input type="radio"/> Orthoclinal slope <input type="radio"/> Plagioclinal slope <input type="radio"/> Cataclinal (generic) slope <input type="radio"/> Cataclinal under-dip slope <input type="radio"/> Cataclinal over-dip slope <input type="radio"/> Cataclinal omo-dip slope					
LANDSLIDE CLASSIFICATION					
Description of the first and second movement			Activity		
1 2 Movement <input type="radio"/> fall <input type="radio"/> topple <input type="radio"/> rotational slide <input type="radio"/> translational slide <input type="radio"/> spread <input type="radio"/> flow	1 2 Material <input type="radio"/> rock <input type="radio"/> debris <input type="radio"/> earth 1 2 Water content <input type="radio"/> dry <input type="radio"/> moist <input type="radio"/> wet <input type="radio"/> very wet	1 2 Velocity <input type="radio"/> extremely slow (< 16 mm/year) <input type="radio"/> very slow (< 1.6 m/year) <input type="radio"/> slow (< 13 m/month) <input type="radio"/> moderate (< 1.8 m/h) <input type="radio"/> rapid (< 3 m/min) <input type="radio"/> very rapid (< 5 m/s) <input type="radio"/> extremely rapid (> 5 m/s)	State <input type="radio"/> active <input type="radio"/> reactivated <input type="radio"/> suspended <input type="radio"/> dormant <input type="radio"/> abandoned <input type="radio"/> stabilised <input type="radio"/> relict	Distribution <input type="radio"/> moving <input type="radio"/> advancing <input type="radio"/> retrogressive <input type="radio"/> widening <input type="radio"/> enlarging <input type="radio"/> diminishing <input type="radio"/> confined	Style <input type="radio"/> single <input type="radio"/> complex <input type="radio"/> composite <input type="radio"/> multiple <input type="radio"/> successive
NOTE: 1. First movement 2. Second movement					
LANDSLIDE CAUSES					
Geological <input type="checkbox"/> weak materials <input type="checkbox"/> sensitive materials <input type="checkbox"/> weathered materials <input type="checkbox"/> sheared materials <input type="checkbox"/> adversely oriented mass discontinuity <input type="checkbox"/> adversely oriented structural discontinuity <input type="checkbox"/> contrast in permeability <input type="checkbox"/> contrast in competence <input type="checkbox"/> jointed or fissured materials	Geomorphological <input type="checkbox"/> tectonic or volcanic uplift <input type="checkbox"/> glacial rebound <input type="checkbox"/> fluvial erosion of slope toe <input type="checkbox"/> marine erosion of slope toe <input type="checkbox"/> glacial erosion of slope toe <input type="checkbox"/> erosion of lateral margins <input type="checkbox"/> deposition loading slope or its crest <input type="checkbox"/> subterranean erosion (piping, solution) <input type="checkbox"/> natural vegetation removal	Physical <input type="checkbox"/> intense rainfall <input type="checkbox"/> prolonged exceptional precipitation <input type="checkbox"/> rapid snow melt <input type="checkbox"/> thawing <input type="checkbox"/> freeze & thaw weathering <input type="checkbox"/> shrink & swell weathering <input type="checkbox"/> rapid drawdown (floods and tides) <input type="checkbox"/> earthquake <input type="checkbox"/> volcanic eruption	Anthropic <input type="checkbox"/> excavation of slope or its toe <input type="checkbox"/> loading of slope or its crest <input type="checkbox"/> rapid drawdown (reservoir) <input type="checkbox"/> critical pool level <input type="checkbox"/> water leakage <input type="checkbox"/> irrigation <input type="checkbox"/> deforestation <input type="checkbox"/> artificial vibrations <input type="checkbox"/> mining or quarrying <input type="checkbox"/> accumulation of fillings		
NOTE: (X) preparatory (■) triggering					

A-2. Illustration of the datasheet produced by Casagli and Ermini (1999) to describe dam-forming landslides.

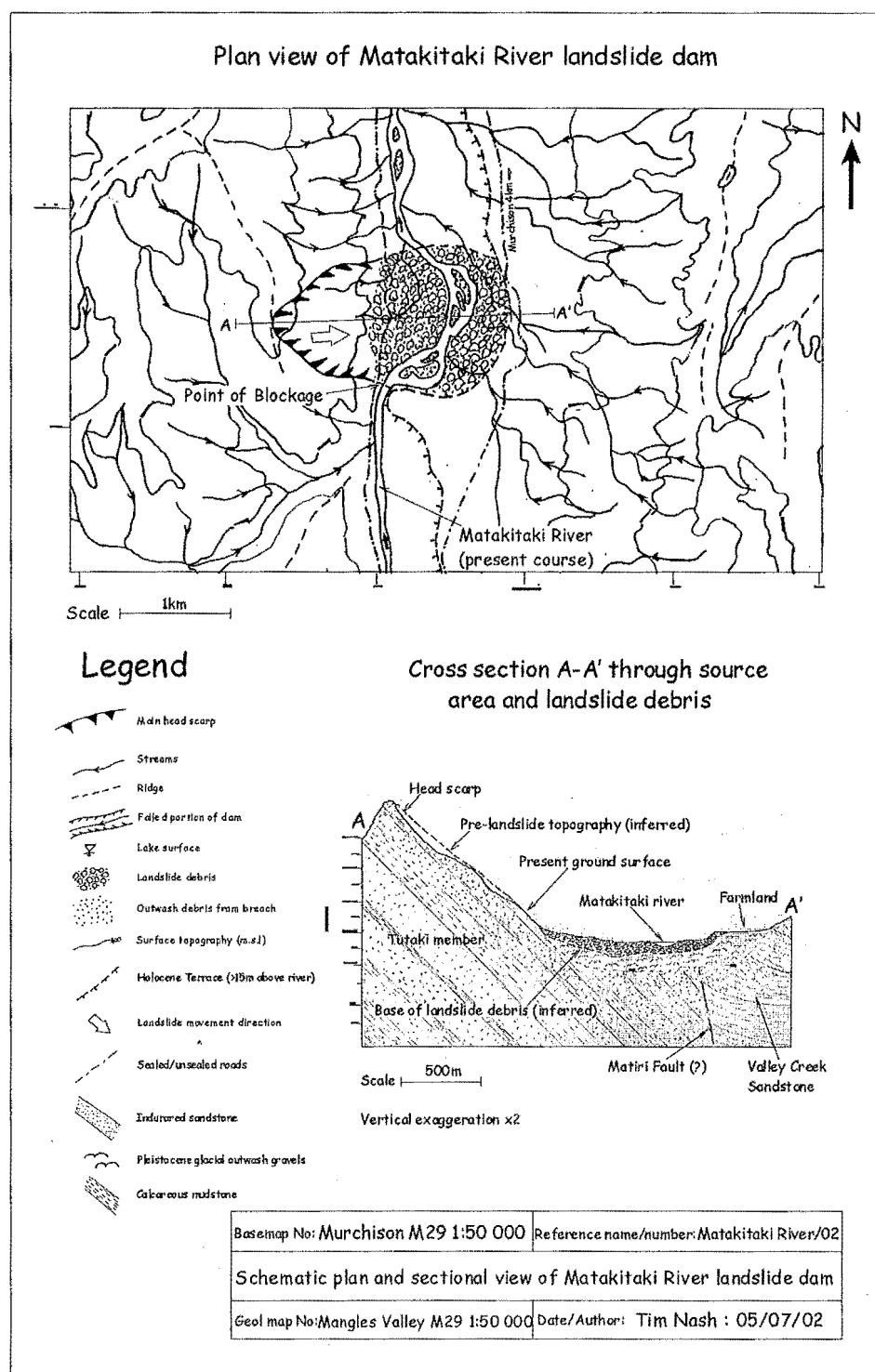
DEBRIS DAM ¹			
Reference number:		Reference name:	
Date of blockage:		NZMG coordinates for dam centre:	
Date of initial dam failure (if failure):		Approximate elevation of dam centre (m):	
Subsequent major dam failure dates:		Classification ² : <input type="radio"/> 1 <input type="radio"/> 2 <input type="radio"/> 3 <input type="radio"/> 4 <input type="radio"/> 5 <input type="radio"/> 6	
ORIGINAL DAM DIMENSIONS			
Crest length (m):	Area of landslide dam (m ²):	Downstream face slope (°):	
Crest width (m):	Volume of landslide dam (x 10 ⁶ m ³):	Upstream face slope (°):	
Crest height (m):	Average baseline length (m):		
PRESENT DAM DIMENSIONS			
Crest length (m):	Area of landslide dam (m ²):	Downstream face slope (°):	
Crest width (m):	Volume of landslide dam (x 10 ⁶ m ³):	Upstream face slope (°):	
Crest height (m):	Average baseline length (m):		
DAM MATERIALS			
Percent matrix =	Angularity	Grading of dam debris	Max grain size (mm):
<input type="radio"/> grain supported	<input type="radio"/> rounded	<input type="radio"/> poorly graded	Min grain size (mm):
<input type="radio"/> intermediate	<input type="radio"/> intermediate	<input type="radio"/> moderately graded	Av. grain size (mm):
<input type="radio"/> matrix supported	<input type="radio"/> angular	<input type="radio"/> well graded	
BREACH CHARACTERISTICS ³			
Average depth (m):	Average width (m):	Breach volume (m ³):	
Breach history			
Failure mechanism (FM)	Acquisition of FM information	Breach shape	Degree of modification ³
<input type="radio"/> overtopping	<input type="radio"/> observed	<input type="radio"/> U shaped	<input type="radio"/> complete (> 90%)
<input type="radio"/> piping	<input type="radio"/> reported/published	<input type="radio"/> V shaped	<input type="radio"/> high (65-90)
<input type="radio"/> mass sliding of landslide dam	<input type="radio"/> personal account	<input type="radio"/> trapezoidal section	<input type="radio"/> moderate (35-65)
<input type="radio"/> modified by eng. works	<input type="radio"/> inferred	<input type="radio"/> piping	<input type="radio"/> low (10-35)
<input type="radio"/> unknown			<input type="radio"/> negligible (< 10%)
LAKE AND CATCHMENT CHARACTERISTICS ⁴			
LAKE			
Lake name:	Length (m):	Present lake condition (since formation)	
Present volume (x10 ⁶ m ³):	Width (m):	<input type="radio"/> existing; no change in level <input type="radio"/> completely infilled	
Original volume (x10 ⁶ m ³):	Max depth (m):	<input type="radio"/> existing; partially infilled <input type="radio"/> drained artificially	
Lake surface elevation (m):	Area (m ²):	<input type="radio"/> partially drained by failure <input type="radio"/> unknown	
Lake deposit thickness (m):	Duration (y/m/d)	<input type="radio"/> drained by failure of dam <input type="radio"/> other ⁵	
CATCHMENT			
River name:	Drainage basin area above landslide dam (km ²):		
Yearly precipitation (mm):	Average monthly precip. (mm):	Max monthly precip. (mm):	
Mean monthly discharge (m ³ /s):	Max monthly discharge (m ³):		
Location/distance of rain gauge:	Location/distance of flow gauge:		
Valley width prior to dam formation ⁶ (m):	Valley elevation prior to dam formation ^{1,6} (m):		
Valley gradient downstream of dam (°):	Valley gradient upstream of dam (°):		
DAMAGE ⁷			
People			
Property/infrastructure			
ADDITIONAL INFORMATION			

¹ All heights measured in metres above mean sea level² Based on the Corta and Schuster (1988) classification of landslide dams³ Expressed as the percentage of dam volume removed⁴ Lake dimensions based on the lake characteristics pre or post dam failure; state in additional information which conditions are described⁵ Information on the state of lake condition other than that stated should be noted in additional information⁶ Valley width and elevation taken from the centre point of the dam prior to formation (estimated) and perpendicular to the major valley axis⁷ Caused by the formation and/or failure of the landslide dam

A-3. Illustration of the datasheet used in the inventory of 26 landslide dams in the Murchison study to document the landslide dam, lake and catchment attributes.

[illegible]

A-4. Illustration of the datasheet produced by Casagli and Ermini (1999) to describe the landslide dam, lake and catchment parameters.



A.5. Sample of the schematic plan and profile maps accompanying each landslide dam in the Murchison dataset. This particular map is of the Matakiki landslide dam, which is the second largest dam-forming landslide in the dataset.

Appendix B

Murchison Dataset (Raw Data on CD)

This Appendix contains:

- Two datasheets detailing the parameters associated with the dam-forming landslide and the dam, lake and catchment for 26 landslide dams in the Murchison dataset;
- A4 schematic plan and section map for 26 landslide dams in the Murchison dataset;
and
- Aerial oblique photo of each landslide in the Murchison dataset.

Appendix C

Synthesised Murchison Data

This appendix contains spreadsheets synthesising the Murchison dataset parameters for 26 landslide dams (Raw data in Appendix B, on CD). Qualitative data is synthesised here by linking a number for the particular parameter to descriptive terminology, which is listed following the respective spreadsheets. Appendix F gives a detailed description for each parameter used in the datasheets.

		1. General								
		Blockage date	Has dam breached or failed since formation*	Has lowering been gradual or instantaneous	Date of Breach or failure of dam*	Evidence for rapid lowering events*	Has dam crest lowered since formation*	Degree of Modification	Stable (s) Unstable (u) Other (o) unknown (un)	Dam Centre Coordinates
1	Lake Stanley	17/06/1929	✓	1	nd	*	✓	1	s	2478245:6021250
2	Marakitaki (Mud)	17/06/1929	✓	1	nd	*	✓	nd	o	2453340:5928725
3	Falls	17/06/1929	nd	1	nd	*	✓	2	s	2430685:5973685
4	Glasseye	17/06/1929	nd	1	nd	*	✓	2	s	2432055:5976820
5	Lake Matiri	17/06/1929	✓	1	nd	*	✓	nd	s	2454570:5949200
6	Lake Marina	17/06/1929	✓	1	nd	*	✓	2	s	2446455:5969720
7	Lake Dora	17/06/1929	nd	na	nd	*	*	na	s	2441965:5963825
8	Kakapo/ Haystack	17/06/1929	✓	nd	nd	nd	✓	nd	u	2448995:5990670
9	Lake Perrine	17/06/1929	✓	2	4/07/1929	✓	✓	5	u	2439890:5961640
10	Matiri (Right Branch)	17/01/1929	*	na	na	*	*	na	s	2457990:5961230
11	Maruia Falls	17/06/1929	✓	1	19/06/1929	*	✓	na	u	2428000:5927300
12	Lower Stanley	17/06/1929	✓	nd	nd	nd	✓	nd	u	2479935:6019625
13	Allen	17/06/1929	✓	nd	nd	nd	✓	2	s	2451025:5974025
14	Beautiful	17/06/1929	✓	nd	nd	nd	✓	2	s	2460595:6004640
15	lake Elmer	17/06/1929	✓	1	nd	*	✓	1	s	2450000:6041500
16	Matiri (Rain Peak)	17/06/1929	✓	2	nd	✓	✓	4	u	2452255:5947410
17	Tangent	17/06/1929	*	nd	nd	*	nd	nd	s	2449785:5984105
18	Upper Matiri	17/06/1929	✓	1	nd	*	✓	2	s	2458850:5961025
19	Lower Lindsay	17/06/1929	✓	1	nd	*	✓	nd	s	2480955:6022480
20	Mercury	17/06/1929	✓	1	nd	*	✓	2	s	2457780:5985699
21	Ferris	17/06/1929	✓	nd	nd	*	✓	nd	un	2455580:6002720
22	Garribaldi	17/06/1929	✓	1	nd	*	✓	3	s	2460245:5999695
23	Lake Moonstone	17/06/1929	✓	1	nd	*	✓	nd	s	2462780:5981200
24	Lake Barfoot	17/06/1929	✓	1	nd	*	✓	2	s	2459490:6007855
25	Ram	24/05/1968	✓	2	29/04/1981	✓	✓	5	u	2429800:5925960
26	Buller	24/05/1968	✓	2	31/05/1968	✓	✓	5	u	2433260:5931880

1. General Cont.			2. Original Dam Dimensions								3. Present Dam Dimensions						
Dam Centre			Crest			Dam			Dam Slope		Crest			Dam			Dam Slope
	Elevation	Classification	Length	Width	Height	Area	Volume	Baseline length	Downstream	Upstream	Length	Width	Height	Area	Volume	Baseline length	Downstream
1	770	3	nd	nd	nd	nd	nd	nd	nd	nd	500	200	70	410000	12500000	1000	18
2	210	1	1200	1350	30	300000	24000000	1350	nd	nd	na	na	na	na	na	na	na
3	95	2	300	570	100	145000	3000000	730	nd	nd	185	570	85	65000	1000000	730	nd
4	130	2	190	470	20	58000	1300000	500	nd	nd	130	470	20	48000	800000	500	nd
5	340	3	nd	nd	nd	nd	nd	nd	nd	nd	380	60	35	300000	3100000	530	7
6	550	3	450	875	40	340000	7800000	1250	nd	nd	400	875	30	290000	5300000	1250	nd
7	140	2	90	30	35	nd	200000	nd	10	nd	90	30	35	nd	200000	nd	10
8	170	1	270	300	10	97000	400000	385	nd	nd	nd	nd	nd	nd	nd	385	nd
9	105	2	205	280	25	73000	1500000	360	nd	nd	na	na	na	na	na	na	na
10	610	3	340	520	40	43000	4000000	600	8	3	340	520	40	43000	4000000	600	8
11	190	1	nd	nd	nd	nd	2500000	625	nd	nd	nd	nd	nd	nd	2500000	625	na
12	610	2	nd	nd	nd	nd	nd	nd	nd	nd	na	na	na	na	na	na	na
13	515	2	345	410	40	120000	2800000	550	nd	nd	310	400	30	100000	2000000	550	nd
14	430	2	250	530	40	25000	2600000	720	nd	nd	180	530	25	20000	900000	1200	nd
15	600	2	470	690	70	350000	4500000	900	nd	nd	430	690	50	350000	4000000	900	nd
16	425	3	240	130	30	23000	1000000	320	13	9	na	na	na	na	na	na	na
17	700	2	nd	nd	nd	nd	nd	nd	nd	nd	130	310	10	70000	400000	nd	nd
18	515	2	180	380	25	60000	1000000	400	nd	nd	160	360	20	50000	800000	450	nd
19	950	2	200	100	70	34000	4000000	520	6	13	200	100	70	34000	4000000	520	6
20	740	3	520	480	20	120000	2000000	850	nd	nd	480	480	15	120000	1600000	850	nd
21	450	2	220	nd	30	nd	nd	nd	nd	nd	150	nd	20	nd	nd	nd	nd
22	618	2	205	530	20	100000	1100000	650	nd	nd	200	500	15	nd	500000	650	nd
23	475	4	nd	nd	nd	nd	nd	nd	nd	nd	150	300	15	nd	600000	300	nd
24	530	4	280	325	30	90000	1300000	nd	nd	nd	230	325	20	70000	800000	756	nd
25	415	3	560	550	40	121000	2800000	650	14	20	na	na	na	na	na	na	na
26	155	2	350	200	20	83000	1000000	830	nd	nd	na	na	na	na	na	na	na

Dam Slope		4. Dam Materials							5. Breach Characteristics						6. Lake Characteristics		
		Matrix			Grain Size				Average			Failure Mechanism		Shape	Lake Name	Volume	
Upstream		Percent	Support	Angularity	Grading	Maximum	Minimum	Average	Depth	Width	Volume	Type	Acquisition of Data			Present	Original
1	10	5	1	3	2	5000	2	250	45	100	1000000	1	4	2	Stanley	6500000	nd
2	na	nd	1	2	3	3000	5	200	nd	nd	nd	4	2	1	Mud / Matakitaiki	0	15000000
3	nd	nd	nd	nd	nd	nd	nd	nd	15	100	1000000	1	4	2	Falls	2000000	nd
4	nd	nd	nd	nd	nd	nd	nd	nd	10	50	500000	1	1	1	na	1000000	1500000
5	6	nd	1	2	3	20000	100	2000	nd	nd	nd	1	1	2	Matiri	6000000	nd
6	nd	nd	nd	nd	nd	nd	nd	nd	10	80	2500000	1	4	1	Marina	2500000	3500000
7	nd	nd	1	2	2	10000	20	200	na	na	na	nd	na	na	Dora	450000	nd
8	nd	nd	nd	nd	nd	nd	nd	nd	5	40	200000	1	4	2	na	0	nd
9	na	5	1	2	3	1500	20	800	nd	nd	nd	1	4	1	Perrine	0	15000000
10	3	5	1	3	2	1000	10	150	na	na	na	na	na	na	na	0	0
11	na	10	1	2	3	1000	5	400	nd	nd	nd	5	2	5	na	0	2000000
12	na	nd	nd	nd	nd	nd	nd	nd	nd	nd	nd	nd	na	nd	na	nd	nd
13	nd	nd	nd	nd	nd	nd	nd	nd	10	40	800000	1	4	1	na	nd	nd
14	nd	nd	nd	nd	nd	nd	nd	nd	15	20	1400000	1	4	nd	na	nd	500000
15	nd	nd	nd	nd	nd	nd	nd	nd	20	100	500000	1	4	1	Elmer	2400000	3500000
16	na	15	2	3	2	1500	10	60	20	200	550000	1	4	2	na	2000	150000
17	nd	nd	nd	nd	nd	nd	nd	nd	nd	nd	nd	nd	na	nd	na	70000	nd
18	nd	nd	nd	nd	nd	nd	nd	nd	5	20	200000	nd	na	nd	na	2000000	nd
19	13	nd	nd	nd	nd	nd	nd	nd	nd	nd	nd	nd	na	nd	na	1100000	nd
20	nd	nd	nd	nd	nd	nd	nd	nd	5	40	400000	1	4	nd	na	nd	nd
21	nd	nd	nd	nd	nd	nd	nd	nd	10	50	nd	nd	na	nd	na	nd	nd
22	nd	nd	nd	nd	nd	nd	nd	nd	5	40	300000	nd	na	nd	Earthquake	2000000	nd
23	nd	nd	2	3	2	5000	10	200	nd	nd	nd	nd	na	nd	Moonstone	600000	nd
24	nd	nd	nd	nd	nd	nd	nd	nd	10	40	500000	1	4	1	Barfoot	500000	nd
25	na	20	3	3	3	4000	1	70	40	100	1000000	1	4	2	na	0	1100000
26	na	nd	nd	3	nd	4000	10	nd	nd	330	800000	1	2	1	na	0	1500000

6. Lake Characteristics									7. Catchment Characteristics			
	Surface Elevation	Evidence for infilling of lake	Length	Width	Depth	Area	Duration	Present Condition	River Name	Drainage Basin Area	Precipitation	
											Yearly	Av. Monthly
1	770	✓	2190	360	20	730000	74/0/13	2	Stanley	33	3694	307
2	210	✓	2500	700	25	2000000	4/0/0 - 30/0/0	6	Matakitaki	875	1550	129
3	85	✗	1665	250	15	208000	74/0/13	2	Falls Creek	15	1853	154
4	30	✗	1900	130	20	130000	74/0/13	7	Glasseye Creek	22	2421	201
5	343	✓	1350	420	35	470000	300	2	Matiri	160	2584	215
6	550	nd	760	270	45	120000	74/0/13	2	Hemphill	11	2584	215
7	137	✗	855	105	15	54000	74/0/13	7	na	8.5	2584	215
8	nd	nd	nd	nd	nd	nd	nd	4	Kakapo	43	2421	201
9	130	✓	5000	450	25	16000000	0/0/6	4	Mokihinui	520	2584	215
10	na	✗	na	na	na	na	na	8	Right tributary Matiri R	5.5	2584	215
11	170	✗	4800	150	15	480000	0/0/2	8	Maruia	1025	2297	191
12	nd	nd	nd	nd	nd	nd	nd	7	Stanley	40	3694	307
13	nd	✗	nd	nd	nd	nd	nd	2	Left Branch Allen	9	2584	215
14	445	✗	500	190	40	30000	nd	3	Beautiful	52	2210	184
15	600	✓	940	175	50	152000	74/0/13	2	Ugly	19	2421	201
16	420	✓	230	100	20	15000	nd	4	West Branch of Matiri R	3.5	2584	215
17	700	✗	130	60	10	6000	74/0/13	7	Tangent Creek	1.5	2421	201
18	515	✓	770	210	25	160000	74/0/14	2	Matiri	38	2584	215
19	930	✗	420	155	30	15100	74/0/13	1	Lindsay Creek	9	1255	104
20	nd	✓	nd	nd	nd	nd	nd	7	Mercury Creek	6	2421	201
21	nd	✓	nd	nd	nd	nd	nd	7	Ferris Creek	5.5	2421	201
22	220	✓	3300	125	20	450000	74/0/13	3	Karamea	850	2210	184
23	475	✓	1300	90	5	120000	nd	3	Karamea	110	2421	201
24	530	✓	750	190	20	80000	nd	2	Beautiful	37	2210	184
25	450	✓	450	300	30	40000	12/11/26	4	Ram Creek	4.5	2322	194
26	100	na	6000	200	12	nd	0/0/1	4	Buller	4400	1931	160

Key for Landslide Dam Debris Attributes

1.0 General

1.1 Date

- **Blockage:** Day, month and year of the dam formation or blockage of river
- **Initial Dam Failure:** Day, month and year of initial dam failure
- **Subsequent Dam Failures:** Day, month and year of any subsequent dam failures

1.2 Dam Centre

- **Coordinates:** New Zealand Map Grid easting and northing of dam centre
- **Elevation:** Height of dam centre above mean sea level

1.3 Classification

1. Type one 2. Type two 3. Type three 4. Type four 5. Type five 6. Type six

2.0 Original Dam Dimensions

2.1 Crest

- **Length:** Length of dam crest measured in meters
- **Width:** Width of dam crest measured in meters
- **Height:** Average height of dam crest above mean sea level

2.2 Area

Area (m²) of landslide dam

2.3 Volume

Volume (m³) of debris blocking the river forming landslide dam

2.4 Baseline Length

Distance (m) from upstream extent of debris to downstream extent of debris

2.5 Dam Slope

- **Downstream:** Angle (° from horizontal) of downstream dam slope
- **Upstream:** Angle (° from horizontal) of upstream dam slope

3.0 Present Dam Dimensions

3.1 Crest

- **Length:** Length of dam crest measured in meters
- **Width:** Width of dam crest measured in meters
- **Height:** Average height of dam crest above mean sea level

3.2 Area

Area (m²) of landslide dam

3.3 Volume

Volume (m³) of debris blocking the river forming landslide dam

3.4 Baseline Length

Distance (m) from upstream extent of debris to downstream extent of debris

3.5 Dam Slope

- **Downstream:** Angle (° from horizontal) of downstream dam slope
- **Upstream:** Angle (° from horizontal) of upstream dam slope

4.0 Dam Materials

4.1 Matrix

- **Percent**
Percentage of matrix to rock
- **Support**
1. Grain supported 2. Intermediate 3. Matrix supported
- **Angularity**
1. Rounded 2. Intermediate 3. Angular
- **Grading (engineering terms)**
1. Poorly Graded 2. Moderately Graded 3. Well Graded

4.2 Grain Size

- **Maximum:** Measured in mm
- **Minimum:** Measured in mm
- **Average:** Measured in mm

5.0 Breach Characteristics

5.1 Average

- **Depth:** Measured in meters
- **Width:** Measured in meters
- **Volume:** Measured in m³

5.2 Failure Mechanism

- **Type**
1. Overtopping 2. Piping 3. Mass sliding of landslide dam 4. Modified by eng works 5. Unknown
- **Acquisition of Data**
1. Observed 2. Reported / Published 3. Personal account 4. Inferred

5.3 Shape

1. U Shape 2. V Shape 3. Trapezoidal section 4. Piping

5.4 Degree of Modification

1. Negligible 2. Low 3. Moderate 4. High 5. Complete

6.0 Lake Characteristics

6.1 Lake Name

Official name of the impounded lake

6.2 Volume

- **Present:** Volume (m^3) of water impounded presently
- **Original:** Volume (m^3) of water impounded before partial or complete failure of dam

6.3 Surface Elevation

Max elevation of lake surface above mean sea level

6.4 Deposit Thickness

Thickness (in meters) of any aggradation or lake deposits

6.5 Length

Length (m) of lake

6.6 Width

Width (m) of lake

6.7 Depth

Depth (m) of lake

6.8 Area

Area (m^2) of lake

6.9 Duration

Year /month/days since lake formation

6.10 Present Condition

1. Existing; no change in lake level
2. Existing; partially infilled
3. Partially drained by failure
4. Drained by failure of dam
5. Completely infilled
6. Drained artificially
7. Unknown
8. Other

7.0 Catchment Characteristics**7.1 River Name**

The official name of the river/stream

7.2 Drainage Basin Area

Area (km^2) of land draining the land above the landslide dam

7.3 Precipitation

- **Yearly:** Recorded total precipitation per year (mm)
- **Av. Monthly:** Average precipitation per month (mm)
- **Max. Monthly:** Max precipitation per month (mm)

7.4 Discharge

- **Mean Monthly:** Average discharge of water at landslide dam location (m^3/s) per month
- **Max. Monthly:** Maximum monthly discharge of water (m^3/s)

7.5 Valley

- **Width:** Width (m) of valley prior to dam formation

- **Elevation:** Height of valley (m above mean sea level) prior to dam formation
- **Downstream Gradient:** Slope ($^\circ$) of valley immediately downstream of dam
- **Upstream Gradient:** Slope ($^\circ$) of valley immediately upstream of dam

8.0 Damage People

- **Landslide:** No. of deaths from landslide
- **Dam:** No. of deaths from dam failure

8.1 Damage Infrastructure

- As for Damage People (replace with infrastructure)

General									Source Dimensions				
Number	Name of dam	Map Series	Map Scale	Sheet No.	NZMG coordinates ¹	Center elevation ²	District	Landuse	Rupture ³			Area ⁴	In Situ Vol. ⁵
									Length	Width	Depth		
1	Lake Stanley	260	1:50 000	M26	2477885:6020565	1000	T	2	1150	360	50	530000	18000000
2	Matakitaki (Mud)	260	1:50 000	M29	2452975:5929240	360	T	1	1080	1000	35	820	19000000
3	Falls	260	1:50 000	L28	2429705:5973415	218	W	2	1170	433	83	440000	22000000
4	Glasseye	260	1:50 000	L28	2431150:5976790	295	W	2	650	1250	30	630000	13000000
5	Lake Matiri	260	1:50 000	M29	2455000:5948840	600	T	2	665	1270	20	700000	9000000
6	Lake Marina	260	1:50 000	L28	2445985:5969645	720	W	2	950	520	30	450000	8000000
7	Lake Dora	260	1:50 000	L28	2441230:5963535	300	W	1	890	480	10	230000	2200000
8	Kakapo / Haystack	260	1:50 000	M27	2450715:5990875	500	W	2	525	490	30	300000	4000000
9	Lake Perrine	260	1:50 000	L28	2439695:5961470	200	W	1	810	456	15	135000	3000000
10	Matiri (Right Branch)	260	1:50 000	M28	2457540:5961130	800	T	2	560	438	40	31000	5000000
11	Maruia Falls	260	1:50 000	L29	2448340:5927155	270	T	2	435	360	20	250000	2500000
12	Lower Stanley	260	1:50 000	M26	2478715:6018595	1100	T	2	970	400	20	230000	4000000
13	Allen	260	1:50 000	M28	2450335:5973835	740	W	2	600	336	40	200000	4200000
14	Beautiful	260	1:50 000	M27	2460125:6004630	660	W	2	600	360	20	300000	2200000
15	Lake Elmer	260	1:50 000	L26	2449200:6014850	920	W	2	830	270	35	160000	4100000
16	Matiri (Rain Peak)	260	1:50 000	M29	2452585:5947960	560	T	2	480	440	35	58000	3800000
17	Tangent	260	1:50 000	L27	2450225:5983830	1040	W	2	500	260	20	100000	1500000
18	Upper Matiri	260	1:50 000	M28	2460085:5961335	800	T	2	500	350	20	200000	1 800000
19	Lower Lindsay	260	1:50 000	M26	2480370:6022060	1300	T	1	360	170	40	44000	2600000
20	Mercury	260	1:50 000	M27	2457570:5985105	1100	W	2	430	330	20	200000	1500000
21	Ferris	260	1:50 000	M27	2454830:6002940	860	W	2	320	420	20	150000	1400000
22	Garribaldi	260	1:50 000	M27	2461065:5998270	660	W	2	400	510	15	240000	1600000
23	Lake Moonstone	260	1:50 000	M27	2460950:5981390	1050	W	2	430	250	20	200000	1100000
24	Lake Barfoot	260	1:50 000	M27	2458990:6007830	800	W	2	640	270	15	360000	1300000
25	Ram	260	1:50 000	L29	2430025:5926355	478	W	2	500	425	40	320000	4400000
26	Buller	260	1:50 000	L29	2433515:5931100	320	W	1	470	330	50	141000	4100000

						Geology					Geology		
Number	Final Bulk'd Vol. ⁵	Head Elev. ³	Toe Elev. ³	Slope		Rock Material			Rock Name	Age	Rock Mass		
				Angle ⁶	Direction ⁶	Weathering	Strength	Fabric			Defect spacing ³	Defect persistence ³	Unit Block Size ³
1	24000000	1400	750	29	29	2	5	1	11	1	3	5	4
2	25000000	600	210	20	90	3	4	2	7	11	4	5	4
3	24000000	315	115	8	340	nd	nd	nd	4	10	nd	nd	nd
4	14000000	280	60	17	90	nd	nd	nd	3	10	nd	nd	nd
5	12000000	860	350	40	280	3	5	2	5	11	6	5	4
6	10500000	950	600	30	90	nd	nd	3	1	4	nd	nd	nd
7	3700000	500	160	26	100	3	4	2	4	10	6	5	4
8	5500000	700	150	30	225	nd	nd	nd	1	4	nd	nd	nd
9	4000000	500	160	26	100	3	4	2	4	10	3	4	4
10	6500000	1070	620	48	80	3	5	3	4	10	6	5	3
11	3200000	295	150	17	263	3	4	2	4	11	4	5	4
12	5300000	1500	680	25	050	nd	nd	nd	8	1	nd	nd	nd
13	5500000	960	520	38	080	nd	nd	3	1	4	nd	nd	nd
14	3000000	1000	470	36	087	nd	nd	3	1	4	nd	nd	nd
15	5500000	1200	620	34	085	nd	nd	3	1	4	nd	nd	nd
16	5000000	675	400	20	220	4	4	3	1	4	5	4	3
17	2000000	1200	730	38	315	nd	nd	nd	1	1	nd	nd	nd
18	2400000	1050	520	30	250	3	5	nd	4	10	nd	nd	nd
19	3500000	1595	940	40	45	nd	nd	nd	8	1	nd	nd	nd
20	2000000	1400	740	44	10	nd	nd	nd	1	4	nd	nd	nd
21	1900000	1070	490	30	100	nd	nd	nd	1	4	nd	nd	nd
22	2100000	1000	240	50	340	nd	nd	2	5	10	nd	nd	nd
23	1500000	1300	470	40	80	3	5	3	7	1	nd	nd	nd
24	1700000	1200	560	32	90	nd	nd	3	1	4	nd	nd	nd
25	5800000	660	280	20	225	4	3	3	1	4	3	3	2
26	5400000	670	135	26	300	3	4	3	1	4	nd	nd	nd

Number	Landslide Classification											
			Initial Movement			Activity						
	Joint/Strata Dip	Joint/Strata Direction	Movement	Velocity	Velocity info	State	Distribution	Style	Landslide Material	Geol. Control	Triggering Mechanism	Subsequent Failures
1	70	135	2	6	1	2	3	4	1	5	1	1
2	50	90	3	6	3	4	5	1	2	2	1	2
3	nd	nd	3	5	1	4	5	1	1	2	1	2
4	17	40	4	5	1	4	4	1	1	2	1	2
5	65	280	3	6	1	2	3	5	1	2	1	1
6	nd	nd	2	5	1	4	5	1	1	1	1	1
7	28	100	3	5	1	4	2	1	1	2	1	2
8	nd	nd	2	6	1	5	4	1	1	3	1	2
9	30	100	1	5	1	4	3	1	1	2	1	1
10	nd	nd	2	6	1	4	5	1	1	3	1	2
11	25	320	3	5	1	5	5	1	1	2	1	2
12	nd	nd	2	6	1	1	5	1	1	nd	1	1
13	nd	nd	3	6	1	4	5	1	1	3	1	2
14	80	260	2	6	1	4	5	1	1	4	1	1
15	nd	nd	2	6	1	4	5	1	1	3	1	1
16	nd	nd	3	5	1	4	5	1	1	5	1	2
17	nd	nd	2	6	1	4	5	1	1	3	1	2
18	40	275	2	5	1	2	4	4	2	5	1	1
19	nd	nd	2	6	1	4	5	4	1	3	1	1
20	nd	nd	1	6	1	4	4	4	1	3	1	1
21	nd	nd	2	5	1	4	5	1	1	nd	1	1
22	40	160	2	6	1	1	2	5	1	nd	1	1
23	70	98	2	5	1	2	6	5	1	6	nd	2
24	80	260	2	6	1	4	5	1	2	3	1	1
25	nd	nd	2	6	1	1	3	1	1	3	2	2
26	43	315	1	6	1	4	3	4	1	4	2	1

Key for Landslide Dam Source Area Attributes

1.0 General

1.1 Map series

260 Scale 1:50 000; Edition 1 1982,
Limited Revision 1998.

1.2 Sheet No.

L26	Heaphy
L27	Karamea
L28	Mokihinui
L29	Inangahua
M26	Cobb
M27	Mount Arthur
M28	Wangapeka
M29	Murchison

1.3 NZMG Coordinates

New Zealand Map Grid Projection
coordinates; Easting/Northing

1.4 Centre Elevation

Elevation above mean sea level measured in
meters

1.5 District

T = Tasman District
B = Buller District

1.6 Land use

1. Shrubs/bushland 2. Forest (native)
3. Forestation 4. Urban areas 5.
Farmland

2.0 Source Dimensions

2.1 Rupture

- **Length:** Distance in meters from the head to the toe of the landslide
- **Width:** Distance in meters from one lateral scarp to the other
- **Depth:** Distance in meters from the pre-failure surface to the failure surface

2.2 In situ volume

Volume (measured in m³) of material that has been displaced from the source area (pre-bulking)

2.3 Final Bulk Volume

Volume (m³) of displaced material that has come to rest at the base of the landslide (33% bulking)

2.4 Head Elevation

The height of the head of the landslide above mean sea level measured in meters

2.5 Toe Elevation

The height of the toe of the landslide above mean sea level measured in meters

3.0 Geology

3.1 Slope

- **Angle** = The angle between the failure surface and the horizontal measured in degrees
- **Direction** = The slope facing direction relative to north measured in degrees

3.2 Rock Material

- **Weathering**
1. Unweathered 2. Slightly weathered 3. Moderately (Mod) weathered 4. Highly weathered
5. Completely weathered 6. Residual Soil
- **Strength**
1. Very weak 2. Weak 3. Mod weak 4. Mod strong 5. Strong 6. Very strong 7. Extremely strong
- **Fabric**
1. Finely layered 2. Coarsely layered 3. Massive 4. Other
- **Rock name**
1. Granite
2. Granodiorite
3. Limestone
4. Sandy/muddy limestone
5. Sandstone
6. Mudstone
7. Alternating Sandstone/mudstone 8. Conglomerate
9. Schist
10. Gneiss
- **Age**
1. Cambrian
2. Ordovician
3. Silurian
4. Devonian
5. Carboniferous
6. Permian
7. Triassic
8. Jurassic
9. Cretaceous
10. Palaeogene
11. Neogene
12. Quaternary

3.3 Rock Mass

- **Defect Spacing**
1. Extremely close 2. Very Close 3. Close
4. Moderate 5. Wide 6. Very wide 7. Extremely wide

- **Defect persistence**
1. Very low 2. Low 3. Moderate 4. High
5. Very high
- **Defect Unit Block Size**
1. Very small 2. Small 3. Medium 4. Large
5. Very large
- **Joint/Strata Dip**
The angle between a joint or strata plane
and the horizontal measured in degrees
- **Joint/Strata Direction**
The facing direction of a joint or strata
plane relative to north measured in degrees

4.0 Landslide Classification

4.1 Initial Movement

- **Movement**
1. Rock fall 2. Rock avalanche 3.
Translational slide 4. Rotational slide 5.
Translational slide 6. Spread 7. Flow
- **Velocity**
1. Very slow 2. Slow 3. Moderate 4. Rapid
5. Very rapid 6. Extremely rapid
- **Velocity Info**
1. Inferred 2. Personal account 3.
Reported/ published 4. Observed

4.2 Activity

- **State**
1. Active 2. Reactivated 3. Suspended 4.
Dormant 5. Abandoned 6. Stabilized
- **Landslide Movement**
1. Advancing 2. Retrogressive 3. Widening
4. Enlarging 5. Diminishing 6. Confined
- **Style**
1. Single 2. Complex 3. Composite 4.
Multiple 5. Successive

4.3 Landslide Material

1. Rock 2. Debris 3. Earth

4.4 Geol. Control

1. Close proximity to active fault 2. Bedding
3. Jointing 4. Weathering 5. bedding and
jointing 6. Foliation

4.5 Triggering Mechanism

1. 1929 Murchison earthquake 2. 1968
Inangahua earthquake 3. Rainfall

4.6 Subsequent failures

1. Yes 2. No

Appendix D

Landslide Triggering Mechanisms

This appendix describes triggering mechanisms for landslides such as 1) rainfall and snowmelt; 2) earthquakes; 3) volcanic eruptions; and 4) additional triggering mechanisms.

D.1 RAINFALL AND SNOWMELT

The rapid infiltration of rainfall, causing soil saturation and a temporary rise in pore water pressures, is thought to be the general mechanism by which landslides are produced during intense rainstorms (Turner and Schuster, 1996). As for earthquake triggering, the intensity and duration of the rainfall is a key contributing factor in exceeding the critical thresholds needed for landslide generation. Antecedent ground water conditions and the effect-response time of the water table levels, can contribute to the amount of water needed to initiate failure of a slope. These water table levels are generally controlled seasonally, with Spring conditions creating saturated conditions in temperate environments.

The type of landslide triggered by rainfall varies with intensity of rainfall, ground moisture conditions, material properties such as cohesion and slope angle, and pore water pressures (Van Asch et al., 1999). For example, debris flows are generally triggered by high surface run-off and high peak discharges. Shallow landslides require the moisture content to become close to saturation at a critical depth, which is determined by the cohesion of the soil and slope angle. Deep seated landslides are, in most cases, triggered by positive pore pressures on the failure surface induced by a rising ground water level (Van Asch et al., 1999)

Rapid snowmelt can occur during warmer periods leading to the infiltration of meltwater into hillside soils or shallow fractured bedrock slopes. This creates higher than normal pore-water pressures within a rock or soil mass leading to a reduction in overall strength and slope instability (Turner and Schuster, 1996). An example of rainfall induced landsliding was: the formation of a landslide dam 500 000m³ in volume, in Eastern Guatemala as a direct result of Hurricane Mitch in November 1998 (Schuster et al., 2001). Swanson *et al.* (1986) also document the formation of 53 landslides in the upper 1,100 km² of the Totsu River catchment, Japan as a result of a heavy rainstorm in 1889.

D.2 EARTHQUAKES

Earthquakes have long been recognised as a major cause of landslides, documentation of which dates back to around 370 B.C. (Keefer, 1984; Seed, 1968). Earthquake motions can induce significant horizontal and vertical dynamic stresses in slopes of any rock type (Fig 1) (Kramer, 1996). These stresses act to produce dynamic normal and shear stresses along potential failure surfaces, previously in a state of static equilibrium, which may or may not

exceed the available shear strength within the rock or soil mass. Peak ground acceleration and duration of strong shaking are also important factors leading to the failure of natural slopes (Schuster and Wieczorek 1989).

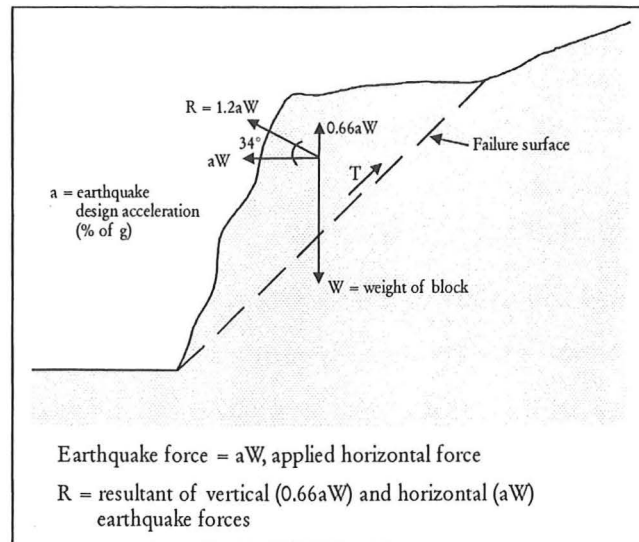


Fig 1. Summary of forces acting on a slope produced during an earthquake.

The size and scale of earthquake-triggered landslides varies generally controlled by the geological setting of a region. For example, in the Pamir Mountains, Tajikistan, the Murgab River was dammed when a massive earthquake triggered rock slide with a volume of $8 \times 10^9 \text{ m}^3$, fell into the valley forming Lake Sarez presently $\sim 4 \times 10^{12} \text{ m}^3$ in volume (ISDR, 2000). In June 1929 an M_s 7.8 earthquake in northwest Nelson, South Island, New Zealand, caused landsliding over an area of $\sim 7000 \text{ km}^2$ and formed a minimum of 39 landslide dams over $500\,000 \text{ m}^3$ in volume (Hancox et al., 2002).

40 historical earthquakes from around the world documented by Keefer (1984), illustrate the most common landslides produced from earthquakes. The type of landslide and area affected by landsliding does vary remarkably; however, it is generally a function of the magnitude of the earthquake, its focal depth, the topography, geology, antecedent ground moisture conditions, and the amplitude, frequency composition, and duration of ground shaking.

Landslides formed at the maximum distance from the epicentre or fault rupture of an earthquake delineate mass movements requiring the least amount of ground shaking to mobilise. Keefer (1986) lists rock falls, rockslides, soil falls, and disrupted soil slides as being initiated by the weakest shaking; larger deep-seated landslides are generally initiated

by stronger and of higher duration shaking generally situated proximal to the seismic source.

Keefer (1984) identified and characterised fourteen types of landslides in his aforementioned study of 40 earthquakes based on material type (rock or soil), nature of movement, velocity, depth to failure surface, and water content. The most common of which were rock falls, disrupted soil slides, and rock slides.

D.3 VOLCANIC ERUPTIONS

Huge landslides on the flanks of volcanoes and adjacent slopes can form as a direct result of volcanic activity. Mass movements from volcanic activity can be grouped into two main categories: debris avalanche and mudflows (also known as lahars) (Francis, 1993). The Mount St Helens volcanic activity preceding the May 1980 eruption and the eruption itself triggered a 2.3 km^3 rockslide off the northern sector of the volcanic cone. The rock slide then disintegrated into a debris avalanche upon mobilisation, depositing debris up to 27km from the source and blocking major tributaries impounding or enlarging five large lakes; of which three remain today (Meyer et al., 1986).

D.4 ADDITIONAL MECHANISMS

Schuster (1993) lists redeposition of debris-flow materials from upstream failures of natural dams, stream undercutting and anthropogenic activity, as additional landslide triggering mechanisms. Perhaps the most significant recent example of an anthropogenically triggered landslide is that of the Vaiont Dam reservoir landslide of 1963. A landslide with a volume $\sim 270 \times 10^6 \text{ m}^3$ moved into the reservoir behind the recently completed 265m tall double thin arch Vaiont dam. The mass moved approximately 500 m at $\sim 30 \text{ m/s}$ displacing $\sim 115 \times 10^6 \text{ m}^3$ of water in the reservoir; the resulting flood wave killed about 2500 people downstream of the dam (Kiersch, 1964). In 1990 a landslide with a volume of $3.6 \times 10^6 \text{ m}^3$, was triggered by seepage from irrigation wastewater in the Pisque River, northern Ecuador. The result was the formation of a natural dam 58m high impounding a lake 2.6km long and reaching a maximum volume of $2.5 \times 10^6 \text{ m}^3$ which failed within 24 days (Asanza et al., 1991).

Appendix E

Predicting Flood Magnitude from Dam Failures

Appendix E details the available techniques used to predict the magnitude of dam-break floods and breach development times from initial overtopping to full breaching reaching its maximum discharge (via flood hydrographs).

The simplest approach in estimating the peak discharge (e.g. Fig 1) from dam-breaks is to use empirically derived correlations relating observed values of peak discharge to some measure of the impoundment or dam such as lake volume, depth of the lake and/or the total drop in lake level during a flood (e.g Costa, 1988; Costa and Schuster, 1988; Evans, 1986; Manville, 2001; Walder and O'Connor, 1997).

Many of these empirically derived regression relationships have been produced to predict dam-break flooding for both constructed and natural earthen dams many of which show the following form:

$$Q_{max} = a X^b$$

Where X is the impoundment or dam characteristic such as lake depth (d) or lake volume (v) and a and b are empirically derived coefficients (Manville, 2001). Manville (2001) sites at least seven different regression equations from three authors; application of which found values separated by an order of magnitude. For example, Costa (1988) proposed a regression equation based on the height of the dam (H) and volume (V) of lake producing the dam factor ($H \times V$) with $r^2 = 0.76$ and $SE = 129\%$:

$$Q_{max} = 181(HV)^{0.43}$$

However, such regression relations show a high degree scatter because factors other than those used in the regression relations, often exert considerable control on the formation of a breach and hence the peak discharge (Manville, 2001; Singh, 1996; Walder and O'Connor, 1997). Scatter also occurs because of the differences in the way the data was collected. Therefore, underestimates of actual peak flow arise from the inability to correctly allow for the translation and attenuation of flood waves from recording sites, some distance downstream, back to the dam location (Manville, 2001).

Regardless of the low accuracy compared to physically based models, regression relations are a useful tool in the rapid assessment of the flood potential following a breach given the short longevity of most landslide dams (Walder and O'Connor, 1997).

A large number of mathematically based dam breach models have been developed to predict dam breach characteristics (i.e. size and time of formation) and the discharge hydrograph (a plot of discharge vs time) deriving from the breaching of both natural and man made earth dams (Fread, 1988) (Table 1).

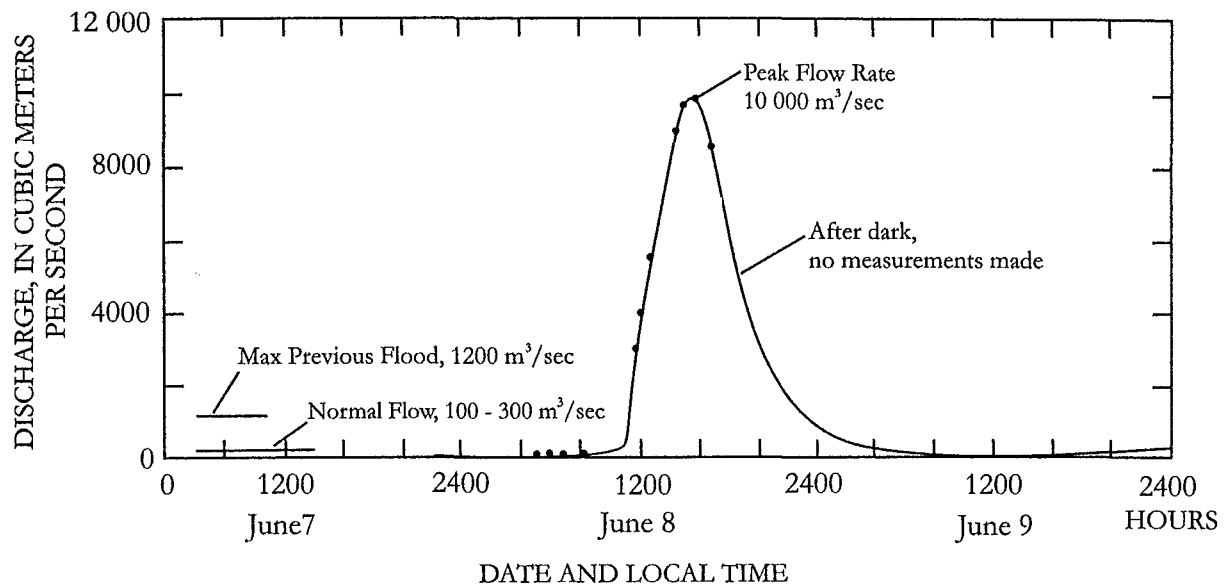


Fig 1. Example of a typical hydrograph of discharge following the failure of landslide dams. This particular hydrograph is from the failure in 1974 of the Mayunmarca landslide dam, Peru (Source: Costa, 1988).

One approach models the discharge through the evolving breach through the application of weir flow equations known as parametric methods (Manville, 2001). These methods commonly require details of the final breach dimensions such as width, sidewall slope and depth and the breach development time (Manville, 2001). Manville (2001) found parametric approaches to be sensitive to a number of input parameters in a simulation of a dam break flood. In particular, dam breach dimensions followed by breach development time seem to have the greatest influence on peak discharge.

Table 1. Summary of mathematically based models to predict dam breach characteristics such as peak flow and breach development times.

Mathematical Model	Year of Development
1 Cristofano Model	1965
2 Harris Wagner (HW) Model	1967
3 BRDAM Model	1981
4 Ponce-Tsivoglou (PT) Model	1981
5 Lou Model	1981
6 Nogueira Model	1984
7 DAMBRK Model	1984
8 SMPDBK Model	1984
9 BREACH Model	1984
10 BEED Model	1987

Walder and O'Connor (1997), propose an effective and less labour intensive physically based dimensionless model of dam-breach formation demonstrating that the hydrograph (peak discharge vs. time) depends on a dimensionless parameter η defined as:

$$\eta = \left(\frac{kV_o}{g^{1/2} d^{7/2}} \right)$$

where k is mean erosion rate of the breach, V_o is the total volume of water drained from the lake, d is drop in lake level during flood, and g is acceleration due to gravity. Graphing the dimensionless peak discharge against the dimensionless parameter η form the basis for predicting peak discharge from known values of lake depth, lake volume and breach erosion rate (Walder and O'Connor, 1997).

A more sophisticated yet labour intensive and mathematically complex evaluation of dam break flood outflows, involves physically based models that relate the erosive force of exiting breach water to the enlargement of the breach (e.g. Table 1) (Manville, 2001). The data requirements and initial conditions needed to run the these models are widely variable, and show high complexity, however they remain the most accurate in assessing the potential flood hydrograph (Table 2).

Physical modelling of landslide dam break flood magnitudes to represent or reproduce flood hydrographs is another method used to identify key variables that influence the peak outburst flow at the dam site upon breaching. The most recent example of such modelling is that of Davies (*pers comm.*, T. Davies, 2003), in his representation of the Poerua River landslide dam in Westland South Island, New Zealand where $10 \times 10^6 \text{ m}^3$ of rock debris fell into the gorge forming a dam 120 m high, which overtopped five days later (Hancox *et al*, 1999). At the time the only available basis for predicting the peak flood discharge was the empirical method of Costa and Schuster (1988); this gave a peak flow rate of about $3000 \text{ m}^3 \text{ s}^{-1}$.

Table 2. Summary table listing the advantages, disadvantages of available methods to predict the dam break flood characteristics and data required for the individual techniques (reproduced from Manville, 2001)

Method	Advantages	Disadvantages	Data required
1 Empirical regression equations (lake and dam characteristics)	Very rapid and simple	Questionable accuracy Large choice of regression relationships	Lake volume, dam height
2 Empirical breach characteristics	Very rapid and simple Can supply first - order input parameters for more sophisticated models	Uncertain accuracy Based on empirical data	Lake volume, depth and surface area
3 Parametric	Rapid (if model is available)	Several choices of weir - flow equation DAMBRK requires some familiarity to operate	Breach dimensions, geometry and development time. Lake volume and geometry
4 Dimensionless	Rapid	Sensitive to lake depth Sensitive to breach width/depth ratio. Little - tested in New Zealand. Requires use of graphs and calculations	Breach development time Lake volume and geometry
5 Physically based	Potentially the most accurate	Requires experience to operate, can be temperamental. Data input slower than other methods. Little-tested in New Zealand	Dam geometry and dimensions. Geotechnical properties of dam material. Lake volume and geometry

In order to gather data on the hydrograph shape generated by overtopping failure of a dam of homogeneous material, a physical laboratory model was designed to represent the filling and overtopping failure of the Poerua dam (Donadini and Kunz, 2001). The details of the geometry of the Poerua gorge were not represented, but the laboratory experiments used a V-shaped valley with 40° side-slopes as is typical of the prototype situation. Fig 2-15 shows the laboratory apparatus in action. A steady inflow rate of 3 l/sec was used in the model to fill and overtop the dam, corresponding to 800 m³s⁻¹ in the prototype corresponding to about a 2-year flood in the Poerua River (*pers comm.*, T. Davies, 2003).

The selection of model dam material took considerable care to represent as best as possible, the material making up the Poerua dam. The failure process modelled was that of overtopping and erosion of the dam crest and downstream face by the outflow.



Fig 2. Physical modelling of the Poerua landslide dam. Note the mass failure of the breach side walls during erosion of the dam material further enlarging the breach width (*pers comm.*, T.Davies, 2003).

Occasionally mass failures occurred prior to or following overtopping (Fig. 2). These made no detectable difference to the outflow hydrograph and so were not considered to affect the results, although whether the model was capable of adequately representing such a process in the prototype is unknown (but doubtful) (*pers comm.*, T. Davies, 2003).

Fig. 2.3 shows the model outflow hydrographs measured with a valley bed slope of 3.5° and various combinations of upstream and downstream dam slopes. Similar results were obtained with a valley bed slope of 5° , but the peak outflow rates were about 20% - 30% lower, depending on the dam batter slopes.

At 5° valley bed slope, the batter slopes most closely corresponding to the Poerua case are 10° upstream and 25° downstream. The peak outflow for this dam geometry was $0.03 \text{ m}^3 \text{ s}^{-1}$ of which was the steady input so the outflow due to the dam break itself was $0.010 \text{ m}^3 \text{ s}^{-1}$.

At the linear scale ratio of 1:150, discharges scale as $(150)^{2.5} = 275568$, so the corresponding prototype dam break outflow is $2756 \text{ m}^3\text{s}^{-1}$. This is of the same order as the inferred peak flow rate at the lower end of the gorge, and also as the predicted peak outflow using the Costa and Schuster (1988) method. The time to empty the lake in this case was about 75 seconds, which at the appropriate time scale of $(150)^{0.5}$ corresponds to about 15 minutes in the prototype (Davies, *pers comm*, 2003).

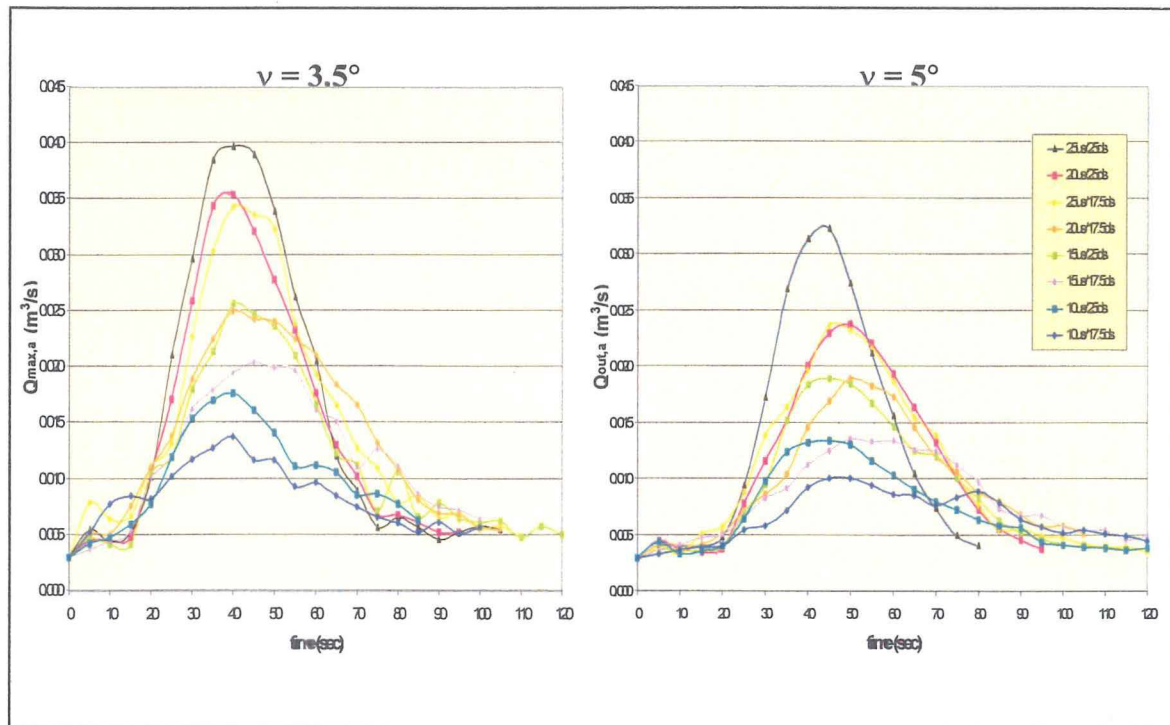


Fig. 2.16. Outflow hydrographs with 3.5° and 5° bed slopes (Source: T. Davies, *pers comm*, 2003).

In summary, there are multiple ways to predict the potential magnitude of a dam break flood with differing levels of accuracy and data input. The following sequential approach in the assessment of a potential dam break flood is proposed by Manville (2001):

- Use empirically derived regression equations and breach characteristics analysis to define the order of magnitude of the peak discharge
- Compare the results of these empirical methods to check for consistency
- Use dimensionless analysis (e.g. Walder and O'Connor, 1997), and parametric analysis to evaluate the sensitivity of the peak discharge to breach development time and to refine peak discharge estimates
- Further refine the breach outflow hydrograph using physical / physically based models
- Application of a safety factor in case of an unforeseen worst-case flood

Appendix F

Parameter Terminology

Appendix F describes the intended meanings of the parameters included in the Murchison dataset.

1) Landslide Characterisation

A. DAM DEBRIS SOURCE AREA:

- *Reference number*: links the landslide dam to the datasheet in appendix 2 and location map in chapter 3
- *Reference name*: documents the name given to the dam or associated lake
- *Date of landslide*: the date the landslide forming the dam occurred
- *NZMG coordinates of source centre*: the New Zealand map grid coordinates locating the centre of the landslide
- *Subsequent landslide failures*: date of any landslides after the date of the landslide forming dam
- *Map edition/scale*: edition of topographic map produced by Land Information New Zealand and the scale used
- *District in which landslide occurred*: states the geographical district where the landslide occurred (see Fig. 1.3)
- *Approximate elevation of landslide centre*: the height of the landslide centre above mean sea level (m)

B. SOURCE DIMENSIONS

- *Rupture length (L_r)*: Fig. A-1-1
- *Rupture width (W_r)*: Fig. A-1-1
- *Rupture depth (D_r)*: the depth (m) from the original surface (inferred) to the slip surface (Fig. A-1-1)
- *Area (A)*: the ground area (m^2) within the landslide boundaries (Fig. A-1-1)
- *Initial landslide volume*: the landslide volume has been quantified based on the assumption that the slide exhibits rotational failure; volume can then be approximated by half an ellipsoid (Fig. A-1-1). The volume of ground displacement by a landslide is thus expressed as: $V_{ls} = \frac{1}{6} \pi D_r W_r L_r$ (N.b. Slight variations in volume quantification may exist)
- *Final landslide volume*: the volume of material that comes to rest at the base of the slope. Expressed assuming a dilation of 33%. (Nicoletti and Sorriso-Valvo, 1991)
- *Head elevation*: the height (m) of the landslide head above mean sea level (Fig. A-1-1)
- *Toe elevation*: the height (m) of the landslide toe above mean sea level
- *Travel angle/azimuth*: the angle ($^\circ$) between the failure surface and the horizontal / the angle ($^\circ$ relative to north) the landslide failure propagates

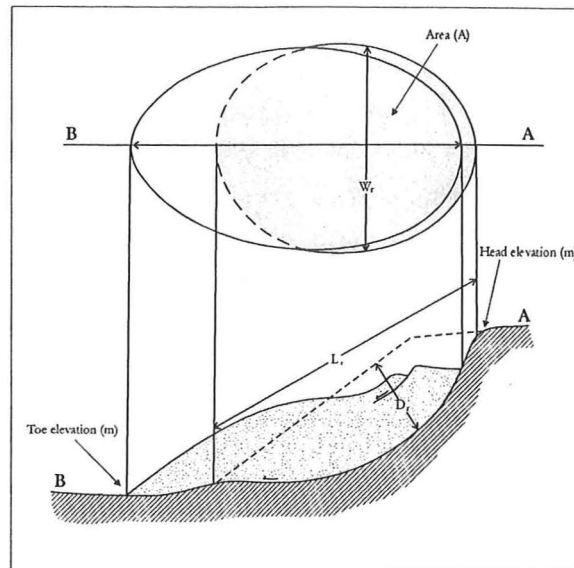


Fig. A-1-1. Landslide dimensions in plan (upper portion) and section (lower portion) illustrating features used in the database (modified from Cruden and Varnes, 1996)

G. GEOLOGY

- *Geological description of source rock*: a general historical geological account of source rock and any tectonic activity that may be affecting the sites proximal to the landslide dam. Where relevant, geological accounts of juxtaposed lithologies can be described
- *Weathering*: qualitative terms following Bell and Pettinga (1983), in their description of rock material based on the discolouration and loss of strength associated with weathering
- *Strength*: qualitative terms following Bell and Pettinga (1983), in their description of rock material based on field estimation of strength.
- *Fabric*: qualitative term based on the layering within the rock material following Bell and Pettinga (1983)
- *Rock name*: the rock type (or lithology) based on the mineralogy and texture following Bell and Pettinga (1983)
- *Defect spacing*: the distance between defects based on qualifying terms following Bell and Pettigna (1983)
- *Defect persistence*: the distance over which a defect can be traced based on qualifying terms following Bell and Pettigna (1983)
- *Average unit block size*: quantitative term based on the defect unit block size following Bell and Pettigna (1983)
- *Dip/direction of joint/strata*: the orientation of a joint or bedding plane defined by the dip of the plane from the horizontal and the direction of the dip relative to north
- *Land use*: defines the main land use within or juxtaposing the landslide and/or dam

D. LANDSLIDE CLASSIFICATION (BASED ON CRUDEN AND VARNES (1996))

D-1 Movement

- *Fall*: No shear displacement takes place; material descends mainly through air

- *Rock avalanche*: rapidly flowing masses of dry debris created by large falls and slides (also known as sturzstroms)
- *Translational slide*: the mass displaces along a planar or undulating surface of rupture, sliding out over the original ground surface
- *Rotational slide*: debris move along a surface of rupture that is curved or concave normally showing little internal deformation
- *Spread*: extension of a cohesive soil rock mass combined with a general subsidence of the fractured mass of cohesive material into softer underlying material
- *Flow*: spatially continuous movement in which surfaces of shear are short lived, closely spaced and usually not preserved. Velocity distribution within the mass resemble those of a viscous liquid

D-2 Velocity

- *Velocity*: determined by the rate at which the landslide moves over time. Average rates are indicated to characterise the slide into one of the 6 velocity classes

D-3 State

- *Active*: currently moving, first time movers or reactivated landslides
- *Reactivated*: active after inactive. Generally moves on pre-existing slide planes
- *Suspended*: landslides that have moved within the last annual cycle but are currently inactive
- *Dormant*: if causes of movement remain apparent the landslide is dormant
- *Stabilised*: toe of slope has been protected against erosion by bank armouring or artificial measures
- *Abandoned*: if mechanisms eroding the toe of a slope are removed (e.g. a river that is eroding a slope at the toe changes course)

D-4 Landslide movement

- *Advancing*: the surface of rupture is extending in direction of movement
- *Retrogressive*: the surface of rupture is extending in the direction opposite to the movement of displaced material
- *Widening*: if surface of rupture is extending in or both lateral margins
- *Enlarging*: movement may be limited to the displaced material or the surface rupture may be enlarging continually adding to the volume of displaced material
- *Diminishing*: volume of material being displaced grows less with time and for those landslides in which no trend is obvious
- *Confined*: have a scarp but no visible surface of rupture in the foot of the displaced mass

D-5 Style

- *Single*: single movement of displaced material, often as an unbroken block
- *Complex*: those that have at least two types of movement
- *Composite*: different movement s occur in different areas of the displaced mass
- *Multiple*: repeated movements of the same type often following enlargement of the surface of rupture

- *Successive*: identical in type to earlier movements but doesn't share the same displaced material or surface of rupture (as in multiple)

D-6 Material

- *Rock*: firm intact bedrock
- *Debris*: loose unconsolidated or poorly cemented aggregate of particles
- *Earth*: superficial slide debris involving the top 2 -3 meters of colluvium/organic matter

E. LANDSLIDE CAUSE

- *Pre existing geological controls*: indicate any major defects (jointing or weathering for example) within the rock mass; tectonic influences that may influence the formation of a landslide
- *Triggering mechanisms*: state how the landslide was initiated (i.e. earthquake or rainfall for example)
- *Subsequent failures*: state the type and extend of any failures after the dam-forming landslide

2) DAM CHARACTERISTICS:

A. DAM DEBRIS

- *Reference number*: links the landslide dam to the datasheet in appendix 2 and location map in chapter 3
- *Reference name*: documents the name given to the dam or associated lake
- *Date of blockage*: the date the blockage occurred
- *NZMG coordinates of dam centre*: the New Zealand map grid coordinates locating the centre of the dam
- *Date of initial dam failure*: date that the dam was breached
- *Approximate elevation of dam centre*: the height of the dam centre above mean sea level (m) prior to failure
- *Subsequent major dam failure dates*: date of any dam failures after the main breaching occurrence
- *Classification*: geomorphic classification of landslide dams based on Costa and Schuster (1988)

B. ORIGINAL DAM DIMENSIONS

- *Crest length*: length (m) of the dam crest measured perpendicular to valley walls pre-failure
- *Crest width*: width (m) of debris at the crest height prior to failure
- *Crest height*: height (m) of debris above the inferred valley floor prior to failure
- *Area of landslide dam*: the area (m²) of debris that blocks the valley forming a dam
- *Volume of landslide dam*: the approximate volume (10⁶ m³) of debris blocking the flow of water. Measurements taken from the height of dam crest in a horizontal line to the valley walls prior to failure of the dam (also referred to as dam footprint)

- *Average baseline length*: the length (m) from the upstream to downstream extent of debris on the valley floor prior to failure
- *Downstream face slope*: the slope (°) of the downstream dam face prior to failure of the dam
- *Upstream face slope*: the slope (°) of the upstream dam face prior to failure of the dam

C. PRESENT DAM DIMENSIONS

- *Crest length*: length (m) of the dam crest measured perpendicular to valley walls post-failure
- *Crest width*: width (m) of debris at the crest height post-failure
- *Crest height*: height (m) of debris above the inferred valley floor post-failure
- *Area of landslide dam*: the area (m²) of debris that blocks the valley forming a dam post-failure.
- *Volume of landslide dam*: the approximate volume (10⁶ m³) of debris blocking the flow of water. Measurements taken from the height of dam crest in a horizontal line to the valley walls post-failure of the dam
- *Average baseline length*: the length (m) from the upstream to downstream extent of debris on the valley floor post-failure
- *Downstream face slope*: the slope (°) of the downstream dam face post-failure of the dam
- *Upstream face slope*: the slope (°) of the upstream dam face post-failure of the dam

D. DAM MATERIALS

- *Percent matrix*: percentage of matrix making up the dam debris
- *Grain supported*: qualitative term suggesting the grain-to-grain contact is the primary internal friction force
- *Intermediate*: qualitative term suggesting the combination of grain-to-grain plus grain-to-matrix contact is producing the main internal friction force
- *Matrix supported*: qualitative term suggesting the grains are not in contact with each other; the matrix produces the majority of the internal frictional force
- *Rounded*: qualitative term based on the high degree of grain or clast rounding within the dam debris
- *Intermediate*: translational qualitative description between highly rounded and angular grains or clasts within the dam material
- *Angular*: qualitative term based on the low degree of rounding of the grains or clasts comprising the dam material
- *Poorly graded*: engineering geological term indicating the dam material is composed predominantly by one size grain or clast
- *Moderately graded*: engineering geological term relating to the translational degree of grading between poorly graded and well graded (see below)
- *Well graded*: engineering geological term indicating the dam material is comprised of grains or clasts that represent the full range of particle sizes (i.e. clay to boulder sizes)

- *Minimum grain size*: the size (mm) of the smallest grain comprising the dam
- *Maximum grain size*: the size (mm) of the largest grain size comprising the dam

E. BREACH CHARACTERISTICS

- *Average depth*: the average depth (m) of the breached section of the dam post failure
- *Average width*: the average width (m) of the breached section of the dam post-failure measured at the original crest height
- *Breach volume*: the amount of material (m^3) eroded from the original dam volume as a result of failure of the dam (using average width and average depth of the breach)
- *Breach history*: brief account describing the breaching of the dam since formation
- *Failure mechanism*: Description of the type of failure mechanism associated with the dam breach (see section 2.3 for definition of failure mechanisms)
- *Acquisition of failure mechanism information*: indicates how the information relating to the failure mechanism was obtained
- *Breach shape*: indicates the general shape of the breach post failure
- *Degree of modification*: based on the volume of material that has been eroded from the original dam material post failure expressed as a percentage of the original dam volume

F. LAKE AND CATCHMENT CHARACTERISTICS

- *Lake name*: the name given to the impounded water
- *Present volume*: the volume (10^6 m^3) of water impounded presently
- *Original volume*: the max volume (10^6 m^3) of water impounded prior to the failure of dam (if applicable)
- *Lake surface elevation*: the present elevation(m) of the lake above mean sea level
- *Lake deposit thickness*. The thickness (m) of lacustrine aggradation upstream of the dam
- *Length*: the average length (m) of the impoundment. State in additional information the use of current or pre-failure lake conditions
- *Width*: the average width (m) of the impoundment. State in additional information the use of current or pre-failure lake conditions
- *Max depth*: the maximum depth (m) of the impoundment. State in additional information the use of current or pre-failure lake conditions
- *Area*: the area (m^2) of the impoundment. State in additional information the use of current or pre-failure lake conditions
- *Duration*: the length of time the water was impounded before breaching (year/month/day)
- *Present lake condition*: indicates the condition of the impoundment at the present time

G. CATCHMENT

- *River name*: the name given to the river or stream affected by the impoundment
- *Drainage basin area above landslide dam*: the catchment size (km^2) upstream of the blockage

- *Yearly precipitation*: the total amount of rain (mm) the area receives per annum
- *Average monthly precipitation*: the average monthly amount of rain (mm) the area receives
- *Maximum monthly precipitation*: the maximum amount of rain (mm) the area has received in one month
- *Mean monthly discharge*: the amount (m^3/s) of water discharging through the dam site averaged over a one month period
- *Maximum monthly discharge*: the maximum amount (m^3/s) of water discharging through the dam site averaged over a one month period
- *Location/distance to rain gauge*: the proximity of the rain gauge to the dam site expressed as a locality and distance (km)
- *Location/distance of flow gauge*: the proximity of the flow gauge to the dam site expressed as a locality and distance (km)
- *Valley width prior to the formation of the dam*: the width (m) at the base of the valley prior to dam formation
- *Valley elevation prior to dam failure*: the elevation (m) above mean sea level of the valley floor prior to the formation of the dam
- *Valley gradient downstream of the dam*: the average slope of the valley ($^{\circ}$) downstream of the dam
- *Valley gradient upstream of the dam*: the average slope of the valley ($^{\circ}$) upstream of the dam

H. DAMAGE

- *People*: the number of people killed as a result of the landslide or failure of dam (state which in additional information)
- *Property/infrastructure*: damage sustained as a result of the landslide or dam failure

Appendix G

Rock Mass and Material Field Descriptions

This appendix contains rock mass terminology from Bell and Pettinga (1983) for use on the dam-forming landslide source rock included in the Murchison dataset.

WEATHERING			STRENGTH			GEOLOGICAL CLASSIFICATION																
TERM	GRADE	ROCK DESCRIPTION	TERM	POINT LOAD STRENGTH INDEX IS(50)	FIELD ESTIMATION OF STRENGTH	CRYSTAL OR GRAIN SIZE	SEDIMENTARY ⁽¹⁾				IGNEOUS ⁽¹⁾								METAMORPHIC ⁽¹⁾⁽²⁾			
							CLASTIC	CHEMORGANIC		Siliceous	Intermediate	Mafic	Ultramafic	FOLIATED	MASSIVE							
6.	* residual soil (RW)	discolouration and complete transformation to soil; original fabric destroyed	1.	extremely strong (ES)	more than 10 can only be chipped with geological hammer	very coarse 6-2																
5	completely weathered (CW)	discolouration and transformation to soil; original fabric largely preserved	2.	very strong (VS)	3 to 10 several hard blows required to break hand specimen	coarse 2																
4.	highly weathered (HW)	material pervasively altered with discolouration and loss of strength; fabric preserved; lithorelicts	3.	strong (S)	1 to 3 few firm blows of hammer required to break specimen	medium																
	moderately weathered (MW)	penetrative discolouration and alteration of rock material, with some loss of strength	4.	moderately strong (MS)	0.3 to 1 breaks readily with one blow of hammer																	
3.	slightly weathered (SW)	slight discolouration of rock fabric; no loss of material strength	5.	moderately weak (MWk)	0.1 to 0.3 broken by hand only with difficulty; small thin pieces broken by finger pressure	fine — 0.06	T															
2.	unweathered (UW)	no discolouration or loss of strength, or any other effects due to weathering	6.	weak (Wk)	0.03 to 0.1 broken by hand; pieces 25 mm or more broken by finger pressure	U F S M V (7)	SILTSTONE (5) SLYVOSTONE (6) CLAYSTONE (8)															
1.			7.	* very weak (VWk)	less than 0.03 crushed or remoulded by hand (grades into soil materials)	very fine 0.002 [mm]																

(1) OTHERS: Specity (43)

